https://doi.org/10.61092/iaea.s5qz-c2k8

INTERNATIONAL ATOMIC ENERGY AGENCY

NUCLEAR DATA SERVICES

DOCUMENTATION SERIES OF THE IAEA NUCLEAR DATA SECTION

IAEA-NDS-0232
August, 2020

Processing of the Evaluated Photonuclear Data Library (IAEA/PD-2019)

Hiroki KAWADA
Tokyo Institute of Technology

Jean-Christophe SUBLET
and
Shin OKUMURA
IAEA Nuclear Data Section

Toshihiko KAWANO
Los Alamos National Laboratory

Nuclear Data Section
International Atomic Energy Agency
P.O. Box 100
A-1400 Vienna
Austria

E-mail: nds.contact-point@iaea.org
Fax: (43-1) 26007
Telephone: (43-1) 2600 21725
Web: http://www-nds.iaea.org/

Disclaimer

Neither the authors nor the IAEA makes any warranty, expressed or implied, or assumes any legal liability or responsibility for the accuracy, completeness or usefulness of any information disclosed, or represents that its use would not infringe privately owned rights.

The IAEA-NDS would appreciate any comment on this report at: nds.contact-point@iaea.org.

Vienna, August, 2020

Abstract

A new IAEA Evaluated Photonuclear Library (IAEA/PD-2019) was produced by the IAEA Coordinated Research Project (CRP). The new library consists of 219 evaluations in total, including 199 new evaluations and 20 evaluations retained from the previous library released in 1999 (IAEA/PD-1999).

This report describes the ENDF-6 data format representations used in the IAEA Photonuclear Data Library (IAEA/PD-2019), the use of ENDF Utility codes, FRENDY, and DeCE for the ENDF-6 data file verification. The report also describes the data processing employed to create an ACE transport library and FISPACT-II inventory-source terms libraries using NJOY2016 (a special patched branch for IAEA/PD-2019) and PREPRO-2019 nuclear data processing systems.

Table of contents

1 Evaluated Photonuclear Data Library (IAEA-PD2019)

The first recommended photo-induced reaction nuclear data library was released in 1999 as the IAEA Photonuclear Data Library (IAEA/PD-1999) assembled under an international coordinated research project (CRP) named "Compilation and Evaluation of Photonuclear Data for Applications" from 1996 to 1999 [1]. The previous library is available at the IAEA-Nuclear Data Section (NDS) website[1], which includes the photonuclear reaction nuclear data for 164 isotopes.

A new CRP was endorsed by the International Nuclear Data Committee during its 2014 meeting in Vienna [2] and was initiated by the IAEA, entitled "Updating the Photonuclear Data Library". As a result of the new CRP [3, 4, 5], an updated version of the IAEA Photonuclear Data Library (IAEA/PD-2019) was produced. The IAEA/PD-2019 includes 219 evaluated files, where the highest photon energy was extended to 200 MeV (some files remained at a maximum energy of 140 MeV). The evaluations have been contributed by China Nuclear Data Center (CNDC) of China Institute of Atomic Energy (CIAE), the Korea Atomic Energy Research Institute (KAERI), the Japan Atomic Energy Agency (JAEA), and the Horia Hulubei National Institute (IFIN-HH) and University of Bucharest (UB) collaboration. Details of the experimental and evaluation efforts in this CRP are explained in the publication [6].

The evaluated data files contained in the IAEA/PD-2019 are in a standard ENDF-6 format [7], however different ENDF-6 data format representations have been used by different evaluators. All of the files were reassembled, a consistent description was given in the header part of each file by the IAEA-NDS. Table 1 gives the complete list of target nuclides with maximum energies, originating evaluation laboratory(s), and file names given in the library. The ENDF-6 library files, graphs, processed application libraries, and their compressed archives are available at the IAEA-NDS website[2]. They can also be downloaded from the IAEA GitHub repository by the terminal command:

```
git clone https://github.com/IAEA-NDS/IAEA-PD2019.git
```

In this report, we describe the ENDF-6 data representation used in each evaluated file of the IAEA/PD-2019 and summarize our procedures for checking and correcting of the ENDF-6 data format, whenever needed, and the data processing to create transport and activation-transmutation libraries. In Section 2, we describe details of the aforementioned ENDF-6 data representations. The type of the data representation of each data file is shown in the right-most column of Table 1. In Section 3, we summarize our procedures for verifying the data format, and checking the correctness and internal physical consistency of the ENDF-6 data files by using ENDF Utility codes (CHEKR, FIZCON, PSYCHE), FRENDY [8], and DeCE [9]. In addition, we describe procedures of the general nuclear data processing to create ACE transport library and FISPACT-II activation libraries using NJOY2016 [10] with a special patch for the IAEA/PD-2019[3] and PREPRO-2019 [11]. These procedures are to meet recommended guidelines as part of the nuclear data verification and validation processes [12].

[1] IAEA/PD-1999: https://nds.iaea.org/photonuclear/photonuclear99/
[2] IAEA/PD-2019: https://nds.iaea.org/photonuclear/
[3] NJOY2016 feature/pn-iaea branch: https://github.com/njoy/NJOY2016/tree/feature/pn-iaea/

Table 1: List of evaluated nuclear data files in the IAEA/PD-2019. The format descriptions numbered from 0 to 5 are shown in the following section. The institute abbreviations are, CNDC: China Nuclear Data Center of CIAE, IFIN-HH: Horia Hulubei National Institute, JAEA: Japan Atomic Energy Agency, JAERI: Japan Atomic Energy Research Institute, KAERI: Korea Atomic Energy Research Institute, NFD: Nippon Nuclear Fuel Development, and UB: University of Bucharest.

Nuclides	MAT number	Evaluation Institute	E_{MAX} (MeV)	Filename	Format description
1-H-2	128	NFD	140	g_1-H-2_0128.endf	0
2-He-3	225	JAEA	140	g_2-He-3_0225.endf	1
3-Li-6	325	JAEA	140	g_3-Li-6_0325.endf	1
3-Li-7	328	JAEA	140	g_3-Li-7_0328.endf	1
4-Be-9	425	CNDC	150	g_4-Be-9_0425.endf	3
6-C-12	625	CNDC	150	g_6-C-12_0625.endf	3
6-C-13	628	KAERI	140	g_6-C-13_0628.endf	1
6-C-14	631	KAERI	200	g_6-C-14_0631.endf	2
7-N-14	725	CNDC	150	g_7-N-14_0725.endf	3
7-N-15	728	KAERI	140	g_7-N-15_0728.endf	1
8-O-16	825	CNDC	150	g_8-O-16_0825.endf	3
8-O-17	828	KAERI	140	g_8-O-17_0828.endf	1
8-O-18	831	KAERI	140	g_8-O-18_0831.endf	1
9-F-19	925	JAEA	140	g_9-F-19_0925.endf	1
11-Na-23	1125	KAERI	140	g_11-Na-23_1125.endf	1
12-Mg-24	1225	KAERI	140	g_12-Mg-24_1225.endf	1
12-Mg-25	1228	KAERI	140	g_12-Mg-25_1228.endf	1
12-Mg-26	1231	KAERI	140	g_12-Mg-26_1231.endf	1
13-Al-27	1325	CNDC	200	g_13-Al-27_1325.endf	3
14-Si-27	1422	KAERI	140	g_14-Si-27_1422.endf	1
14-Si-28	1425	KAERI	140	g_14-Si-28_1425.endf	1
14-Si-29	1428	KAERI	140	g_14-Si-29_1428.endf	1
14-Si-30	1431	KAERI	140	g_14-Si-30_1431.endf	1
16-S-32	1625	KAERI	140	g_16-S-32_1625.endf	1
16-S-33	1628	KAERI	140	g_16-S-33_1628.endf	1
16-S-34	1631	KAERI	140	g_16-S-34_1631.endf	1
16-S-36	1637	KAERI	140	g_16-S-36_1637.endf	1
17-Cl-35	1725	JAEA	200	g_17-Cl-35_1725.endf	1
17-Cl-37	1731	JAEA	200	g_17-Cl-37_1731.endf	1
18-Ar-36	1825	JAEA	200	g_18-Ar-36_1825.endf	1
18-Ar-38	1831	JAEA	200	g_18-Ar-38_1831.endf	1
18-Ar-40	1837	JAEA	200	g_18-Ar-40_1837.endf	1
19-K-39	1925	JAEA	200	g_19-K-39_1925.endf	1
19-K-40	1928	JAEA	200	g_19-K-40_1928.endf	1
19-K-41	1931	JAEA	200	g_19-K-41_1931.endf	1
20-Ca-40	2025	JAEA	140	g_20-Ca-40_2025.endf	1
20-Ca-42	2031	KAERI	140	g_20-Ca-42_2031.endf	1
20-Ca-43	2034	KAERI	140	g_20-Ca-43_2034.endf	1
20-Ca-44	2037	JAEA	140	g_20-Ca-44_2037.endf	1
20-Ca-46	2043	KAERI	140	g_20-Ca-46_2043.endf	1

Table 1 The list of IAEA/PD-2019 evaluated nuclear data files. (Continued)

Nuclides	MAT	Evaluation	E_{MAX} (MeV)	Filename	Format description
20-Ca-48	2049	JAEA	140	g_20-Ca-48_2049.endf	1
21-Sc-45	2125	JAEA	200	g_21-Sc-45_2125.endf	1
22-Ti-46	2225	JAEA	200	g_22-Ti-46_2225.endf	1
22-Ti-47	2228	JAEA	200	g_22-Ti-47_2228.endf	1
22-Ti-48	2231	JAEA	200	g_22-Ti-48_2231.endf	1
22-Ti-49	2234	JAEA	200	g_22-Ti-49_2234.endf	1
22-Ti-50	2237	JAEA	200	g_22-Ti-50_2237.endf	1
23-V-50	2325	JAEA	200	g_23-V-50_2325.endf	1
23-V-51	2328	JAEA	200	g_23-V-51_2328.endf	1
24-Cr-50	2425	CNDC	200	g_24-Cr-50_2425.endf	4
24-Cr-52	2431	JAEA	200	g_24-Cr-52_2431.endf	1
24-Cr-53	2434	CNDC	200	g_24-Cr-53_2434.endf	4
24-Cr-54	2437	CNDC	200	g_24-Cr-54_2437.endf	4
25-Mn-55	2525	JAEA	200	g_25-Mn-55_2525.endf	1
26-Fe-54	2625	JAEA	200	g_26-Fe-54_2625.endf	1
26-Fe-56	2631	JAEA	200	g_26-Fe-56_2631.endf	1
26-Fe-57	2634	JAEA	200	g_26-Fe-57_2634.endf	1
26-Fe-58	2637	JAEA	200	g_26-Fe-58_2637.endf	1
27-Co-59	2725	IFIN-HH,UB	200	g_27-Co-59_2725.endf	5
28-Ni-58	2825	JAEA	200	g_28-Ni-58_2825.endf	1
28-Ni-60	2831	JAEA	200	g_28-Ni-60_2831.endf	1
28-Ni-61	2834	JAEA	200	g_28-Ni-61_2834.endf	1
28-Ni-62	2837	JAEA	200	g_28-Ni-62_2837.endf	1
28-Ni-64	2843	JAEA	200	g_28-Ni-64_2843.endf	1
29-Cu-63	2925	JAEA	200	g_29-Cu-63_2925.endf	1
29-Cu-65	2931	JAEA	200	g_29-Cu-65_2931.endf	1
30-Zn-64	3025	KAERI	200	g_30-Zn-64_3025.endf	2
30-Zn-66	3031	JAEA	200	g_30-Zn-66_3031.endf	1
30-Zn-67	3034	JAEA	200	g_30-Zn-67_3034.endf	1
30-Zn-68	3037	JAEA	200	g_30-Zn-68_3037.endf	1
30-Zn-70	3043	JAEA	200	g_30-Zn-70_3043.endf	1
32-Ge-70	3225	JAEA	200	g_32-Ge-70_3225.endf	1
32-Ge-72	3231	JAEA	200	g_32-Ge-72_3231.endf	1
32-Ge-73	3234	JAEA	200	g_32-Ge-73_3234.endf	1
32-Ge-74	3237	JAEA	200	g_32-Ge-74_3237.endf	1
32-Ge-76	3243	JAEA	200	g_32-Ge-76_3243.endf	1
33-As-75	3325	KAERI	200	g_33-As-75_3325.endf	2
34-Se-76	3431	KAERI	200	g_34-Se-76_3431.endf	2
34-Se-78	3437	KAERI	200	g_34-Se-78_3437.endf	2
34-Se-80	3443	KAERI	200	g_34-Se-80_3443.endf	2
34-Se-82	3449	KAERI	200	g_34-Se-82_3449.endf	2
38-Sr-84	3825	JAEA	200	g_38-Sr-84_3825.endf	1
38-Sr-86	3831	JAEA	200	g_38-Sr-86_3831.endf	1
38-Sr-87	3834	JAEA	200	g_38-Sr-87_3834.endf	1

Table 1 The list of IAEA/PD-2019 evaluated nuclear data files. (Continued)

Nuclides	MAT	Evaluation	E_{MAX} (MeV)	Filename	Format description
38-Sr-88	3837	JAEA	200	g_38-Sr-88_3837.endf	1
38-Sr-90	3843	JAEA	200	g_38-Sr-90_3843.endf	1
39-Y-89	3925	IFIN-HH,UB	200	g_39-Y-89_3925.endf	5
40-Zr-90	4025	CNDC	200	g_40-Zr-90_4025.endf	4
40-Zr-91	4028	KAERI	200	g_40-Zr-91_4028.endf	2
40-Zr-92	4031	JAEA	200	g_40-Zr-92_4031.endf	1
40-Zr-93	4034	JAEA	200	g_40-Zr-93_4034.endf	1
40-Zr-94	4037	KAERI	200	g_40-Zr-94_4037.endf	2
40-Zr-96	4043	JAEA	200	g_40-Zr-96_4043.endf	1
41-Nb-93	4125	JAEA	200	g_41-Nb-93_4125.endf	1
41-Nb-94	4128	JAEA	200	g_41-Nb-94_4128.endf	1
42-Mo-100	4249	JAEA	200	g_42-Mo-100_4249.endf	1
42-Mo-92	4225	JAEA	200	g_42-Mo-92_4225.endf	1
42-Mo-94	4231	JAEA	200	g_42-Mo-94_4231.endf	1
42-Mo-95	4234	JAEA	200	g_42-Mo-95_4234.endf	1
42-Mo-96	4237	JAEA	200	g_42-Mo-96_4237.endf	1
42-Mo-97	4240	JAEA	200	g_42-Mo-97_4240.endf	1
42-Mo-98	4243	JAEA	200	g_42-Mo-98_4243.endf	1
44-Ru-98	4431	JAEA	200	g_44-Ru-98_4431.endf	1
45-Rh-103	4525	IFIN-HH,UB	200	g_45-Rh-103_4525.endf	5
46-Pd-102	4625	JAEA	200	g_46-Pd-102_4625.endf	1
46-Pd-104	4631	JAEA	200	g_46-Pd-104_4631.endf	1
46-Pd-105	4634	JAEA	200	g_46-Pd-105_4634.endf	1
46-Pd-106	4637	JAEA	200	g_46-Pd-106_4637.endf	1
46-Pd-107	4640	JAEA	200	g_46-Pd-107_4640.endf	1
46-Pd-108	4643	JAEA	200	g_46-Pd-108_4643.endf	1
46-Pd-110	4649	JAEA	200	g_46-Pd-110_4649.endf	1
47-Ag-107	4725	JAEA	200	g_47-Ag-107_4725.endf	1
47-Ag-108	4728	JAEA	200	g_47-Ag-108_4728.endf	1
47-Ag-109	4731	JAEA	200	g_47-Ag-109_4731.endf	1
48-Cd-106	4825	JAEA	200	g_48-Cd-106_4825.endf	1
48-Cd-108	4831	JAEA	200	g_48-Cd-108_4831.endf	1
48-Cd-110	4837	JAEA	200	g_48-Cd-110_4837.endf	1
48-Cd-111	4840	JAEA	200	g_48-Cd-111_4840.endf	1
48-Cd-112	4843	JAEA	200	g_48-Cd-112_4843.endf	1
48-Cd-113	4846	JAEA	200	g_48-Cd-113_4846.endf	1
48-Cd-114	4849	JAEA	200	g_48-Cd-114_4849.endf	1
48-Cd-116	4855	JAEA	200	g_48-Cd-116_4855.endf	1
49-In-115	4931	KAERI	200	g_49-In-115_4931.endf	2
50-Sn-112	5025	JAEA	200	g_50-Sn-112_5025.endf	1
50-Sn-114	5031	JAEA	200	g_50-Sn-114_5031.endf	1
50-Sn-115	5034	JAEA	200	g_50-Sn-115_5034.endf	1
50-Sn-116	5037	KAERI	200	g_50-Sn-116_5037.endf	2
50-Sn-117	5040	JAEA	200	g_50-Sn-117_5040.endf	1

Table 1 The list of IAEA/PD-2019 evaluated nuclear data files. (Continued)

Nuclides	MAT	Evaluation	E_{MAX} (MeV)	Filename	Format description
50-Sn-118	5043	CNDC	200	g_50-Sn-118_5043.endf	4
50-Sn-119	5046	JAEA	200	g_50-Sn-119_5046.endf	1
50-Sn-120	5049	JAEA	200	g_50-Sn-120_5049.endf	1
50-Sn-122	5055	JAEA	200	g_50-Sn-122_5055.endf	1
50-Sn-124	5061	JAEA	200	g_50-Sn-124_5061.endf	1
51-Sb-121	5125	JAEA	200	g_51-Sb-121_5125.endf	1
51-Sb-123	5131	JAEA	200	g_51-Sb-123_5131.endf	1
52-Te-120	5225	JAEA	200	g_52-Te-120_5225.endf	1
52-Te-122	5231	JAEA	200	g_52-Te-122_5231.endf	1
52-Te-123	5234	JAEA	200	g_52-Te-123_5234.endf	1
52-Te-124	5237	JAEA	200	g_52-Te-124_5237.endf	1
52-Te-125	5240	JAEA	200	g_52-Te-125_5240.endf	1
52-Te-126	5243	JAEA	200	g_52-Te-126_5243.endf	1
52-Te-128	5249	JAEA	200	g_52-Te-128_5249.endf	1
52-Te-130	5255	JAEA	200	g_52-Te-130_5255.endf	1
53-I-127	5325	JAEA	200	g_53-I-127_5325.endf	1
53-I-129	5331	JAEA	200	g_53-I-129_5331.endf	1
54-Xe-132	5449	JAEA	200	g_54-Xe-132_5449.endf	1
55-Cs-133	5525	KAERI	200	g_55-Cs-133_5525.endf	2
55-Cs-135	5531	JAEA	200	g_55-Cs-135_5531.endf	1
55-Cs-137	5537	JAEA	200	g_55-Cs-137_5537.endf	1
56-Ba-138	5649	KAERI	200	g_56-Ba-138_5649.endf	2
57-La-139	5728	JAEA	200	g_57-La-139_5728.endf	1
58-Ce-140	5837	KAERI	200	g_58-Ce-140_5837.endf	2
58-Ce-142	5843	KAERI	200	g_58-Ce-142_5843.endf	2
59-Pr-141	5925	JAEA	200	g_59-Pr-141_5925.endf	1
60-Nd-142	6025	KAERI	200	g_60-Nd-142_6025.endf	2
60-Nd-143	6028	KAERI	200	g_60-Nd-143_6028.endf	2
60-Nd-144	6031	KAERI	200	g_60-Nd-144_6031.endf	2
60-Nd-145	6034	KAERI	200	g_60-Nd-145_6034.endf	2
60-Nd-146	6037	KAERI	200	g_60-Nd-146_6037.endf	2
60-Nd-148	6043	KAERI	200	g_60-Nd-148_6043.endf	2
60-Nd-150	6049	KAERI	200	g_60-Nd-150_6049.endf	2
62-Sm-144	6225	JAEA	200	g_62-Sm-144_6225.endf	1
62-Sm-147	6234	JAEA	200	g_62-Sm-147_6234.endf	1
62-Sm-148	6237	JAEA	200	g_62-Sm-148_6237.endf	1
62-Sm-149	6240	JAEA	200	g_62-Sm-149_6240.endf	1
62-Sm-150	6243	JAEA	200	g_62-Sm-150_6243.endf	1
62-Sm-151	6246	JAEA	200	g_62-Sm-151_6246.endf	1
62-Sm-152	6249	JAEA	200	g_62-Sm-152_6249.endf	1
62-Sm-154	6255	JAEA	200	g_62-Sm-154_6255.endf	1
63-Eu-153	6331	KAERI	200	g_63-Eu-153_6331.endf	2
64-Gd-156	6437	JAEA	200	g_64-Gd-156_6437.endf	1
64-Gd-157	6440	JAEA	200	g_64-Gd-157_6440.endf	1

Table 1 The list of IAEA/PD-2019 evaluated nuclear data files. (Continued)

Nuclides	MAT	Evaluation	E_{MAX} (MeV)	Filename	Format description
64-Gd-158	6443	JAEA	200	g_64-Gd-158_6443.endf	1
64-Gd-160	6449	JAEA	200	g_64-Gd-160_6449.endf	1
65-Tb-158	6522	JAEA	200	g_65-Tb-158_6522.endf	1
65-Tb-159	6525	IFIN-HH,UB	200	g_65-Tb-159_6525.endf	5
66-Dy-162	6643	JAEA	200	g_66-Dy-162_6643.endf	1
66-Dy-163	6646	JAEA	200	g_66-Dy-163_6646.endf	1
67-Ho-165	6725	IFIN-HH,UB	200	g_67-Ho-165_6725.endf	5
68-Er-166	6837	JAEA	200	g_68-Er-166_6837.endf	1
68-Er-170	6849	JAEA	200	g_68-Er-170_6849.endf	1
69-Tm-169	6925	IFIN-HH,UB	200	g_69-Tm-169_6925.endf	5
71-Lu-175	7125	KAERI	200	g_71-Lu-175_7125.endf	2
72-Hf-174	7225	JAEA	200	g_72-Hf-174_7225.endf	1
72-Hf-176	7231	JAEA	200	g_72-Hf-176_7231.endf	1
72-Hf-177	7234	JAEA	200	g_72-Hf-177_7234.endf	1
72-Hf-178	7237	JAEA	200	g_72-Hf-178_7237.endf	1
72-Hf-179	7240	JAEA	200	g_72-Hf-179_7240.endf	1
72-Hf-180	7243	JAEA	200	g_72-Hf-180_7243.endf	1
73-Ta-181	7328	IFIN-HH,UB	200	g_73-Ta-181_7328.endf	5
74-W-180	7425	CNDC	200	g_74-W-180_7425.endf	4
74-W-182	7431	CNDC	200	g_74-W-182_7431.endf	4
74-W-183	7434	CNDC	200	g_74-W-183_7434.endf	4
74-W-184	7437	CNDC	200	g_74-W-184_7437.endf	4
74-W-186	7443	CNDC	200	g_74-W-186_7443.endf	4
75-Re-185	7525	JAEA	200	g_75-Re-185_7525.endf	1
75-Re-187	7531	JAEA	200	g_75-Re-187_7531.endf	1
76-Os-186	7631	KAERI	200	g_76-Os-186_7631.endf	2
76-Os-188	7637	KAERI	200	g_76-Os-188_7637.endf	2
76-Os-189	7640	KAERI	200	g_76-Os-189_7640.endf	2
76-Os-190	7643	KAERI	200	g_76-Os-190_7643.endf	2
76-Os-192	7649	KAERI	200	g_76-Os-192_7649.endf	2
78-Pt-194	7837	JAEA	200	g_78-Pt-194_7837.endf	1
79-Au-197	7925	JAEA	200	g_79-Au-197_7925.endf	1
82-Pb-206	8231	JAEA	200	g_82-Pb-206_8231.endf	1
82-Pb-207	8234	JAEA	200	g_82-Pb-207_8234.endf	1
82-Pb-208	8237	JAEA	200	g_82-Pb-208_8237.endf	1
83-Bi-209	8325	KAERI	200	g_83-Bi-209_8325.endf	2
88-Ra-226	8834	JAEA	200	g_88-Ra-226_8834.endf	1
90-Th-232	9040	JAEA	200	g_90-Th-232_9040.endf	1
92-U-233	9222	JAEA	200	g_92-U-233_9222.endf	1
92-U-234	9225	JAEA	200	g_92-U-234_9225.endf	1
92-U-235	9228	JAEA	200	g_92-U-235_9228.endf	1
92-U-236	9231	JAEA	200	g_92-U-236_9231.endf	1
92-U-238	9237	JAEA	200	g_92-U-238_9237.endf	1
93-Np-237	9346	JAEA	200	g_93-Np-237_9346.endf	1

Table 1 The list of IAEA/PD-2019 evaluated nuclear data files. (Continued)

Nuclides	MAT	Evaluation	E_{MAX} (MeV)	Filename	Format description
94-Pu-238	9434	JAEA	200	g_94-Pu-238_9434.endf	1
94-Pu-239	9437	JAEA	200	g_94-Pu-239_9437.endf	1
94-Pu-241	9443	JAEA	200	g_94-Pu-241_9443.endf	1

2 ENDF Format Description for Photonuclear Data

Depending on the original photonuclear ENDF-6 data format representation adopted in any particular file, processing steps and application forms may differ. The type of data representation for each evaluated file is shown in the right-most column of Table 1.

2.1 General Data Format

The majority of photonuclear data files in the IAEA/PD-2019 contains a total photo-absorption cross section $\sigma_a(E_\gamma)$ in MF3 (File 3: cross sections) MT5 (reaction type 5: reaction cross section), while cross sections for each reaction, given as the production of emitted particles and residual nuclei, are stored in MF6 (File 6: product energy and angular distributions) by its fraction or the so-called multiplicity. The typical MF – MT combination for photonuclear data library is as follows.

```
MF    1
 451
MF    3
    5
MF    6
    5
```

An example of $\sigma_a(E_\gamma)$ given in the MF3/MT5 representation is shown by the solid curve in Figure 1. The neutron multiplicity $y_n(E_\gamma)$, shown by the dashed curve, is given in MF6/MT5 and ZAP (product identifier) = 1. Note that ZAP is the product identifier $1000 \times Z + A$ and ZAP = 1 means neutron, ZAP = 0 means gamma. The $(\gamma, x\mathrm{n})$ reaction cross section (*i.e.* inclusive neutron production cross section) is given by the product $\sigma_a(E_\gamma) \times y_a(E_\gamma)$, which is shown by the dotted curve.

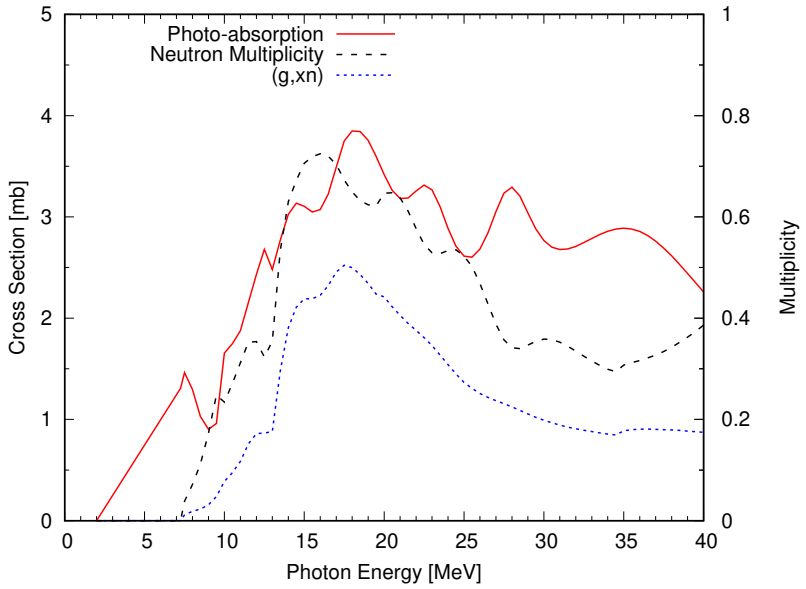

Figure 1: Photo-absorption cross section σ_a of ^{7}Li, neutron multiplicity, and $^7\mathrm{Li}(\gamma, x\mathrm{n})$ cross section in the IAEA/PD-2019.

Similarly, one can see the proton multiplicities in ZAP = 1001 subsection, ZAP = 1002 is for the deuteron, 2004 is for the α-particle, and *etc.* This kind of data representation is sometimes referred to as "inclusive data", because $(\gamma, x\mathrm{n})$ is composed of all the neutron emission chan-

nels, such as $(\gamma, \mathrm{n}) + (\gamma, 2\mathrm{n}) + (\gamma, \mathrm{np}) + \ldots$ Hence the residual nucleus is not explicit, needs to be derived, unless explicitly specified in MF8/MT5.

The table below summarizes the relation between ZAP and actual reaction channels for some selected cases. When ZAP is $1000(Z-1)+A-2$, such cross section involves (γ, α), $(\gamma, \mathrm{n}^3\mathrm{He})$, $(\gamma, 2\mathrm{d})$, and so on. However, this might be predominantly (γ, α) at low energies below the Q value of multiple particle emission.

ZAP	reaction	note
1	$(\gamma, x\mathrm{n})$	neutron multiplicity
1001	$(\gamma, x\mathrm{p})$	proton multiplicity
1002	$(\gamma, x\mathrm{d})$	deuteron multiplicity
2004	$(\gamma, x\alpha)$	α-particle multiplicity
$1000Z + A - 1$	(γ, n)	explicit one-neutron emission
$1000Z + A - 2$	$(\gamma, 2\mathrm{n})$	explicit two-neutron emission
$1000Z + A - 3$	$(\gamma, 3\mathrm{n})$	explicit three-neutron emission
$1000(Z-1) + A - 1$	(γ, p)	explicit one-proton emission
$1000(Z-1) + A - 2$	$(\gamma, \mathrm{d}) + (\gamma, \mathrm{np})$	one-deuteron emission until np-channel opens, then two channels cannot be separated
$1000(Z-2) + A - 4$	$(\gamma, \alpha) + \ldots$	one-α channel until other channels open
0	(γ, γ)	gamma multiplicity

2.2 Experimental Data Representation

Experimental photonuclear reaction data are usually obtained by directly counting the number of emitted particles, or by measuring the residual nucleus radioactivity. For energies above the multi-particle emission threshold, more than one combination of emitted light-particles can accompany the same number of produced neutrons or can lead to the same residual nucleus, respectively. For example, an experimental data set that is reported as the (γ, xn) cross section could have charged particles emitted concurrently with one-neutron emission, *i.e.,* $(\gamma, \mathrm{n}) + (\gamma, \mathrm{np}) + (\gamma, \mathrm{n2p}) + \ldots$, depending on the incident photon energy.

When the charged-particle emission is negligible, usually for heavy nuclei, the measured one-neutron emission cross section is identical to the cross section for the production of $(Z, A-1)$ nucleus, and the two-neutron emission is equal to the production of $(Z, A-2)$, and so on. However, when the charged-particle emission is non-negligible, then the measured one-neutron emission cross section $\sigma_{1\mathrm{n}X}$ should read

$$\sigma_{1\mathrm{n}X} = \sigma(\gamma, 1\mathrm{n}) + \sigma(\gamma, \mathrm{np}) + \sigma(\gamma, \mathrm{n}\alpha) + \ldots \ , \tag{1}$$

and same for $\sigma(\gamma, 2\mathrm{n}X)$, $\sigma(\gamma, 3\mathrm{n}X)$, and *etc*. Thus, $\sigma(\gamma, i\mathrm{n}X)$ is understood to be the inclusive i-neutron emission cross section, where X stands for anything except for i-neutrons.

The photo-neutron production cross section is defined in two ways, either involving the neutron

multiplicity or not. We denote the photo-neutron yield (or production) cross section $\sigma_{x\mathrm{n}}$ as

$$\begin{aligned}\sigma_{x\mathrm{n}} &= \sigma(\gamma,1\mathrm{n})+\sigma(\gamma,\mathrm{np})+\sigma(\gamma,\mathrm{n}\alpha)+\ldots \\ &+ 2\sigma(\gamma,2\mathrm{n})+2\sigma(\gamma,2\mathrm{np})+2\sigma(\gamma,2\mathrm{n}\alpha)+\ldots \\ &+ 3\sigma(\gamma,3\mathrm{n})+3\sigma(\gamma,3\mathrm{np})+3\sigma(\gamma,3\mathrm{n}\alpha)+\ldots, \\ &= \sum_i i\sigma_{i\mathrm{n}X}\ , \end{aligned} \tag{2}$$

and the total photo-neutron cross section $\sigma_{S\mathrm{n}}$ as

$$\begin{aligned}\sigma_{S\mathrm{n}} &= \sigma(\gamma,1\mathrm{n})+\sigma(\gamma,\mathrm{np})+\sigma(\gamma,\mathrm{n}\alpha)+\ldots \\ &+ \sigma(\gamma,2\mathrm{n})+\sigma(\gamma,2\mathrm{np})+\sigma(\gamma,2\mathrm{n}\alpha)+\ldots \\ &+ \sigma(\gamma,3\mathrm{n})+\sigma(\gamma,3\mathrm{np})+\sigma(\gamma,3\mathrm{n}\alpha)+\ldots \\ &= \sum_i \sigma_{i\mathrm{n}X}\ . \end{aligned} \tag{3}$$

When the photo-charged particle emission cross sections — $\sigma(\gamma,p)$, $\sigma(\gamma,\alpha)$, and *etc.*, — are negligible, and no photo-fission occurs, $\sigma_{S\mathrm{n}}$ is the same as the photo-absorption cross section σ_a.

2.3 Format Description: Type 0 for ^{2}H by NFD

The evaluated data file of ^{2}H was taken from JENDL/PD-2016.1 [13, 14], and it was modified to use the MF6/MT50 combination instead of MT28. This allows to process the data for both activation-transmutation and transport purposes. Additionally, some original coefficients produced negative probabilities, this was fixed by using the PREPRO/LEGEND code [11]. The MF – MT combination is as follows.

```
MF   1
 451
MF   3
   3  50
MF   6
  50
```

The 2-D and 3-D plots by VIEWR (NJOY2016) and PREPRO-2019 are attached in Appendix A.1.

2.4 Format Description: Type 1 by JAEA and KAERI

The majority of photo-nuclear data files are compiled in a commonly used way, where σ_a is given in MF3/MT5 and MF6 contains the emitted particle and residual nucleus multiplicities as explained in Section 2.1. Typical MF – MT combination for these cases is as follows.

```
MF   1
 451
MF   3
   5
MF   6
   5
```

MF6/MT5 is sub-divided by ZAP to indicate the emitted particles or the residual nuclei. These sub-sections may include ZAP of 0 (photon), 1 (neutron), 1001 (proton), 1002 (deuteron), 1003 (triton), 2003 (^{3}He), and 2004 (α-particle) for the light particles, as well as all the possible $1000Z+A$ numbers of residual nuclei.

Additionally, heavy fissionable nuclei contain MT452, MT455 and MT456 (average number of total, delayed and prompt neutrons) in MF1, and explicit MT18 (photo-fission cross section) in MF3 as follows.

```
MF   1
 451 452 455 456
MF   3
   3   5  18
MF   5
 455
MF   6
   5  18
```

As an example, we tabulate the data given in the ^{19}F data file. First the particle (neutron, proton, and deuteron) production cross sections are stored as;

```
#    [  925 :  6 :   5 ]     9 -  19
# Energy and angle distribution
#           NK            25  number of subsections
#          ZAP             1
#          LIP             0  product modifier
#          LAW             1  distribution law
#           NP           230  yield energy points
#   Energy[eV]  CrossSec [b]  Multiplicity  CrossSec x M
 4.0122000e+06 0.0000000e+00 0.0000000e+00 0.0000000e+00
 1.0431000e+07 8.3487645e-03 0.0000000e+00 0.0000000e+00
 1.0600000e+07 9.7649000e-03 2.8793000e-02 2.8116077e-04
...

#          ZAP          1001
#          LIP             0  product modifier
#          LAW             1  distribution law
#           NP            38  yield energy points
#   Energy[eV]  CrossSec [b]  Multiplicity  CrossSec x M
 4.0122000e+06 0.0000000e+00 0.0000000e+00 0.0000000e+00
 7.9941000e+06 2.5844178e-03 0.0000000e+00 0.0000000e+00
 1.0000000e+07 5.6487000e-03 7.1876000e-09 4.0600596e-11
...

#          ZAP          1002
#          LIP             0  product modifier
#          LAW             1  distribution law
#           NP            35  yield energy points
#   Energy[eV]  CrossSec [b]  Multiplicity  CrossSec x M
 4.0122000e+06 0.0000000e+00 0.0000000e+00 0.0000000e+00
 1.3814000e+07 1.6588000e-02 0.0000000e+00 0.0000000e+00
 1.6000000e+07 1.8624000e-02 5.6340000e-09 1.0492762e-10
...
```

then the residual nucleus production cross sections are given as follows.

```
#          ZAP          9016
#          LIP             0  product modifier
#          LAW             0  distribution law
#           NP            23  yield energy points
#   Energy[eV]  CrossSec [b]  Multiplicity  CrossSec x M
 4.0122000e+06 0.0000000e+00 0.0000000e+00 0.0000000e+00
 3.6381000e+07 5.0463795e-03 0.0000000e+00 0.0000000e+00
 4.0000000e+07 3.4827600e-03 2.6913000e-08 9.3731520e-11
...

#          ZAP          9017
#          LIP             0  product modifier
#          LAW             0  distribution law
#           NP           185  yield energy points
#   Energy[eV]  CrossSec [b]  Multiplicity  CrossSec x M
 4.0122000e+06 0.0000000e+00 0.0000000e+00 0.0000000e+00
 1.9580000e+07 2.1371000e-02 0.0000000e+00 0.0000000e+00
 1.9600000e+07 2.1397000e-02 5.3576000e-03 1.1463657e-04
...

#          ZAP          9018
#          LIP             0  product modifier
#          LAW             0  distribution law
#           NP           230  yield energy points
#   Energy[eV]  CrossSec [b]  Multiplicity  CrossSec x M
```

```
 4.0122000e+06 0.0000000e+00 0.0000000e+00 0.0000000e+00
 1.0431000e+07 8.3487645e-03 0.0000000e+00 0.0000000e+00
 1.0600000e+07 9.7649000e-03 2.8793000e-02 2.8116077e-04
...
```

The plot of MF3/MT5 cross section and the residual multiplicities in MF6/MT5 of ^{19}F data file extracted by DeCE code is shown in Figure 2.

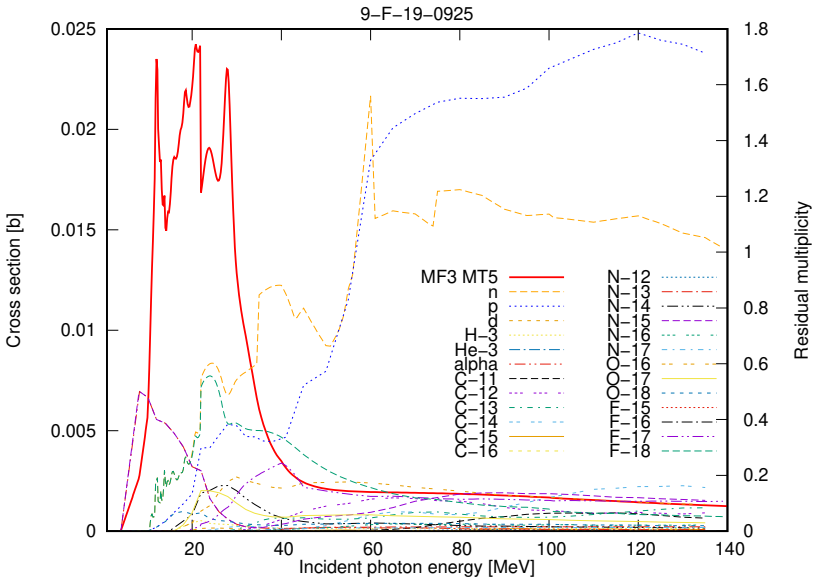

Figure 2: The MF3/MT5 cross section and the residual multiplicities in MF6/MT5 of ^{19}F data file extracted by DeCE code. Only selected residuals are shown in the legend for simplicity.

Although the ZAP = 1 section stands for the neutron emission, we cannot assume a unique (γ, n) cross section from this section unless there are no open channels other than the one-neutron emission. While the production of ZAP = 9018 (^{18}F) is explicitly for the (γ, n) cross section. These cross sections should be identical until $(\gamma, 1\mathrm{n}X)$ channels open up.

For example, the experimental $^{19}\mathrm{F}(\gamma, 1\mathrm{n})$ and $(\gamma, 2\mathrm{n})$ data can be compared directly with the subsection ZAP = 9018 and 9017, while the experimental $^{19}\mathrm{F}(\gamma, x\mathrm{n})$ data should be compared with the sum of subsections ZAP = 9018, 9017, 9016, as well as some other charged particle emission channels that include neutron emission, together with the neutron multiplicities as in Eq. (2).

As another example, the ^{56}Fe data file includes σ_a in MF3/MT5, MF6 gives the production ratios of different reactions. Each subsection for the ZAP numbers of 0 (photon), 1 (neutron), 1001 (proton), 1002 (deuteron), 1003 (triton), 2003 (^{3}He), and 2004 (α-particle) includes the multiplicity of these particles, and all the other ZAP numbers ranging from 14026 to 26056 indicate the residual nucleus production cross sections as shown in Figure 3.

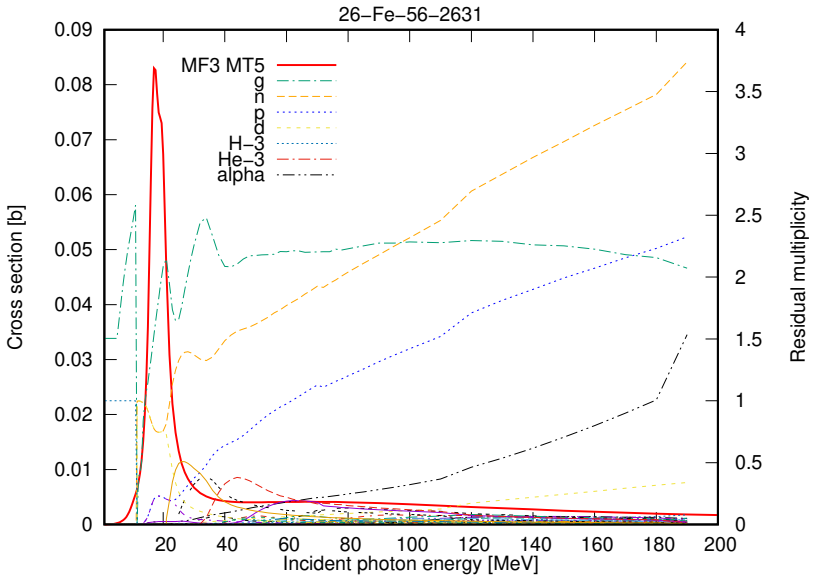

Figure 3: The MF3/MT5 cross section and the residual multiplicities in MF6/MT5 of ^{56}Fe data file extracted by DeCE code. Only selected residuals are shown in the legend for simplicity.

The experimental photo-neutron yield $\sigma_{x\mathrm{n}}$ data are compared directly with the ZAP = 1 subsection, while we cannot know the total photo-neutron cross section $\sigma_{S\mathrm{n}}$ exactly from the evaluated file. $\sigma_{S\mathrm{n}}$ could be the sum of subsections ZAP = 26055 (1n) and 26054 (2n) at low energies. ZAP = 25054 might be a part of it, but it contains both (γ, np) and (γ, d), and the deuteron contribution must be subtracted.

For some actinides such as ^{237}Np, ^{238}Pu, and *etc*., MF6/MT5 contains the very large neutron (ZAP = 1) multiplicity in the high energy range as shown in Figure 4 as an example. This is a known issue and its effect on the cross sections is quite small and is considered to be negligible.

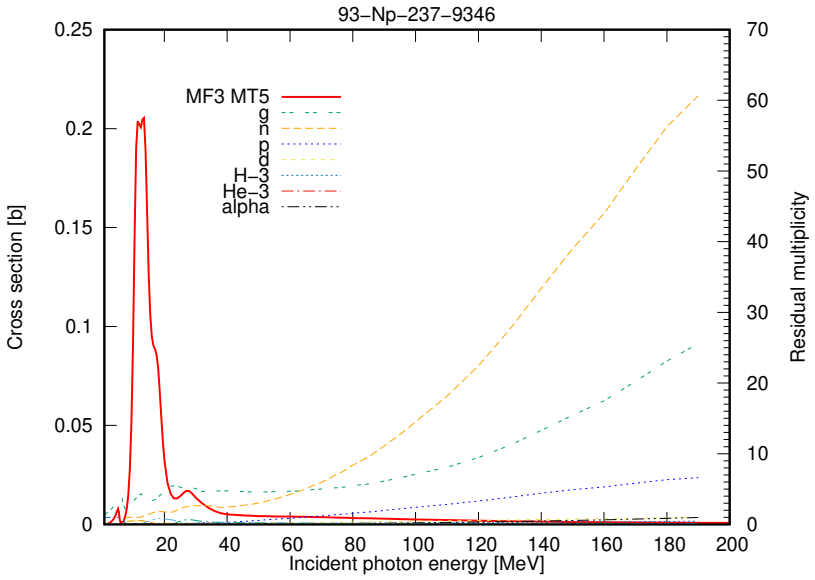

Figure 4: The MF3/MT5 cross section and the residual multiplicities in MF6/MT5 of ^{237}Np data file extracted by DeCE code. Only selected residuals are shown in the legend for simplicity.

The 2-D and 3-D plots of ^{92}Zr data file by VIEWR (NJOY2016) and PREPRO-2019 are attached in Appendix A.2 as an example.

2.5 Format Description: Type 2 by KAERI

Similar to the JAEA files described in Section 2.4, these evaluated files additionally include MF8/MT5 as a dictionary in order to specify the isomeric status of the residuals, which are automatically created by the ENDF-6 format generator TEFAL [15]. The MF – MT combination is as follows.

```
MF   1
 451
MF   3
   3   5
MF   6
   5
MF   8
   5
```

The 2-D and 3-D plots of ^{91}Zr data file by VIEWR (NJOY2016) and PREPRO-2019 are attached in Appendix A.3 as an example.

2.6 Format Description: Type 3 by CNDC for Light Nuclides

The evaluations of light nuclides such as ^{9}Be, ^{12}C, ^{14}N, ^{16}O, and ^{27}Al by CNDC, categorized as the type 3, give σ_a in MF3/MT3 as a non-elastic scattering cross section. All of the explicit cross sections are given in MF3, including MT16 $(\gamma, 2\mathrm{n})$, MT23 $(\gamma, \mathrm{np3}\alpha)$, MT28 $(\gamma, \mathrm{np}$, MT32 (γ, nd), *etc.* The typical MF – MT combination is as follows.

```
MF   1
 451
MF   3
   3  16  23  28  32  34  35  36  44  50 102 108 109 111 112 113 114 115 116 117
 118 600 601 602 603 650 651 700 701 702 703 704 705 706 707 750 751 752 753 754
 755 756 757 758 800 801 802 803 804
MF   6
  16  23  28  32  34  35  36  44  50 108 109 111 112 113 114 115 116 117 118 600
 601 602 603 650 651 700 701 702 703 704 705 706 707 750 751 752 753 754 755 756
 757 758 800 801 802 803 804
```

The experimental $(\gamma, x\mathrm{n})$ should be constructed by summing all the channels that emit neutrons as follows.

$$\begin{aligned}\sigma_{x\mathrm{n}} &= 2(\gamma, 2\mathrm{n}) + (\gamma, \mathrm{n3}\alpha) + (\gamma, \mathrm{np}) + (\gamma, \mathrm{nd}) + (\gamma, \mathrm{n}^3\mathrm{He}) + (\gamma, \mathrm{nd2}\alpha) \\ &+ (\gamma, \mathrm{nt2}\alpha) + (\gamma, \mathrm{n2p}) + (\gamma, \mathrm{n}_0) + (\gamma, \mathrm{n}_1) + \ldots \end{aligned} \quad (4)$$

The 2-D and 3-D plots of ^{12}C data file by VIEWR (NJOY2016) and PREPRO-2019 are attached in Appendix A.4 as an example.

2.7 Format Description: Type 4 by CNDC for Medium-Mass Nuclides

In the case of evaluations for some medium-mass nuclei such as $^{50-54}$Cr, $^{180-160}$W and ^{90}Zr by CNDC, σ_a is stored in MF3/MT5, and MF6/MT5 contains only light residual (particles) multiplicities. In addition to that, MT201–206 in MT3 are also given (note that MT207 is missing) where these are redundant since they can be calculated by $\sigma_a\times$ residual multiplicity in MF6/MT5. The typical MF – MT combination is as follows.

```
MF    1
 451
MF    3
    5 201 203 204 205 206
MF    6
    5
```

As an example, the comparison of MF3/MT201–206 cross sections and $\sigma_a \times$ residual multiplicity in MF6 in ^{182}W data file is shown in Figure 5.

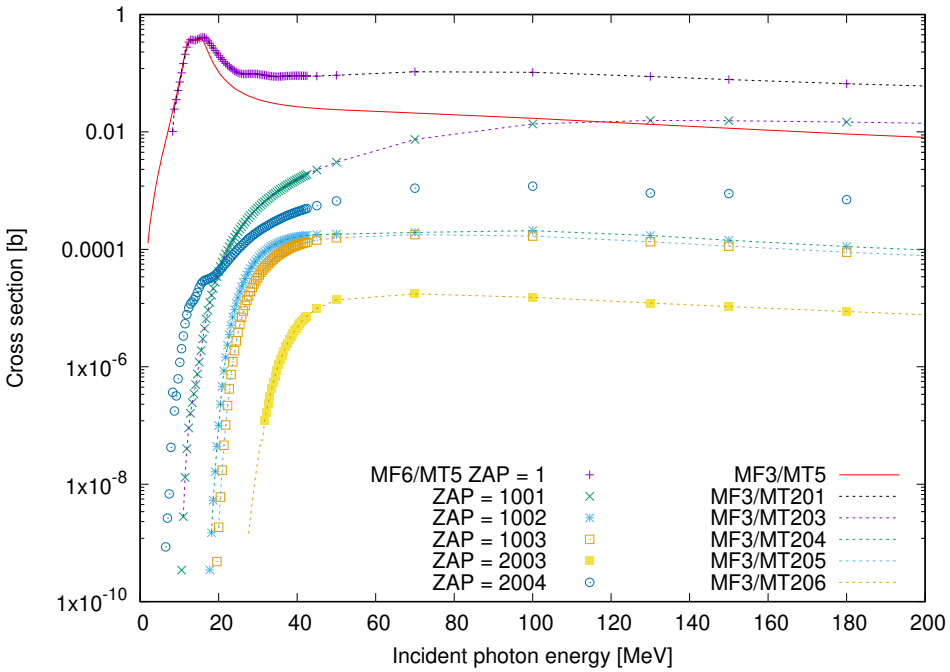

Figure 5: ^{182}W photo-absorption cross section σ_a given in MF3/MT5 (solid curve), and particle production cross sections in MF3/MT201–206 shown by the dotted curves. The calculated production cross sections, $\sigma_a \times$ residual multiplicity in MF6, are shown by the symbols.

The 2-D and 3-D plots of ^{182}W data file by VIEWR (NJOY2016) and PREPRO-2019 are attached in Appendix A.5 as an example.

2.8 Format Description: Type 5 by IFIN-HH/UB

The files evaluated based on EMPIRE code calculations are; the conversion into the ENDF-6 format is done with the EMPEND code using "exclusive data" representation for the first three emitted neutrons and protons (see below for details) and all possible combinations with deuteron, He-3 and tritium emissions. An example of MF–MT combinations for a Ta-181 target data file follows. An individual reaction cross sections can be found in MF3 in the same manner as for the neutron-induced data files, *e.g.*, the MF3/MT16 corresponds to $(\gamma, 2\mathrm{n})$, or the MF3/MT600 corresponds to the reaction (γ, p) in which the emitted proton leaves the residual nucleus in its ground state, *etc*. This data representation also contains the cross section for discrete level information for emitted neutrons, protons and alphas in MF3, MT51 series, MT600 series and MT800 series, respectively, as well as the continuum information in MF3, MT91, MT649, and MT849. Corresponding angular distributions both for the discrete levels and the continuum are stored in MF6 with the corresponding MT.

Additionally, higher (above three emitted neutrons or protons) neutron and/or proton emitted

combinations are stored in the "inclusive" representation in MF3/MT5 sorted by the corresponding residual nucleus.

```
MF   1
 451
MF   3
   1   4   5  11  16  17  22  28  32  33  34  41  42  44  50  51  52  53  54  55
  56  57  58  59  60  61  62  63  64  65  66  67  68  69  70  71  72  73  74  75
  76  77  78  79  80  81  82  83  84  85  86  87  88  89  91 102 104 105 106 111
 112 115 116 600 601 602 603 604 605 606 607 608 609 610 611 612 613 614 615 616
 617 618 619 620 621 622 623 624 625 626 627 628 629 630 631 632 633 634 635 636
 637 638 639 649 800 801 802 803 804 805 806 807 808 809 810 811 812 813 814 815
 816 817 818 819 820 821 822 823 824 825 826 827 828 829 830 831 832 833 834 835
 836 837 838 839 849
MF   6
   5  11  16  17  22  28  32  33  34  41  42  44  50  51  52  53  54  55  56  57
  58  59  60  61  62  63  64  65  66  67  68  69  70  71  72  73  74  75  76  77
  78  79  80  81  82  83  84  85  86  87  88  89  91 102 104 105 106 111 112 115
 116 600 601 602 603 604 605 606 607 608 609 610 611 612 613 614 615 616 617 618
 619 620 621 622 623 624 625 626 627 628 629 630 631 632 633 634 635 636 637 638
 639 649 800 801 802 803 804 805 806 807 808 809 810 811 812 813 814 815 816 817
 818 819 820 821 822 823 824 825 826 827 828 829 830 831 832 833 834 835 836 837
 838 839 849
MF   8
   4   5  22  23  24  25  29  30  35  36  37  45 103 107 108 109 112 114
MF   10
   4   5  22  23  24  25  29  30  35  36  37  45 103 107 108 109 112 114
MF   12
  51  52  53  54  55  56  57  58  59  60  61  62  63  64  65  66  67  68  69  70
  71  72  73  74  75  76  77  78  79  80  81  82  83  84  85  86  87  88  89 601
 602 603 604 605 606 607 608 609 610 611 612 613 614 615 616 617 618 619 620 621
 622 623 624 625 626 627 628 629 630 631 632 633 634 635 636 637 638 639 801 802
 803 804 805 806 807 808 809 810 811 812 813 814 815 816 817 818 819 820 821 822
 823 824 825 826 827 828 829 830 831 832 833 834 835 836 837 838 839
MF   14
  51  52  53  54  55  56  57  58  59  60  61  62  63  64  65  66  67  68  69  70
  71  72  73  74  75  76  77  78  79  80  81  82  83  84  85  86  87  88  89 601
 602 603 604 605 606 607 608 609 610 611 612 613 614 615 616 617 618 619 620 621
 622 623 624 625 626 627 628 629 630 631 632 633 634 635 636 637 638 639 801 802
 803 804 805 806 807 808 809 810 811 812 813 814 815 816 817 818 819 820 821 822
 823 824 825 826 827 828 829 830 831 832 833 834 835 836 837 838 839
```

Both the photo-neutron yield $\sigma_{x\mathrm{n}}$ and total photo-neutron cross section $\sigma_{S\mathrm{n}}$ should be reconstructed by adding all corresponding partial cross sections that contain emitted neutrons. If we limit ourselves to exclusive reactions at low energies, and approximate equations that can be used, follow:

$$\sigma_{x\mathrm{n}} = (4) + 2\times(16) + 3\times(17) + (22) + (28) + (33) + (34) + 2\times(41) + 3\times(42) + (44) \quad (5)$$

and

$$\sigma_{S\mathrm{n}} = (4) + (16) + (17) + (22) + (28) + (33) + (34) + (41) + (42) + (44) \quad (6)$$

where the number in parenthesis is MT.

The 2-D and 3-D plots of ^{181}Ta data file with above ENDF-6 data representation by VIEWR (NJOY2016) and PREPRO-2019 are attached in Appendix A.6 as an example.

3 Format Verification Procedures

The main objective here is to verify that all the evaluated files are sufficient, readable, and usable to some extent. The ENDF-6 data formatter/processing codes, DeCE [9], NJOY2016 [10], PREPRO-2019 [11], and FRENDY [8] were deployed to verify the format correctness, internal physical consistency, cross section, angular and emitted spectra, and data processing. Figure 6 shows the procedures employed, where the steps involved are to check, edit the file format, fix issues if any, and finally generate transport and activation-transmutation-source terms application libraries.

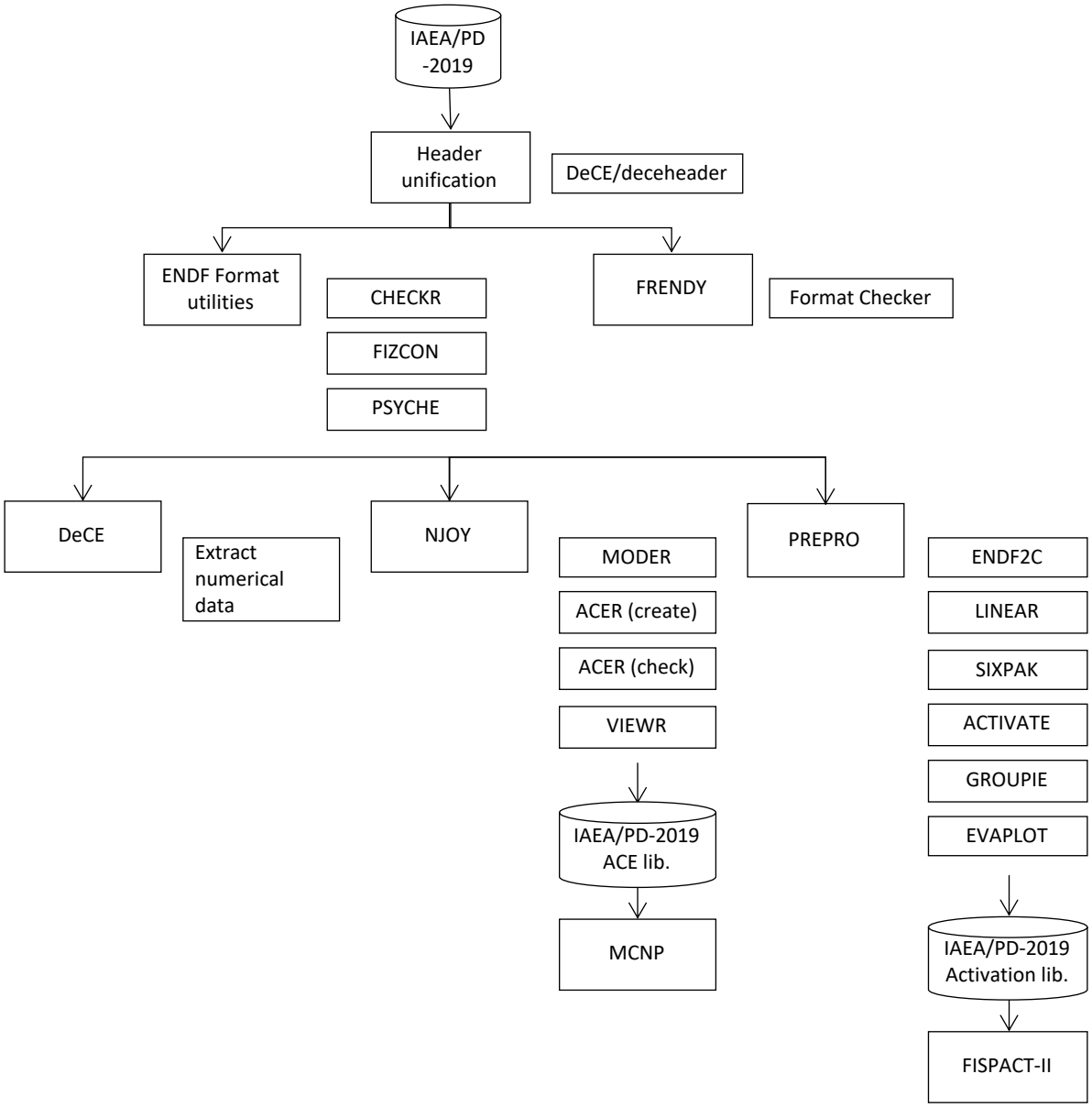

Figure 6: Adopted sequence of the data validation and verification procedure for the IAEA/PD-2019.

3.1 Header Modifications

The IAEA-NDS assembled the ENDF format files evaluated by the participating institutes, and compiled all the collected files into the unified IAEA library as follows;

- Check the MAT number, and fix the number if it is not in the regular definition,
- Unify the file names to follow the standard naming convention, `g_Z-element-A_MAT.endf`, where Z is the atomic and A is the mass numbers,
- Remove all the non-ASCII characters, such as the tab code (\t),
- Convert the line break of CR+LF (Windows) to LF (Unix) by the dos2unix format converter, and
- Delete the line numbers in column by the DeCE code [9].

In order to unify the data format, we applied DeCE [9] to all the files to modify the MF = 1 (File 1: General information) MT = 451 (Type 451: Descriptive Data and Directory) section. We updated the following parameters with DeCE.

Parameters	Values
LRP	-1
AWI	0
NSUB	0
NLIB	38
LREL	0
NVER	2019

where NSUB = 0 denotes the Photonuclear data sub library, NLIB = 38 indicates the IAEA Photonuclear data library, and LREL and NVER are the release and version numbers of the library.

The HSUB in MF1/MT451 of all the files were also updated by the deceheader code, which is one of the tools included in the DeCE package [9].

Parameters	Values
REF	NDS 163 109 (2020)
DDATE	DIST-JUN20
LIBNAME	IAEA/PD-2019
SUBLIB	PHOTO-NUCLEAR DATA
FORMAT	ENDF-6 FORMAT

Applying DeCE and deceheader, the header part of the IAEA/PD-2019 files becomes, e.g.,

```
 JENDL/PD-2016.1  Te-123                                                1 0  0
 5.212300+4 1.218485+2         -1          0         38          15234 1451
 0.000000+0 0.000000+0          0          0          0          65234 1451
 0.000000+0 2.000000+8          0          0          0       20195234 1451
 0.000000+0 0.000000+0          0          0         53          35234 1451
 52-Te-123 JAEA       EVAL-APR19 N.Iwamoto                       5234 1451
NDS 163 109 (2020)    DIST-JUN20                                 5234 1451
----IAEA/PD-2019      MATERIAL 5234                              5234 1451
-----PHOTO-NUCLEAR DATA                                          5234 1451
------ENDF-6 FORMAT                                             5234 1451
```

3.2 Verification of Formal Correctness and Internal Consistency

3.2.1 ENDF-6 Format Check by ENDF Utilities

We utilized the well-known ENDF utilities, CHECKR (Version 8.24), FIZCON, and PSYCHE, to verify the format correctness and internal physical consistency. These utility codes are available in the EMPIRE [16] package.

- CHECKR checks the format correctness,
- FIZCON tests the internal consistency of given data, and
- PSYCHE performs more strict inspections of physics content.

Almost all errors detected by CHECKR were removed by fixing these data files by the evaluator or IAEA-NDS in case if it's straightforward. For the files given in the data-form type 5, CHECKR generates an error message saying existence of MF3/MT1, as follows;

```
PROGRAM CHECKR VERSION 8.24                                  Run on 07-Jul-2020

Input File Specification-----------------------g_67-Ho-165_6725.dat
Check the Entire File

FILE IS UNSEQUENCED. NO SEQUENCE TESTS WILL BE DONE

 Check material  67-Ho-165  MAT 6725
  ERROR(S) FOUND IN MAT=6725, MF= 3, MT=  1
     MT=   1 INVALID                                  RECORD NUMBER     716
     Encountered     1 errors,       0 warnings
 Done CHECKR
```

Since MF3/MT1 is the total cross section of particle-induced reaction, this is not defined in the photonuclear data case. This message can be resolved by removing the section or sorted during the processing that will always sum all linearised-unionised partials.

Although FIZCON claims some errors regarding the physical internal inconsistency of MT5 between MF3 and MF6 (followings are examples), no actions were taken. For the interpretation of the messages from these checking codes, the original documentation should be consulted.

```
PROGRAM FIZCON VERSION 8.18                                  Run on 07-Jul-2020

Input File Specification-----------------------g_67-Ho-165_6725.dat
Check the Entire File
Sum Up Tests will be Omitted
Deviant Point Check will be Omitted
Consecutive Equal Value Check will be Omitted

TAPE BEING PROCESSED IS NUMBERED    1
   LABEL IS   EMPEND Processing file : ho165-g.out


 Check material  67-Ho-165  MAT 6725


  ERROR(S) FOUND IN MAT=6725, MF= 6, MT=  5
     SECTION DOES NOT SPAN THE SAME ENERGY RANGE AS FILE   3, MT=   5
```

```
  ERROR(S) FOUND IN MAT=6725, MF= 6, MT=800
     ENERGY RANGE FOR DISTRIBUTIONS IN LIST RECORDS
         INCONSISTENT WITH TAB1 RECORD                SEQUENCE NUMBER     1
     SECTION DOES NOT SPAN THE SAME ENERGY RANGE AS FILE   3, MT= 800

  ERROR(S) FOUND IN MAT=6725, MF= 6, MT=849
     SECTION DOES NOT SPAN THE SAME ENERGY RANGE AS FILE   3, MT= 849

     Encountered    22 errors,       0 warnings
 Done FIZCON

—

PROGRAM FIZCON VERSION 8.18                                Run on 07-Jul-2020

Input File Specification-----------------------g_39-Y-89_3925.dat
Check the Entire File
Sum Up Tests will be Omitted
Deviant Point Check will be Omitted
Consecutive Equal Value Check will be Omitted

TAPE BEING PROCESSED IS NUMBERED    1
   LABEL IS   EMPEND Processing file : y89-g.out------------------------------

  ERROR(S) - MISSING SECTIONS IN MAT 3925 MF  6
     PRESENCE OF FILE 3, MT=  74 REQUIRES AN EQUIVALENT SECTION IN FILE 6
     PRESENCE OF FILE 3, MT=  75 REQUIRES AN EQUIVALENT SECTION IN FILE 6
     PRESENCE OF FILE 3, MT=  76 REQUIRES AN EQUIVALENT SECTION IN FILE 6
     PRESENCE OF FILE 3, MT=  77 REQUIRES AN EQUIVALENT SECTION IN FILE 6
     PRESENCE OF FILE 3, MT=  78 REQUIRES AN EQUIVALENT SECTION IN FILE 6
     PRESENCE OF FILE 3, MT=  79 REQUIRES AN EQUIVALENT SECTION IN FILE 6
     PRESENCE OF FILE 3, MT=  80 REQUIRES AN EQUIVALENT SECTION IN FILE 6
     PRESENCE OF FILE 3, MT=  81 REQUIRES AN EQUIVALENT SECTION IN FILE 6
     PRESENCE OF FILE 3, MT=  82 REQUIRES AN EQUIVALENT SECTION IN FILE 6
     PRESENCE OF FILE 3, MT=  83 REQUIRES AN EQUIVALENT SECTION IN FILE 6
     PRESENCE OF FILE 3, MT=  84 REQUIRES AN EQUIVALENT SECTION IN FILE 6

 Check material  39-Y - 89  MAT 3925
  ERROR(S) FOUND IN MAT=3925, MF=12, MT= 73
     THE ENERGY OF HIGHEST LEVEL MUST BE 0.0000E+00
     Encountered    11 errors,       0 warnings
 Done FIZCON
```

3.2.2 ENDF-6 Format Check by FRENDY

The nuclear data processing system FRom Evaluated Nuclear Data librarY to any application (FRENDY(1.02.003)) [8] has capability of checking ENDF-6 data scheme and format, which is internally called ENDF6Parser. In order to invoke ENDF6Parser, which will be a stand-alone module in the next update of FRENDY, we execute the RECONR module using the following input.

```
reconr
 20  21
'Check Zr90 for IAEA-PD'
 4025
 1.00E-01  0.00
 0
stop
```

Most of the IAEA/PD-2019 files went through the ENDF6Parser test of FRENDY except for ^{89}Y in which FRENDY reported FATAL ERROR.

```
************************
*                      *
*  !!! FATAL ERROR !!!  *
*                      *
************************

  <Class name>
    ReconstructXSMerger

  <Function name>
    calc_total_inelastic_scat_xs()

  <Error Message>
    The energy grid of inelastic scatter xs is not unit.
```

3.2.3 ENDF-6 Content Check by DeCE

It should be distinguished between the ENDF-6 format including data structure and the data in the ENDF-6 format. First, we employed DeCE [9] to confirm the data structure described in Section 2.1. DeCE was also used to extract the residual product yield, the total photo-absorption cross section in MF3/MT5, and to multiply these two sections to obtain the production cross section. To extract point wise cross section from MF3/MT5, DeCE takes command line options of `-t` for the MT and `-f` for the MF numbers as follows.

```
% dece -f3 -t5 g_52-Te-128_5249.dat
```

Similarly, to extract the multiplicity of residual products from MF6/MT5 is as follows.

```
% dece -f6 -t5 g_52-Te-128_5249.dat
```

The σ_a in MF3/MT5 and residual nucleus multiplicities in MF6/MT5 were checked and corrected if it is crucial after consultation with the evaluator.

DeCE's option -s (scan) shows the MF – MT combinations in the particular file given in the command as follows.

```
% dece -s g_52-Te-128_5249.dat
```

This option was used to check MF and MT combinations in each data file and some of outputs are shown in Section 2.3 – 2.8.

3.3 Processing for Applications

The data processing codes, such as NJOY2016 [10], PREPRO-2019 [11], and FRENDY [8], convert evaluated nuclear data files in the ENDF-6 format into an application-code-specific data format. The application codes include Monte Carlo particle transport simulation, or inventory-source terms, and facilitate the overall validation of the library for different applications. Unfortunately, FRENDY has not yet implemented the photonuclear data processing, therefore we employed NJOY2016 and PREPRO-2019.

3.3.1 PREPRO-2019

We utilized the following codes in PREPRO-2019 [11]:

1. ENDF2C to convert ENDF-6 data to a compatible form to be read uniquely by C, C++ and FORTRAN code alike,
2. LINEAR to linearize and unionize cross section as tables with data point/grid using a single interpolation laws between tabulated points,
3. SIXPAK to extract the activation-transmutation yields,
4. ACTIVATE to distributes to isomeric states when necessary,
5. GROUPIE to transform from point wise to group wise forms, and
6. EVALHARD1 to produce hard-copy plot of the application forms.

A single usage of LEGEND was done for changing MF4/MT2 Legendre coefficients that produces negative polynomial to LAW = 2 LANG = 12 for MF3/MT3, MF3/MT50 and MF6/MT50 for ^{2}H.

3.3.2 NJOY2016

The NJOY nuclear data processing system [10] can produce an ACE type u (continuous photonuclear) library, which can then be used by Monte Carlo radiation transport codes, such as MCNP [17] or SERPENT [18]. However, it transpired during checking that some of the IAEA/PD-2019 data representations could not be properly processed by NJOY2016 [19]. This occurs when in the evaluated file LAW = 1, LANG = 1 but NA != 0 sequence is used: outgoing angular parameters are given in conjunction with Legendre coefficients. This is legal in ENDF-6 format but is not yet handled for photonuclear data processing.

Therefore, a patched version of NJOY2016[4], implementing an approximate work-around, was used to produce the ACE library for the IAEA/PD-2019. In this patched version of July 2020, the so-called ACE LAW = 61 format, which is the continuum energy-angle distribution form (ACE LAW = 61 format, named for ENDF MF = 6, LAW = 1), in the IAEA/PD-2019 is set to isotropic distributions. This approximation occurs in some, though not all, channels of the 153 evaluations of the IAEA/PD-2019. As soon as the issue is resolved for the tandem NJOY-MCNP an updated library will be produced.

Following is an example of NJOY input to invoke the MODER, ACER, and VIEWR modules. The second ACER and VIEWR assist a quality assurance check process and visualize the content of an ACE file in 2-D or 3-D plots.

[4]NJOY2016 feature/pn-iaea branch: https://github.com/njoy/NJOY2016/tree/feature/pn-iaea/

```
moder
20 21/
acer
20 21 0 31 32/
5 1 1/
'Ace Zr90 IAEA-PD'/
4025/
acer
0 31 33 34 36/
7 1 1 -1/
'Ace Zr90 IAEA-PD2019'/
viewr
33 36/
stop
```

Note that ACE files released from IAEA-NDS website will be replaced as soon as NJOY2016 is fixed to process the photonuclear data properly.

4 Summary

A new IAEA Evaluated Photonuclear Library (IAEA/PD-2019) has been assembled and released [6] as a result of the IAEA Coordinated Research Project, which benefits from significant progress made in the theoretical and experimental research in the last two decades. The new library includes 219 evaluations including 199 new evaluations, while 20 evaluations were retained from the previous library released in 1999 (IAEA/PD-1999) [1]. Significant improvements have been made compared to its predecessor, in terms of physical contents, target landscape and energy range.

Since the different ENDF-6 data format representations have been used by different evaluators in the IAEA/PD-2019, we described the ENDF-6 data format representations. A consistent description was given in the header part of each file, and verification of format correctness and internal physical consistency check of ENDF-6 data files were carried out by employing ENDF Utility codes, FRENDY, and DeCE. The ACE transport library and FISPACT-II libraries were created using NJOY2016 (a special patched branch for the IAEA/PD-2019) and PREPRO-2019 nuclear data processing systems.

Pushing for better representation of nuclear reaction physics in a necessary rigid ENDF-6 data format sometimes involves an undesirable information loss. As we reported, the data representation in the IAEA/PD-2019 is not unified, although it is in fact a common situation to many general purpose nuclear data libraries. Such differences may lead to some ambiguities in scrutinizing and validating each data file, and in processing the data for application libraries; a common robust unified data representation leading to standardized processing is certainly desirable.

Acknowledgements

The authors thank Andrej Trkov for his support and valuable discussion on the ENDF-6 format of photonuclear data library. The authors also thank Kenichi Tada for his support of using FRENDY. The IAEA-NDS acknowledges the internship program "The Nuclear Regulation Human Resource Development Program (ANSET: Advanced Nuclear 3S Education and Training)" entrusted to Tokyo Institute of Technology by the Nuclear Regulation Agency of Japan, for supporting this work. The IAEA-NDS thanks all institutions and scientists who produced the IAEA Photonuclear Data Library 2019 and assisted data verification and processing, and preparing this report.

Reference

[1] International Atomic Energy Agency. Handbook on photonuclear data for applications cross-sections and spectra. IAEA-TECDOC-1178, IAEA, Vienna, 2000.

[2] A. J. Koning and R. Capote. Report of the IAEA Nuclear Data Section to the International Nuclear Data Committee for the period January 2014-December 2015. IAEA Report INDC(NDS)-0725, IAEA, Vienna, 2016.

[3] S. Goriely and P. Dimitriou. Updating the photonuclear data library and generating a reference database for photon strength functions. IAEA Report INDC(NDS)-0712, IAEA, Vienna, 2016.

[4] S. Goriely, M. Wiedeking, and P. Dimitriou. Updating the photonuclear data library and generating a reference database for photon strength functions. IAEA Report INDC(NDS)-0745, IAEA, Vienna, 2018.

[5] M. Wiedekin, D. Filipescu, and P. Dimitriou. Updating photonuclear data library and generating a reference database for photon strength functions. IAEA Report INDC(NDS)-0777, IAEA, Vienna, 2019.

[6] T. Kawano, Y. S. Cho, P. Dimitriou, D. Filipescu, N. Iwamoto, V. Plujko, X. Tao, H. Utsunomiya, V. Varlamov, R. Xu, R. Capote, I. Gheorghe, O. Gorbachenko, Y.L. Jin, T. Renstrom, M. Sin, K. Stopani, Y. Tian, G. M. Tveten, J.M. Wang, T. Belgya, R. Firestone, S. Goriely, J. Kopecky, M. Krticka, R. Schwengner, S. Siem, and M. Wiedeking. IAEA photonuclear data library 2019. *Nucl. Data Sheets*, 163:109, 2020.

[7] A. Trkov, M. Herman, and D. A. Brown. ENDF-6 Formats Manual, Data Formats and Procedures for the Evaluated Nuclear Data Files, ENDF/B-VI, ENDF/B-VII and ENDF/B-VIII. ENDF-102, BNL-203218-2018-INRE, Brookhaven National Laboratory, 2018.

[8] K. Tada, Y. Nagaya, S. Kunieda, K. Suyama, and T. Fukahori. Development and verification of a new nuclear data processing system FRENDY. *J. Nucl. Sci. Technol.*, 54(7):806–817, 2017.

[9] T. Kawano. DeCE: the ENDF-6 data interface and nuclear data evaluation assist code. *J. Nucl. Sci. Technol.*, 56(11):1029–1035, 2019.

[10] R. E. MacFarlane and A. C. Kahler. Methods for processing ENDF/B-VII with NJOY. *Nucl. Data Sheets*, 111(12):2739 – 2890, 2010.

[11] D. E. Cullen. PREPRO 2019 ENDF/B pre-processing codes (ENDF/B-VIII verified). IAEA Report IAEA-NDS-0229, IAEA, Vienna, 2019.

[12] A. Trkov. Guidelines for nuclear data verification and validation. IAEA Report INDC(SEC)-0107, IAEA, Vienna, 2005.

[13] N. Iwamoto, K. Kosako, and T. Murata. Photonuclear data file. *JAEA-Conf*, 2016-004:53–58, 2016.

[14] N. Iwamoto. JENDL photonuclear data file 2016 revision 1. *J. Nucl. Sci. Technol.*, to be submitted, 2020.

[15] A. Koning. TEFAL-1.26: Making nuclear data libraries using TALYS. *User manual, Nucl. Res. Consult. Group (NRG), unpublished*, 01 2010.

[16] M. Herman, R. Capote, B.V. Carlson, P. Obložinský, M. Sin, A. Trkov, H. Wienke, and V. Zerkin. EMPIRE: Nuclear reaction model code system for data evaluation. *Nucl. Data Sheets*, 108:2655, 2007.

[17] X-5 Monte Carlo Team. MCNP: – A General Monte Carlo N-Particle Transport Code, Version 5. LA-UR-03-1987, Los Alamos National Laboratory, 2003.

[18] J. Leppanen, M. Pusa, T. Viitanen, V. Valtavirta, and T. Kaltiaisenaho. The Serpent Monte Carlo code: Status, development and applications in 2013. *Ann. Nucl. Energy*, 82:142 – 150, 2015.

[19] W. Haeck. New IAEA photonuclear data library does not process (issue #156 on NJOY2016 Github), 04 2020. https://github.com/njoy/NJOY2016/issues/156.

Appendix A Examples of Processing

A.1 Example of ^{2}H File Processing (File Type 0: ^{2}H by NFD)

A.1.1 Transport Library

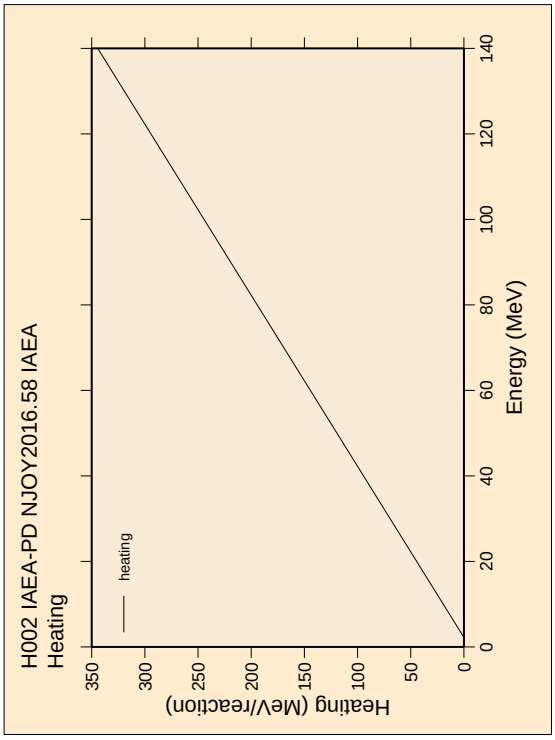

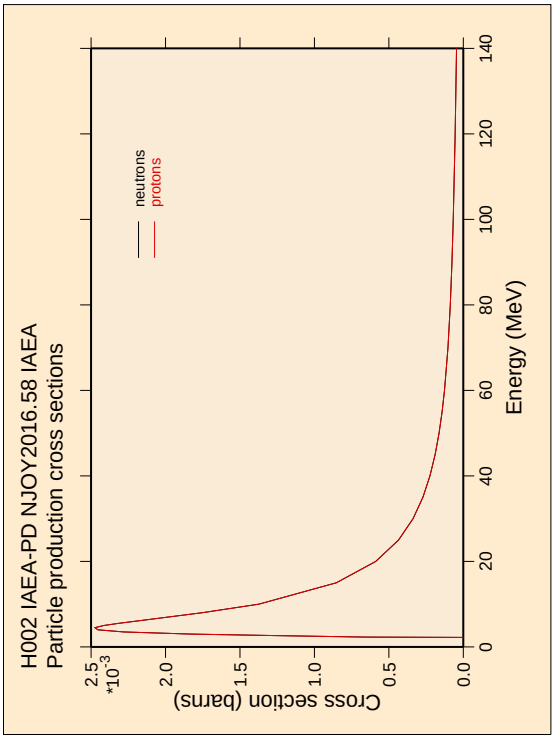

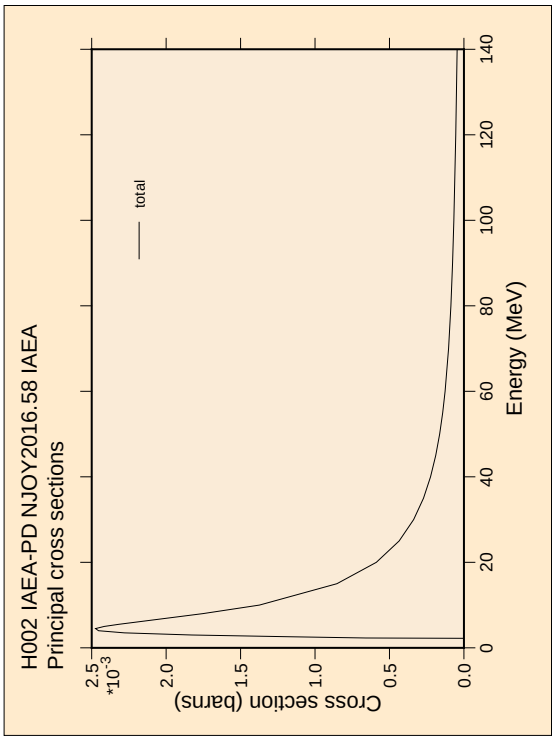

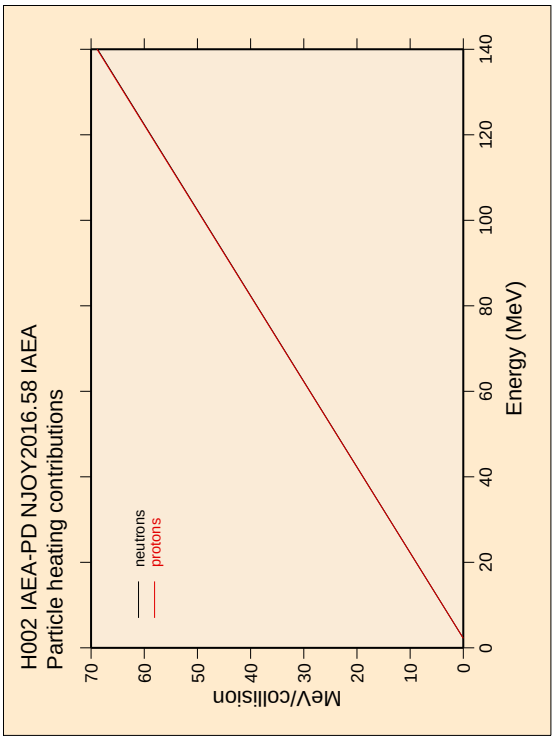

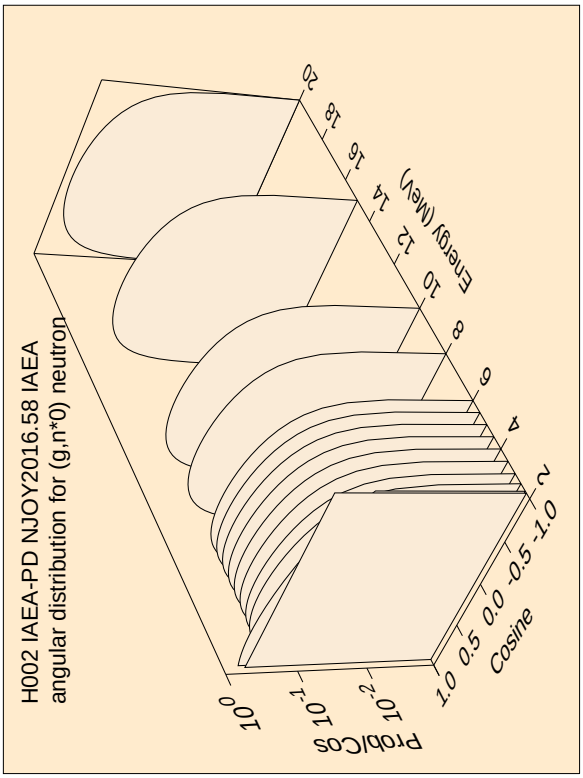
H002 IAEA-PD NJOY2016.58 IAEA
angular distribution for (g,n*0) neutron
Prob|Cos
Energy (MeV)
Cosine

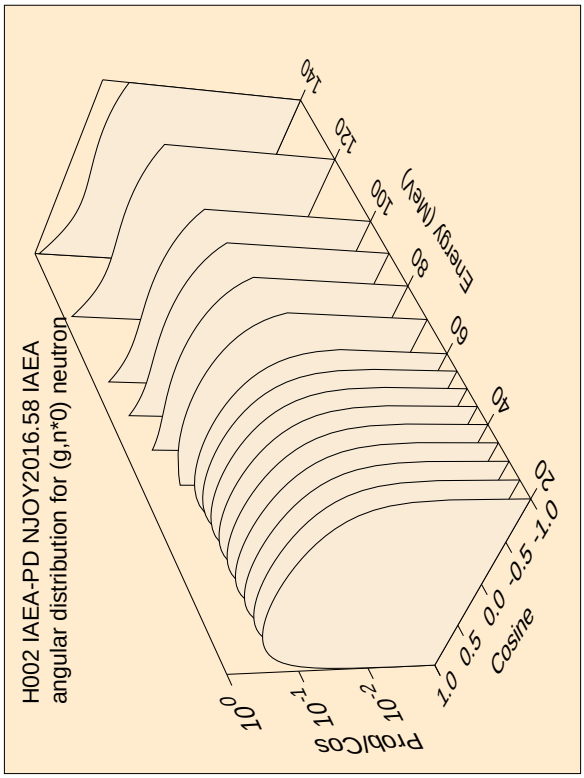
H002 IAEA-PD NJOY2016.58 IAEA
angular distribution for (g,n*0) neutron
Prob|Cos
Energy (MeV)
Cosine

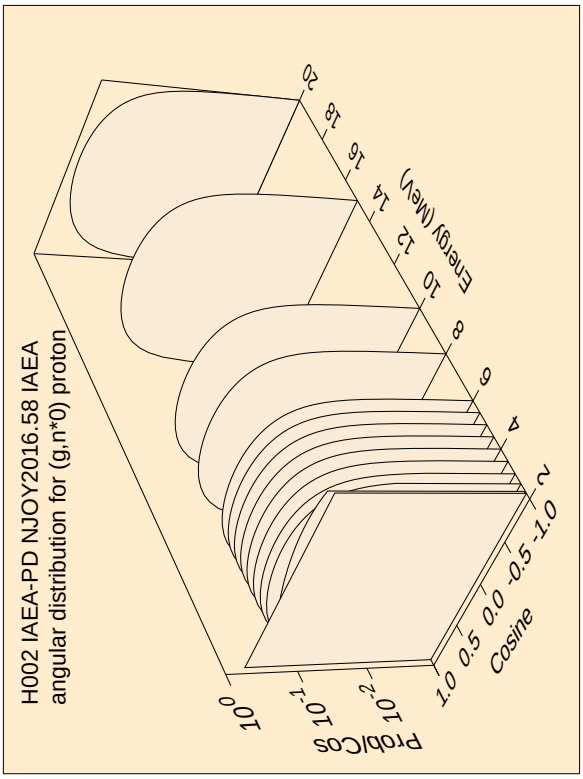
H002 IAEA-PD NJOY2016.58 IAEA
angular distribution for (g,n*0) proton
Prob|Cos
Energy (MeV)
Cosine

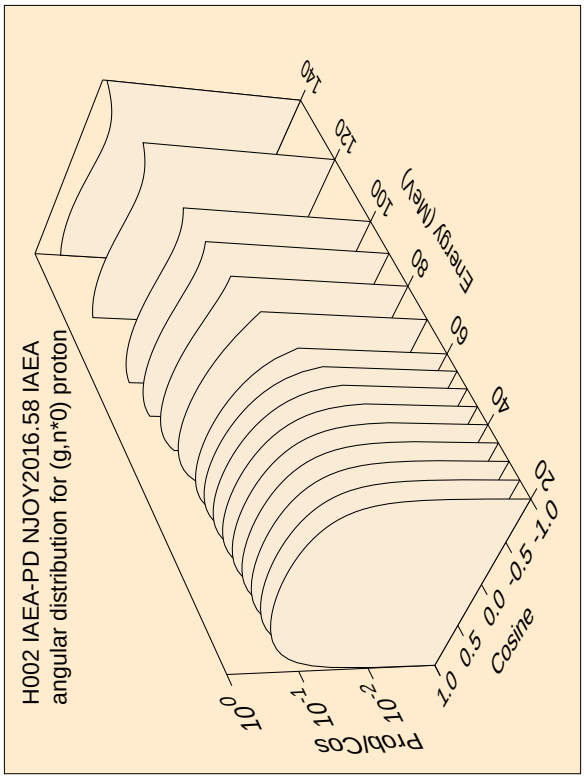
H002 IAEA-PD NJOY2016.58 IAEA
angular distribution for (g,n*0) proton
Prob|Cos
Energy (MeV)
Cosine

A.1.2 Activation Library

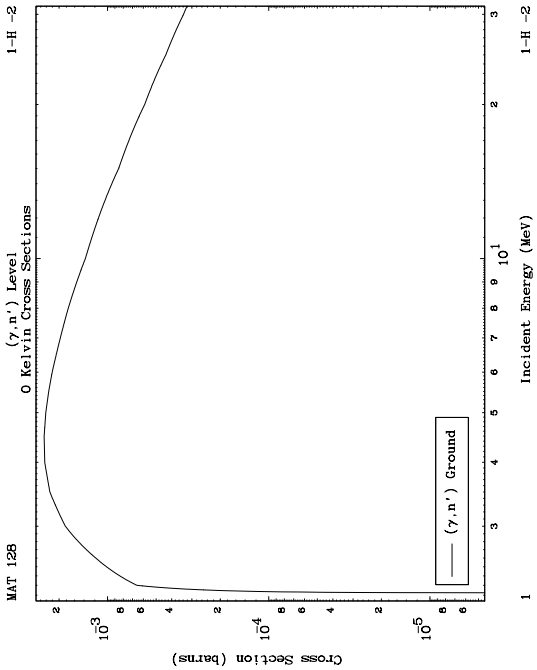

A.2 Example of ^{92}Zr File Processing (File Type 1: JAEA and KAERI)

A.2.1 Transport Library

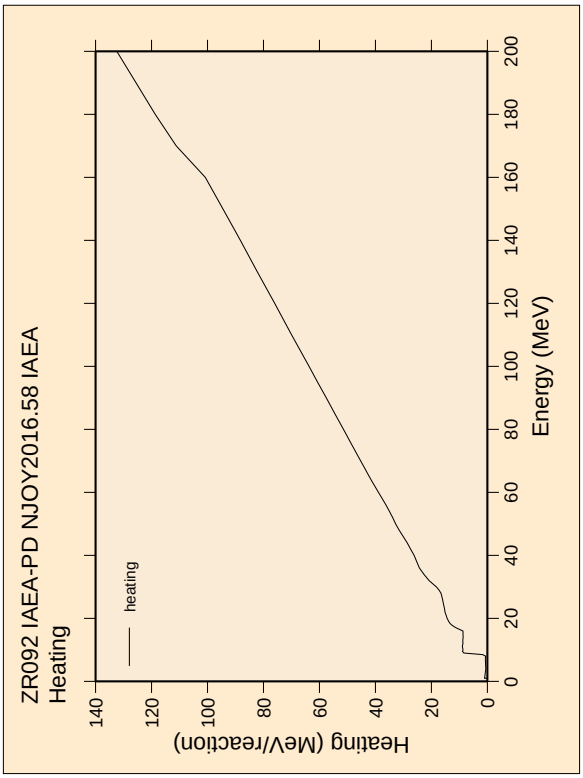

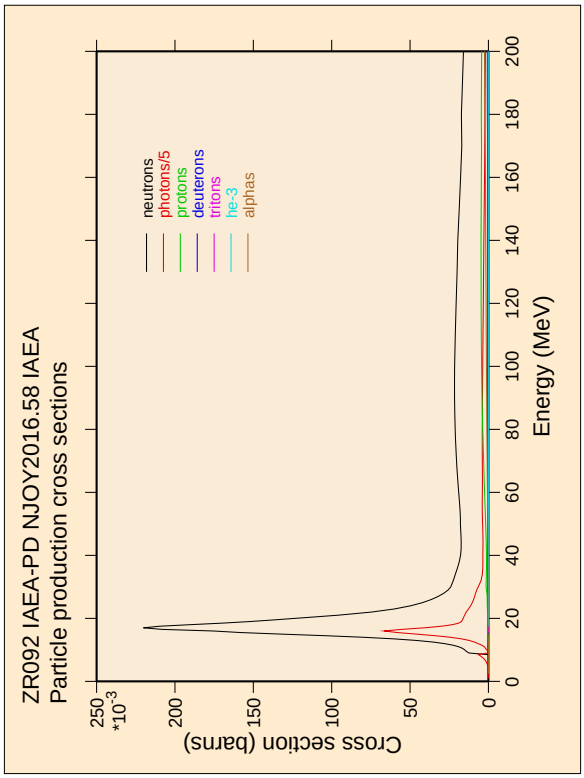

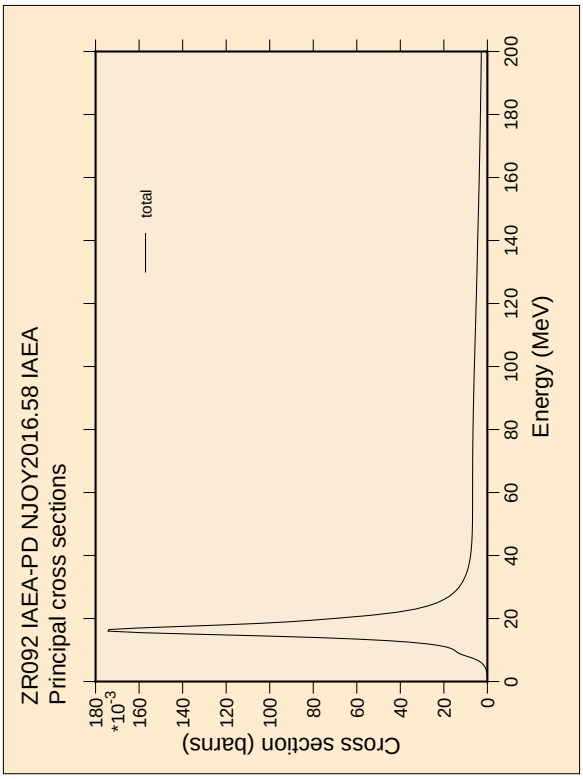

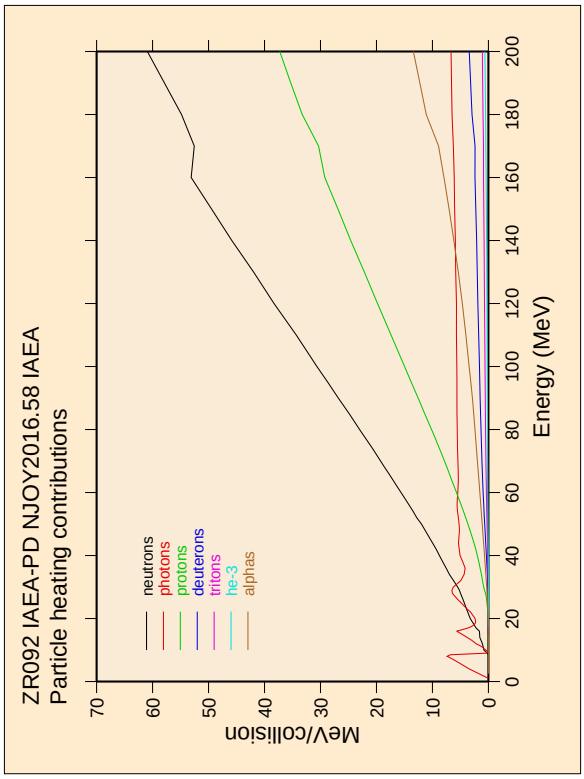

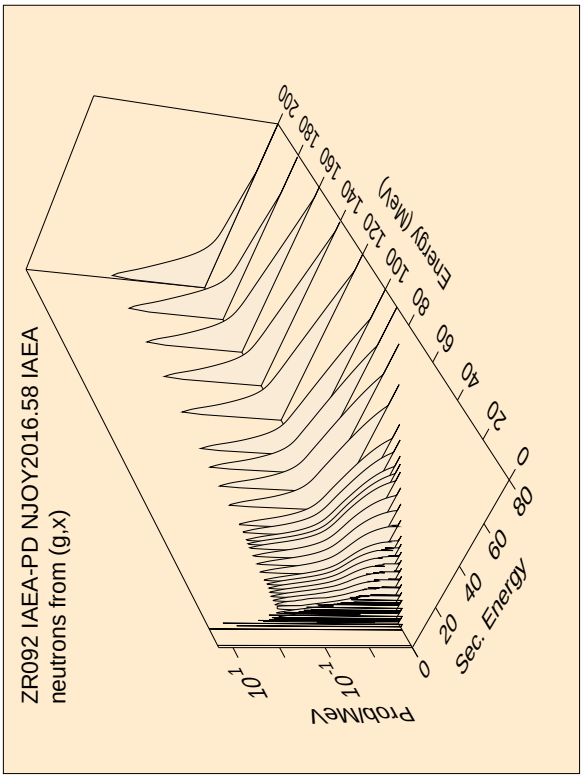
ZR092 IAEA-PD NJOY2016.58 IAEA
neutrons from (g,x)
Prob/MeV
Energy (MeV)
Sec. Energy

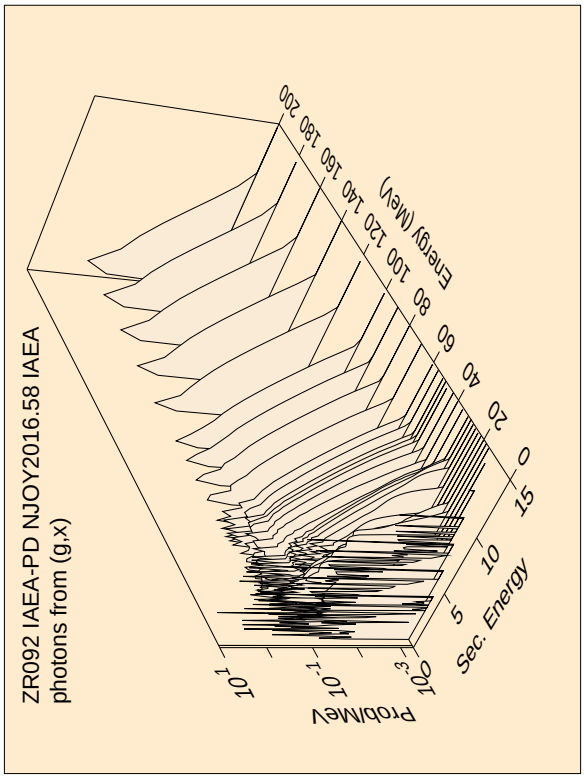
ZR092 IAEA-PD NJOY2016.58 IAEA
photons from (g,x)
Prob/MeV
Energy (MeV)
Sec. Energy

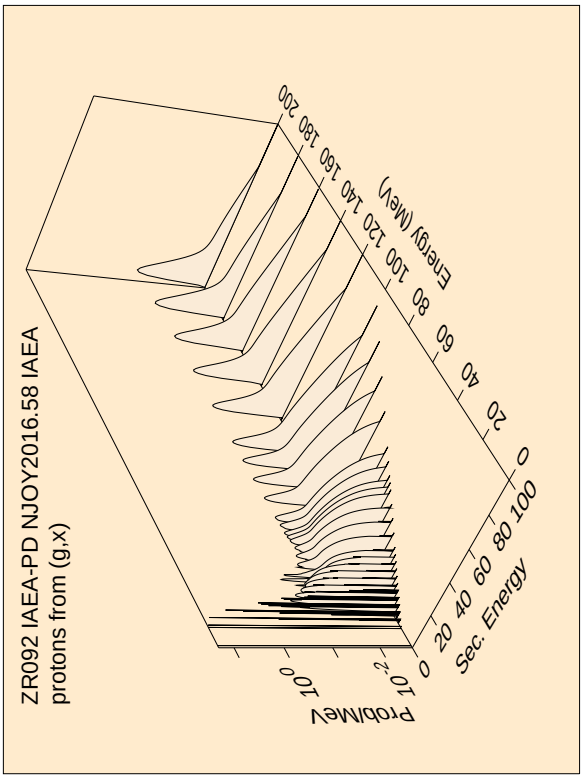
ZR092 IAEA-PD NJOY2016.58 IAEA
protons from (g,x)
Prob/MeV
Energy (MeV)
Sec. Energy

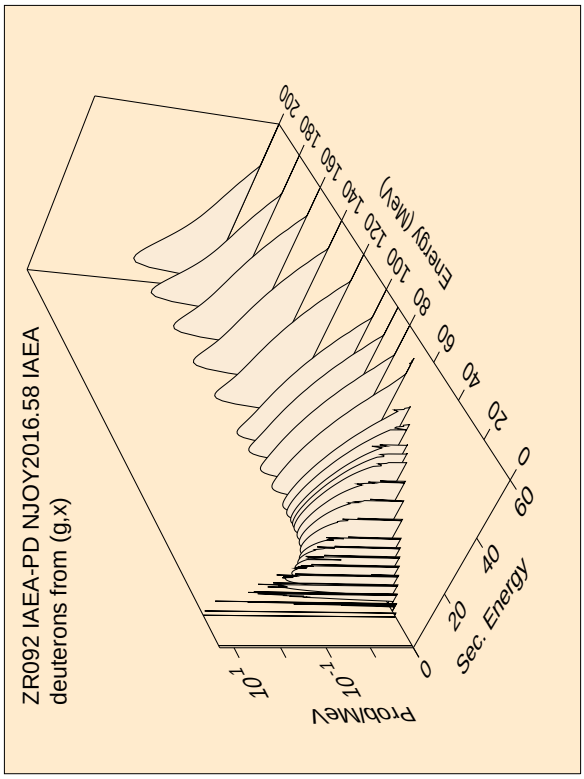
ZR092 IAEA-PD NJOY2016.58 IAEA
deuterons from (g,x)
Prob/MeV
Energy (MeV)
Sec. Energy

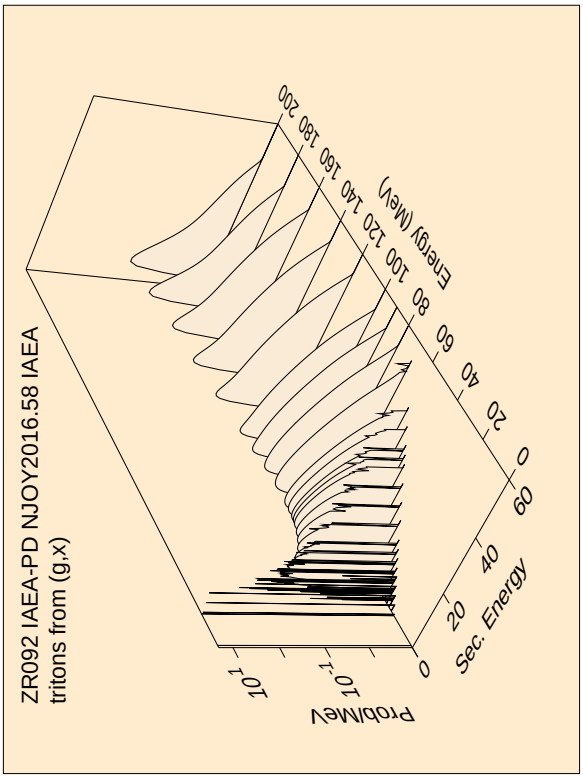
ZR092 IAEA-PD NJOY2016.58 IAEA
tritons from (g,x)
Prob/MeV
Energy (Mev)
Sec. Energy

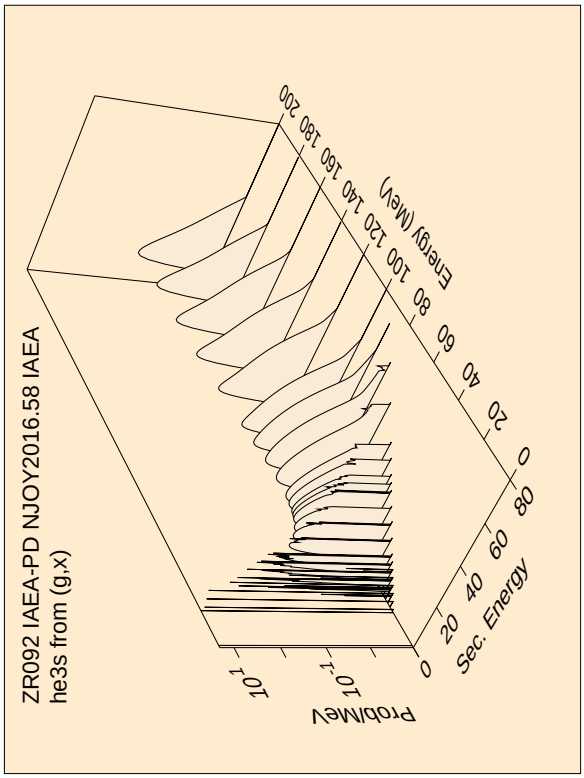
ZR092 IAEA-PD NJOY2016.58 IAEA
he3s from (g,x)
Prob/MeV
Energy (Mev)
Sec. Energy

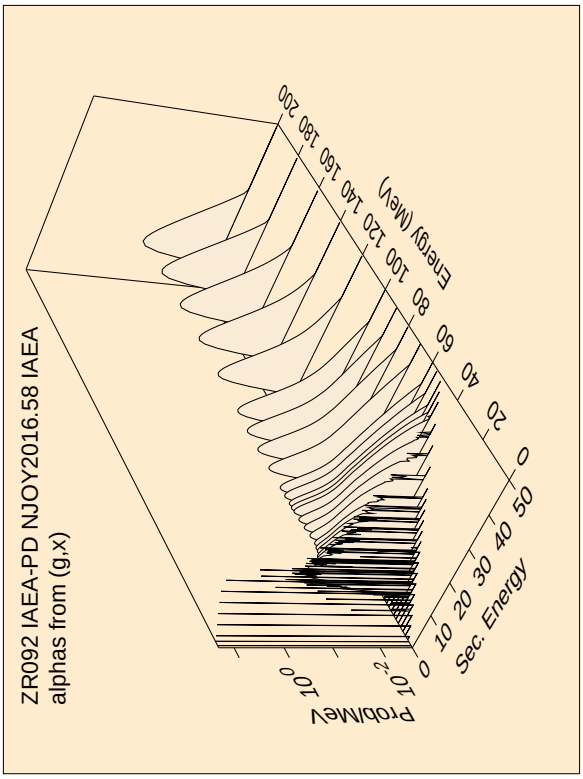
ZR092 IAEA-PD NJOY2016.58 IAEA
alphas from (g,x)
Prob/MeV
Energy (Mev)
Sec. Energy

A.2.2 Activation Library

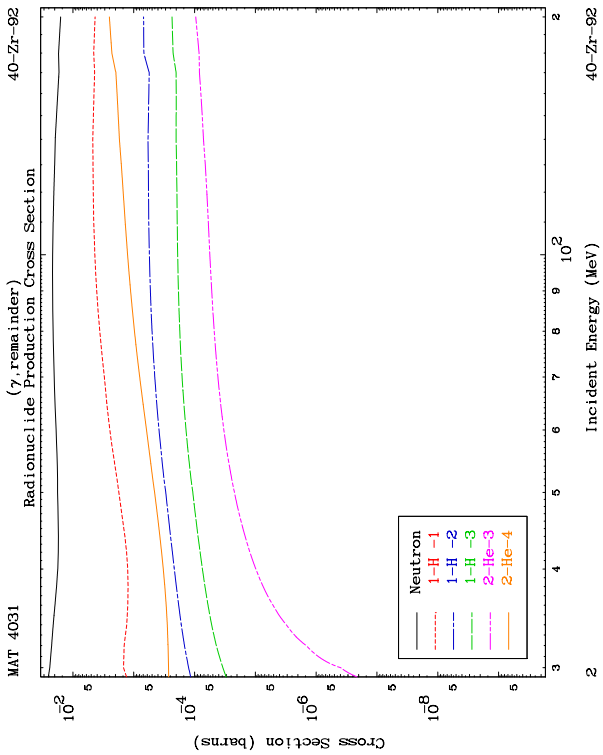

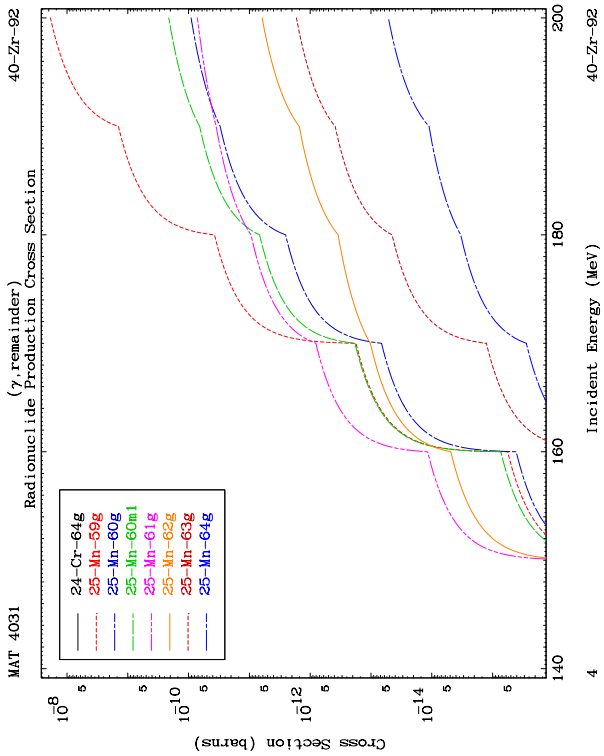

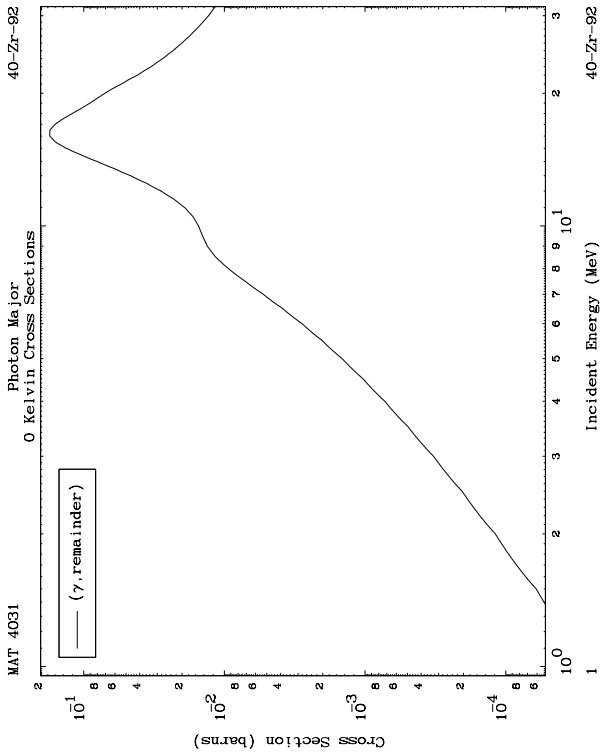

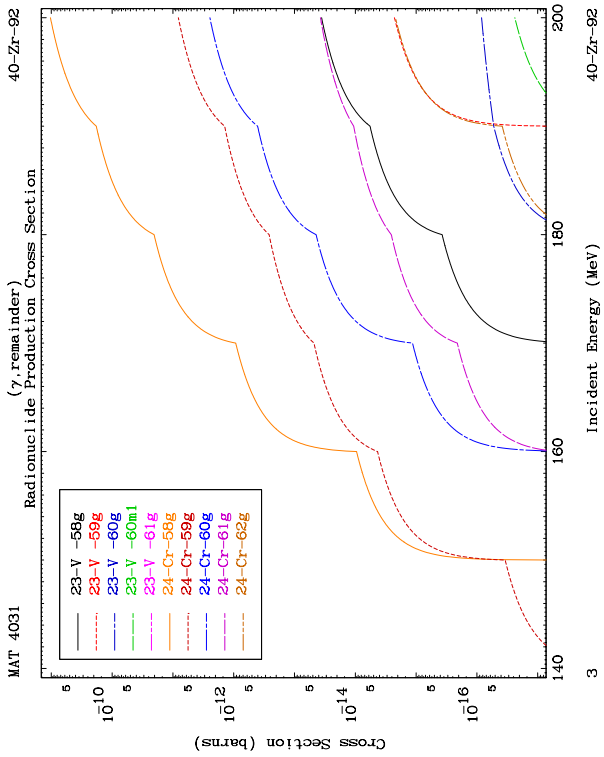

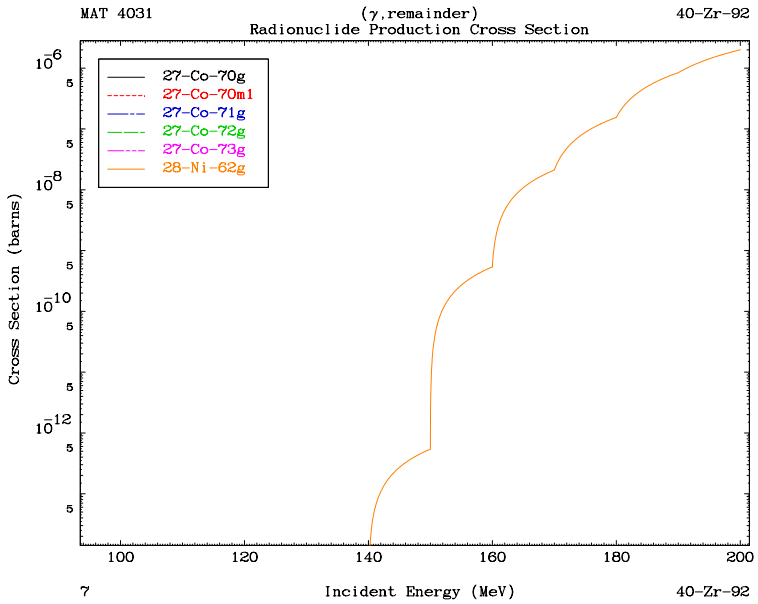
MAT 4031
(γ,remainder)
40-Zr-92
Radionuclide Production Cross Section
27-Co-70g
27-Co-70m1
27-Co-71g
27-Co-72g
27-Co-73g
28-Ni-62g
Cross Section (barns)
Incident Energy (MeV)
7
40-Zr-92

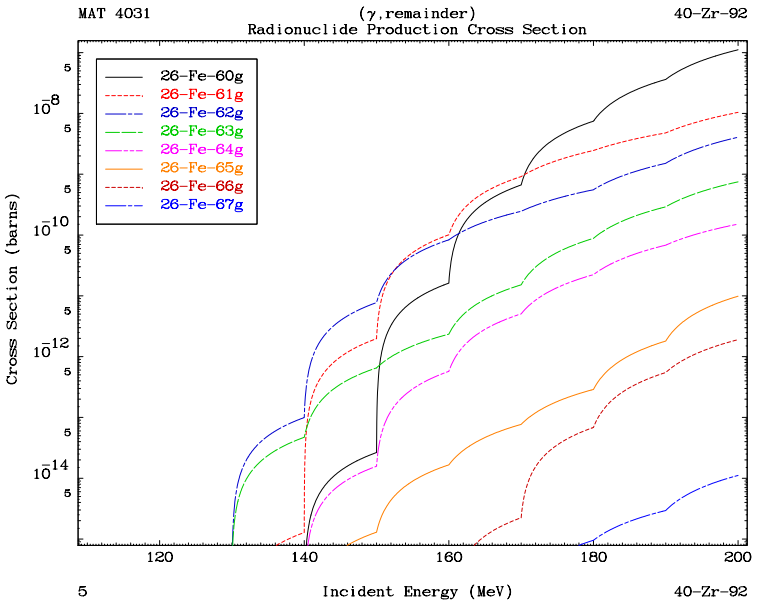
MAT 4031
(γ,remainder)
40-Zr-92
Radionuclide Production Cross Section
26-Fe-60g
26-Fe-61g
26-Fe-62g
26-Fe-63g
26-Fe-64g
26-Fe-65g
26-Fe-66g
26-Fe-67g
Cross Section (barns)
Incident Energy (MeV)
5
40-Zr-92

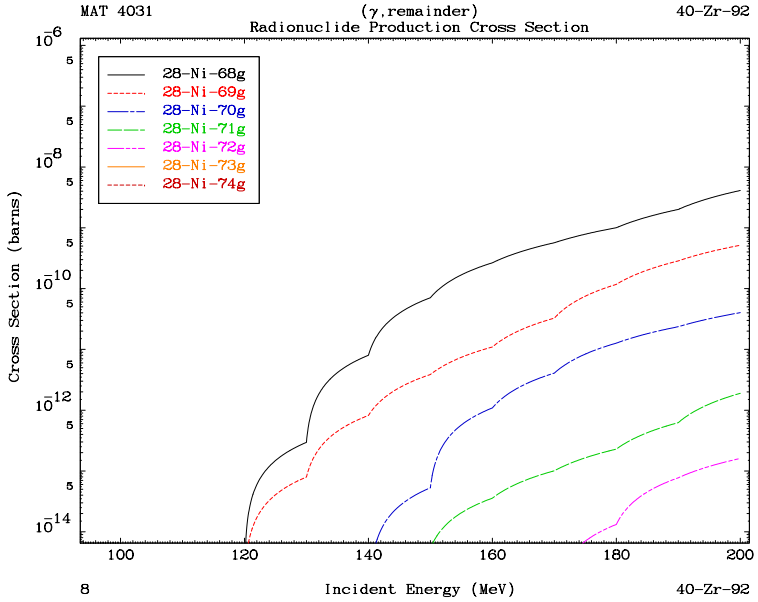
MAT 4031
(γ,remainder)
40-Zr-92
Radionuclide Production Cross Section
28-Ni-68g
28-Ni-69g
28-Ni-70g
28-Ni-71g
28-Ni-72g
28-Ni-73g
28-Ni-74g
Cross Section (barns)
Incident Energy (MeV)
8
40-Zr-92

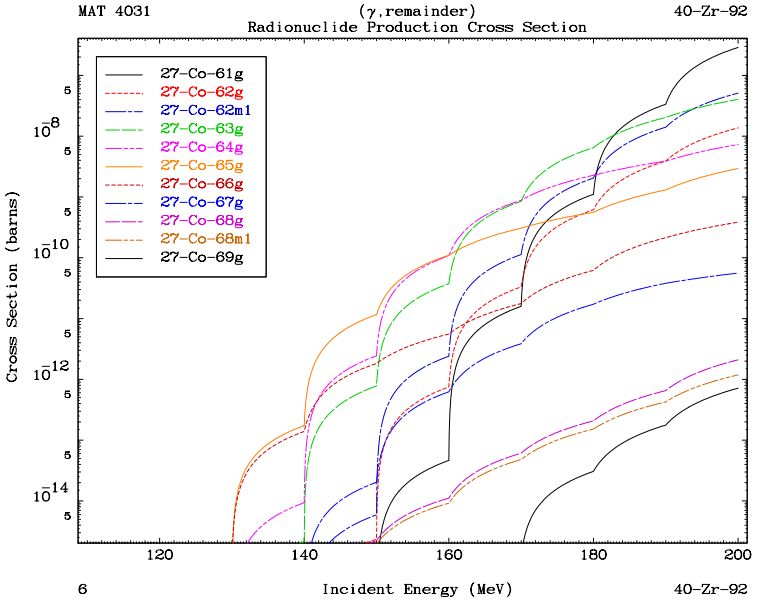
MAT 4031
(γ,remainder)
40-Zr-92
Radionuclide Production Cross Section
27-Co-61g
27-Co-62g
27-Co-62m1
27-Co-63g
27-Co-64g
27-Co-65g
27-Co-66g
27-Co-67g
27-Co-68g
27-Co-68m1
27-Co-69g
Cross Section (barns)
Incident Energy (MeV)
6
40-Zr-92

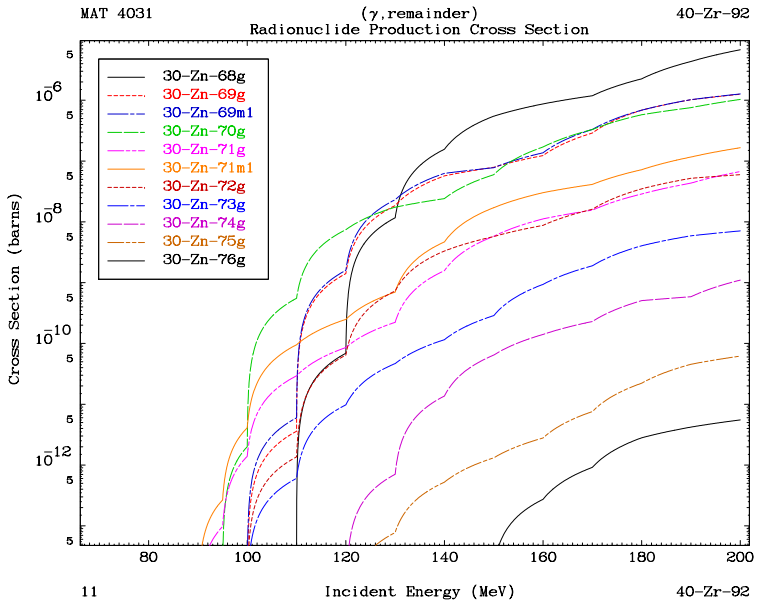
MAT 4031
(γ,remainder)
40-Zr-92
Radionuclide Production Cross Section
30-Zn-68g
30-Zn-69g
30-Zn-69m1
30-Zn-70g
30-Zn-71g
30-Zn-71m1
30-Zn-72g
30-Zn-73g
30-Zn-74g
30-Zn-75g
30-Zn-76g
Cross Section (barns)
Incident Energy (MeV)
11
40-Zr-92

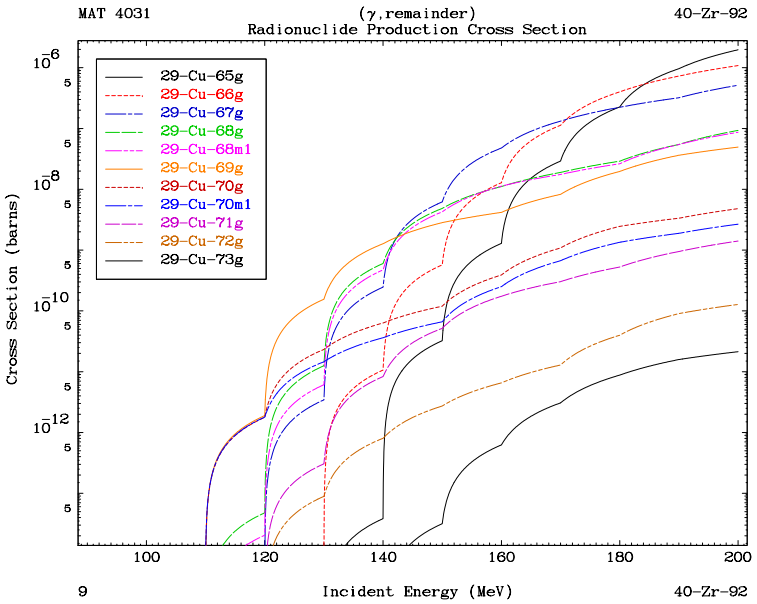
MAT 4031
(γ,remainder)
40-Zr-92
Radionuclide Production Cross Section
29-Cu-65g
29-Cu-66g
29-Cu-67g
29-Cu-68g
29-Cu-68m1
29-Cu-69g
29-Cu-70g
29-Cu-70m1
29-Cu-71g
29-Cu-72g
29-Cu-73g
Cross Section (barns)
Incident Energy (MeV)
9
40-Zr-92

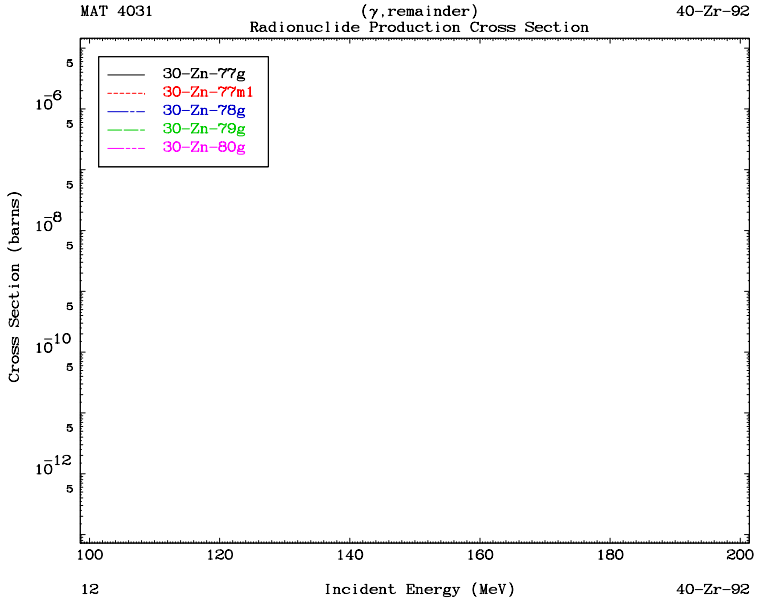
MAT 4031
(γ,remainder)
40-Zr-92
Radionuclide Production Cross Section
30-Zn-77g
30-Zn-77m1
30-Zn-78g
30-Zn-79g
30-Zn-80g
Cross Section (barns)
Incident Energy (MeV)
12
40-Zr-92

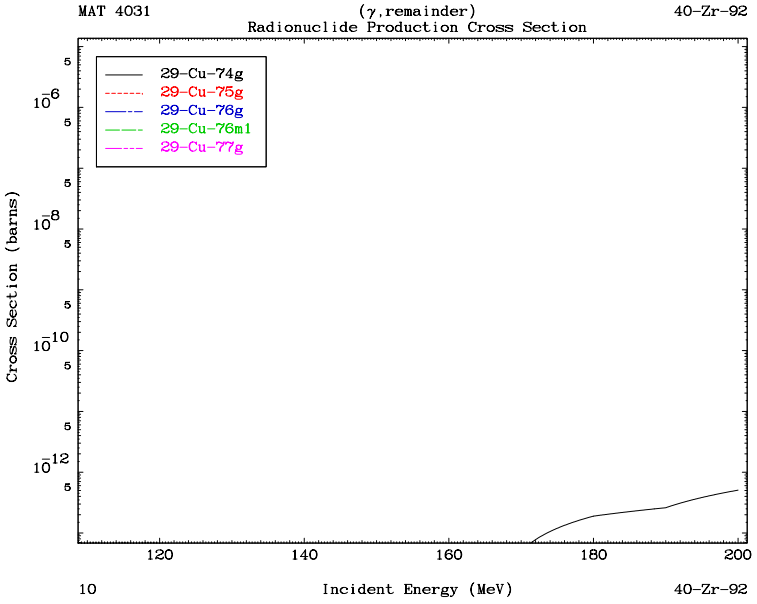
MAT 4031
(γ,remainder)
40-Zr-92
Radionuclide Production Cross Section
29-Cu-74g
29-Cu-75g
29-Cu-76g
29-Cu-76m1
29-Cu-77g
Cross Section (barns)
Incident Energy (MeV)
10
40-Zr-92

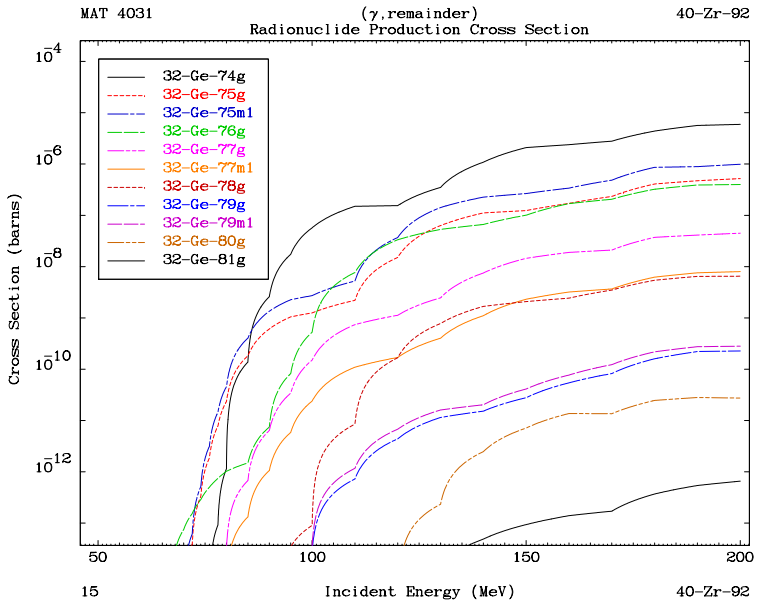
MAT 4031
(γ,remainder)
40-Zr-92
Radionuclide Production Cross Section
32-Ge-74g
32-Ge-75g
32-Ge-75m1
32-Ge-76g
32-Ge-77g
32-Ge-77m1
32-Ge-78g
32-Ge-79g
32-Ge-79m1
32-Ge-80g
32-Ge-81g
Cross Section (barns)
Incident Energy (MeV)
15
40-Zr-92

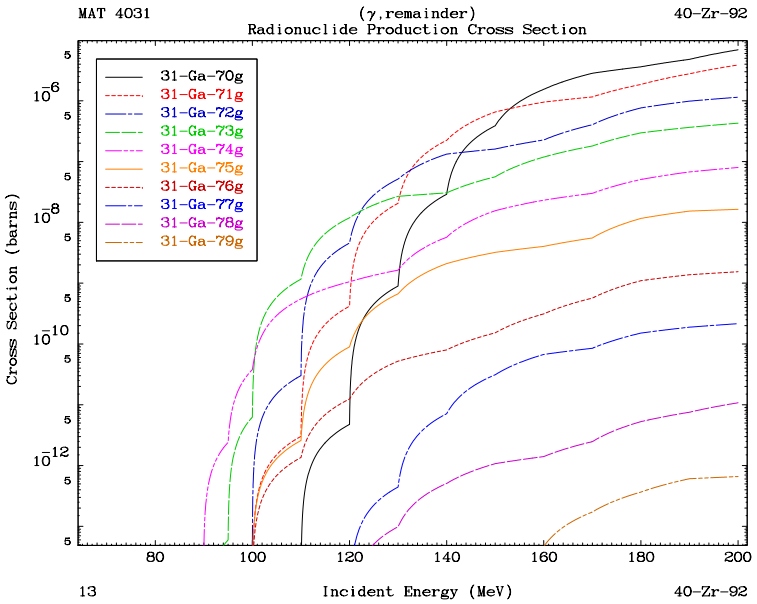
MAT 4031
(γ,remainder)
40-Zr-92
Radionuclide Production Cross Section
31-Ga-70g
31-Ga-71g
31-Ga-72g
31-Ga-73g
31-Ga-74g
31-Ga-75g
31-Ga-76g
31-Ga-77g
31-Ga-78g
31-Ga-79g
Cross Section (barns)
Incident Energy (MeV)
13
40-Zr-92

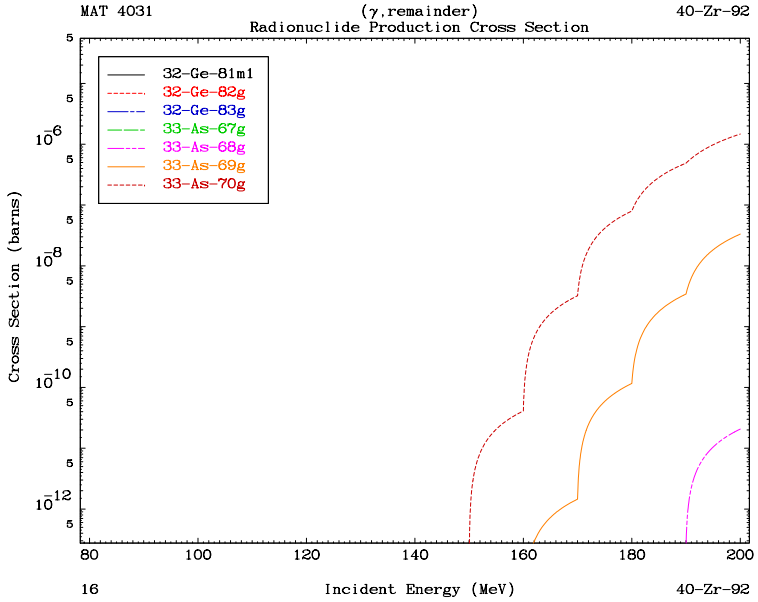
MAT 4031
(γ,remainder)
40-Zr-92
Radionuclide Production Cross Section
32-Ge-81m1
32-Ge-82g
32-Ge-83g
33-As-67g
33-As-68g
33-As-69g
33-As-70g
Cross Section (barns)
Incident Energy (MeV)
16
40-Zr-92

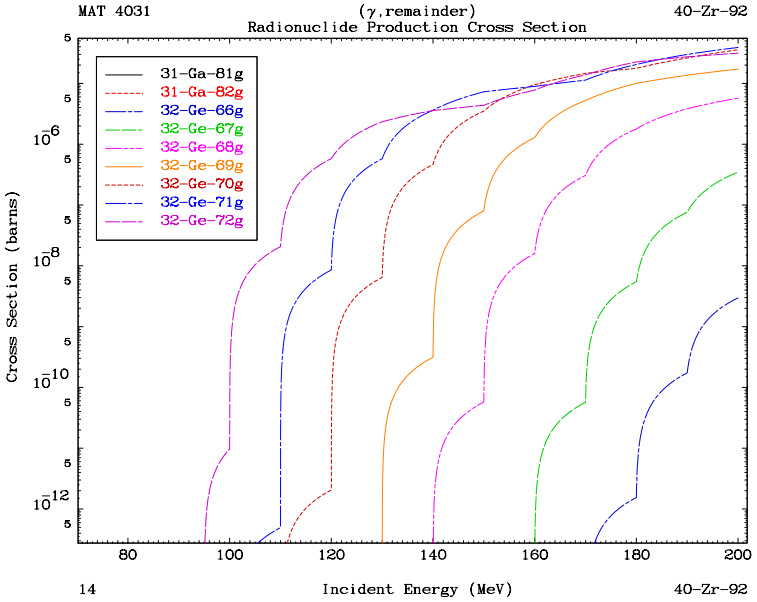
MAT 4031
(γ,remainder)
40-Zr-92
Radionuclide Production Cross Section
31-Ga-81g
31-Ga-82g
32-Ge-66g
32-Ge-67g
32-Ge-68g
32-Ge-69g
32-Ge-70g
32-Ge-71g
32-Ge-72g
Cross Section (barns)
Incident Energy (MeV)
14
40-Zr-92

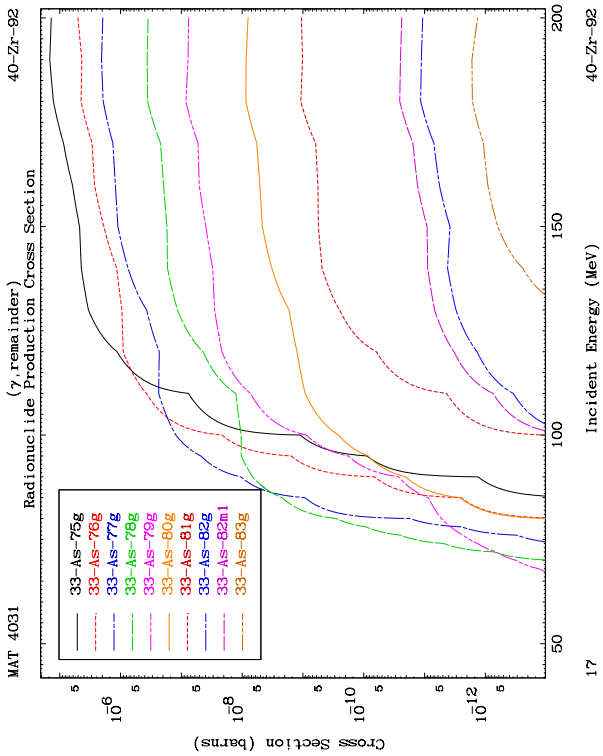
MAT 4031
(γ,remainder)
Radionuclide Production Cross Section
40-Zr-92
33-As-75g
33-As-76g
33-As-77g
33-As-78g
33-As-79g
33-As-80g
33-As-81g
33-As-82g
33-As-82m1
33-As-83g
Cross Section (barns)
Incident Energy (MeV)
17

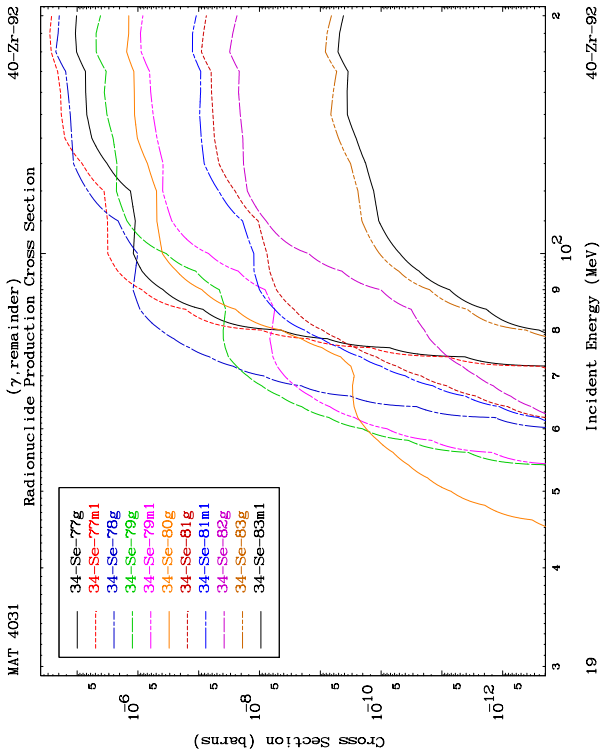
MAT 4031
(γ,remainder)
Radionuclide Production Cross Section
40-Zr-92
34-Se-77g
34-Se-77m1
34-Se-78g
34-Se-79g
34-Se-79m1
34-Se-80g
34-Se-81g
34-Se-81m1
34-Se-82g
34-Se-83g
34-Se-83m1
Cross Section (barns)
Incident Energy (MeV)
19

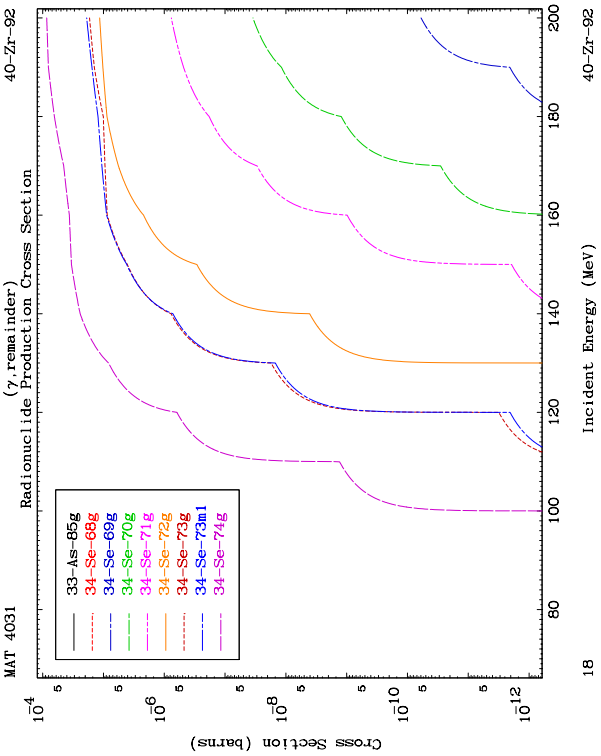
MAT 4031
(γ,remainder)
Radionuclide Production Cross Section
40-Zr-92
33-As-85g
34-Se-68g
34-Se-69g
34-Se-70g
34-Se-71g
34-Se-72g
34-Se-73g
34-Se-73m1
34-Se-74g
Cross Section (barns)
Incident Energy (MeV)
18

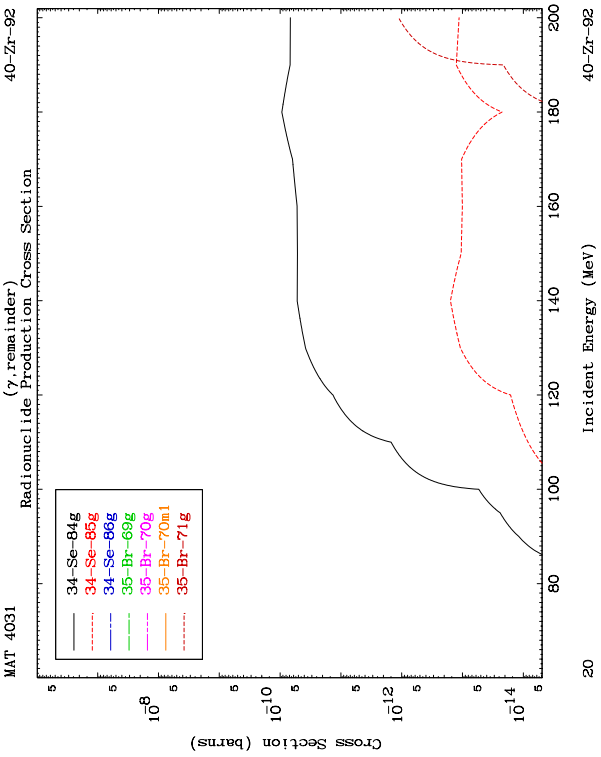
MAT 4031
(γ,remainder)
Radionuclide Production Cross Section
40-Zr-92
34-Se-84g
34-Se-85g
34-Se-86g
35-Br-69g
35-Br-70g
35-Br-70m1
35-Br-71g
Cross Section (barns)
Incident Energy (MeV)
20

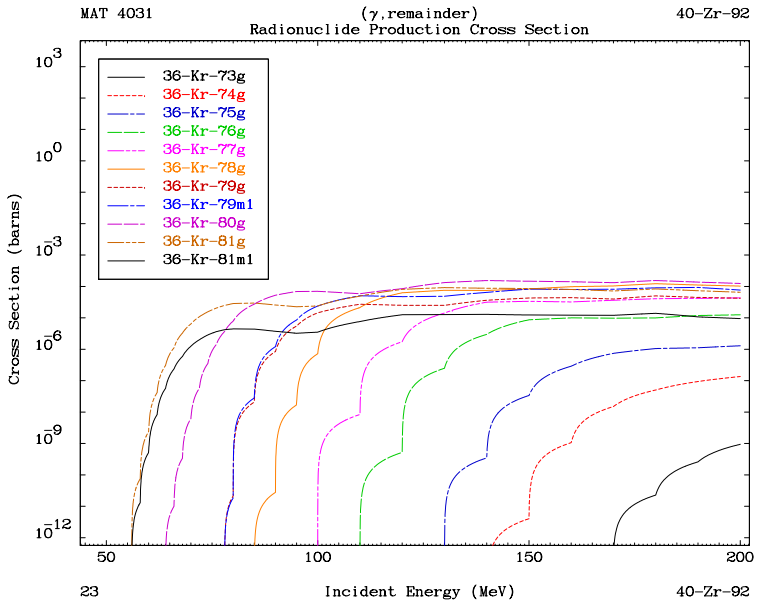
MAT 4031
(γ,remainder)
40-Zr-92
Radionuclide Production Cross Section
36-Kr-73g
36-Kr-74g
36-Kr-75g
36-Kr-76g
36-Kr-77g
36-Kr-78g
36-Kr-79g
36-Kr-79m1
36-Kr-80g
36-Kr-81g
36-Kr-81m1
Cross Section (barns)
Incident Energy (MeV)
23
40-Zr-92

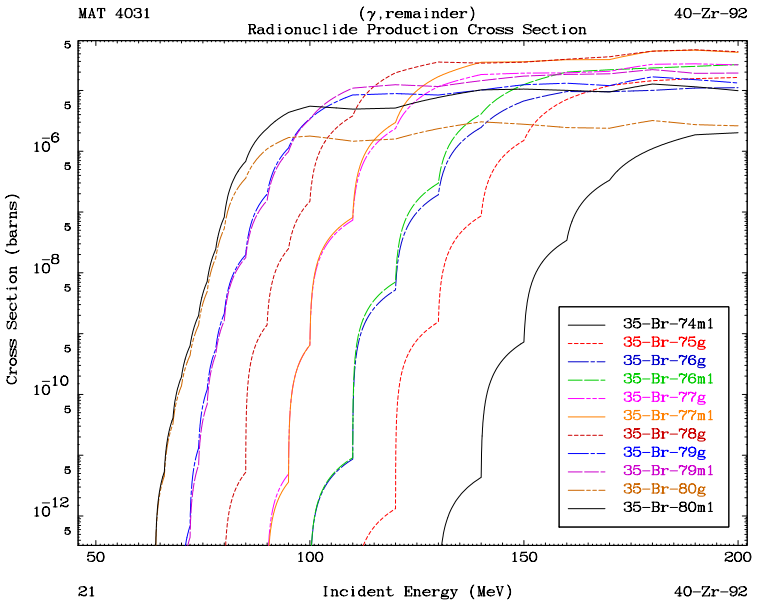
MAT 4031
(γ,remainder)
40-Zr-92
Radionuclide Production Cross Section
35-Br-74m1
35-Br-75g
35-Br-76g
35-Br-76m1
35-Br-77g
35-Br-77m1
35-Br-78g
35-Br-79g
35-Br-79m1
35-Br-80g
35-Br-80m1
Cross Section (barns)
Incident Energy (MeV)
21
40-Zr-92

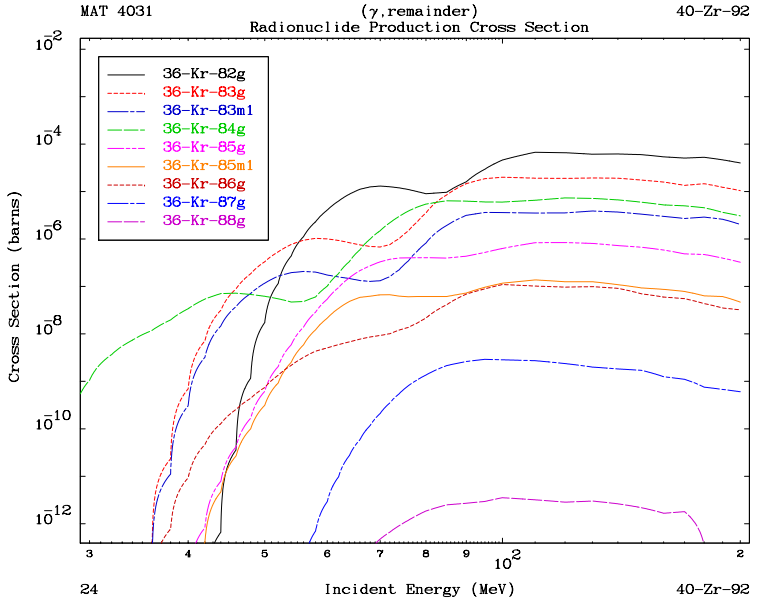
MAT 4031
(γ,remainder)
40-Zr-92
Radionuclide Production Cross Section
36-Kr-82g
36-Kr-83g
36-Kr-83m1
36-Kr-84g
36-Kr-85g
36-Kr-85m1
36-Kr-86g
36-Kr-87g
36-Kr-88g
Cross Section (barns)
Incident Energy (MeV)
24
40-Zr-92

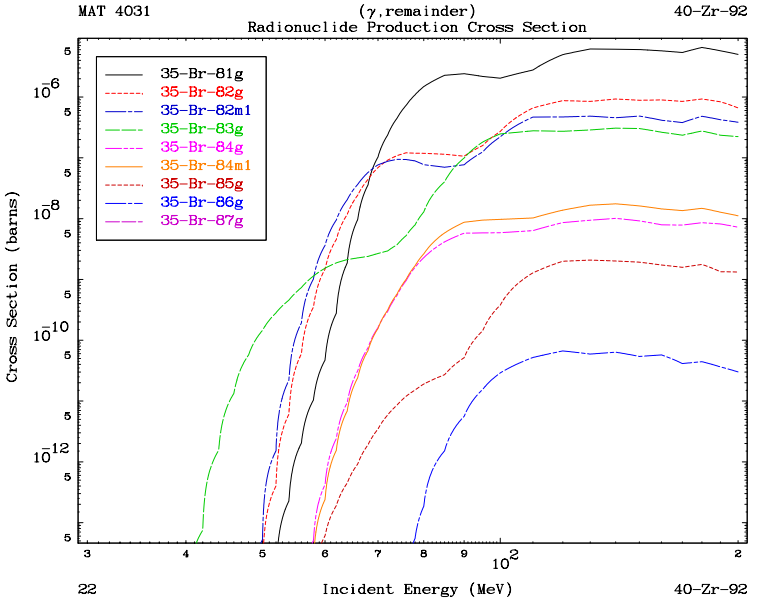
MAT 4031
(γ,remainder)
40-Zr-92
Radionuclide Production Cross Section
35-Br-81g
35-Br-82g
35-Br-82m1
35-Br-83g
35-Br-84g
35-Br-84m1
35-Br-85g
35-Br-86g
35-Br-87g
Cross Section (barns)
Incident Energy (MeV)
22
40-Zr-92

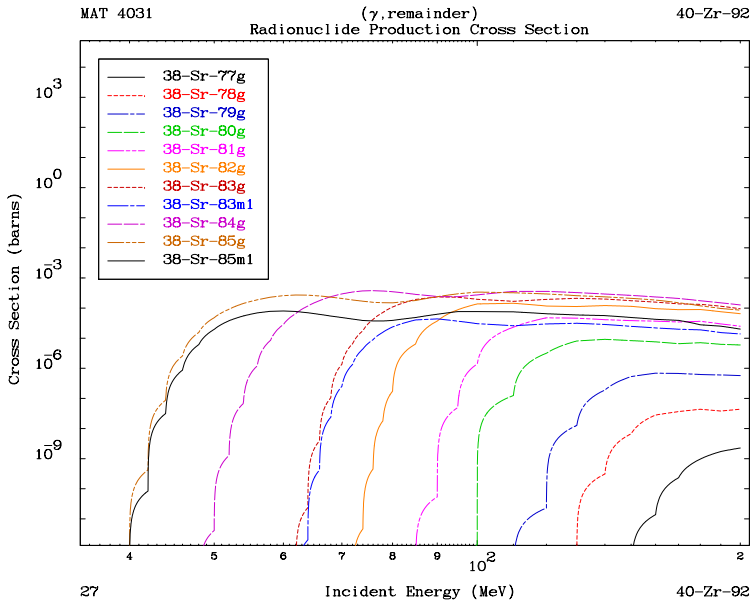
MAT 4031
(γ,remainder)
40-Zr-92
Radionuclide Production Cross Section
38-Sr-77g
38-Sr-78g
38-Sr-79g
38-Sr-80g
38-Sr-81g
38-Sr-82g
38-Sr-83g
38-Sr-83m1
38-Sr-84g
38-Sr-85g
38-Sr-85m1
Cross Section (barns)
Incident Energy (MeV)
27
40-Zr-92

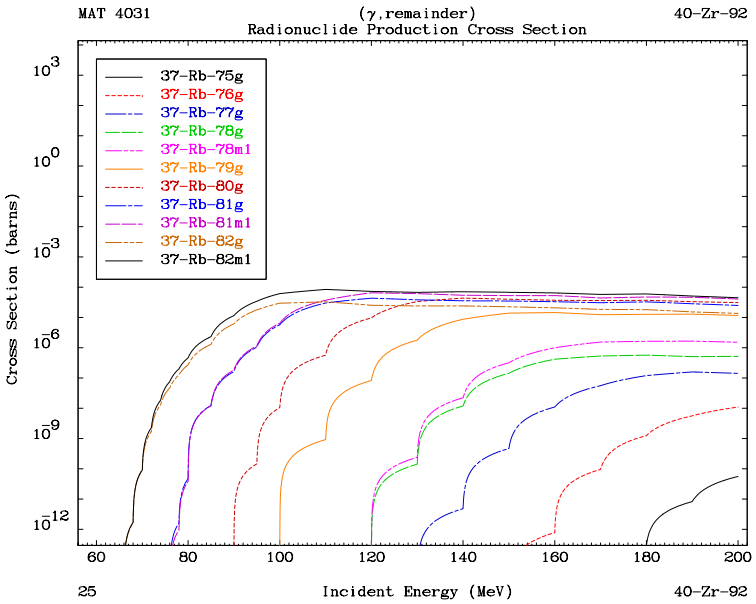
MAT 4031
(γ,remainder)
40-Zr-92
Radionuclide Production Cross Section
37-Rb-75g
37-Rb-76g
37-Rb-77g
37-Rb-78g
37-Rb-78m1
37-Rb-79g
37-Rb-80g
37-Rb-81g
37-Rb-81m1
37-Rb-82g
37-Rb-82m1
Cross Section (barns)
Incident Energy (MeV)
25
40-Zr-92

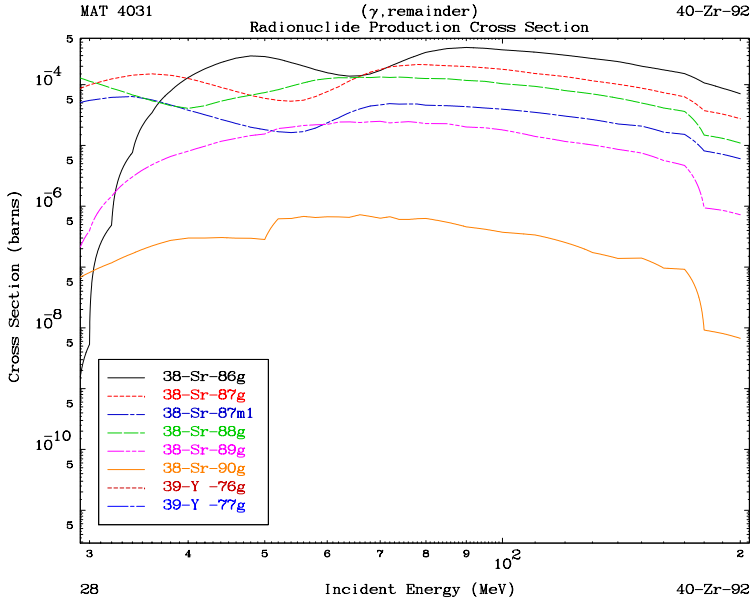
MAT 4031
(γ,remainder)
40-Zr-92
Radionuclide Production Cross Section
38-Sr-86g
38-Sr-87g
38-Sr-87m1
38-Sr-88g
38-Sr-89g
38-Sr-90g
39-Y -76g
39-Y -77g
Cross Section (barns)
Incident Energy (MeV)
28
40-Zr-92

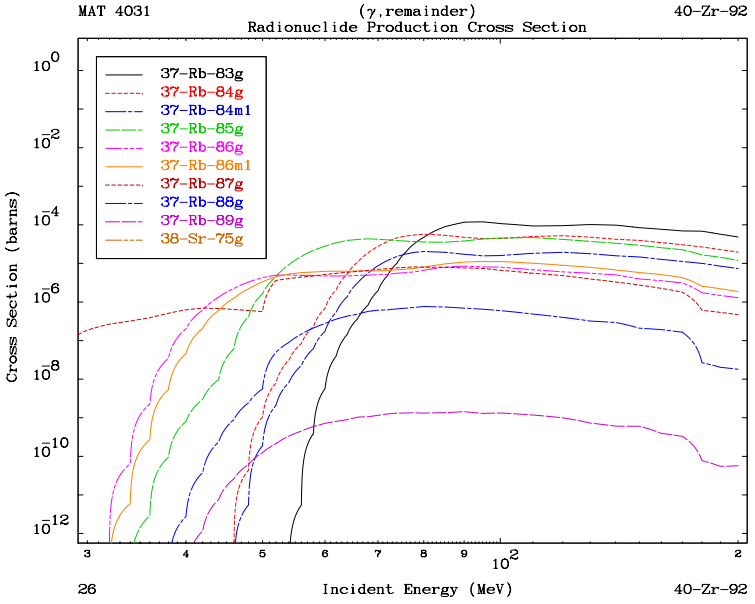
MAT 4031
(γ,remainder)
40-Zr-92
Radionuclide Production Cross Section
37-Rb-83g
37-Rb-84g
37-Rb-84m1
37-Rb-85g
37-Rb-86g
37-Rb-86m1
37-Rb-87g
37-Rb-88g
37-Rb-89g
38-Sr-75g
Cross Section (barns)
Incident Energy (MeV)
26
40-Zr-92

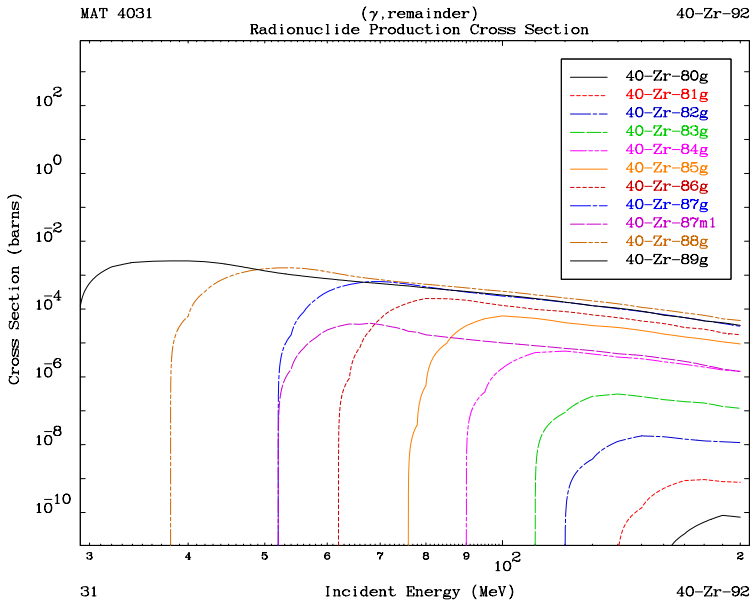
MAT 4031
(γ,remainder)
40-Zr-92
Radionuclide Production Cross Section
40-Zr-80g
40-Zr-81g
40-Zr-82g
40-Zr-83g
40-Zr-84g
40-Zr-85g
40-Zr-86g
40-Zr-87g
40-Zr-87m1
40-Zr-88g
40-Zr-89g
Cross Section (barns)
Incident Energy (MeV)
31
40-Zr-92

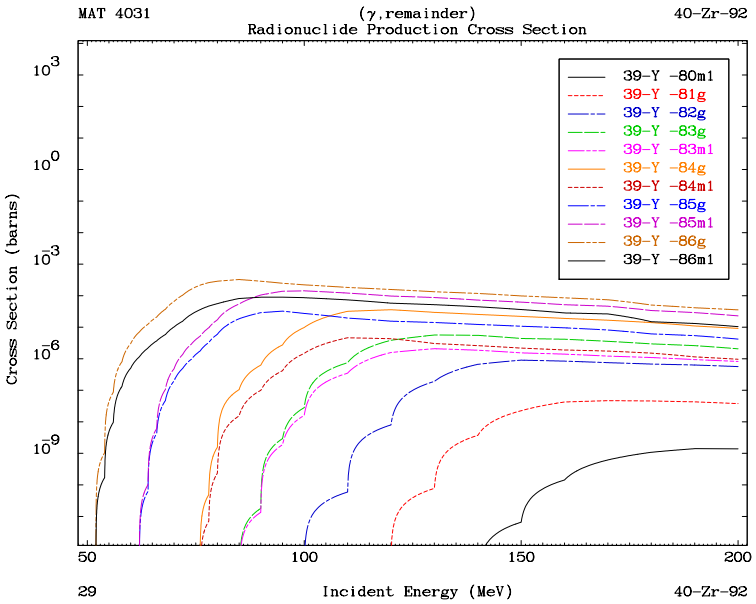
MAT 4031
(γ,remainder)
40-Zr-92
Radionuclide Production Cross Section
39-Y -80m1
39-Y -81g
39-Y -82g
39-Y -83g
39-Y -83m1
39-Y -84g
39-Y -84m1
39-Y -85g
39-Y -85m1
39-Y -86g
39-Y -86m1
Cross Section (barns)
Incident Energy (MeV)
29
40-Zr-92

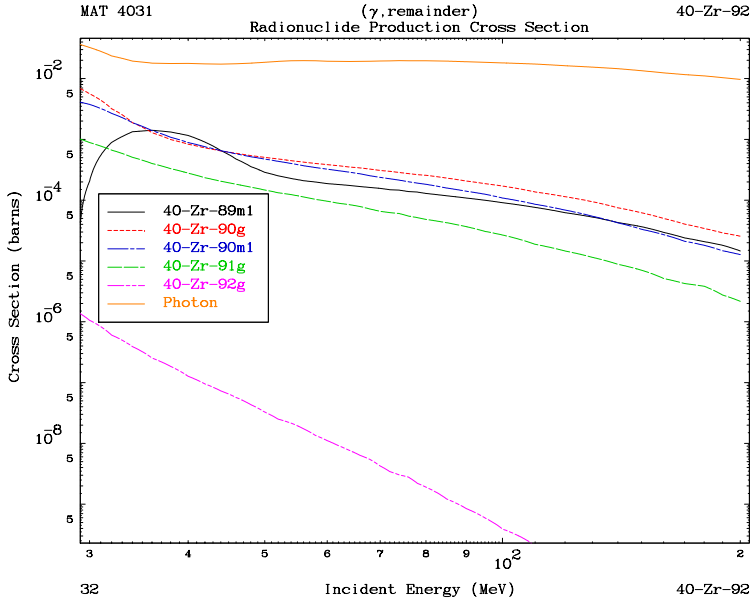
MAT 4031
(γ,remainder)
40-Zr-92
Radionuclide Production Cross Section
40-Zr-89m1
40-Zr-90g
40-Zr-90m1
40-Zr-91g
40-Zr-92g
Photon
Cross Section (barns)
Incident Energy (MeV)
32
40-Zr-92

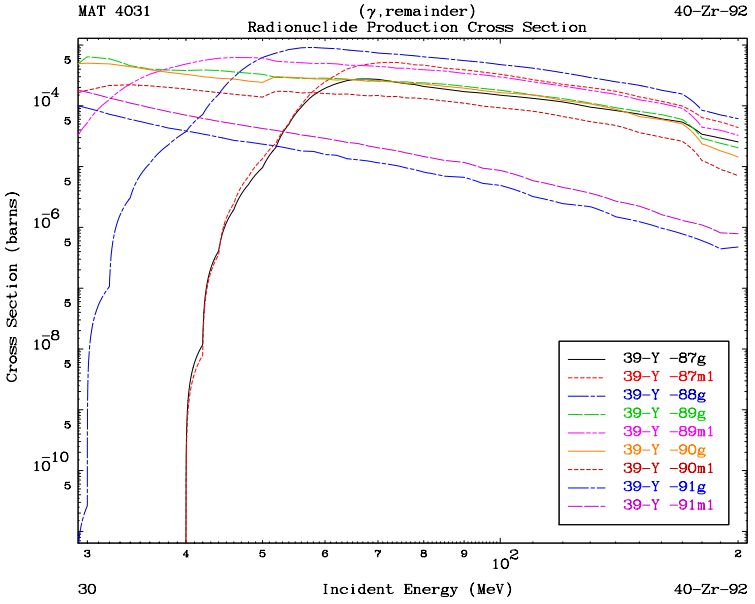
MAT 4031
(γ,remainder)
40-Zr-92
Radionuclide Production Cross Section
39-Y -87g
39-Y -87m1
39-Y -88g
39-Y -89g
39-Y -89m1
39-Y -90g
39-Y -90m1
39-Y -91g
39-Y -91m1
Cross Section (barns)
Incident Energy (MeV)
30
40-Zr-92

A.3 Example of ^{91}Zr File Processing (File Type 2: KAERI)

A.3.1 Transport Library

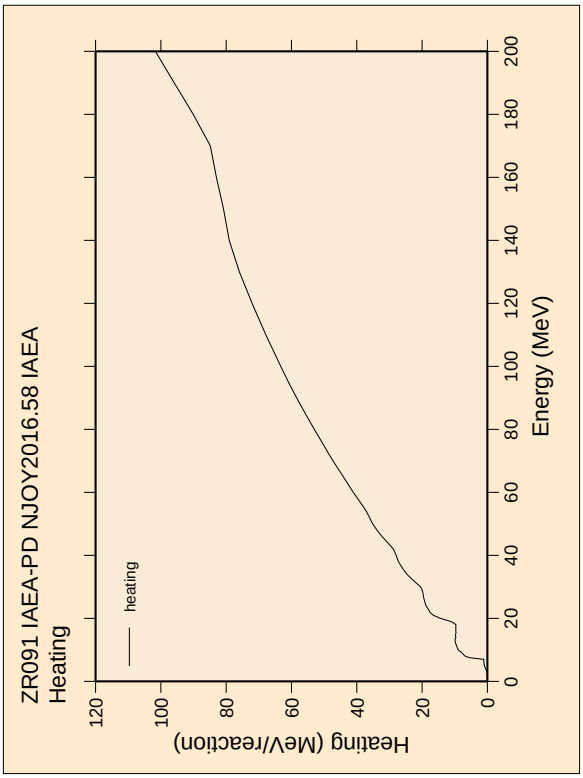

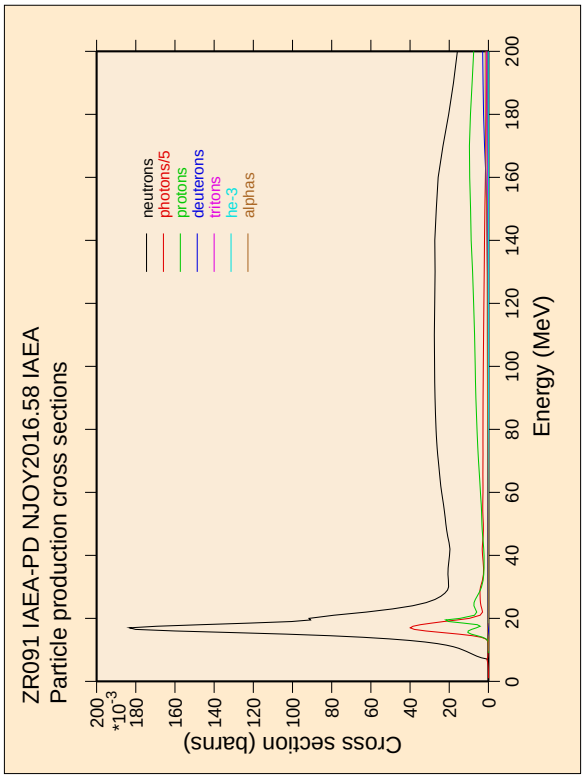

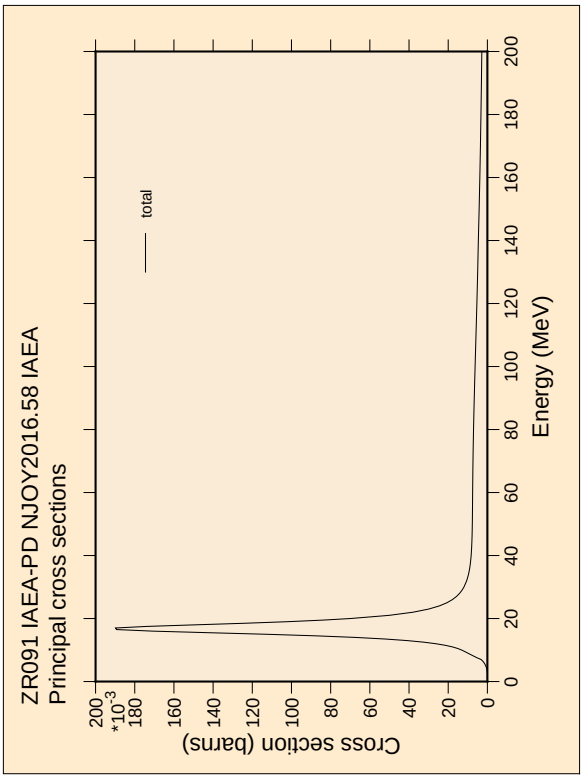

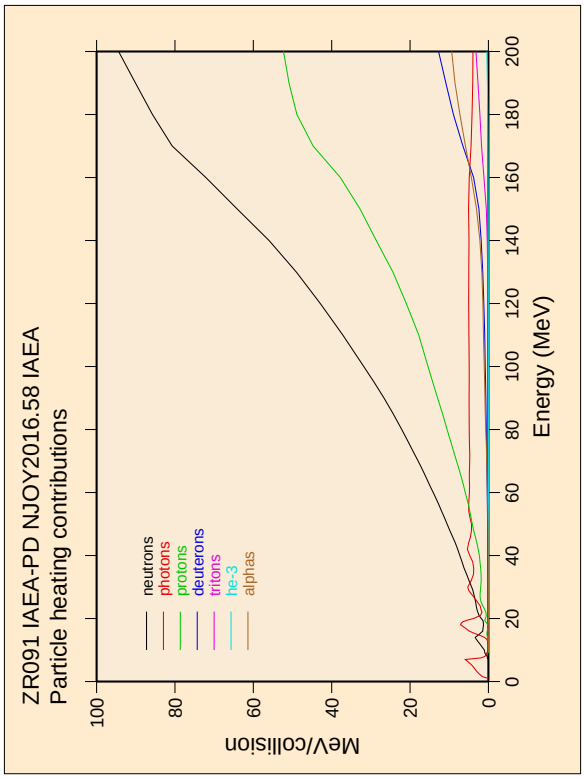

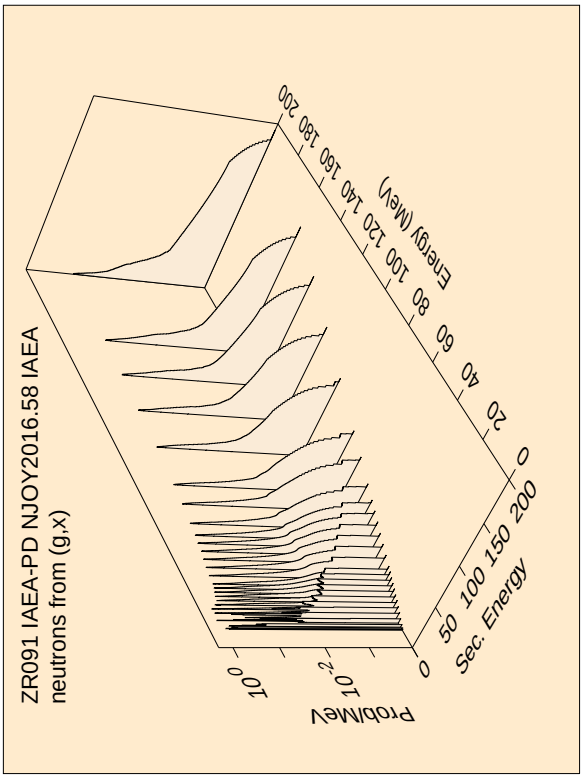
ZR091 IAEA-PD NJOY2016.58 IAEA
neutrons from (g,x)
Prob/MeV
Energy (Mev)
Sec. Energy

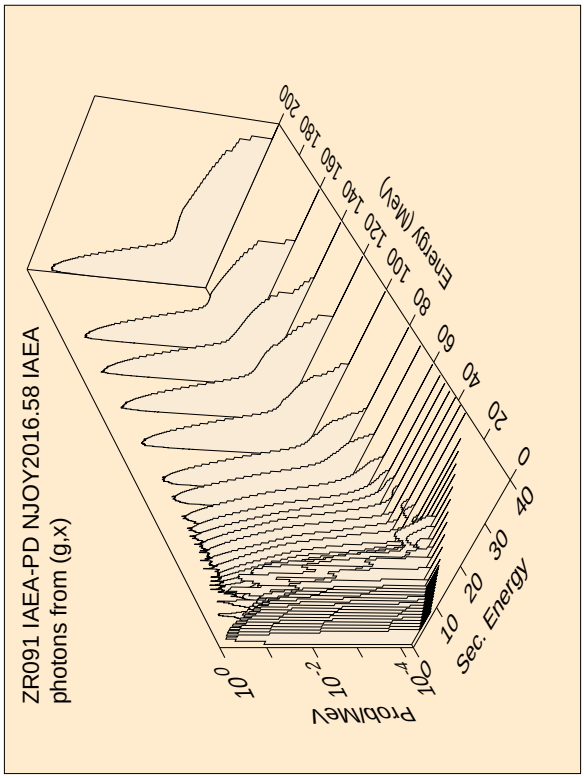
ZR091 IAEA-PD NJOY2016.58 IAEA
photons from (g,x)
Prob/MeV
Energy (Mev)
Sec. Energy

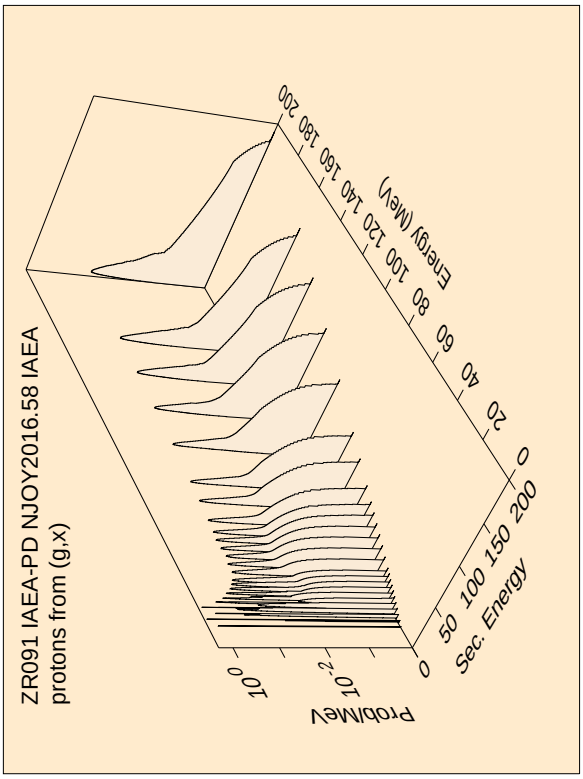
ZR091 IAEA-PD NJOY2016.58 IAEA
protons from (g,x)
Prob/MeV
Energy (Mev)
Sec. Energy

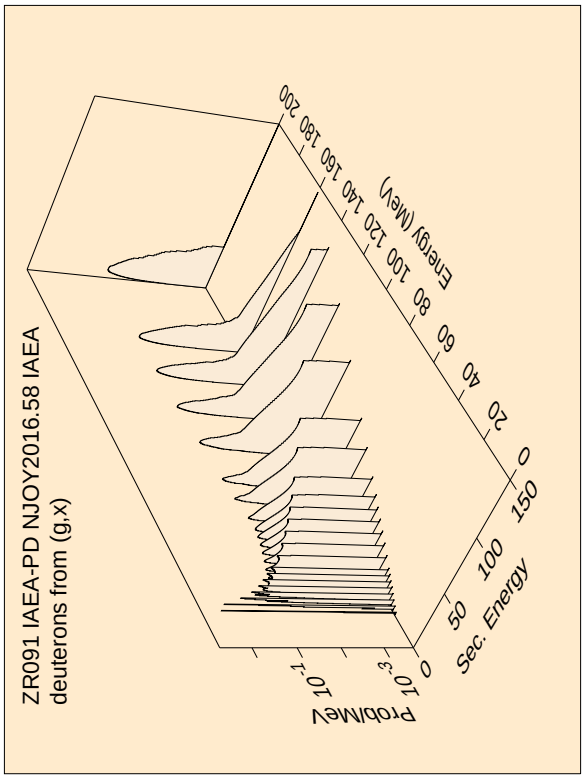
ZR091 IAEA-PD NJOY2016.58 IAEA
deuterons from (g,x)
Prob/MeV
Energy (Mev)
Sec. Energy

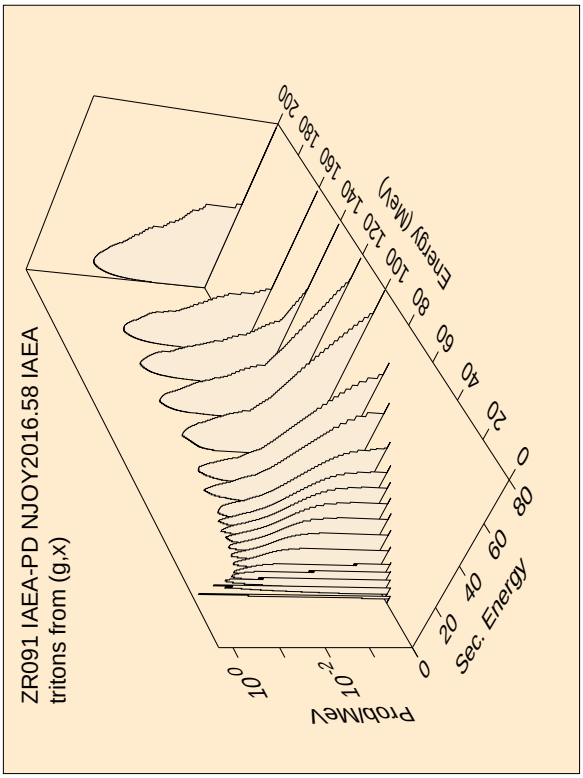
ZR091 IAEA-PD NJOY2016.58 IAEA
tritons from (g,x)
Prob/MeV
Energy (Mev)
Sec. Energy

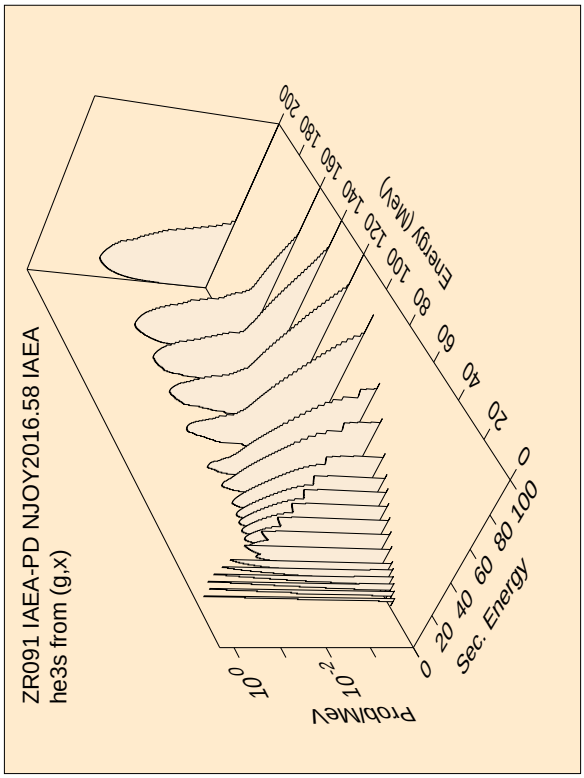
ZR091 IAEA-PD NJOY2016.58 IAEA
he3s from (g,x)
Prob/MeV
Energy (Mev)
Sec. Energy

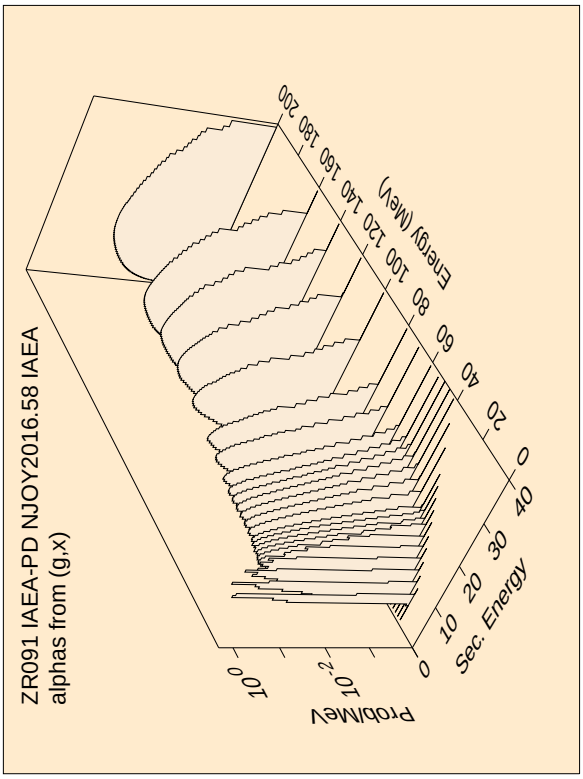
ZR091 IAEA-PD NJOY2016.58 IAEA
alphas from (g,x)
Prob/MeV
Energy (Mev)
Sec. Energy

A.3.2 Activation Library

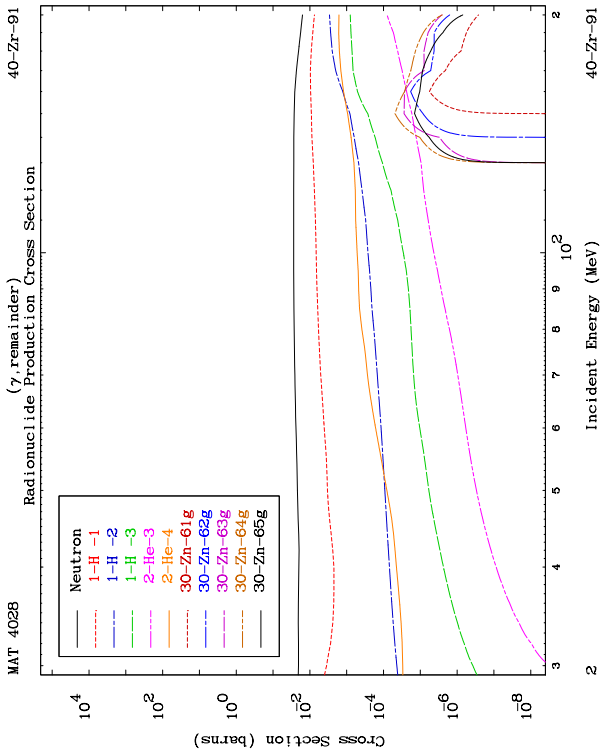

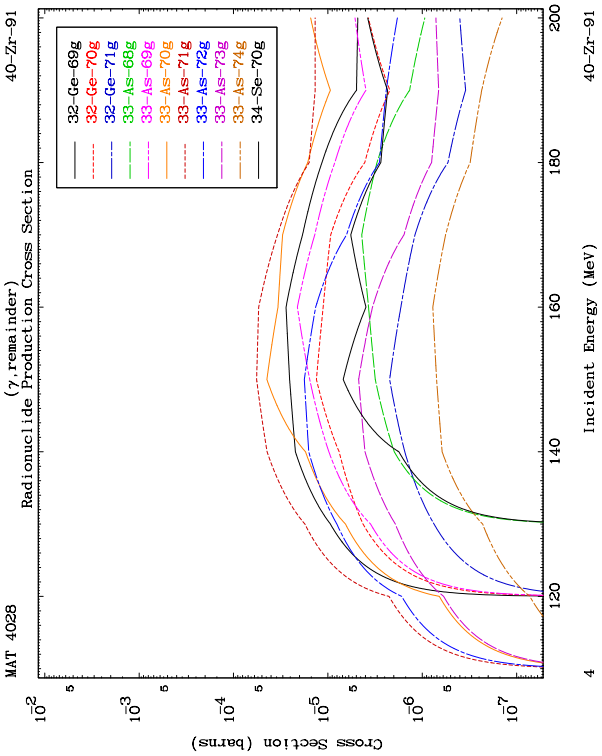

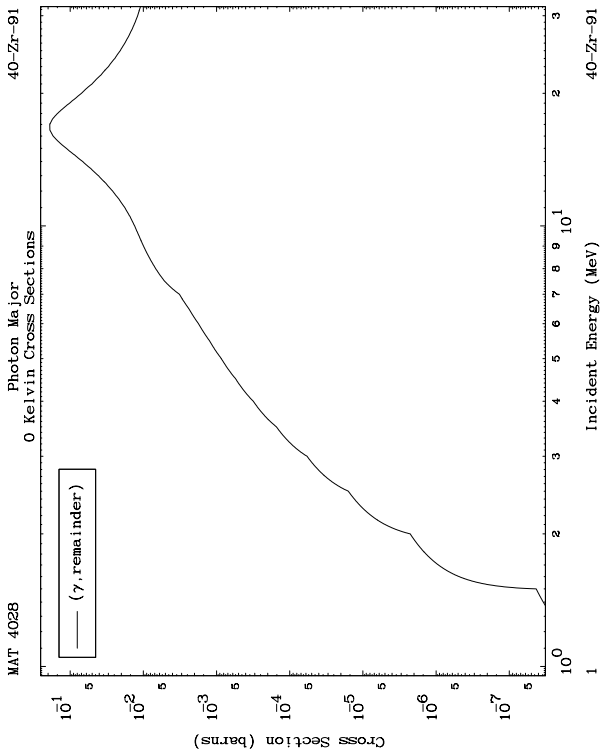

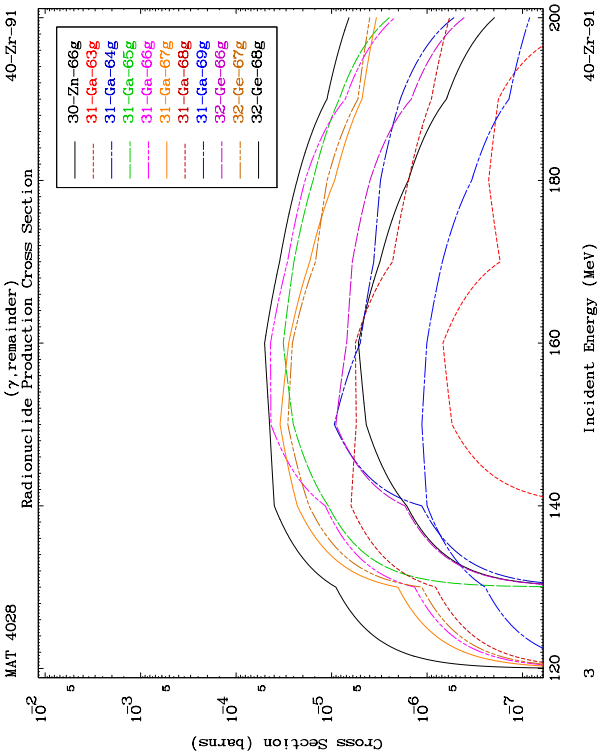

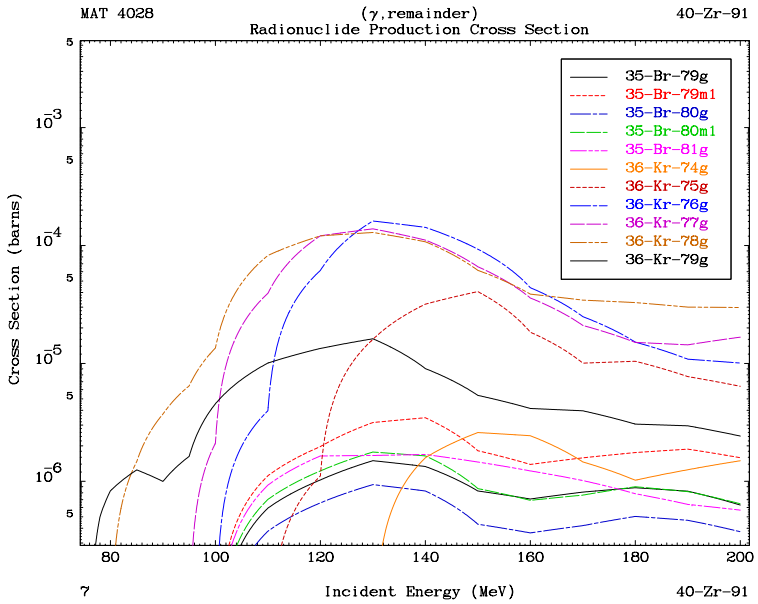
MAT 4028
(γ,remainder)
40-Zr-91
Radionuclide Production Cross Section
35-Br-79g
35-Br-79m1
35-Br-80g
35-Br-80m1
35-Br-81g
36-Kr-74g
36-Kr-75g
36-Kr-76g
36-Kr-77g
36-Kr-78g
36-Kr-79g
Cross Section (barns)
Incident Energy (MeV)
7
40-Zr-91

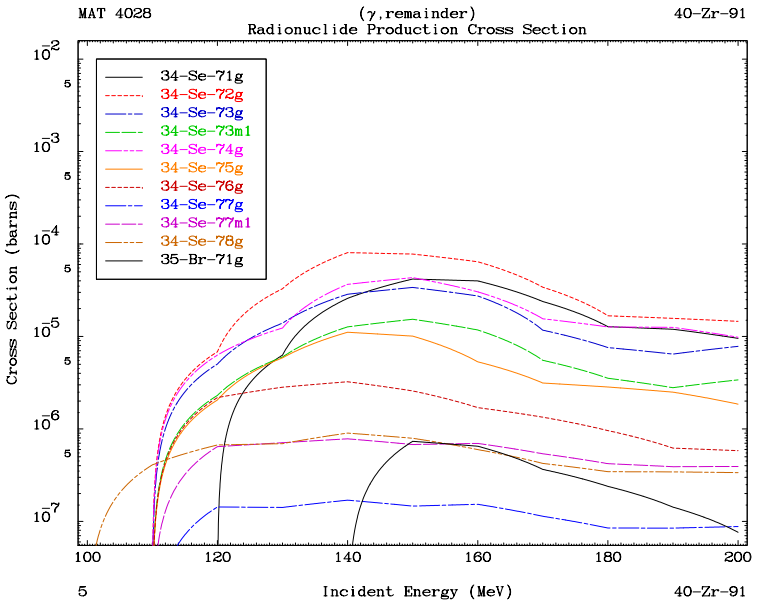
MAT 4028
(γ,remainder)
40-Zr-91
Radionuclide Production Cross Section
34-Se-71g
34-Se-72g
34-Se-73g
34-Se-73m1
34-Se-74g
34-Se-75g
34-Se-76g
34-Se-77g
34-Se-77m1
34-Se-78g
35-Br-71g
Cross Section (barns)
Incident Energy (MeV)
5
40-Zr-91

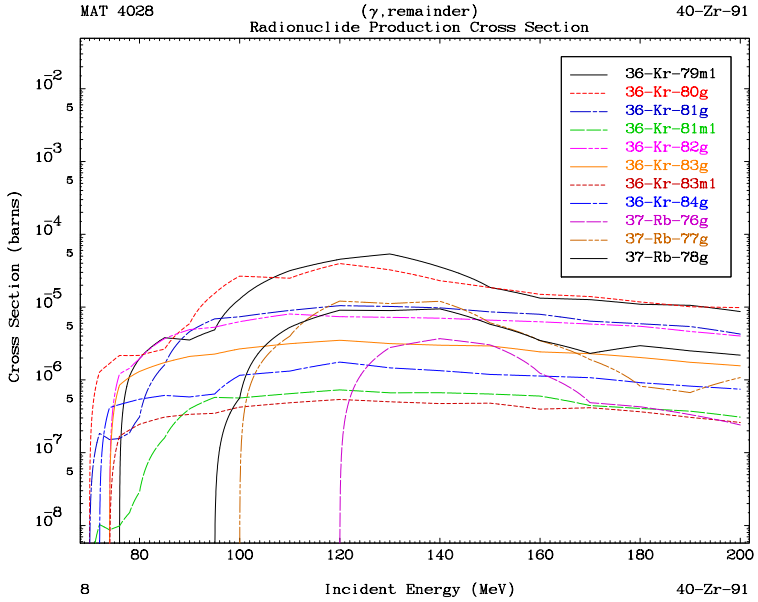
MAT 4028
(γ,remainder)
40-Zr-91
Radionuclide Production Cross Section
36-Kr-79m1
36-Kr-80g
36-Kr-81g
36-Kr-81m1
36-Kr-82g
36-Kr-83g
36-Kr-83m1
36-Kr-84g
37-Rb-76g
37-Rb-77g
37-Rb-78g
Cross Section (barns)
Incident Energy (MeV)
8
40-Zr-91

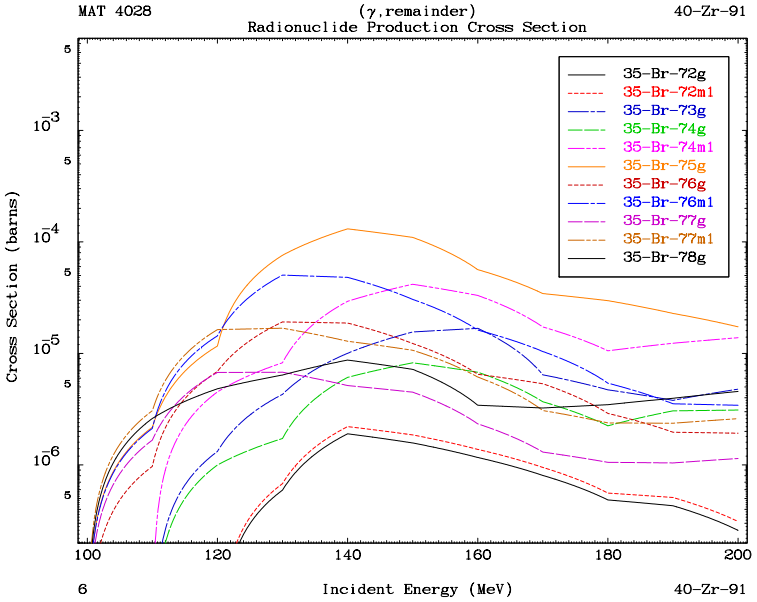
MAT 4028
(γ,remainder)
40-Zr-91
Radionuclide Production Cross Section
35-Br-72g
35-Br-72m1
35-Br-73g
35-Br-74g
35-Br-74m1
35-Br-75g
35-Br-76g
35-Br-76m1
35-Br-77g
35-Br-77m1
35-Br-78g
Cross Section (barns)
Incident Energy (MeV)
6
40-Zr-91

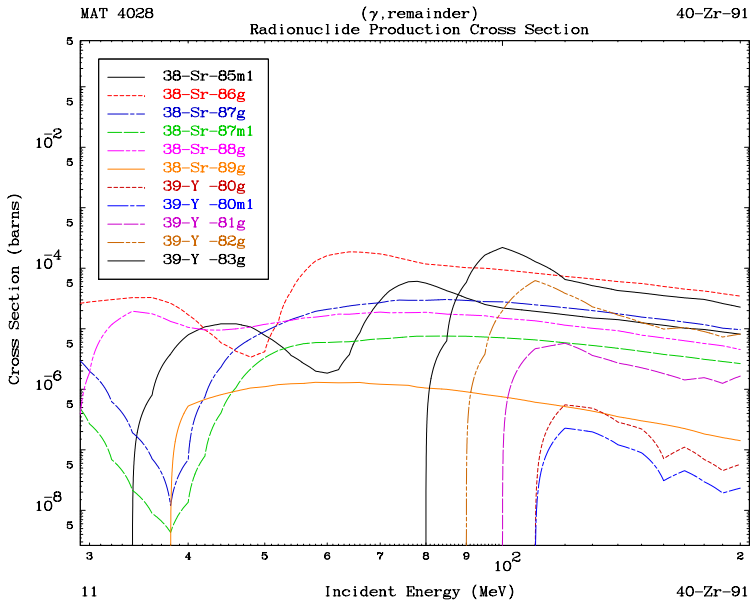
MAT 4028
(γ,remainder)
40-Zr-91
Radionuclide Production Cross Section
38-Sr-85m1
38-Sr-86g
38-Sr-87g
38-Sr-87m1
38-Sr-88g
38-Sr-89g
39-Y -80g
39-Y -80m1
39-Y -81g
39-Y -82g
39-Y -83g
Cross Section (barns)
Incident Energy (MeV)
11
40-Zr-91

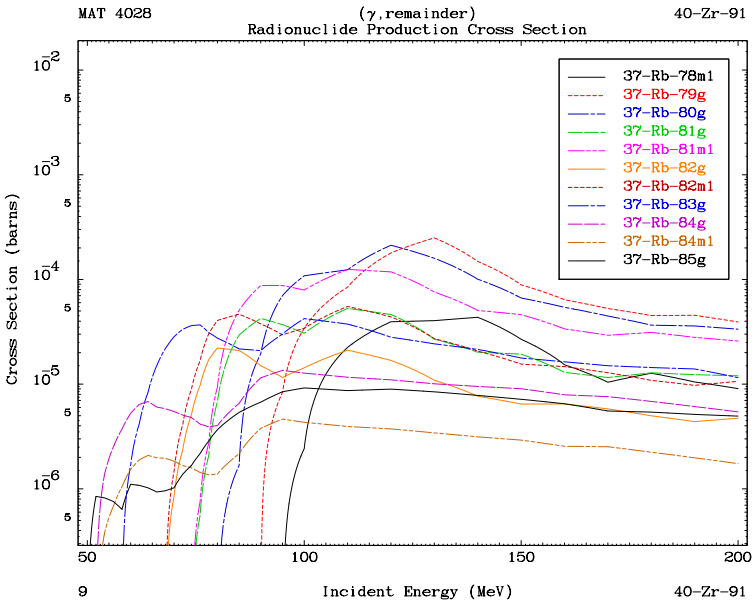
MAT 4028
(γ,remainder)
40-Zr-91
Radionuclide Production Cross Section
37-Rb-78m1
37-Rb-79g
37-Rb-80g
37-Rb-81g
37-Rb-81m1
37-Rb-82g
37-Rb-82m1
37-Rb-83g
37-Rb-84g
37-Rb-84m1
37-Rb-85g
Cross Section (barns)
Incident Energy (MeV)
9
40-Zr-91

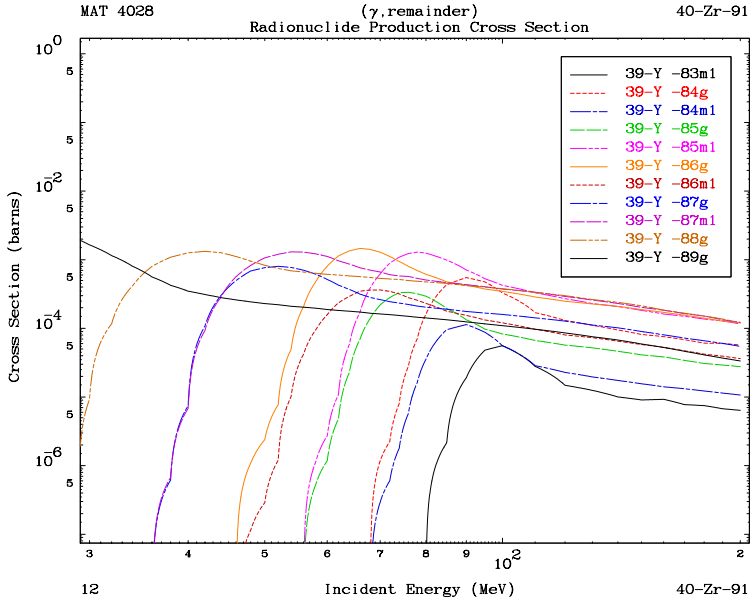
MAT 4028
(γ,remainder)
40-Zr-91
Radionuclide Production Cross Section
39-Y -83m1
39-Y -84g
39-Y -84m1
39-Y -85g
39-Y -85m1
39-Y -86g
39-Y -86m1
39-Y -87g
39-Y -87m1
39-Y -88g
39-Y -89g
Cross Section (barns)
Incident Energy (MeV)
12
40-Zr-91

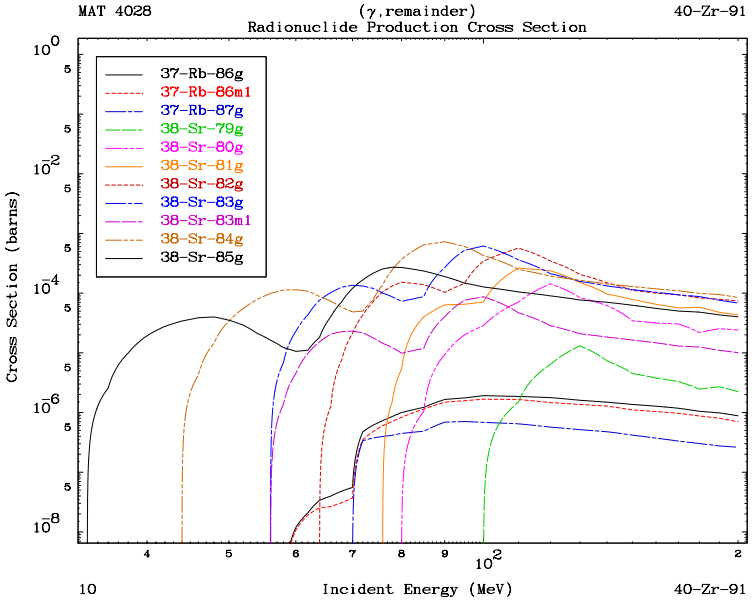
MAT 4028
(γ,remainder)
40-Zr-91
Radionuclide Production Cross Section
37-Rb-86g
37-Rb-86m1
37-Rb-87g
38-Sr-79g
38-Sr-80g
38-Sr-81g
38-Sr-82g
38-Sr-83g
38-Sr-83m1
38-Sr-84g
38-Sr-85g
Cross Section (barns)
Incident Energy (MeV)
10
40-Zr-91

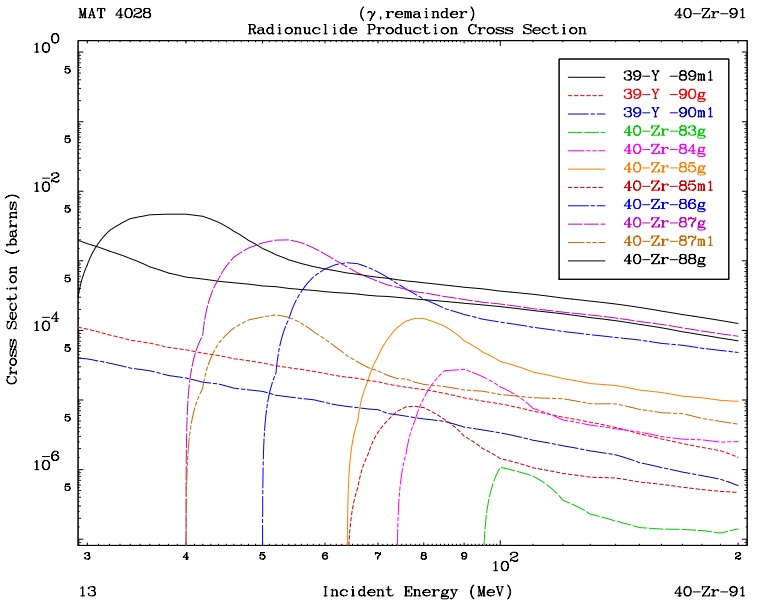
MAT 4028
(γ,remainder)
40-Zr-91
Radionuclide Production Cross Section
39-Y -89m1
39-Y -90g
39-Y -90m1
40-Zr-83g
40-Zr-84g
40-Zr-85g
40-Zr-85m1
40-Zr-86g
40-Zr-87g
40-Zr-87m1
40-Zr-88g
Cross Section (barns)
Incident Energy (MeV)
13
40-Zr-91

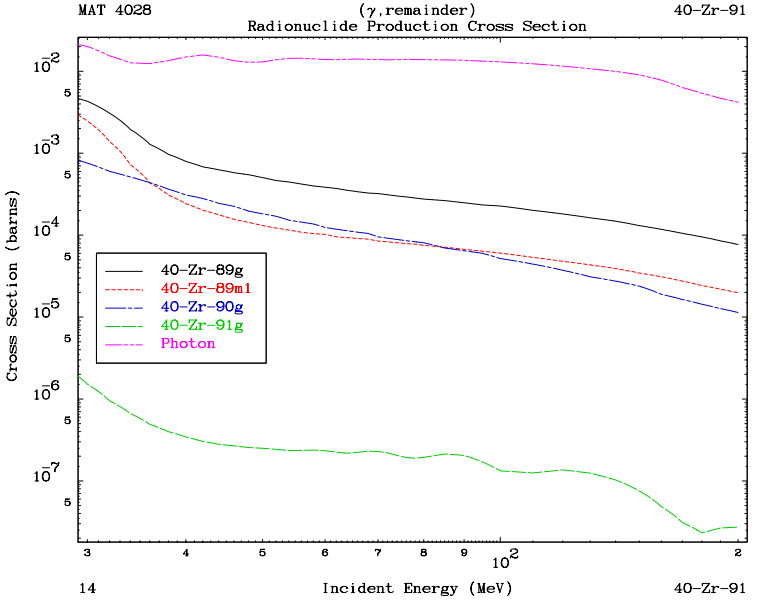
MAT 4028
(γ,remainder)
40-Zr-91
Radionuclide Production Cross Section
40-Zr-89g
40-Zr-89m1
40-Zr-90g
40-Zr-91g
Photon
Cross Section (barns)
Incident Energy (MeV)
14
40-Zr-91

A.4 Example of ^{12}C File Processing (File Type 3: CNDC - Light Nuclides)

A.4.1 Transport Library

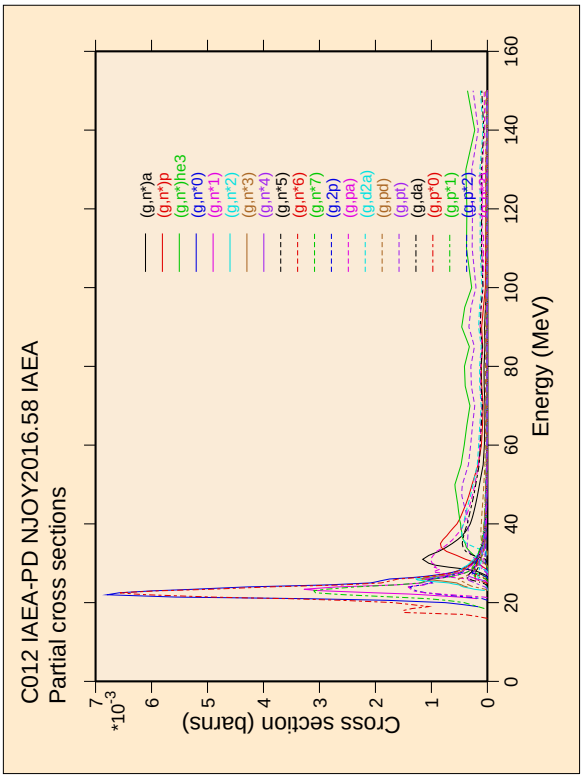

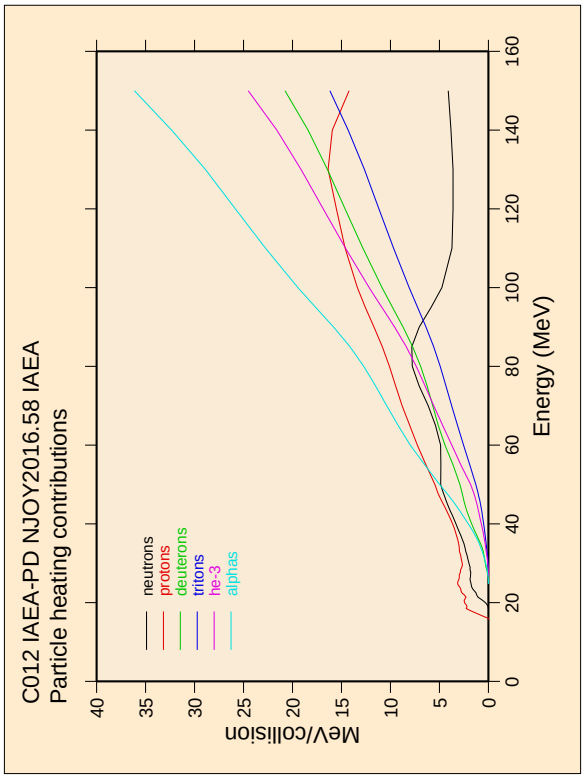

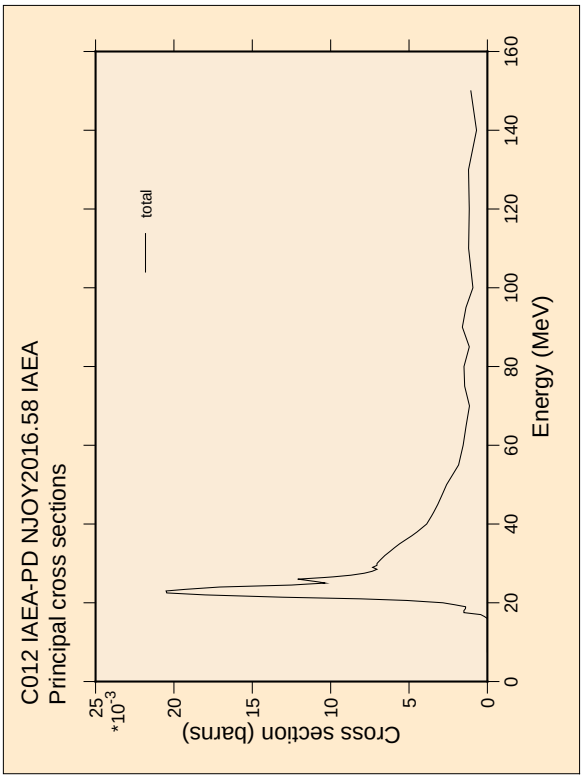

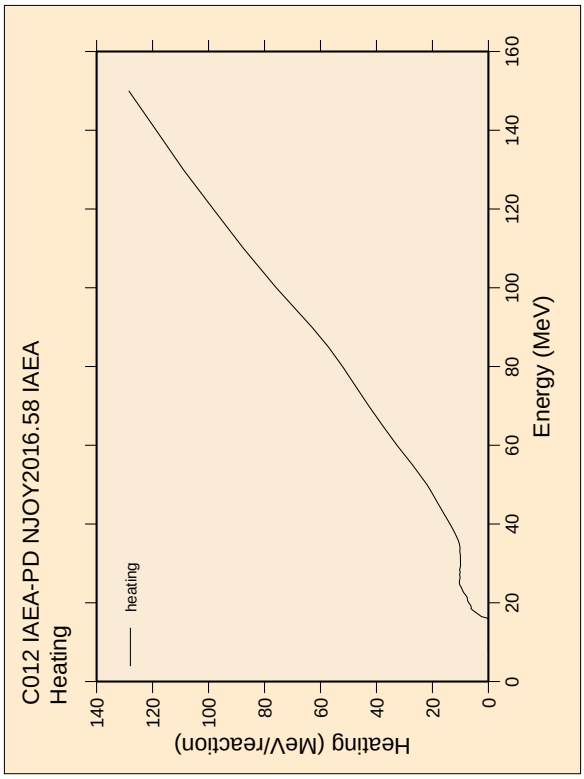

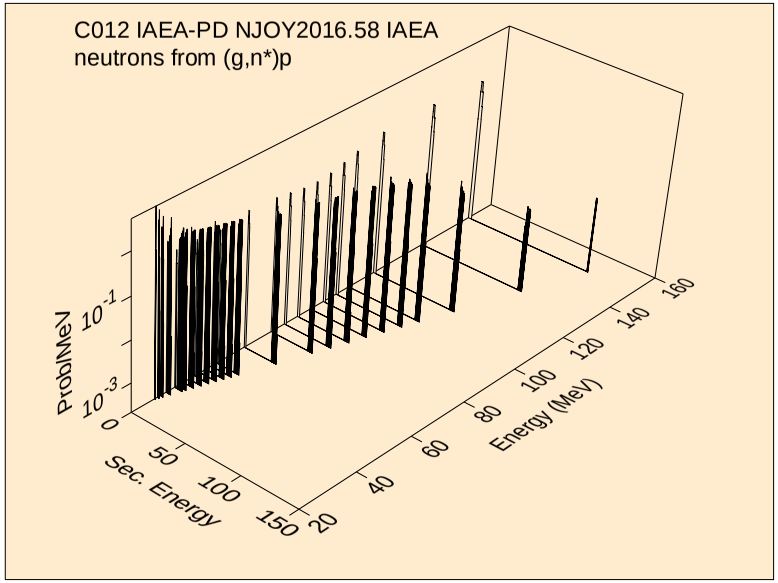
C012 IAEA-PD NJOY2016.58 IAEA
neutrons from (g,n*)p
Prob/MeV
Sec. Energy
Energy (MeV)

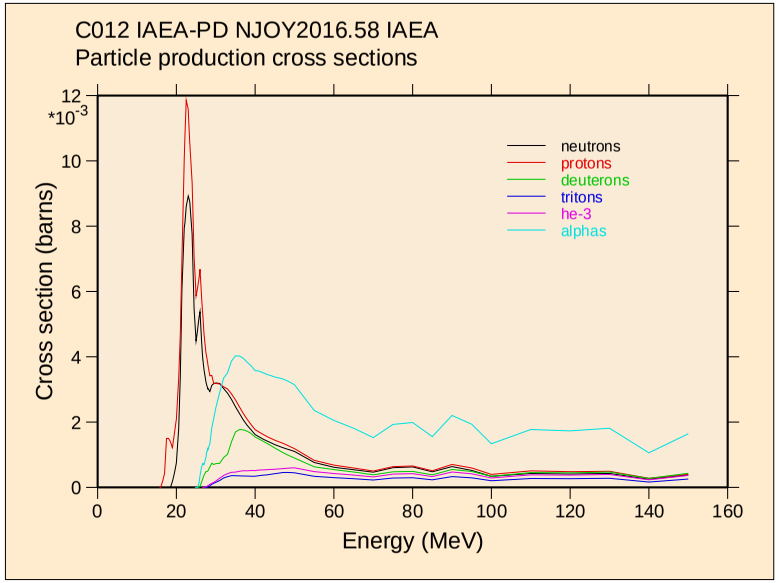
C012 IAEA-PD NJOY2016.58 IAEA
Particle production cross sections
Cross section (barns)
Energy (MeV)
neutrons
protons
deuterons
tritons
he-3
alphas

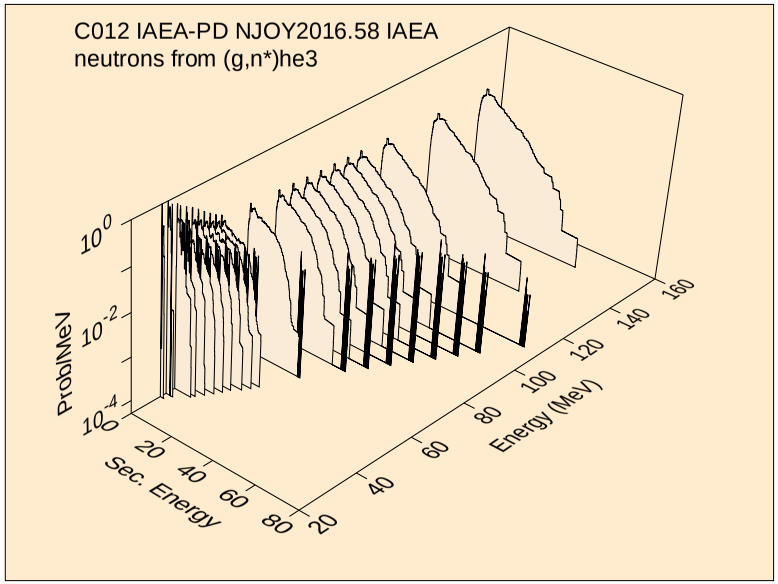
C012 IAEA-PD NJOY2016.58 IAEA
neutrons from (g,n*)he3
Prob/MeV
Sec. Energy
Energy (MeV)

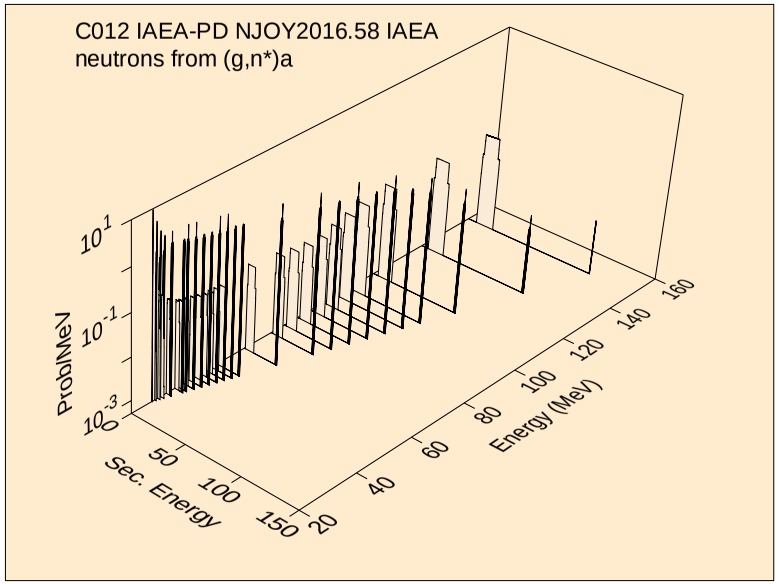
C012 IAEA-PD NJOY2016.58 IAEA
neutrons from (g,n*)a
Prob/MeV
Sec. Energy
Energy (MeV)

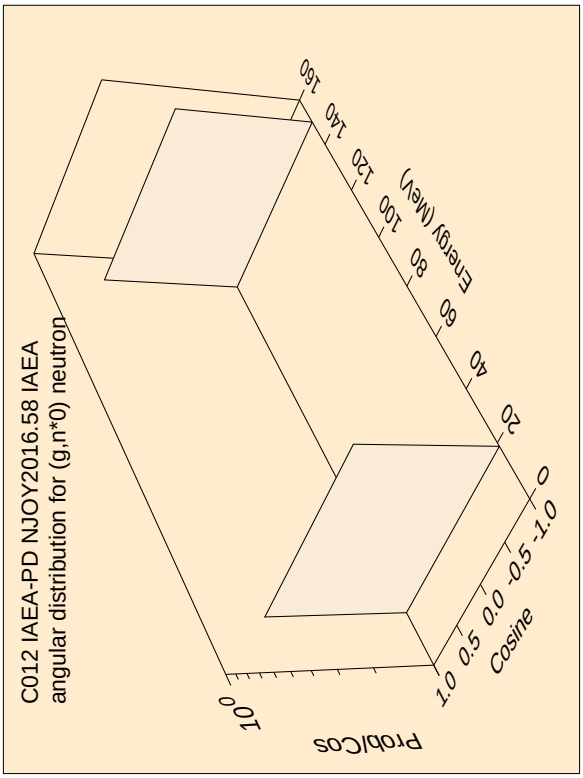
C012 IAEA-PD NJOY2016.58 IAEA
angular distribution for (g,n*0) neutron
Prob/Cos
Energy (MeV)
Cosine

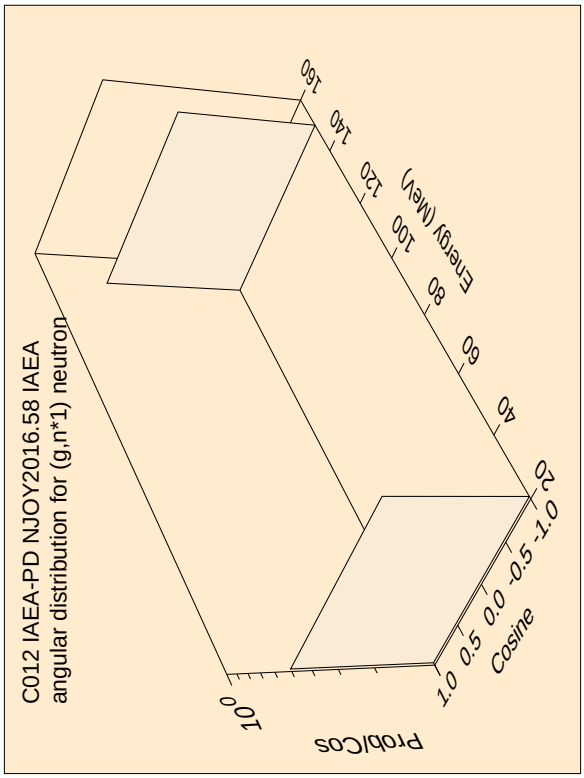
C012 IAEA-PD NJOY2016.58 IAEA
angular distribution for (g,n*1) neutron
Prob/Cos
Energy (MeV)
Cosine

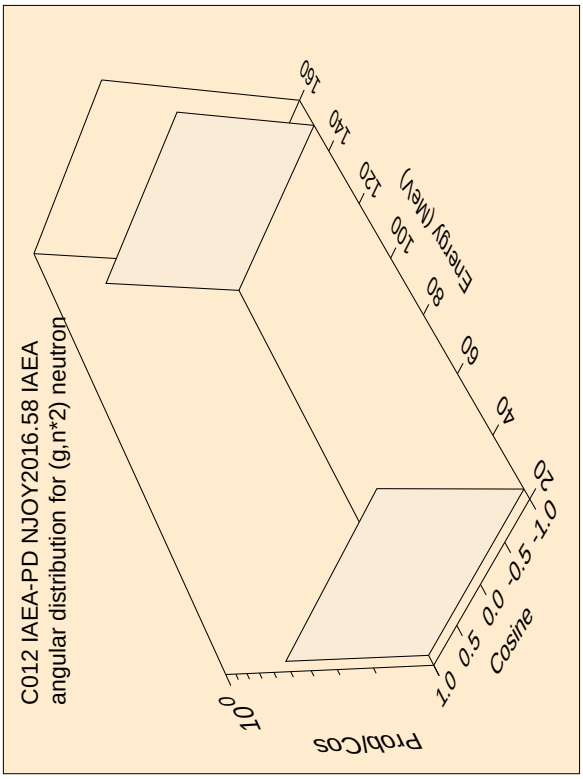
C012 IAEA-PD NJOY2016.58 IAEA
angular distribution for (g,n*2) neutron
Prob/Cos
Energy (MeV)
Cosine

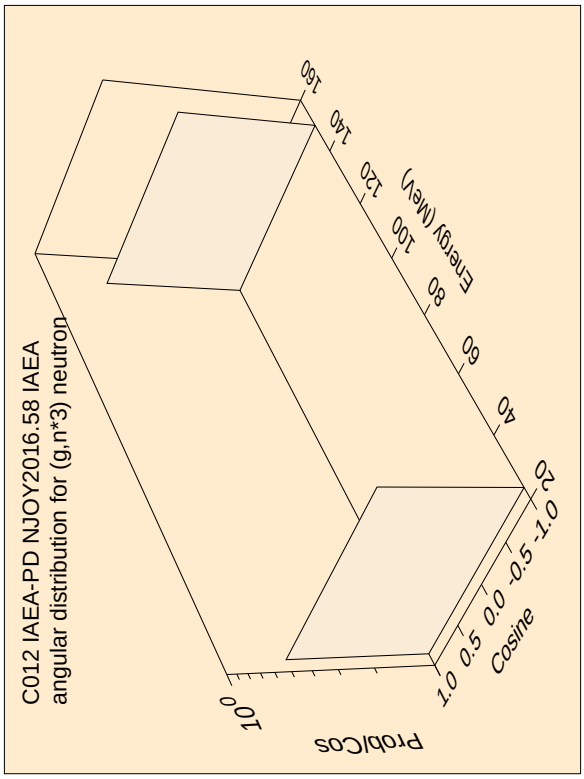
C012 IAEA-PD NJOY2016.58 IAEA
angular distribution for (g,n*3) neutron
Prob/Cos
Energy (MeV)
Cosine

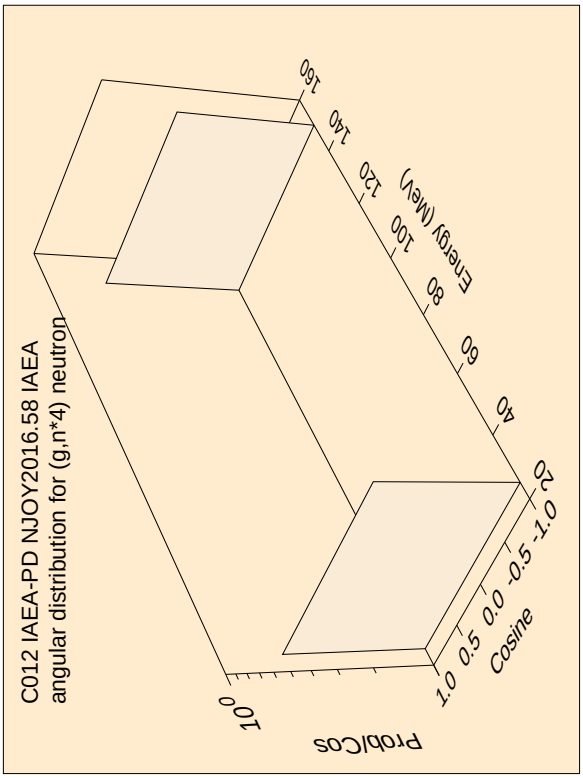
C012 IAEA-PD NJOY2016.58 IAEA
angular distribution for (g,n*4) neutron
Prob/Cos
Energy (MeV)
Cosine

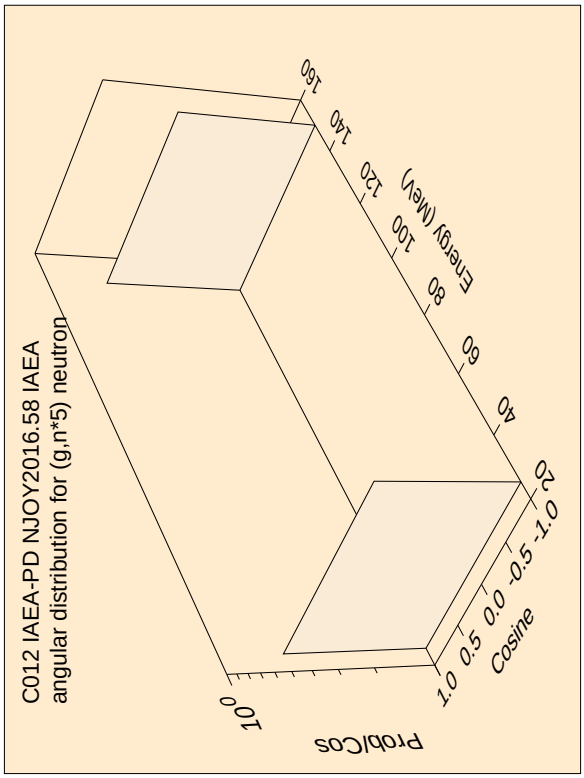
C012 IAEA-PD NJOY2016.58 IAEA
angular distribution for (g,n*5) neutron
Prob/Cos
Energy (MeV)
Cosine

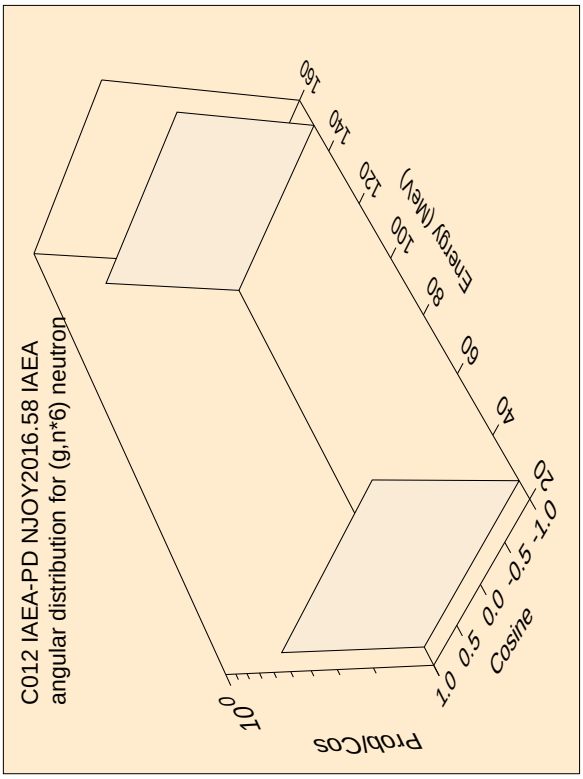
C012 IAEA-PD NJOY2016.58 IAEA
angular distribution for (g,n*6) neutron
Prob/Cos
Energy (MeV)
Cosine

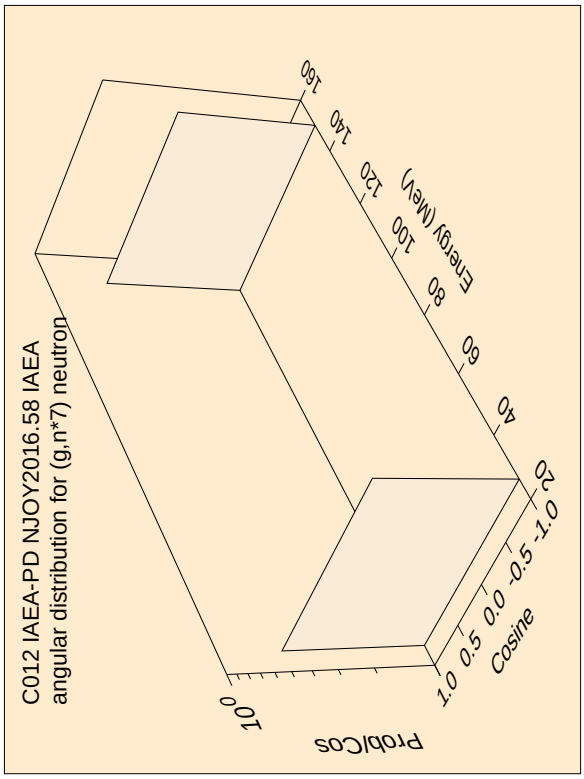
C012 IAEA-PD NJOY2016.58 IAEA
angular distribution for (g,n*7) neutron
Prob/Cos
Energy (MeV)
Cosine

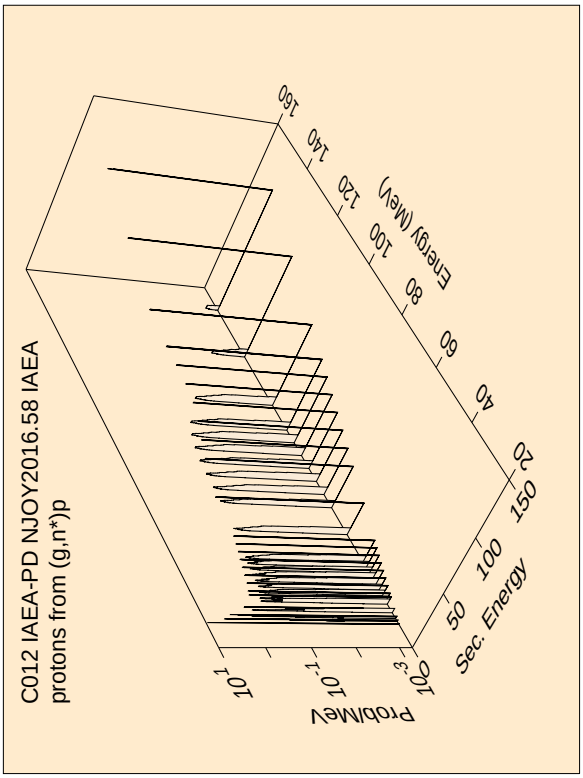
C012 IAEA-PD NJOY2016.58 IAEA
protons from (g,n*)p
Prob/MeV
Energy (Mev)
Sec. Energy

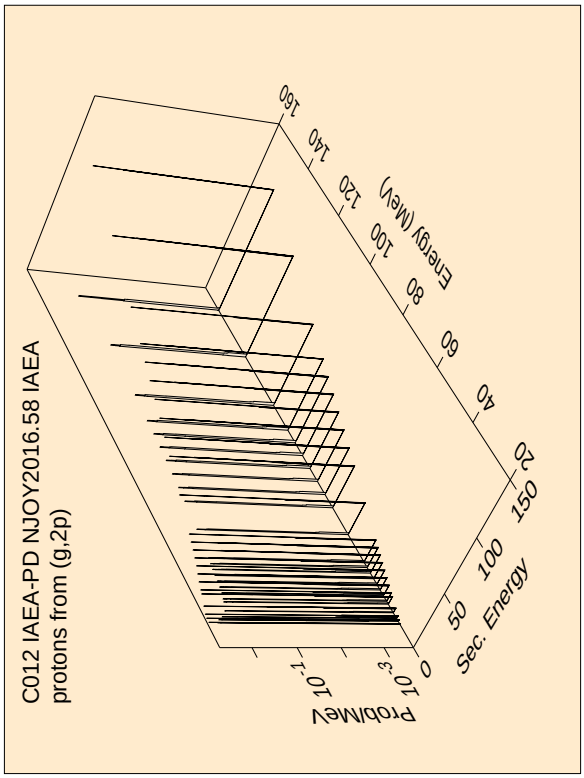
C012 IAEA-PD NJOY2016.58 IAEA
protons from (g,2p)
Prob/MeV
Energy (Mev)
Sec. Energy

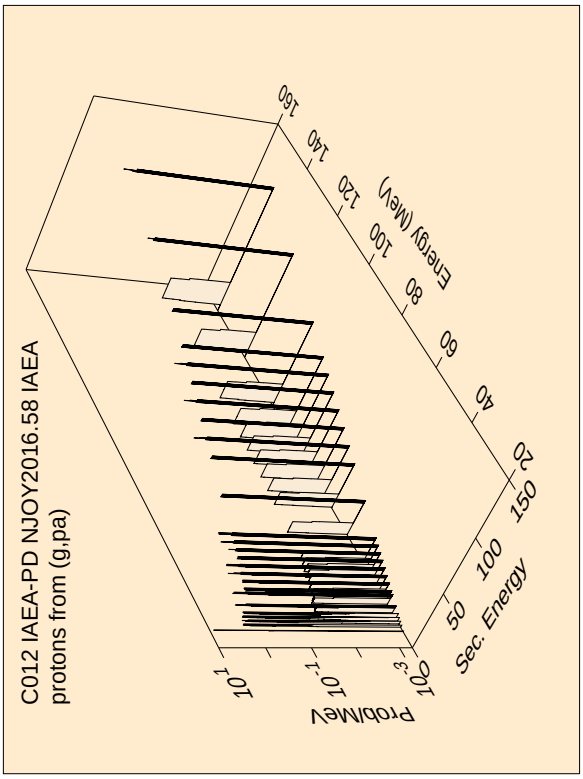
C012 IAEA-PD NJOY2016.58 IAEA
protons from (g,pa)
Prob/MeV
Energy (Mev)
Sec. Energy

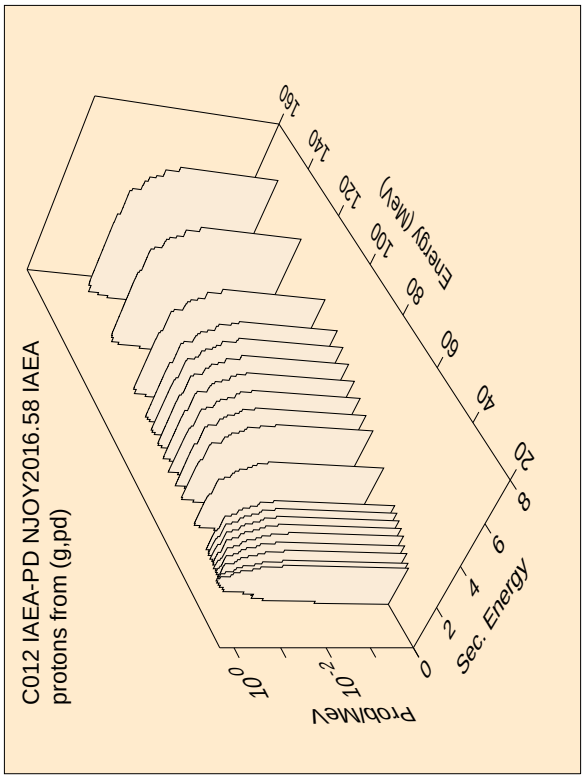
C012 IAEA-PD NJOY2016.58 IAEA
protons from (g,pd)
Prob/MeV
Energy (Mev)
Sec. Energy

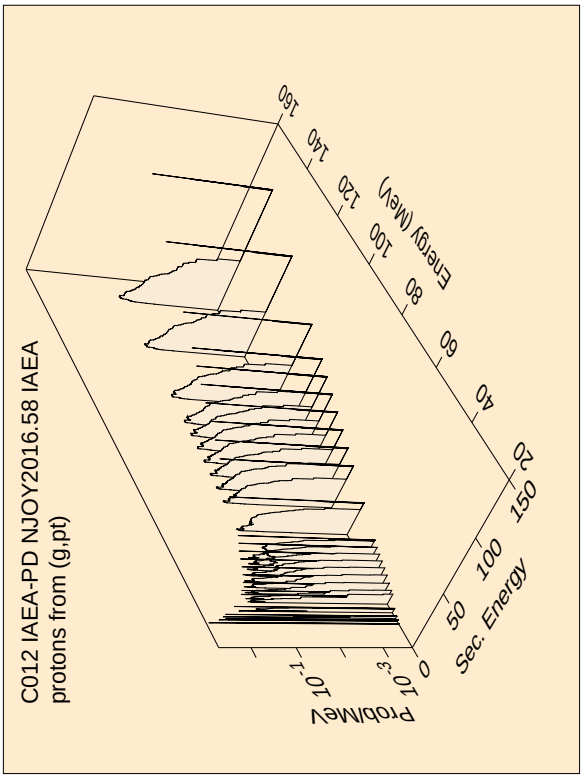
C012 IAEA-PD NJOY2016.58 IAEA
protons from (g,pt)
Prob/MeV
Sec. Energy
Energy (Mev)

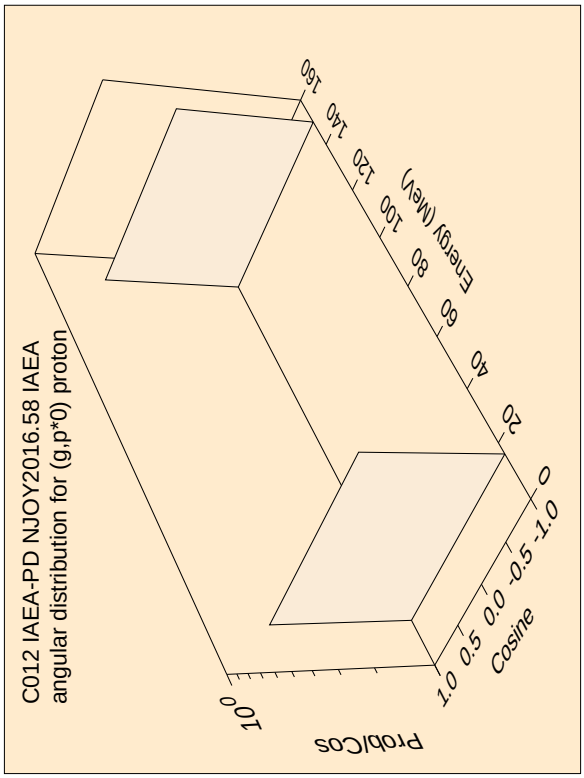
C012 IAEA-PD NJOY2016.58 IAEA
angular distribution for (g,p*0) proton
Prob/Cos
Cosine
Energy (Mev)

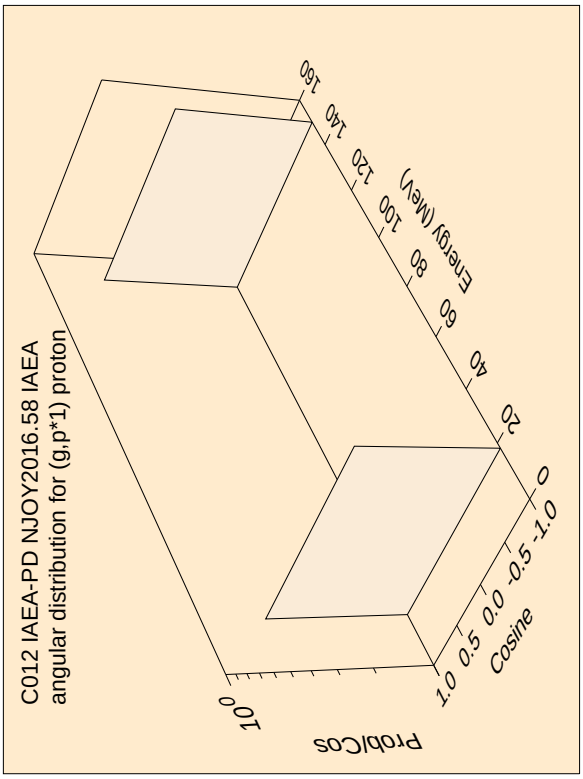
C012 IAEA-PD NJOY2016.58 IAEA
angular distribution for (g,p*1) proton
Prob/Cos
Cosine
Energy (Mev)

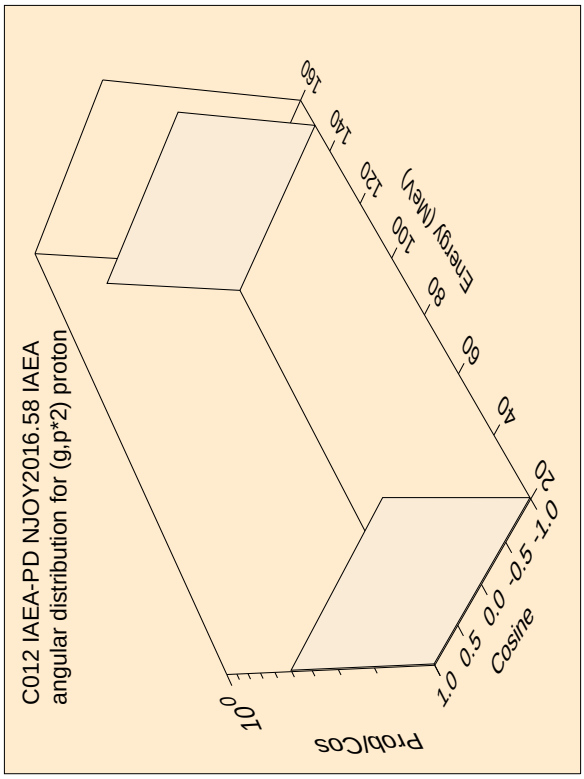
C012 IAEA-PD NJOY2016.58 IAEA
angular distribution for (g,p*2) proton
Prob/Cos
Cosine
Energy (Mev)

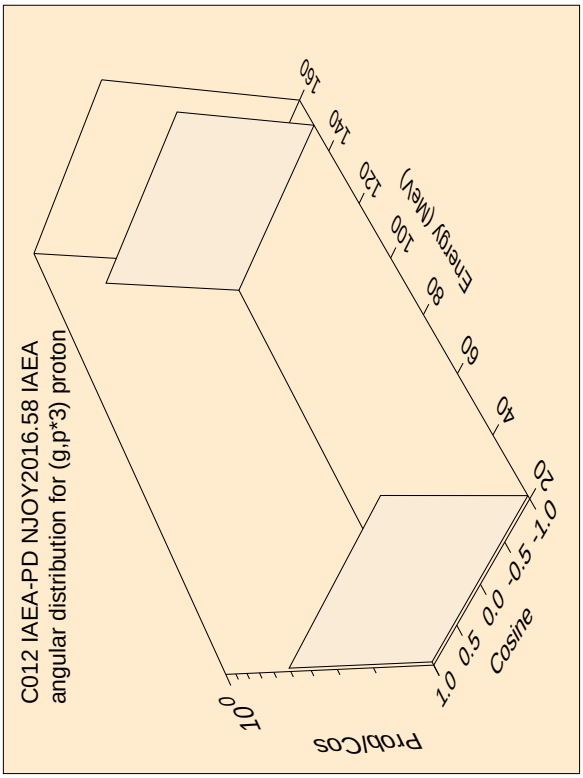
C012 IAEA-PD NJOY2016.58 IAEA
angular distribution for (g,p*3) proton
Prob/Cos
Energy (MeV)
Cosine

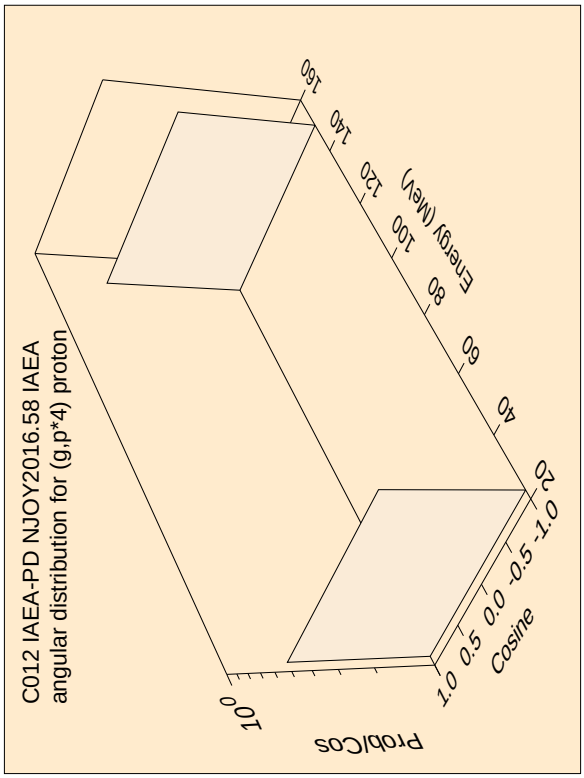
C012 IAEA-PD NJOY2016.58 IAEA
angular distribution for (g,p*4) proton
Prob/Cos
Energy (MeV)
Cosine

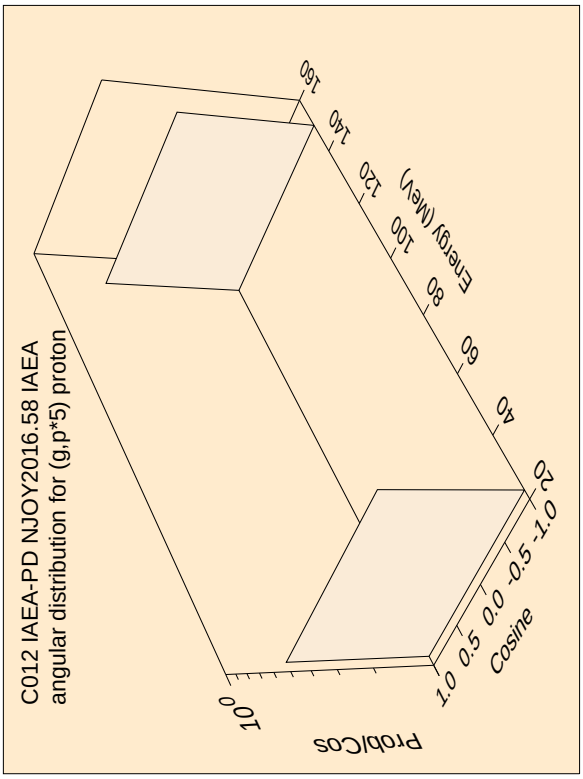
C012 IAEA-PD NJOY2016.58 IAEA
angular distribution for (g,p*5) proton
Prob/Cos
Energy (MeV)
Cosine

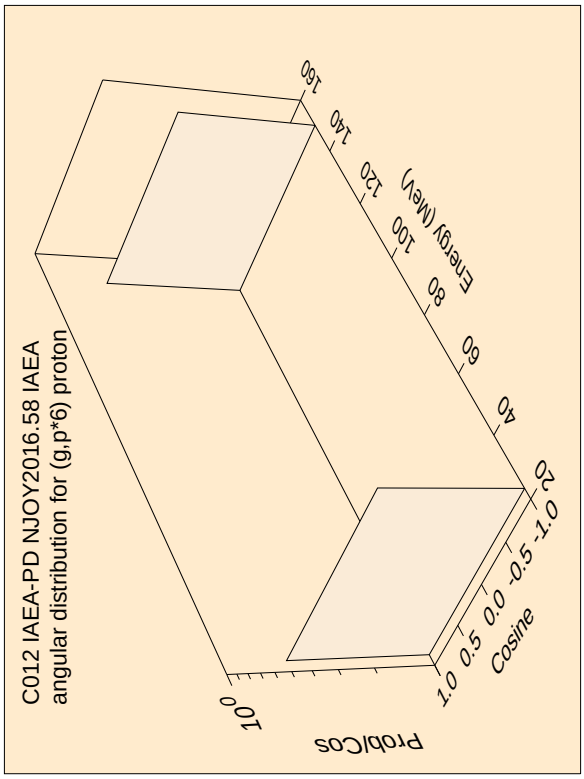
C012 IAEA-PD NJOY2016.58 IAEA
angular distribution for (g,p*6) proton
Prob/Cos
Energy (MeV)
Cosine

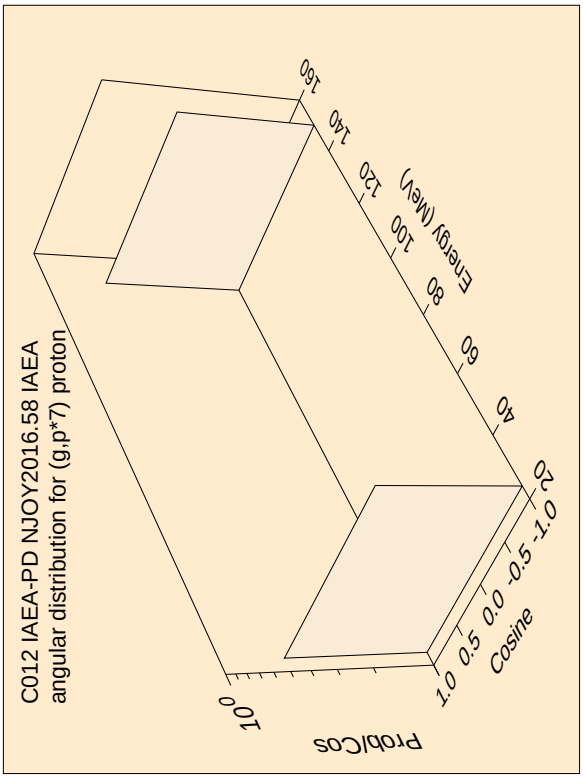
C012 IAEA-PD NJOY2016.58 IAEA
angular distribution for (g,p*7) proton
Prob/Cos
Cosine
Energy (Mev)

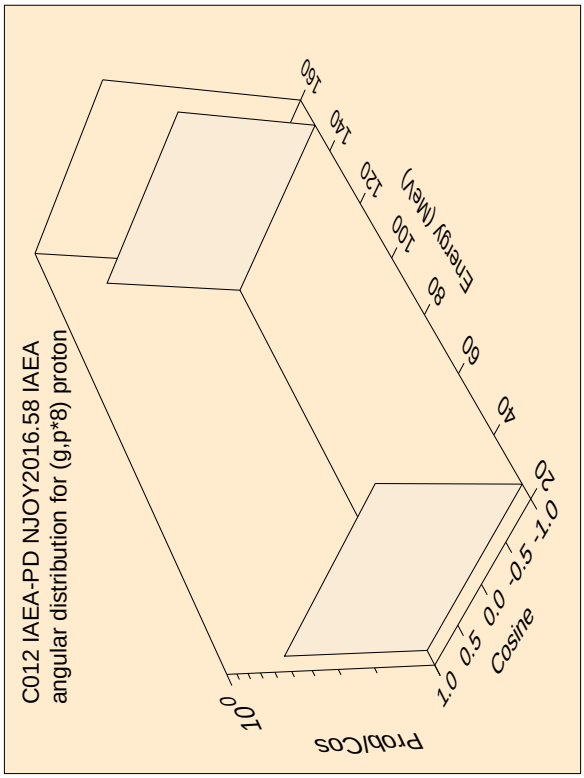
C012 IAEA-PD NJOY2016.58 IAEA
angular distribution for (g,p*8) proton
Prob/Cos
Cosine
Energy (Mev)

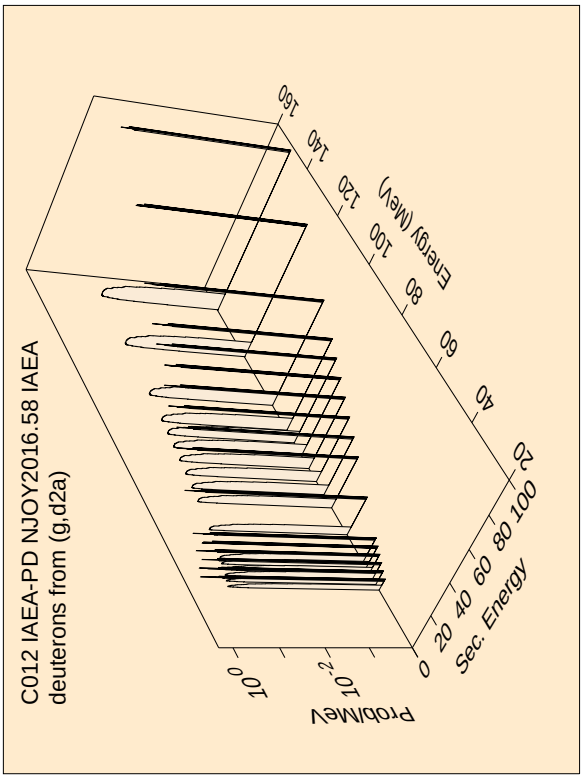
C012 IAEA-PD NJOY2016.58 IAEA
deuterons from (g,d2a)
Prob/MeV
Sec. Energy
Energy (Mev)

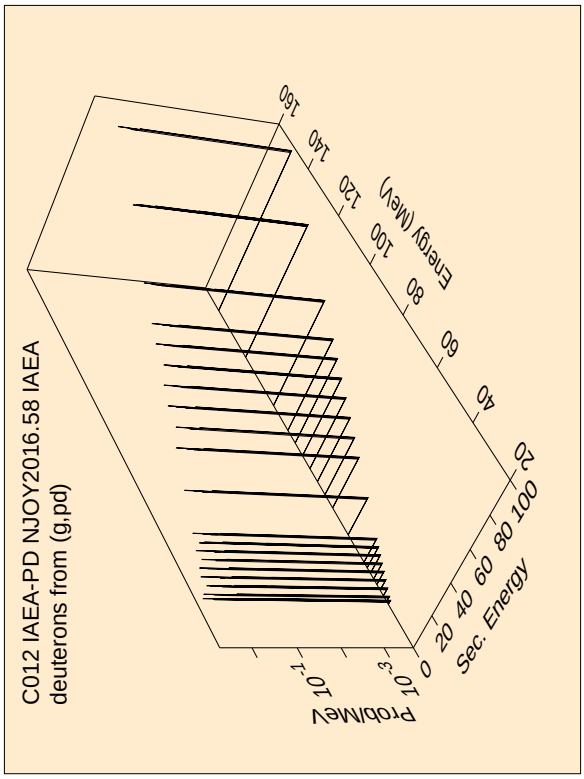
C012 IAEA-PD NJOY2016.58 IAEA
deuterons from (g,pd)
Prob/MeV
Sec. Energy
Energy (Mev)

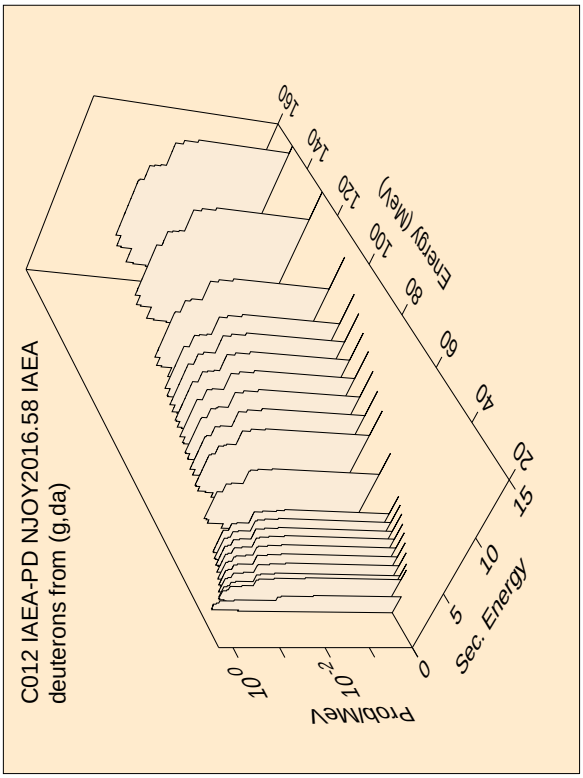
C012 IAEA-PD NJOY2016.58 IAEA
deuterons from (g,da)
Prob/MeV
Sec. Energy
Energy (Mev)

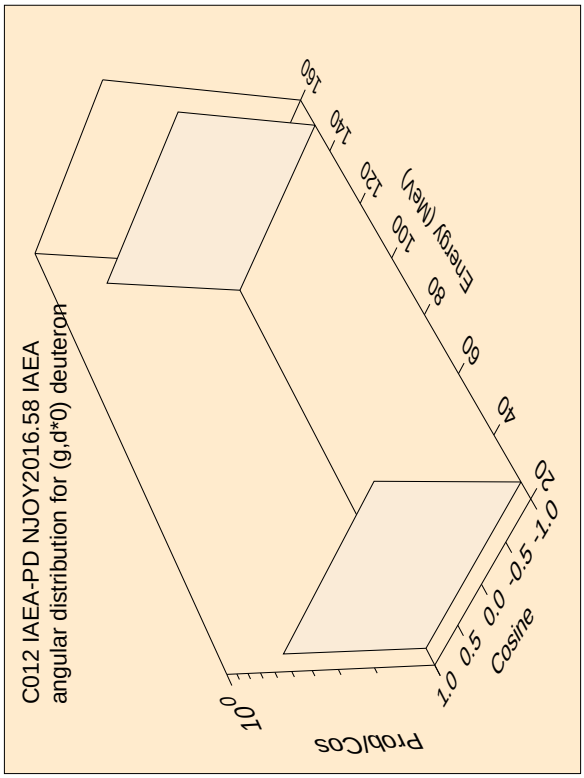
C012 IAEA-PD NJOY2016.58 IAEA
angular distribution for (g,d*0) deuteron
Prob/Cos
Cosine
Energy (Mev)

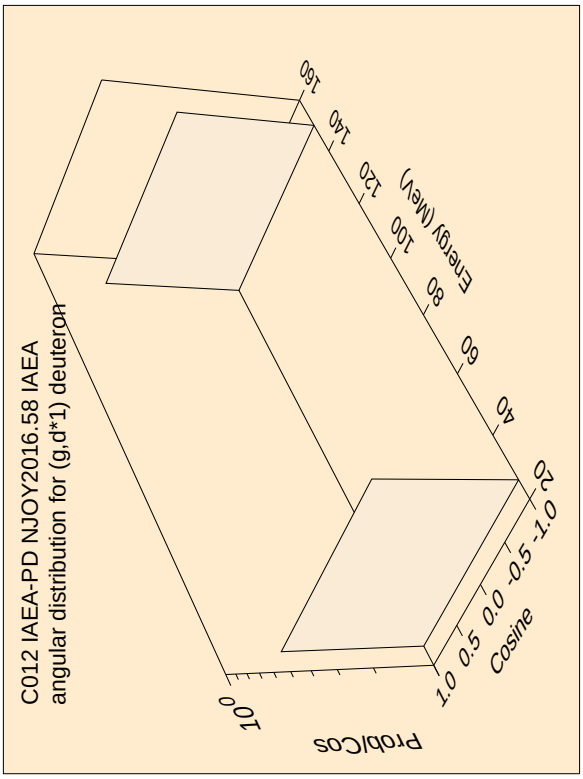
C012 IAEA-PD NJOY2016.58 IAEA
angular distribution for (g,d*1) deuteron
Prob/Cos
Cosine
Energy (Mev)

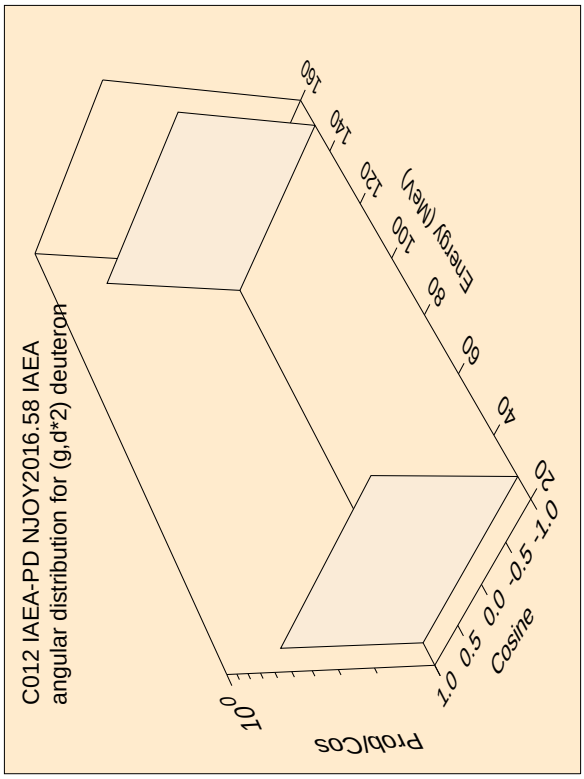
C012 IAEA-PD NJOY2016.58 IAEA
angular distribution for (g,d*2) deuteron
Prob/Cos
Cosine
Energy (Mev)

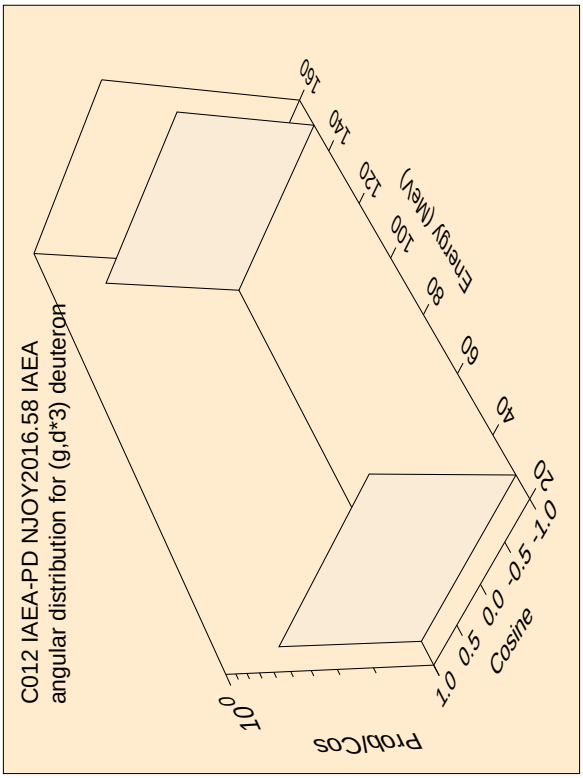
C012 IAEA-PD NJOY2016.58 IAEA
angular distribution for (g,d*3) deuteron
Prob/Cos
Cosine
Energy (Mev)

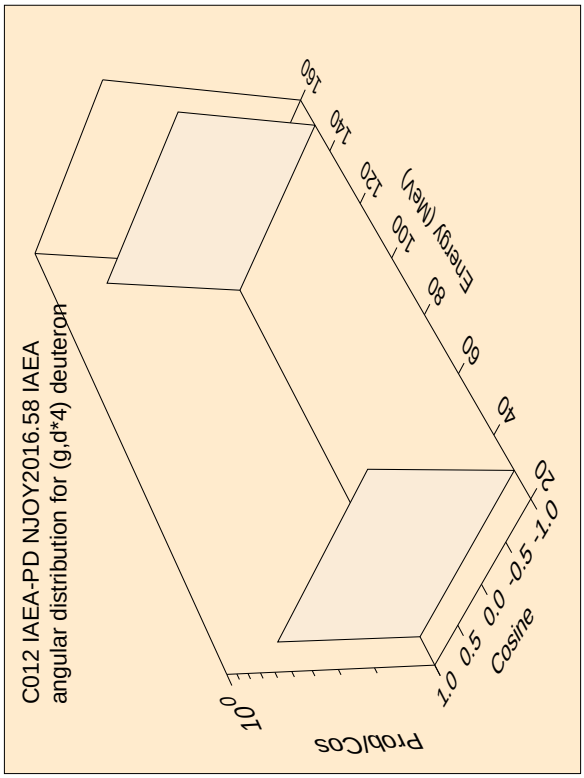
C012 IAEA-PD NJOY2016.58 IAEA
angular distribution for (g,d*4) deuteron
Prob/Cos
Cosine
Energy (Mev)

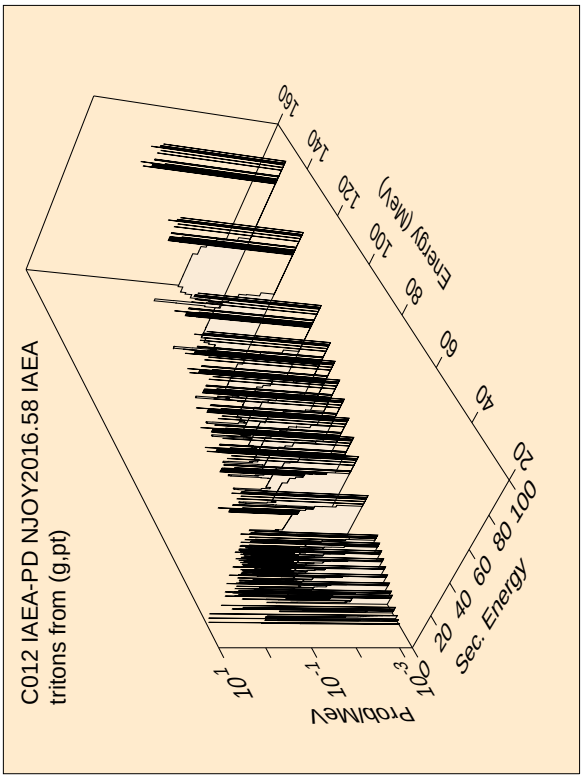
C012 IAEA-PD NJOY2016.58 IAEA
tritons from (g,pt)
Prob/MeV
Sec. Energy
Energy (Mev)

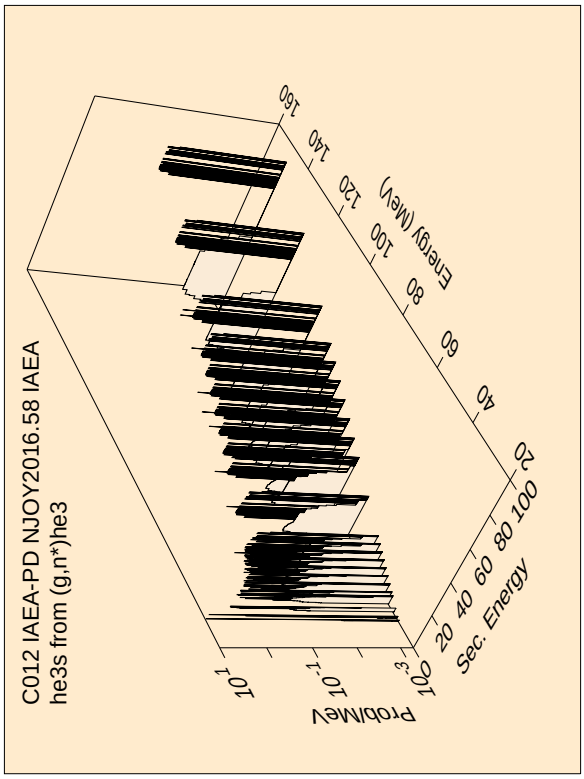
C012 IAEA-PD NJOY2016.58 IAEA
he3s from (g,n*)he3
Prob/MeV
Sec. Energy
Energy (Mev)

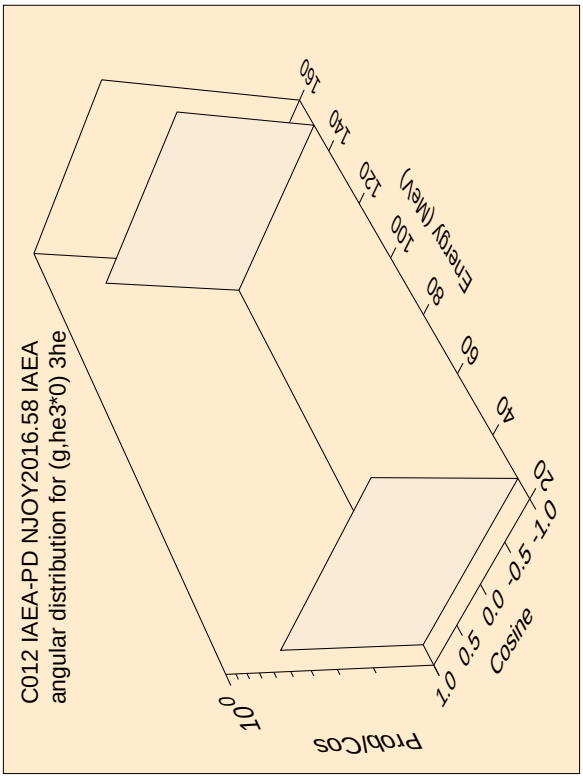
C012 IAEA-PD NJOY2016.58 IAEA
angular distribution for (g,he3*0) 3he
Prob/Cos
Cosine
Energy (Mev)

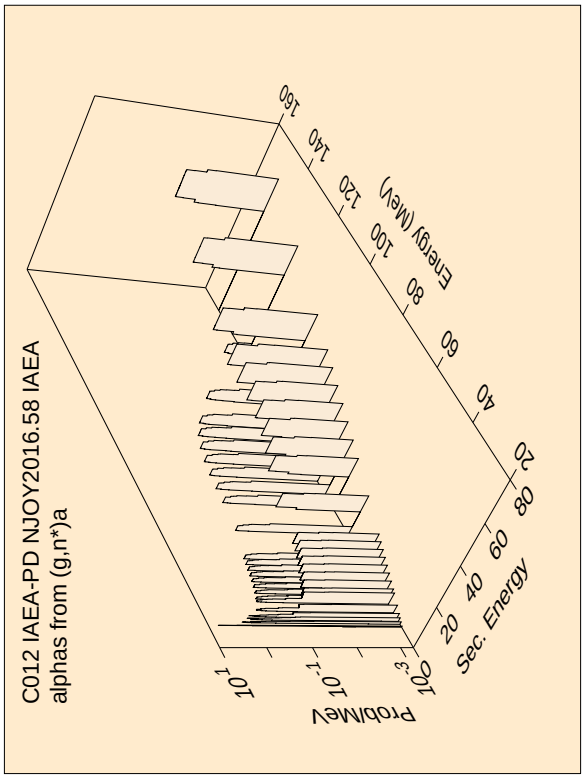
C012 IAEA-PD NJOY2016.58 IAEA
alphas from (g,n*)a
Prob/MeV
Sec. Energy
Energy (Mev)

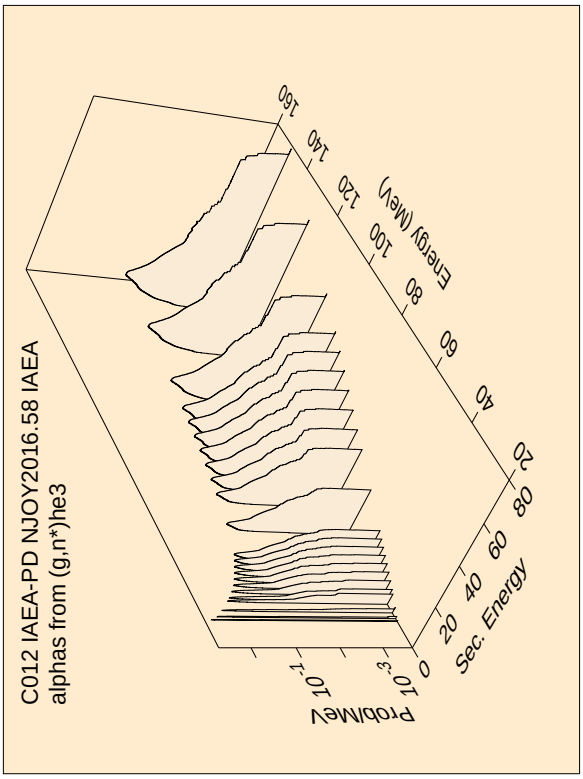
C012 IAEA-PD NJOY2016.58 IAEA
alphas from (g,n*)he3
Prob/MeV
Sec. Energy
Energy (Mev)

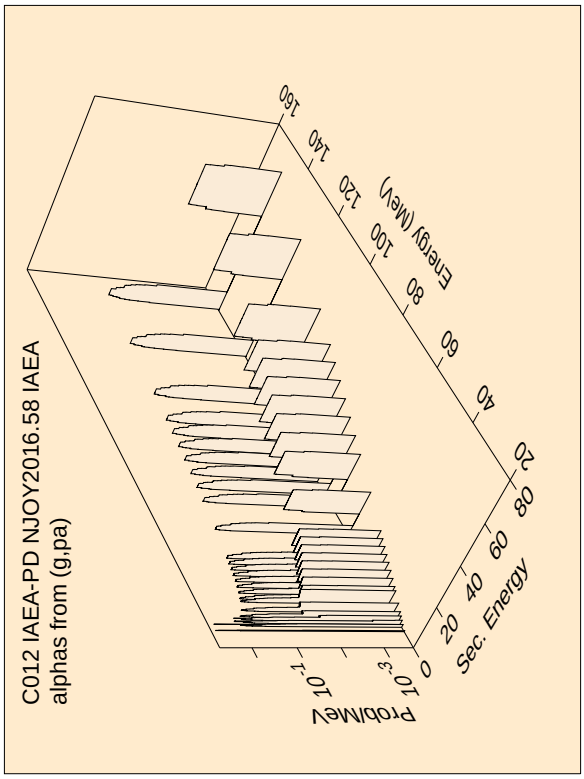
C012 IAEA-PD NJOY2016.58 IAEA
alphas from (g,pa)
Prob/MeV
Sec. Energy
Energy (Mev)

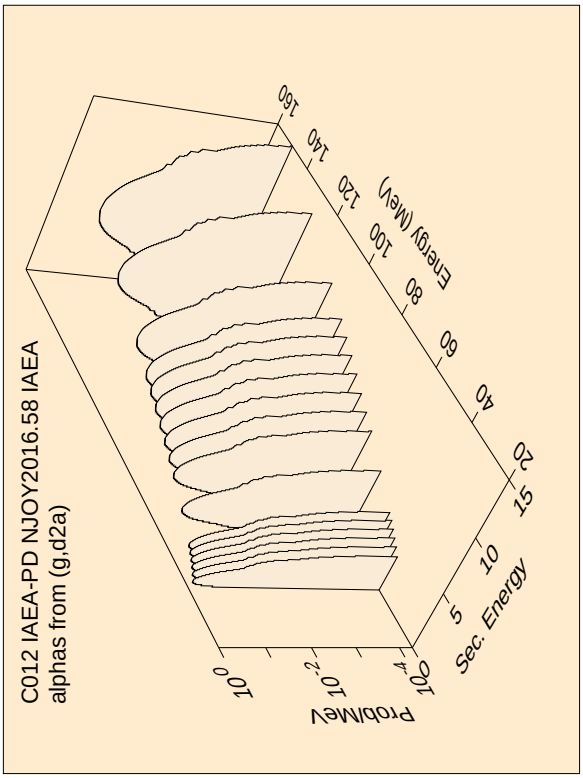
C012 IAEA-PD NJOY2016.58 IAEA
alphas from (g,d2a)
Prob/MeV
Energy (Mev)
Sec. Energy

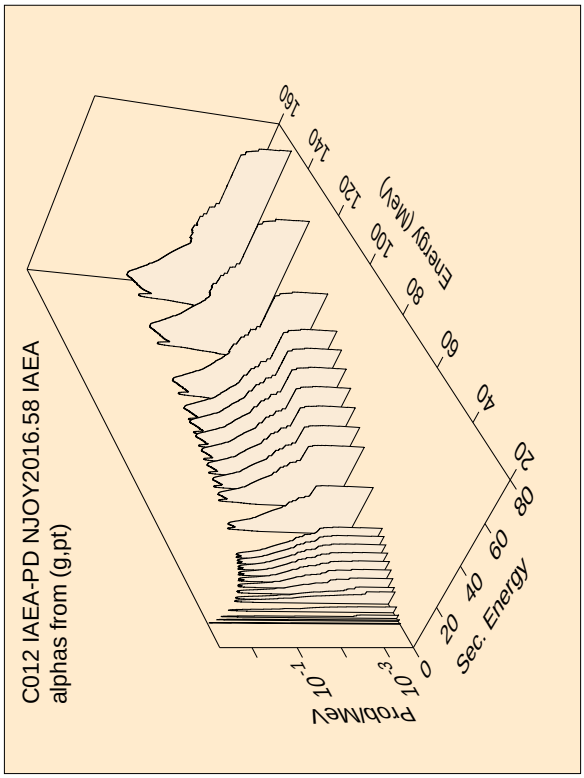
C012 IAEA-PD NJOY2016.58 IAEA
alphas from (g,pt)
Prob/MeV
Energy (Mev)
Sec. Energy

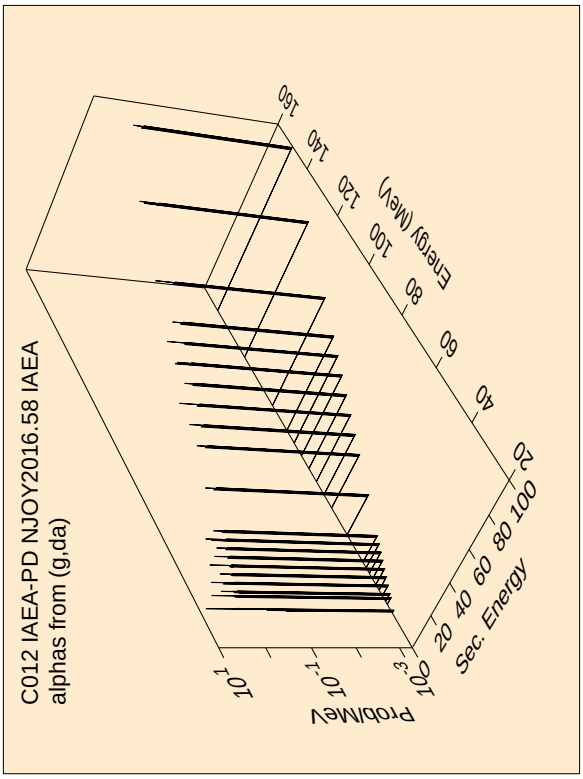
C012 IAEA-PD NJOY2016.58 IAEA
alphas from (g,da)
Prob/MeV
Energy (Mev)
Sec. Energy

A.4.2 Activation Library

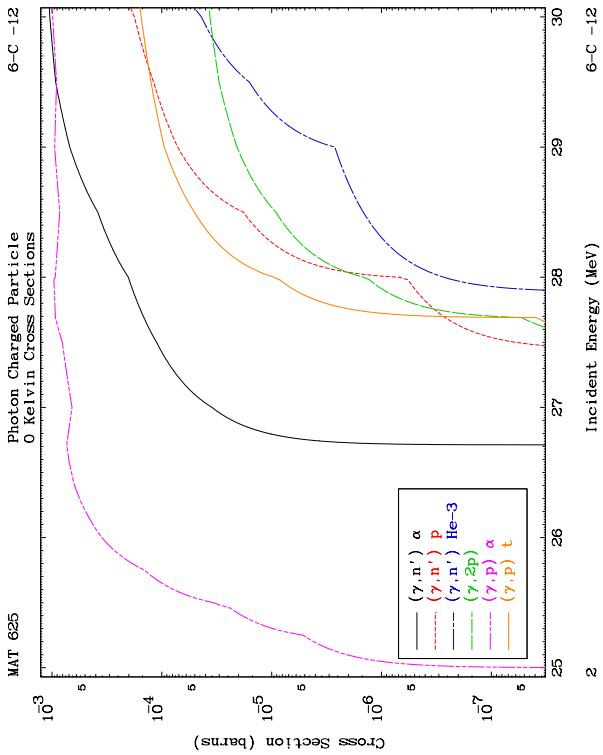

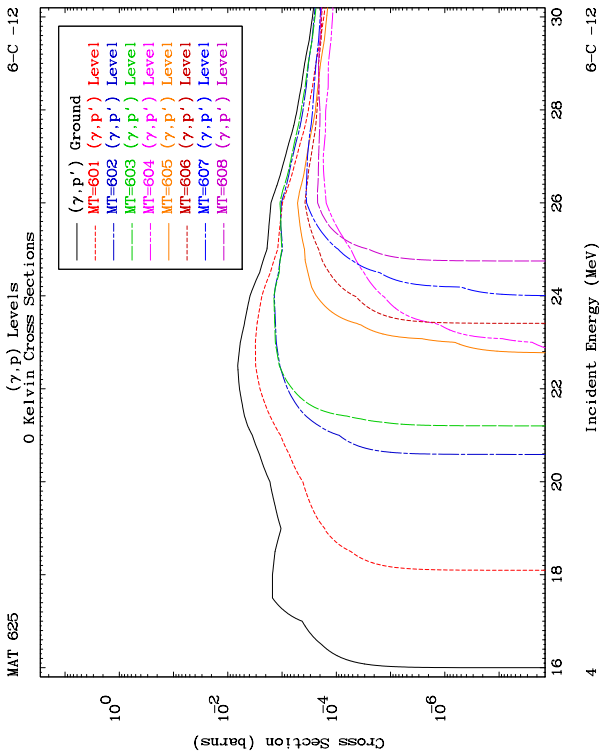

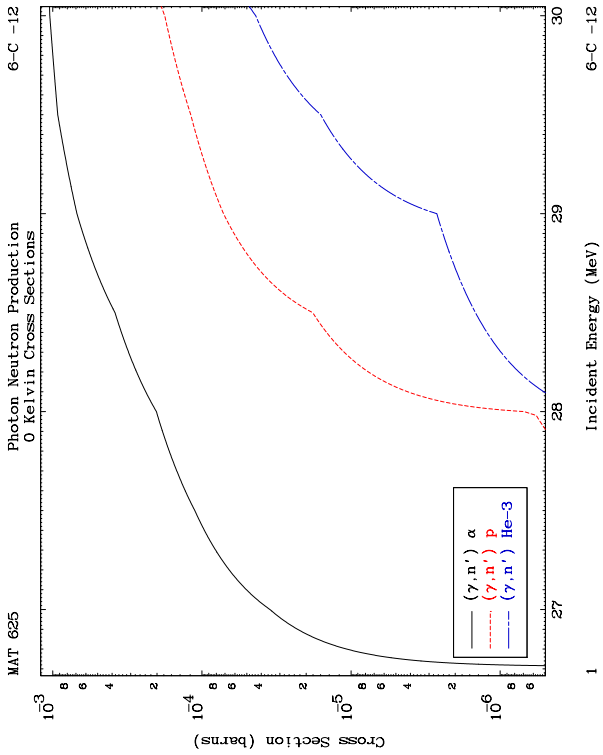

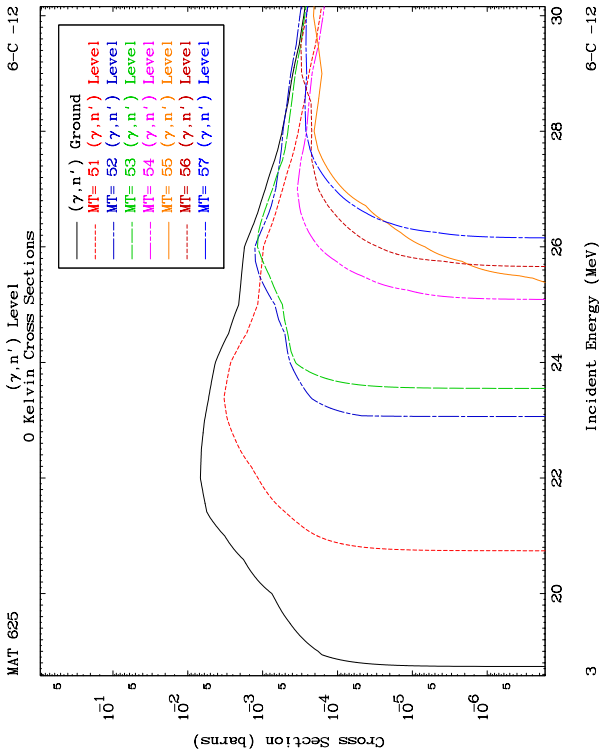

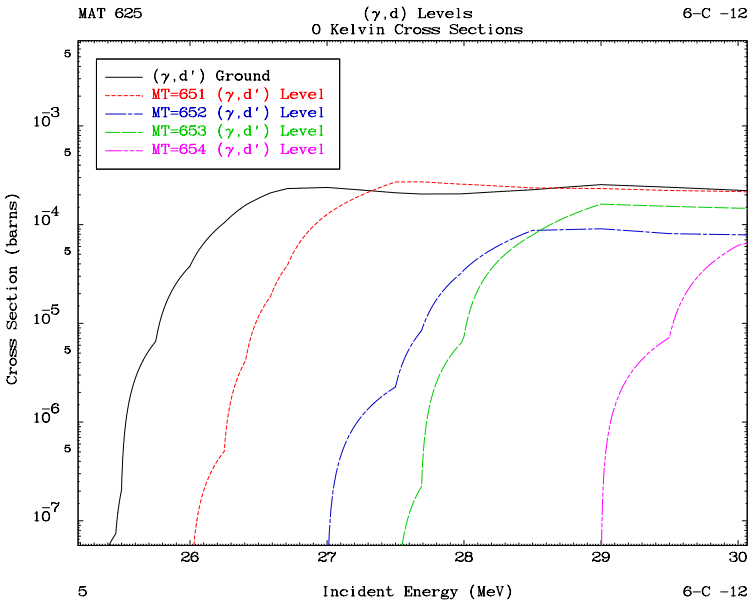
MAT 625
(γ,d) Levels
0 Kelvin Cross Sections
6-C -12
(γ,d') Ground
MT=651 (γ,d') Level
MT=652 (γ,d') Level
MT=653 (γ,d') Level
MT=654 (γ,d') Level
Cross Section (barns)
Incident Energy (MeV)
5
6-C -12

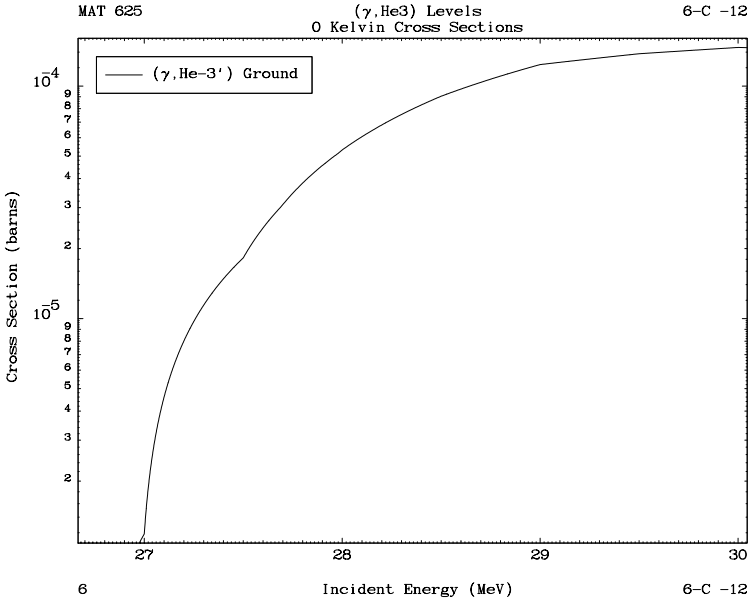
MAT 625
(γ,He3) Levels
0 Kelvin Cross Sections
6-C -12
(γ,He-3') Ground
Cross Section (barns)
Incident Energy (MeV)
6
6-C -12

A.5 Example of ^{182}W File Processing (File Type 4: CNDC - Midium-Mass Nuclides)

A.5.1 Transport Library

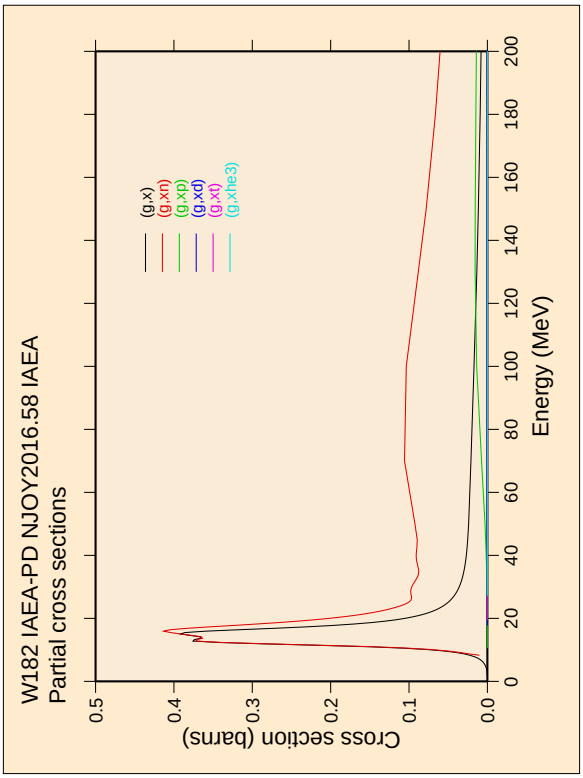

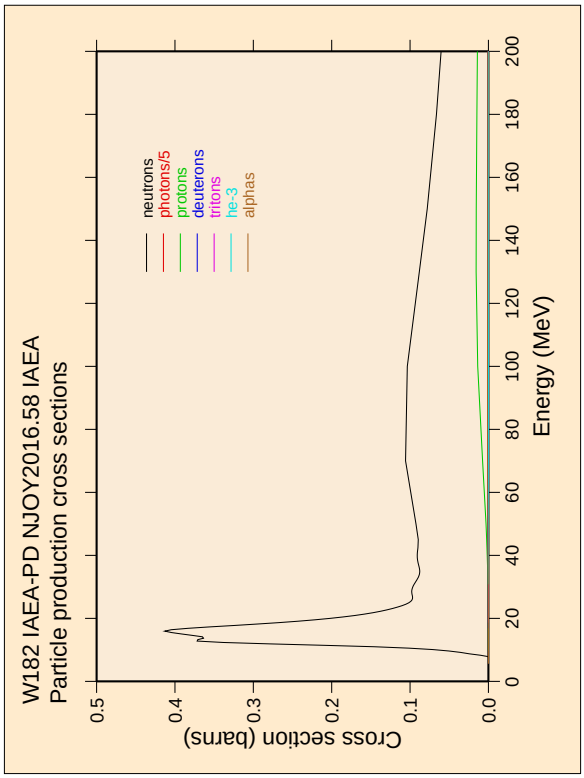

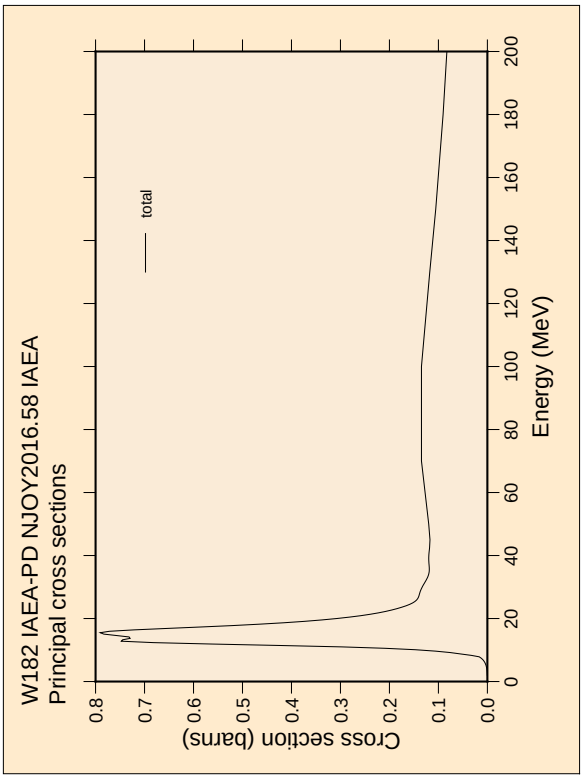

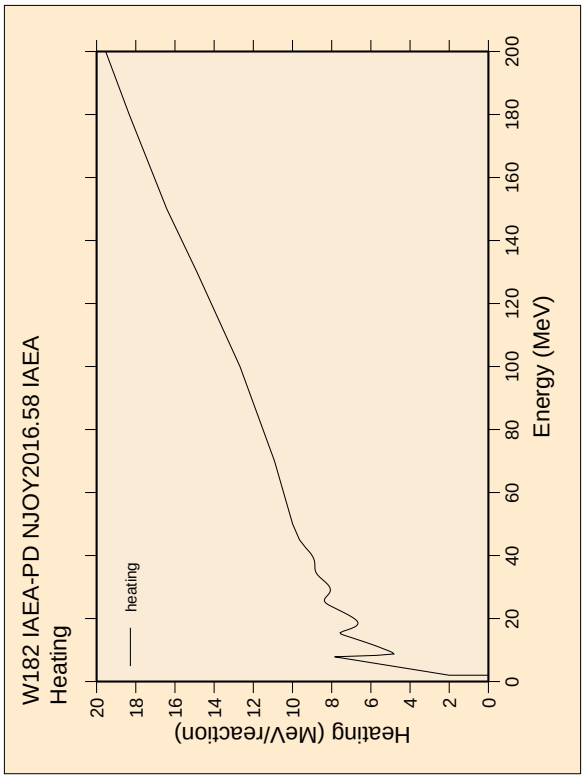

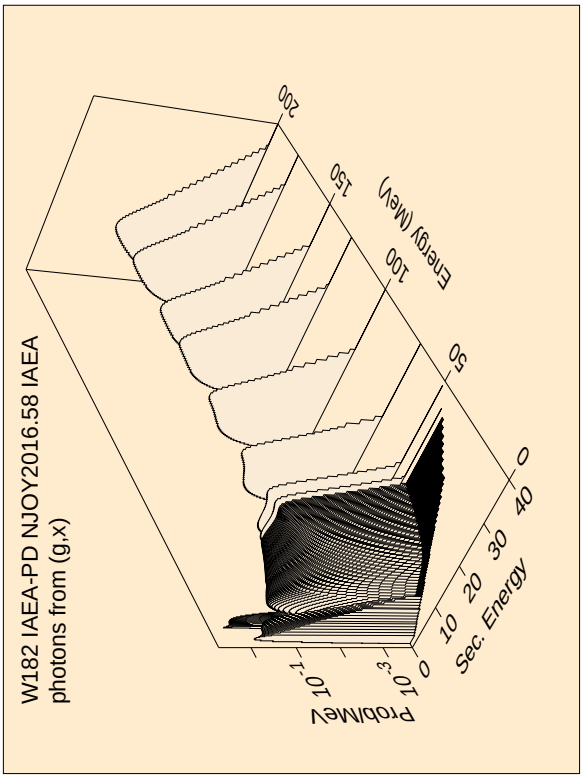
W182 IAEA-PD NJOY2016.58 IAEA
photons from (g,x)
Energy (MeV)
200
150
100
50
0
Sec. Energy
0
10
20
30
40
Prob/MeV
0
10^-3
10^-1

A.5.2 Activation Library

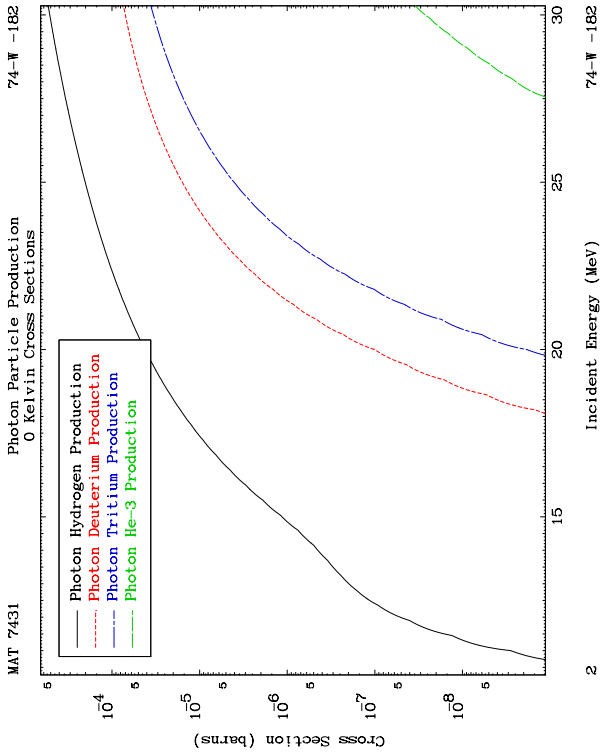

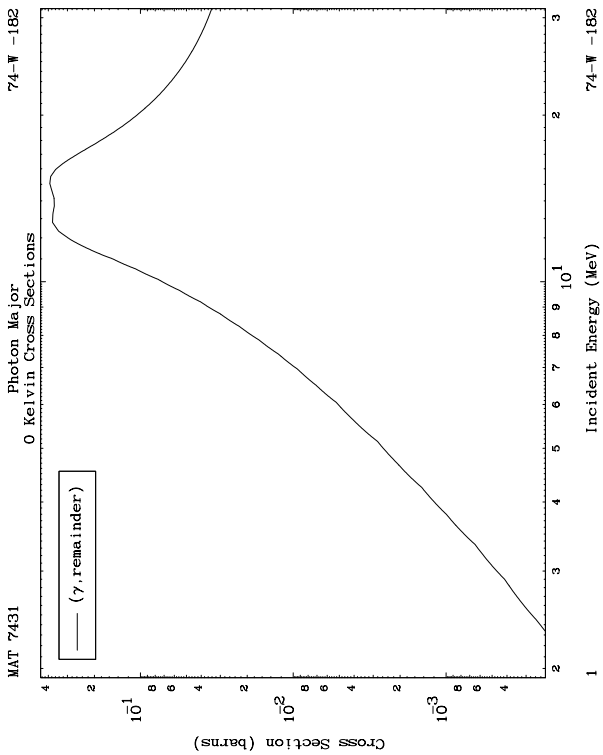

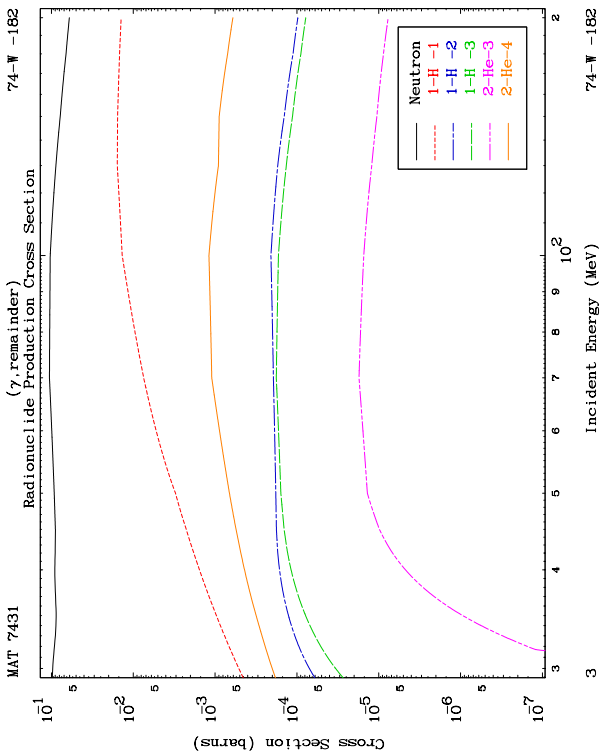

A.6 Example of ^{181}Ta File Processing (File Type 5: IFIN-HH/UB)

A.6.1 Transport Library

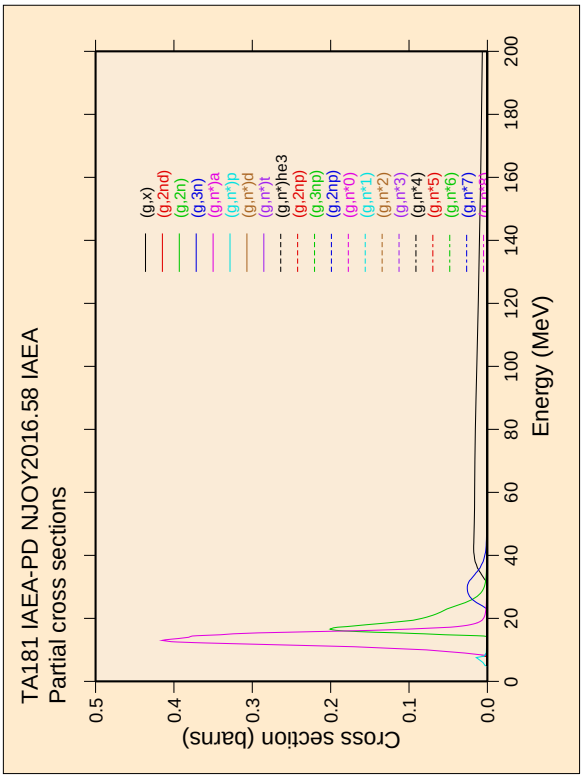

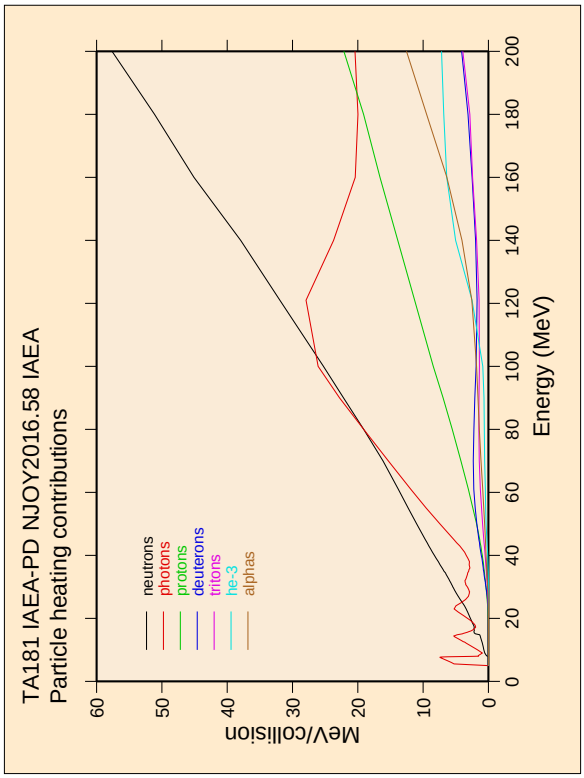

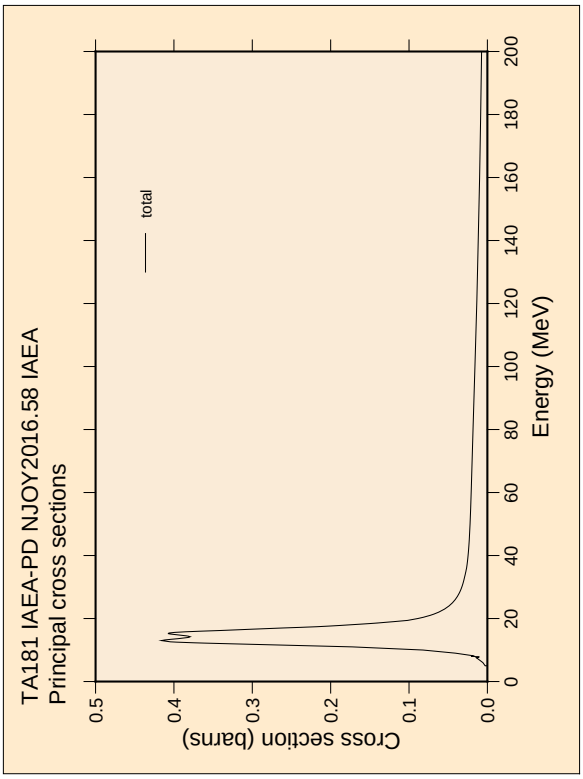

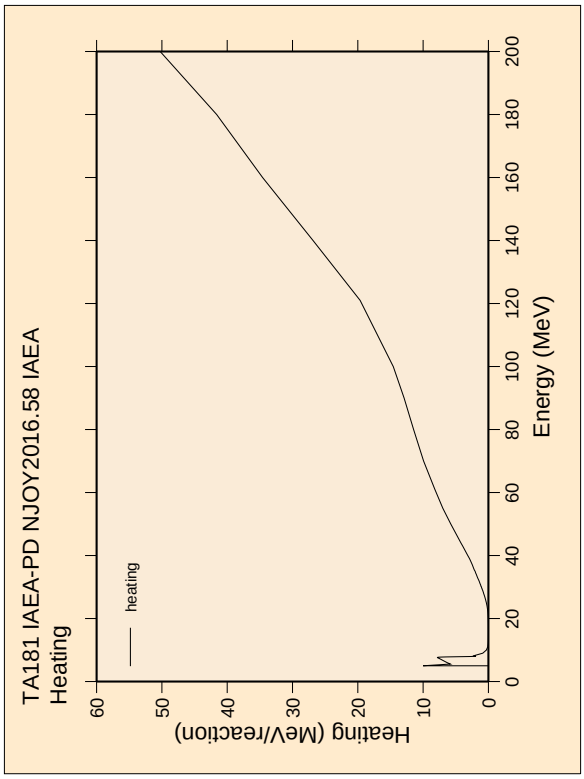

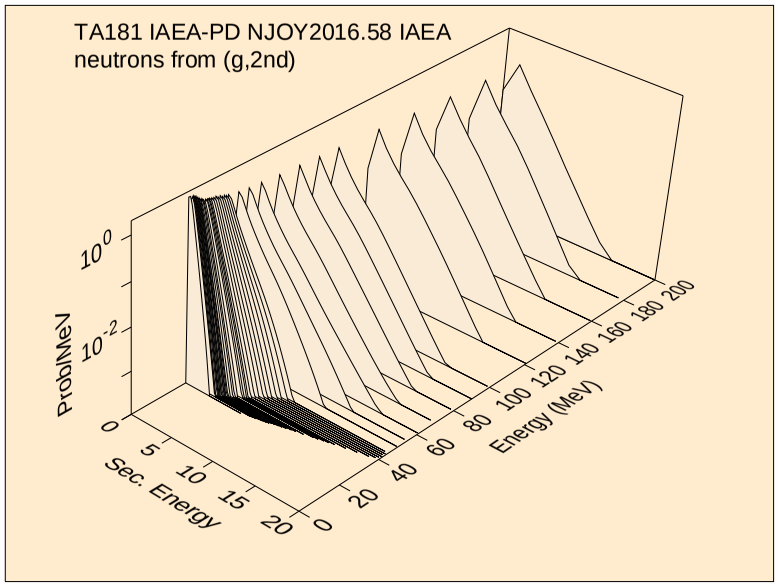
TA181 IAEA-PD NJOY2016.58 IAEA
neutrons from (g,2nd)
Prob/MeV
10^{0}
10^{-2}
0
5
10
15
20
Sec. Energy
0
20
40
60
80
100
120
140
160
180
200
Energy (MeV)

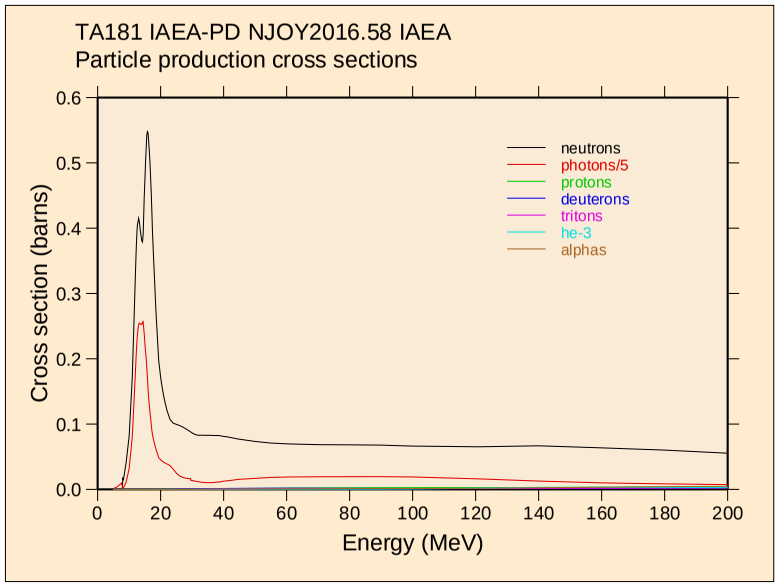
TA181 IAEA-PD NJOY2016.58 IAEA
Particle production cross sections
Cross section (barns)
0.0
0.1
0.2
0.3
0.4
0.5
0.6
0
20
40
60
80
100
120
140
160
180
200
Energy (MeV)
neutrons
photons/5
protons
deuterons
tritons
he-3
alphas

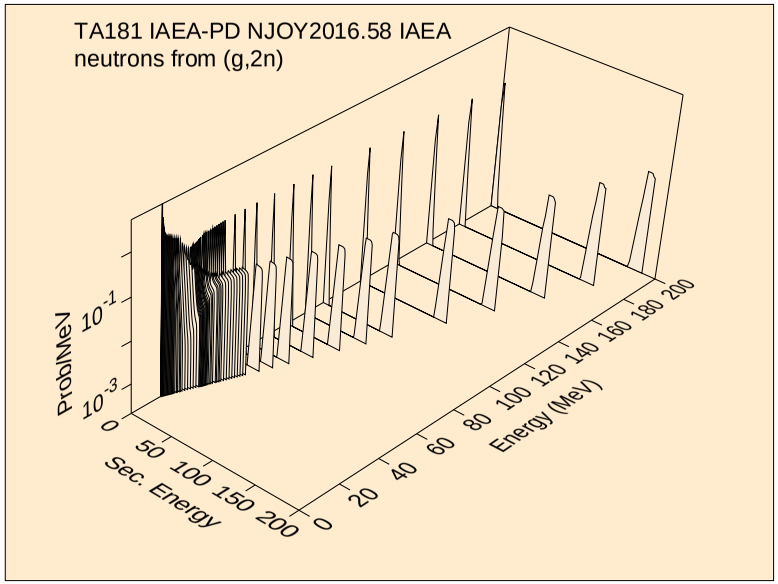
TA181 IAEA-PD NJOY2016.58 IAEA
neutrons from (g,2n)
Prob/MeV
10^{-1}
10^{-3}
0
50
100
150
200
Sec. Energy
0
20
40
60
80
100
120
140
160
180
200
Energy (MeV)

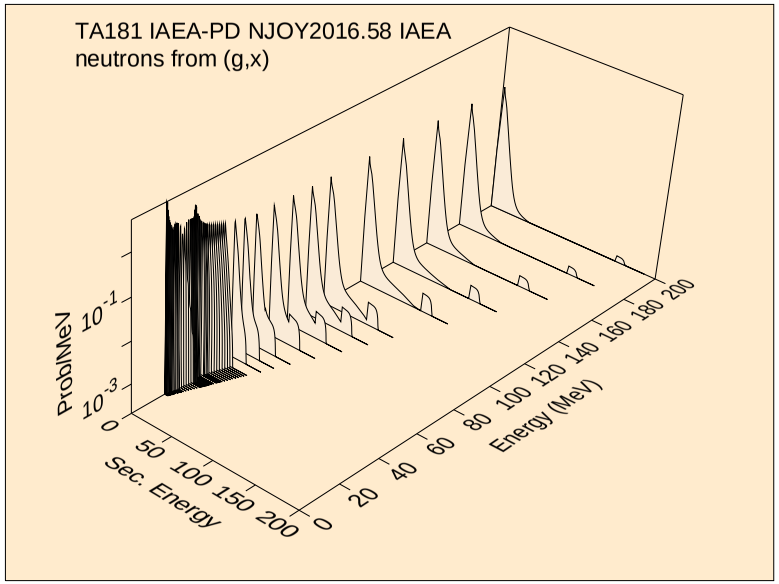
TA181 IAEA-PD NJOY2016.58 IAEA
neutrons from (g,x)
Prob/MeV
10^{-1}
10^{-3}
0
50
100
150
200
Sec. Energy
0
20
40
60
80
100
120
140
160
180
200
Energy (MeV)

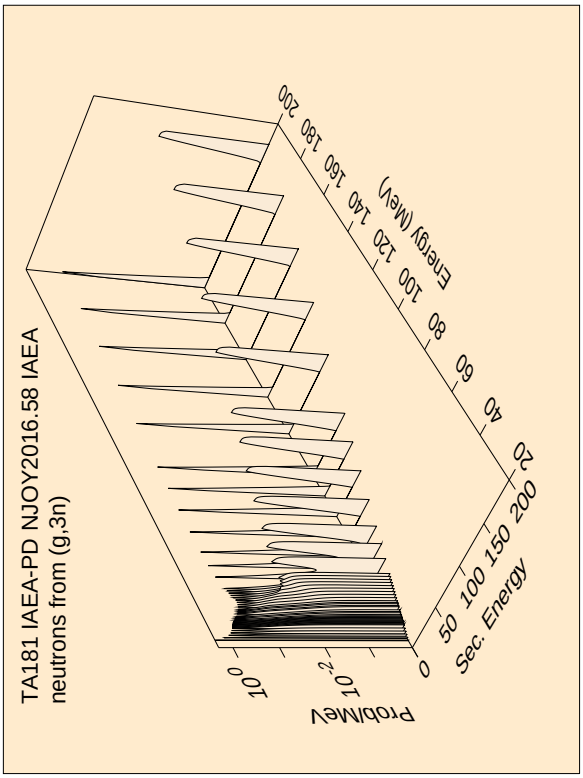
TA181 IAEA-PD NJOY2016.58 IAEA
neutrons from (g,3n)
Prob/MeV
Energy (Mev)
Sec. Energy

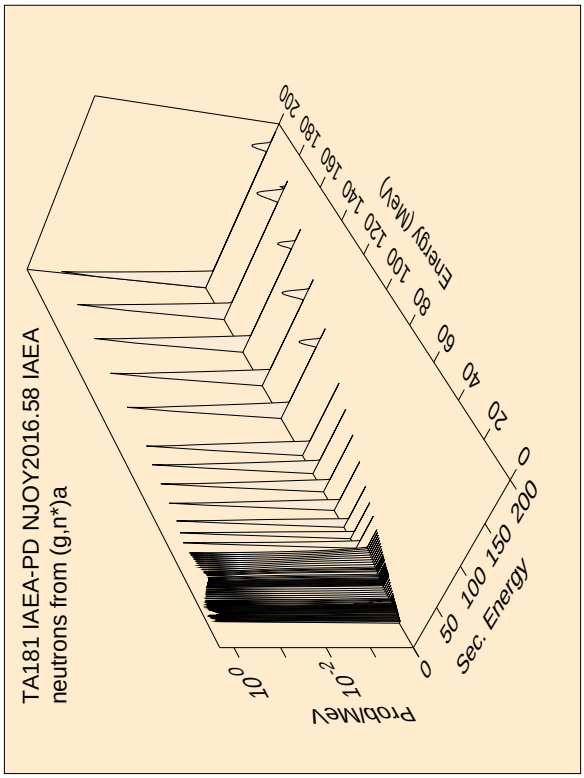
TA181 IAEA-PD NJOY2016.58 IAEA
neutrons from (g,n*)a
Prob/MeV
Energy (Mev)
Sec. Energy

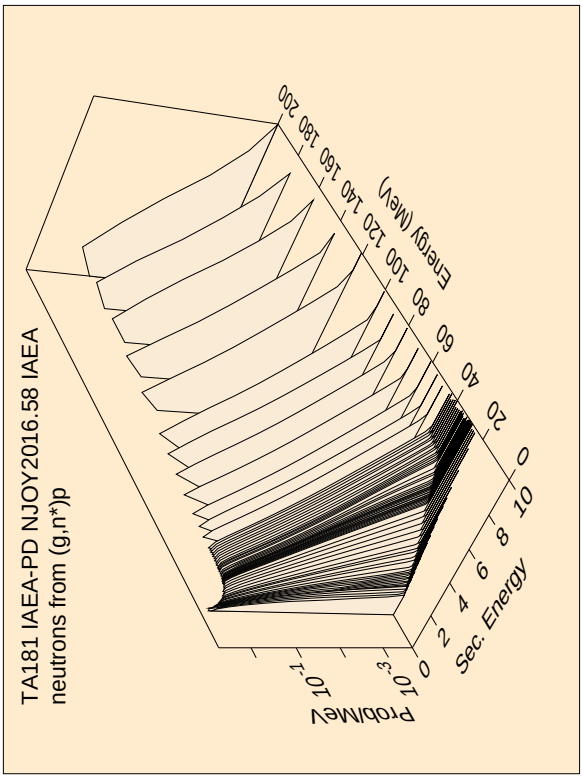
TA181 IAEA-PD NJOY2016.58 IAEA
neutrons from (g,n*)p
Prob/MeV
Energy (Mev)
Sec. Energy

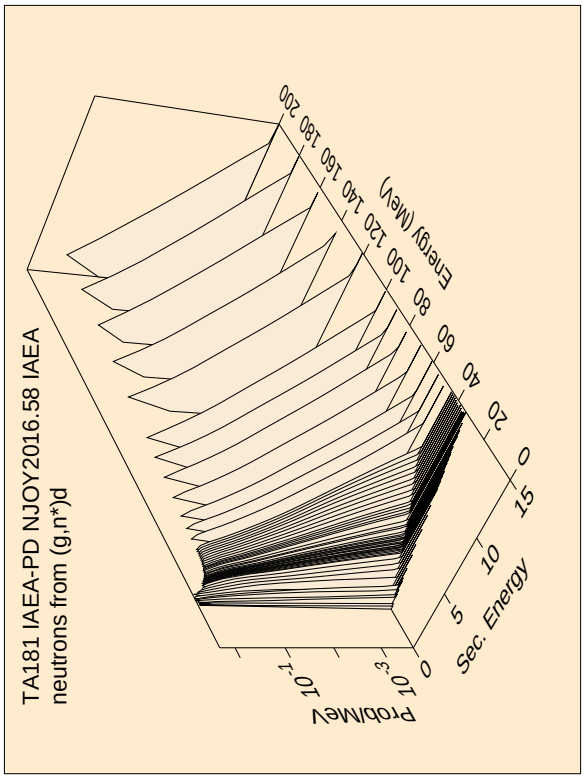
TA181 IAEA-PD NJOY2016.58 IAEA
neutrons from (g,n*)d
Prob/MeV
Energy (Mev)
Sec. Energy

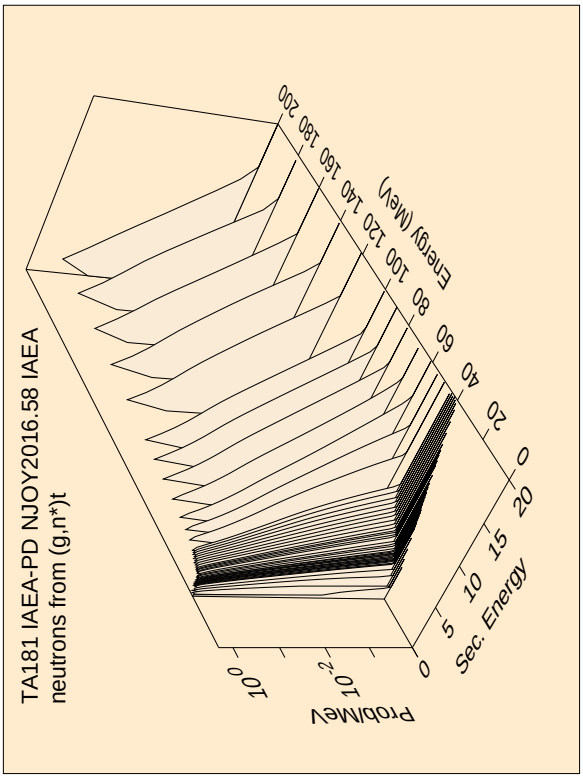
TA181 IAEA-PD NJOY2016.58 IAEA
neutrons from (g,n*)t
Prob/MeV
Energy (Mev)
Sec. Energy

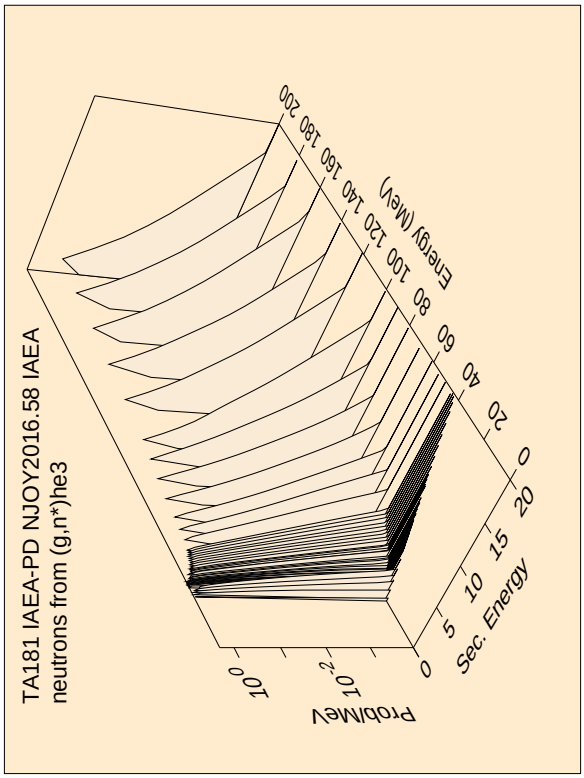
TA181 IAEA-PD NJOY2016.58 IAEA
neutrons from (g,n*)he3
Prob/MeV
Energy (Mev)
Sec. Energy

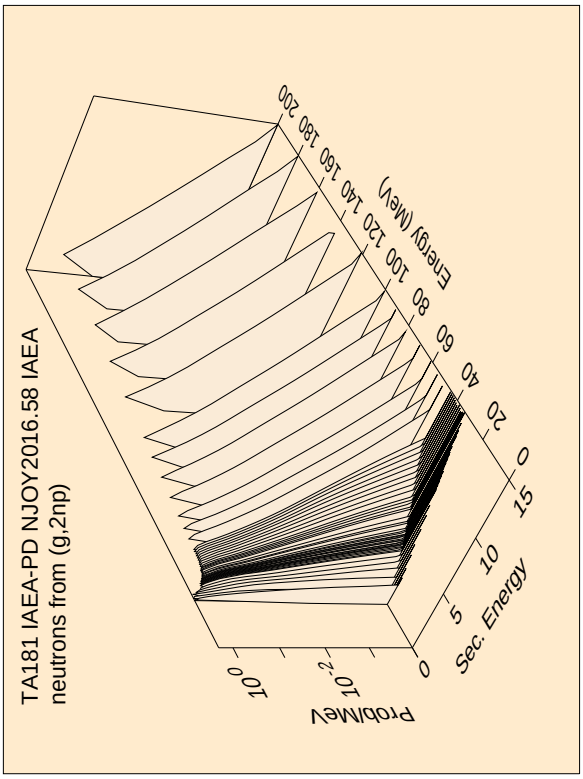
TA181 IAEA-PD NJOY2016.58 IAEA
neutrons from (g,2np)
Prob/MeV
Energy (Mev)
Sec. Energy

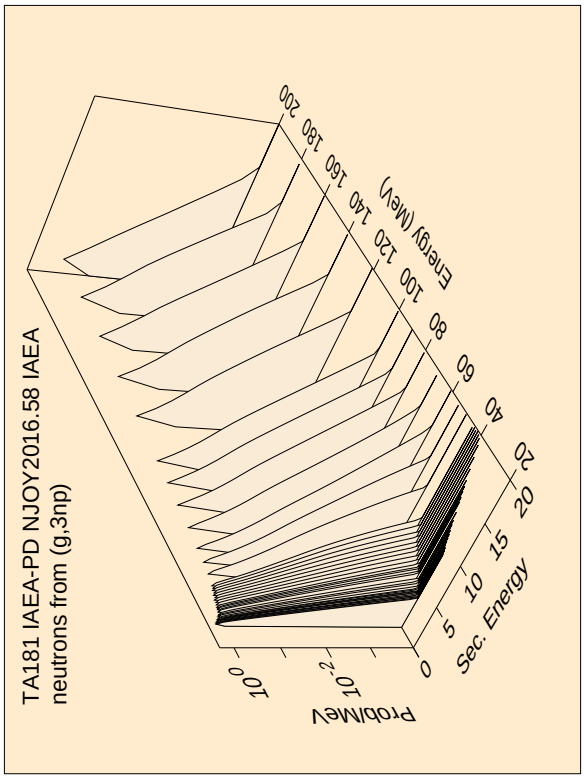
TA181 IAEA-PD NJOY2016.58 IAEA
neutrons from (g,3np)
Prob/MeV
Energy (Mev)
Sec. Energy

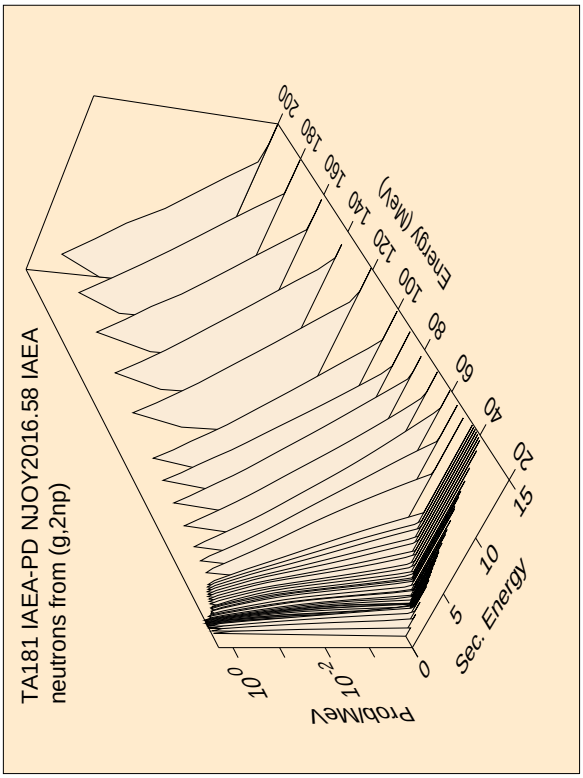
TA181 IAEA-PD NJOY2016.58 IAEA
neutrons from (g,2np)
Prob/MeV
Sec. Energy
Energy (Mev)

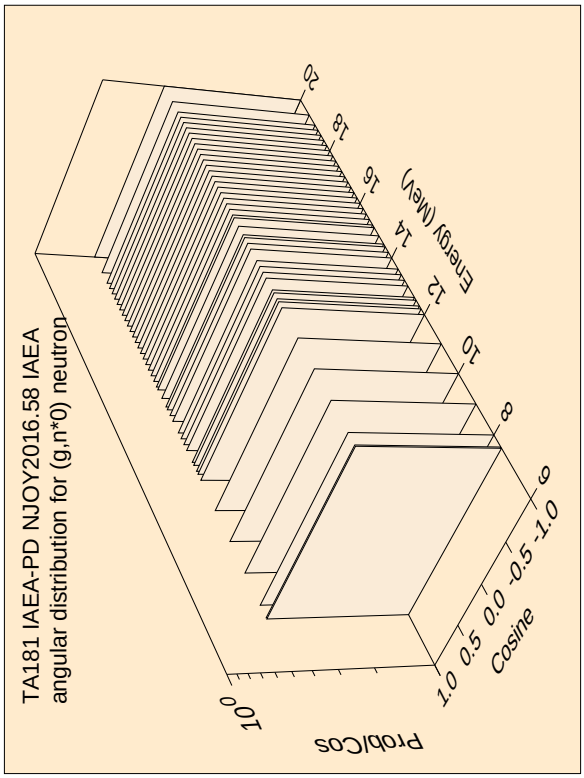
TA181 IAEA-PD NJOY2016.58 IAEA
angular distribution for (g,n*0) neutron
Prob/Cos
Cosine
Energy (Mev)

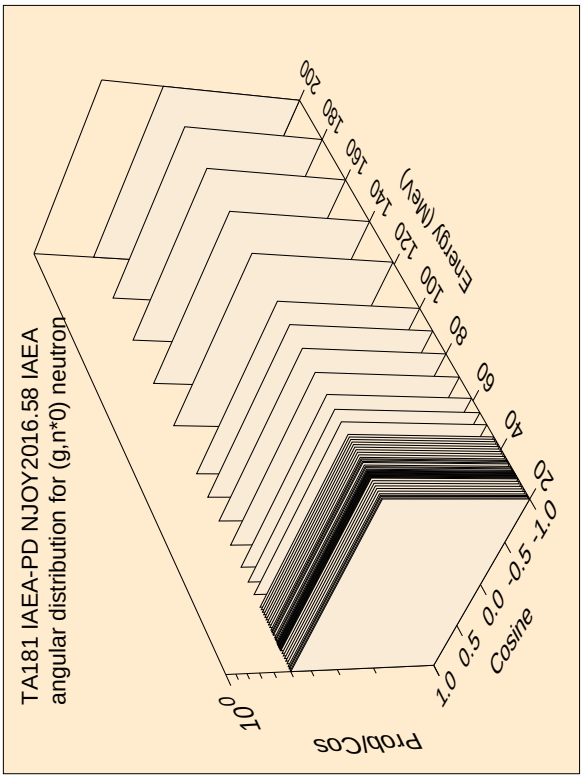
TA181 IAEA-PD NJOY2016.58 IAEA
angular distribution for (g,n*0) neutron
Prob/Cos
Cosine
Energy (Mev)

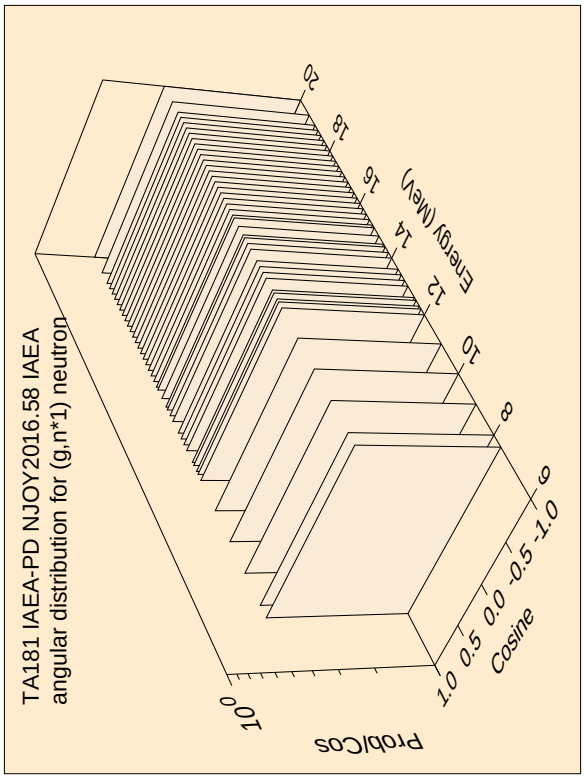
TA181 IAEA-PD NJOY2016.58 IAEA
angular distribution for (g,n*1) neutron
Prob/Cos
Cosine
Energy (Mev)

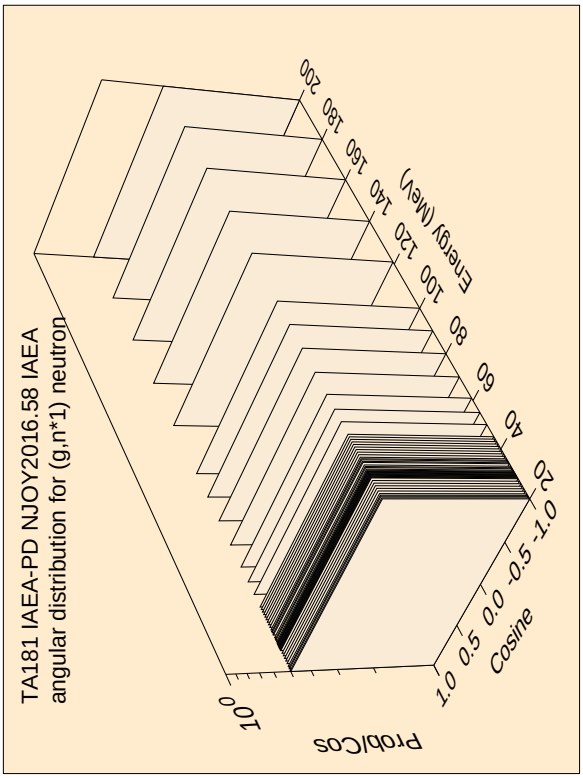
TA181 IAEA-PD NJOY2016.58 IAEA
angular distribution for (g,n*1) neutron
Prob/Cos
Cosine
Energy (MeV)

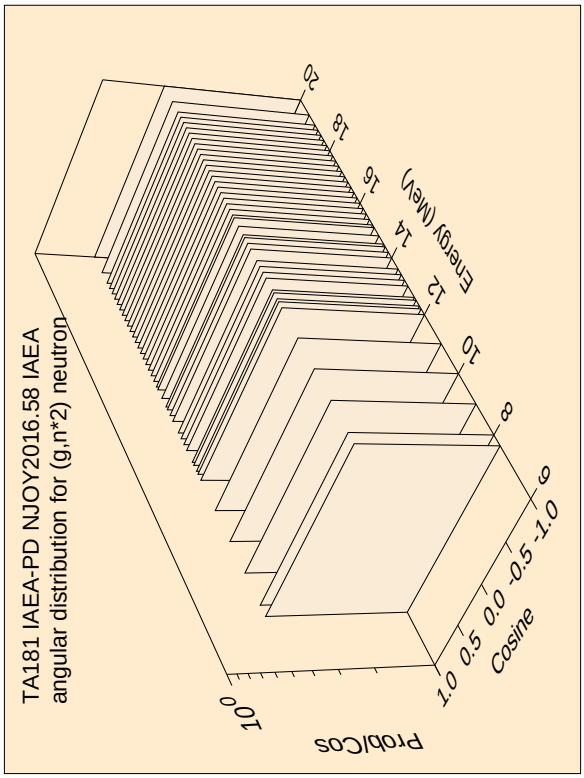
TA181 IAEA-PD NJOY2016.58 IAEA
angular distribution for (g,n*2) neutron
Prob/Cos
Cosine
Energy (MeV)

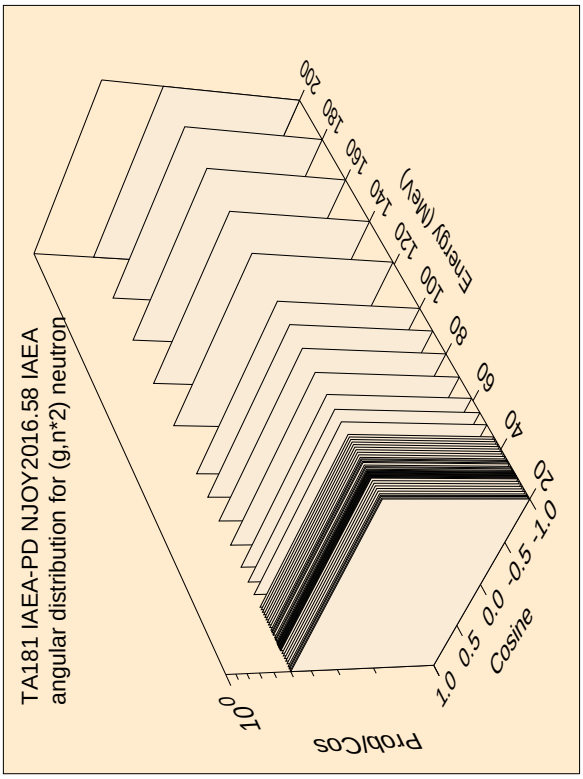
TA181 IAEA-PD NJOY2016.58 IAEA
angular distribution for (g,n*2) neutron
Prob/Cos
Cosine
Energy (MeV)

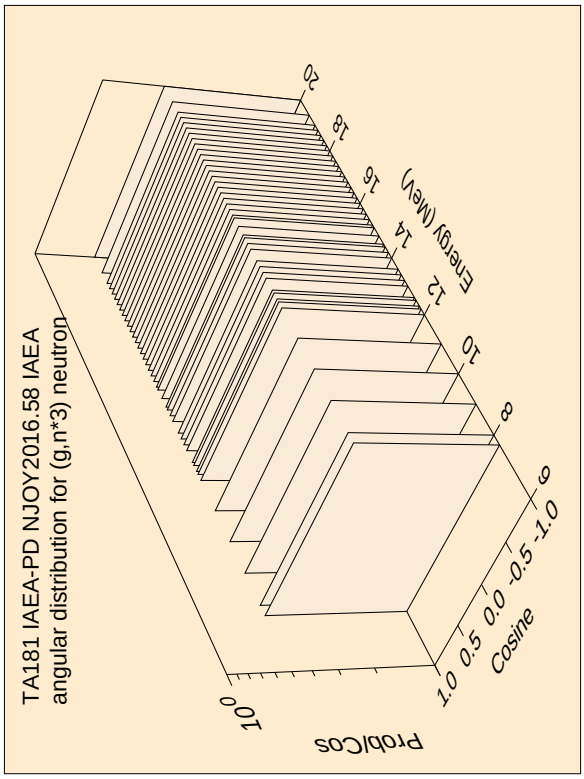
TA181 IAEA-PD NJOY2016.58 IAEA
angular distribution for (g,n*3) neutron
Prob/Cos
Cosine
Energy (MeV)

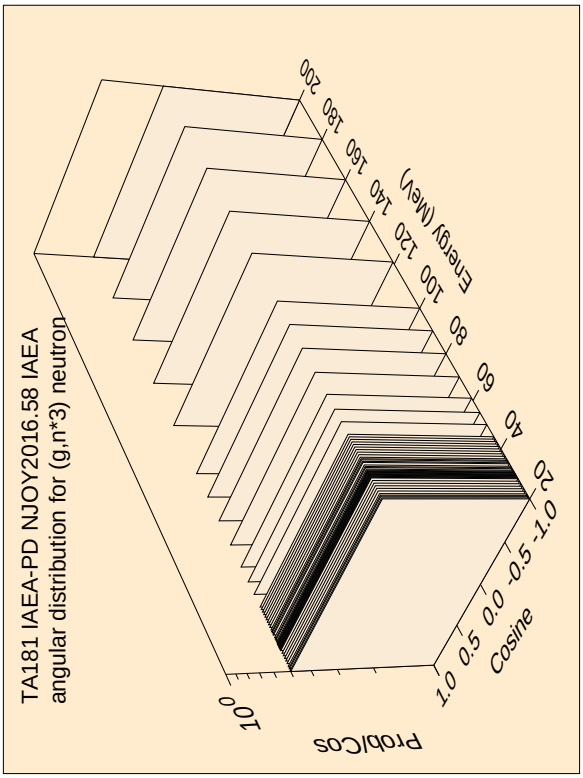
TA181 IAEA-PD NJOY2016.58 IAEA
angular distribution for (g,n*3) neutron
Prob/Cos
Cosine
Energy (MeV)

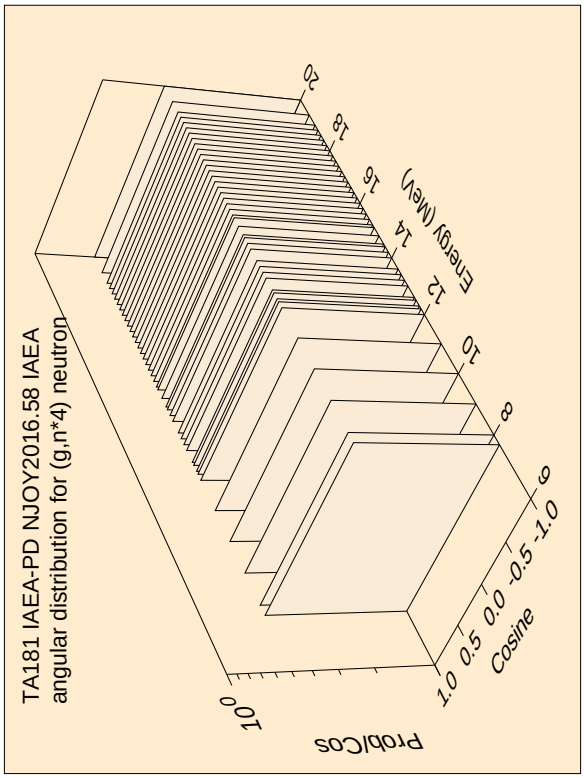
TA181 IAEA-PD NJOY2016.58 IAEA
angular distribution for (g,n*4) neutron
Prob/Cos
Cosine
Energy (MeV)

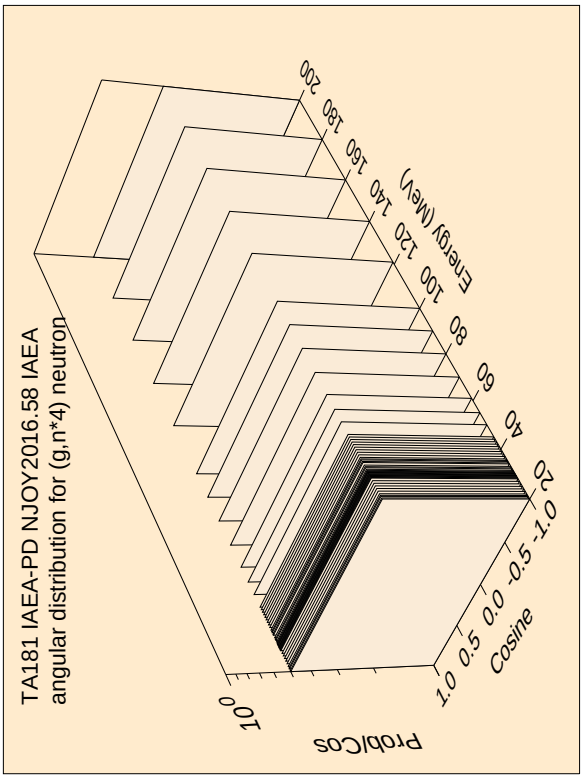
TA181 IAEA-PD NJOY2016.58 IAEA
angular distribution for (g,n*4) neutron
Prob/Cos
Cosine
Energy (MeV)

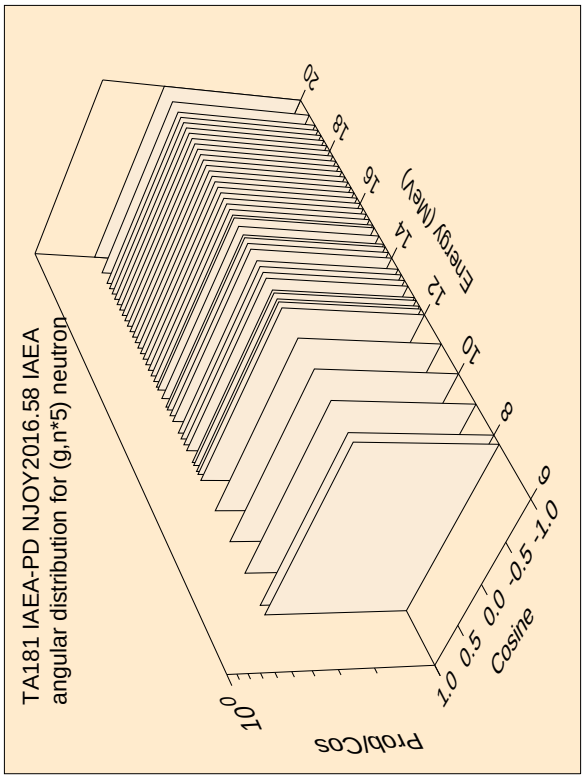
TA181 IAEA-PD NJOY2016.58 IAEA
angular distribution for (g,n*5) neutron
Prob/Cos
Cosine
Energy (MeV)

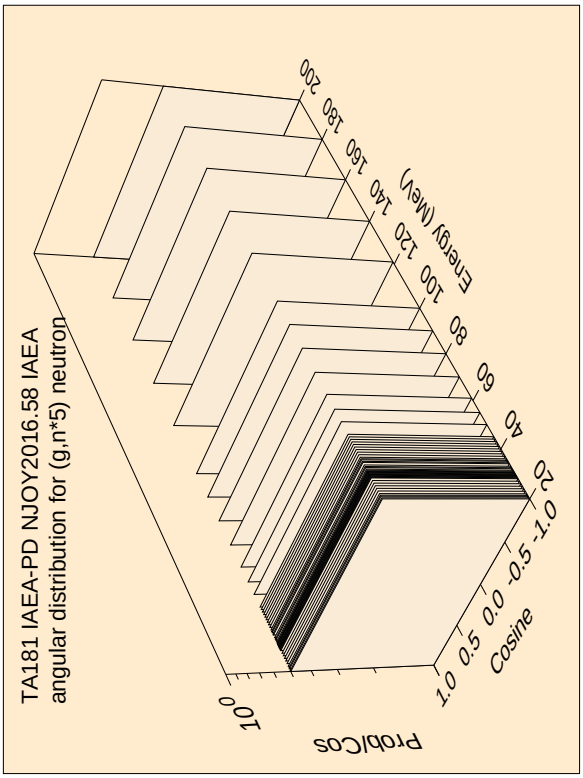
TA181 IAEA-PD NJOY2016.58 IAEA
angular distribution for (g,n*5) neutron
Prob/Cos
Cosine
Energy (MeV)

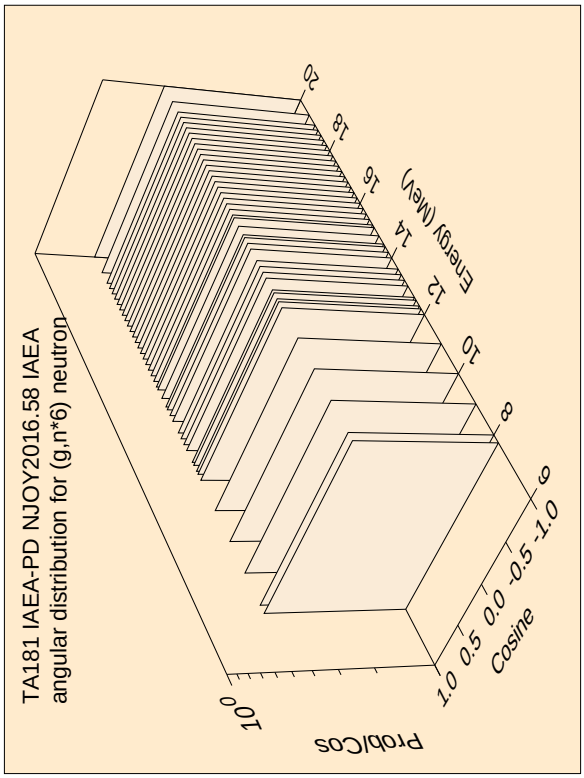
TA181 IAEA-PD NJOY2016.58 IAEA
angular distribution for (g,n*6) neutron
Prob/Cos
Cosine
Energy (MeV)

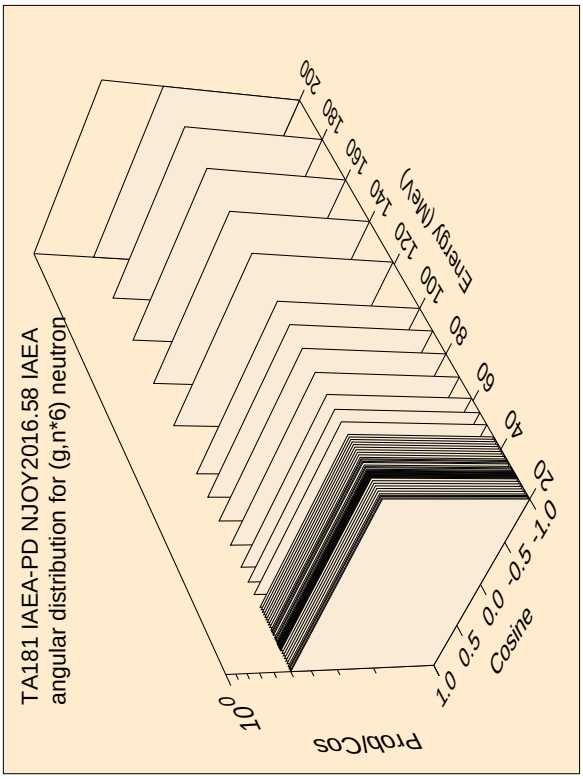
TA181 IAEA-PD NJOY2016.58 IAEA
angular distribution for (g,n*6) neutron
Prob/Cos
Cosine
Energy (MeV)

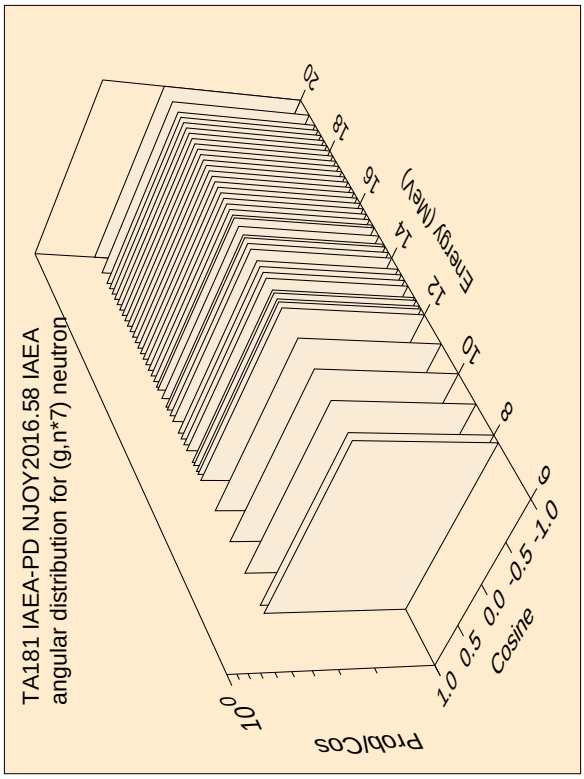
TA181 IAEA-PD NJOY2016.58 IAEA
angular distribution for (g,n*7) neutron
Prob/Cos
Cosine
Energy (MeV)

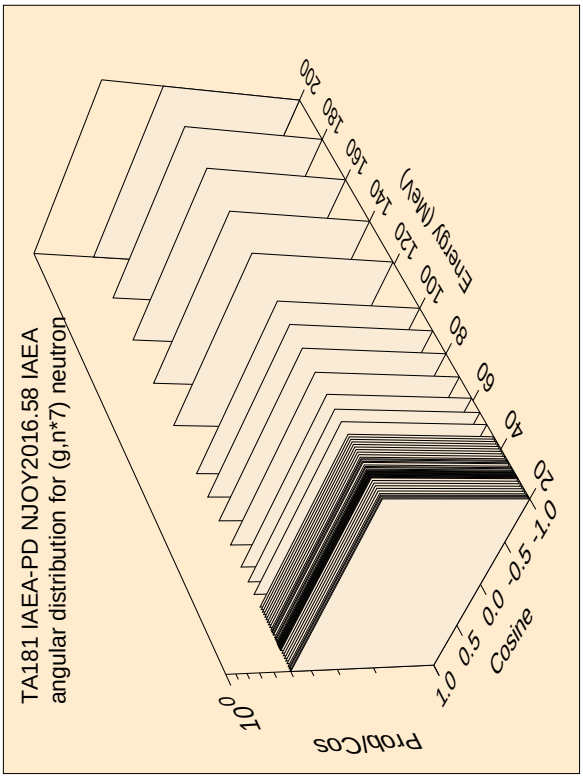
TA181 IAEA-PD NJOY2016.58 IAEA
angular distribution for (g,n*7) neutron
Prob/Cos
Energy (MeV)
Cosine

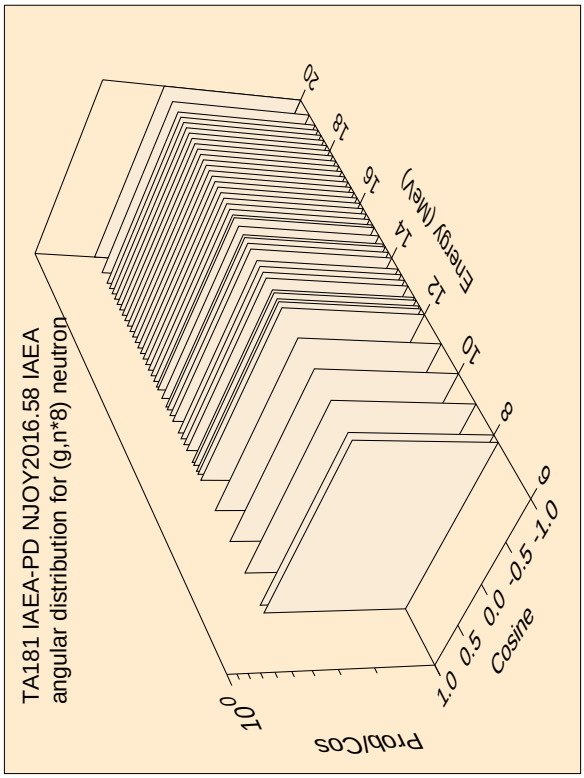
TA181 IAEA-PD NJOY2016.58 IAEA
angular distribution for (g,n*8) neutron
Prob/Cos
Energy (MeV)
Cosine

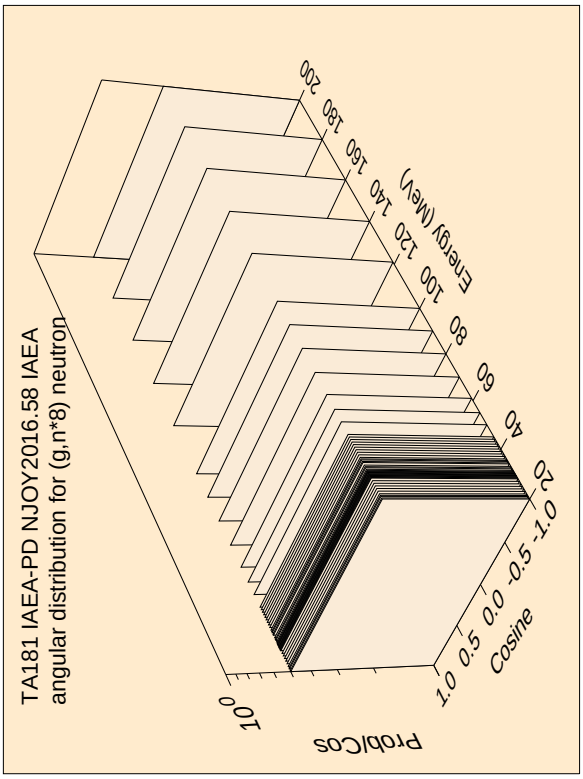
TA181 IAEA-PD NJOY2016.58 IAEA
angular distribution for (g,n*8) neutron
Prob/Cos
Energy (MeV)
Cosine

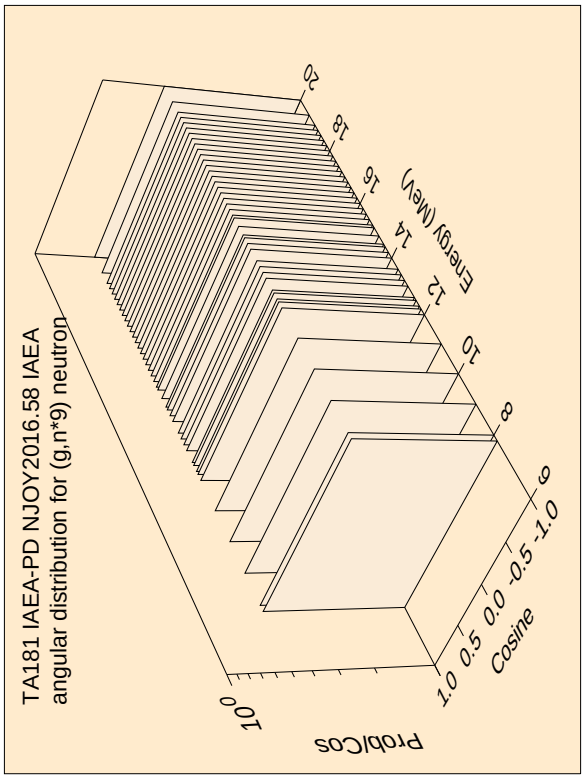
TA181 IAEA-PD NJOY2016.58 IAEA
angular distribution for (g,n*9) neutron
Prob/Cos
Energy (MeV)
Cosine

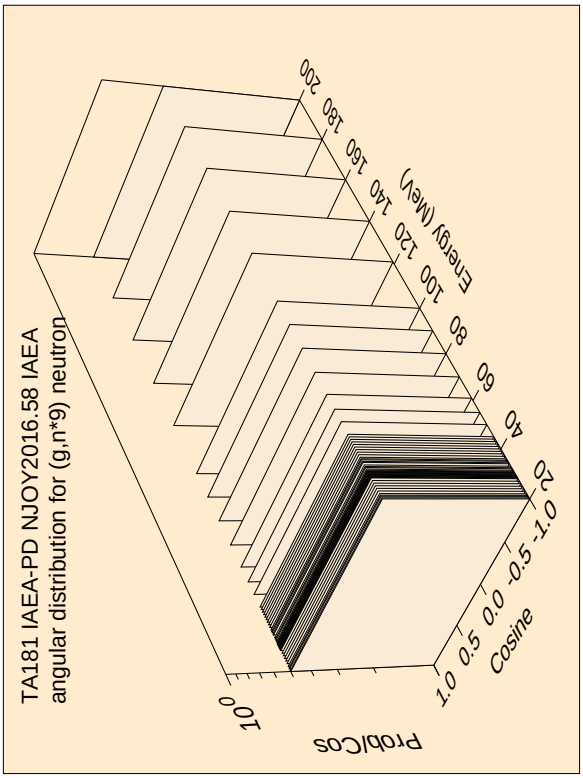
TA181 IAEA-PD NJOY2016.58 IAEA
angular distribution for (g,n*9) neutron
Prob/Cos
Cosine
Energy (MeV)

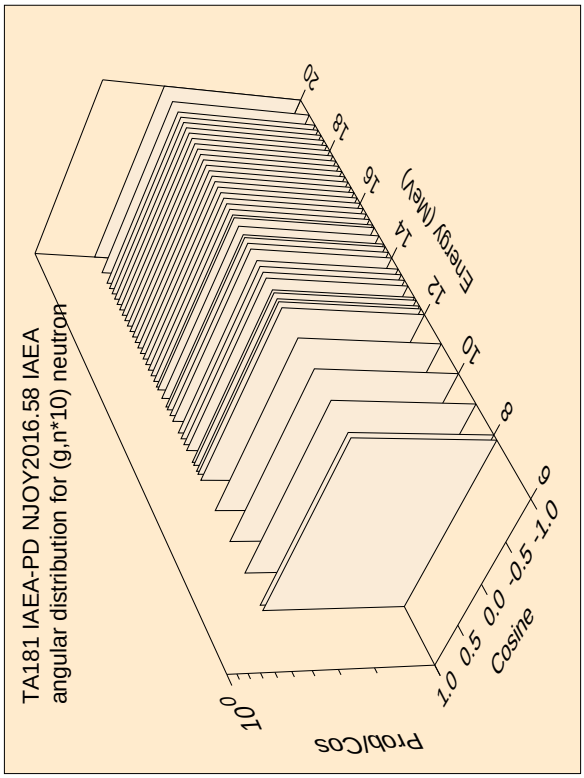
TA181 IAEA-PD NJOY2016.58 IAEA
angular distribution for (g,n*10) neutron
Prob/Cos
Cosine
Energy (MeV)

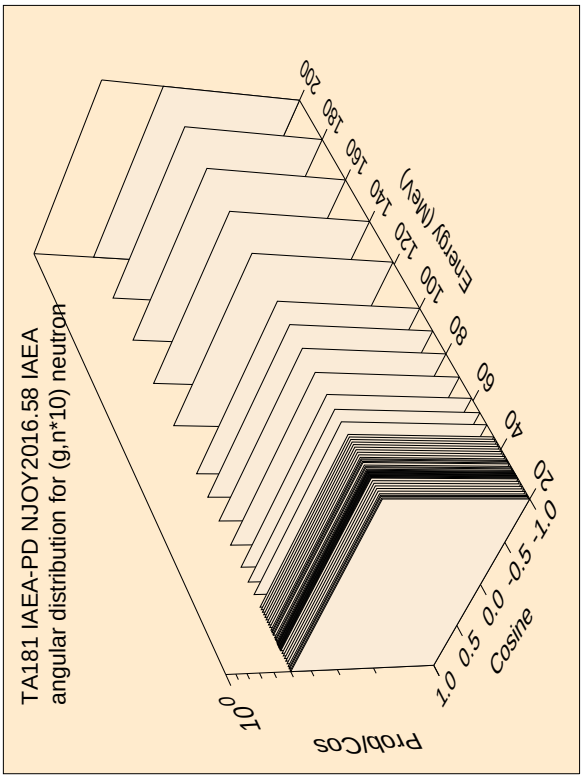
TA181 IAEA-PD NJOY2016.58 IAEA
angular distribution for (g,n*10) neutron
Prob/Cos
Cosine
Energy (MeV)

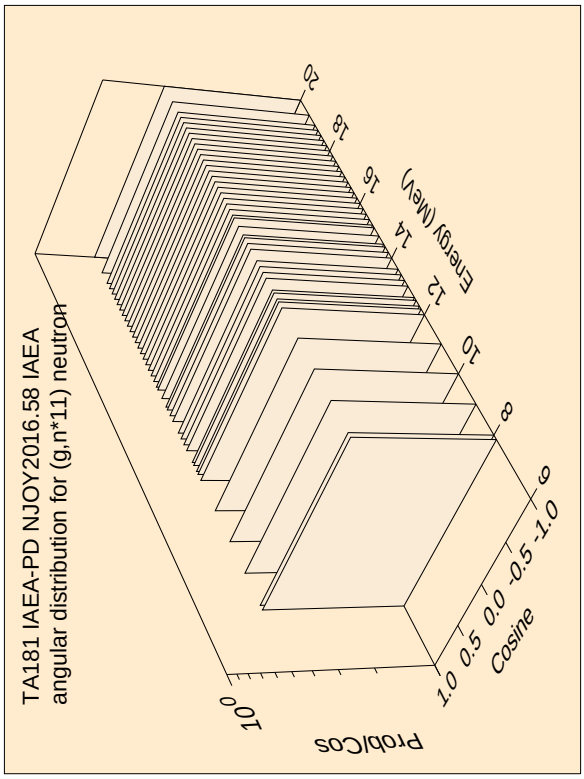
TA181 IAEA-PD NJOY2016.58 IAEA
angular distribution for (g,n*11) neutron
Prob/Cos
Cosine
Energy (MeV)

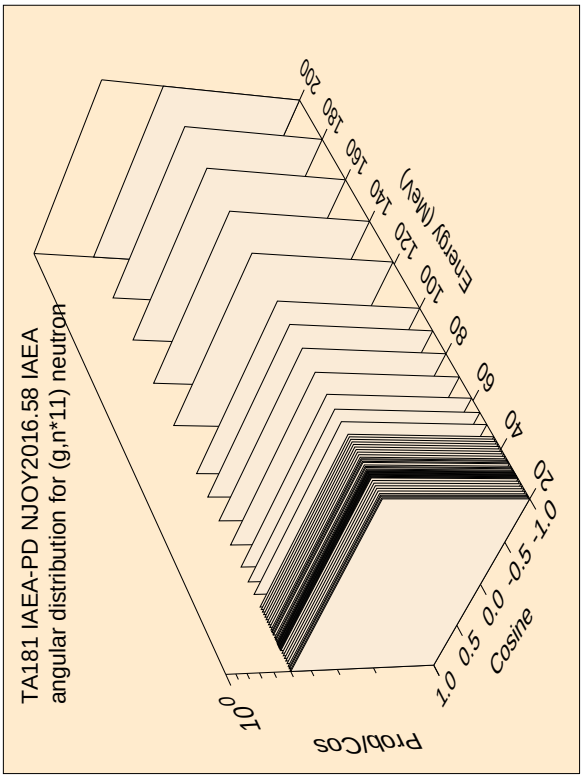
TA181 IAEA-PD NJOY2016.58 IAEA
angular distribution for (g,n*11) neutron
Prob/Cos
Cosine
Energy (MeV)

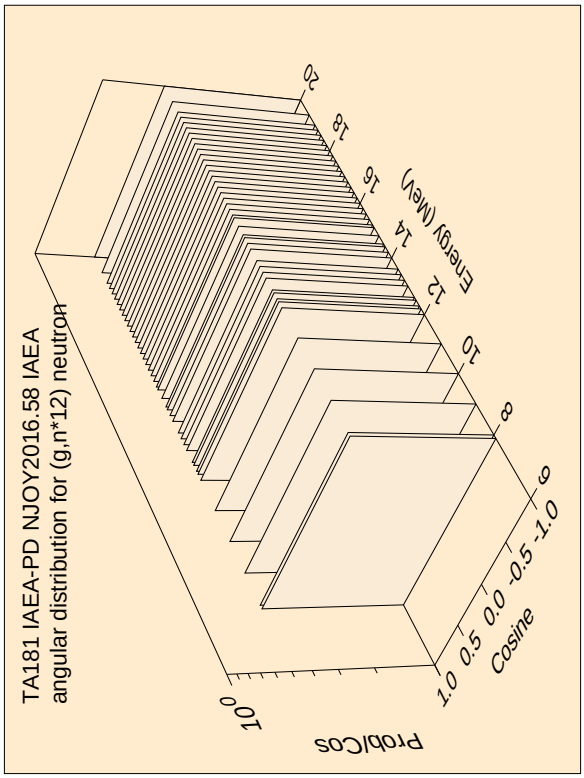
TA181 IAEA-PD NJOY2016.58 IAEA
angular distribution for (g,n*12) neutron
Prob/Cos
Cosine
Energy (MeV)

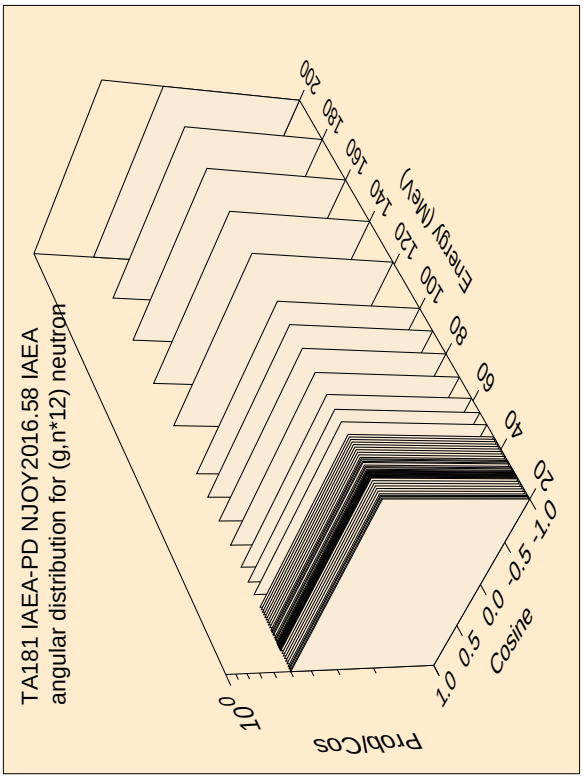
TA181 IAEA-PD NJOY2016.58 IAEA
angular distribution for (g,n*12) neutron
Prob/Cos
Cosine
Energy (MeV)

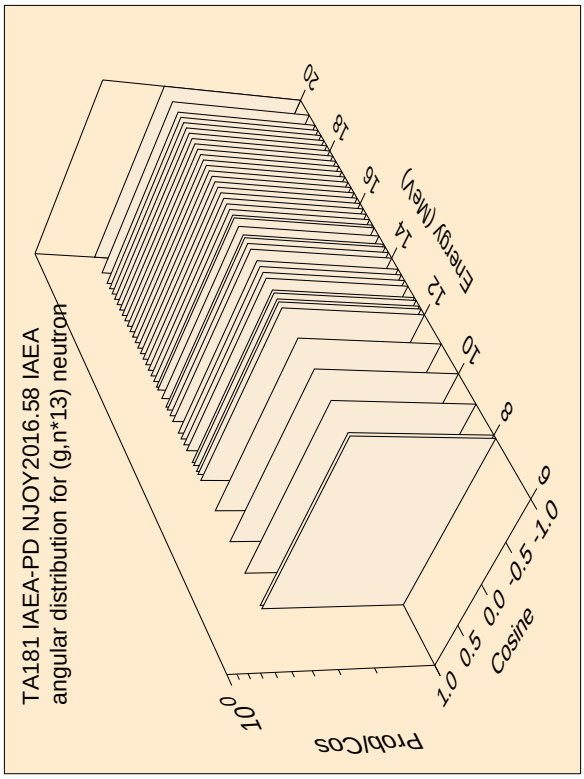
TA181 IAEA-PD NJOY2016.58 IAEA
angular distribution for (g,n*13) neutron
Prob/Cos
Cosine
Energy (MeV)

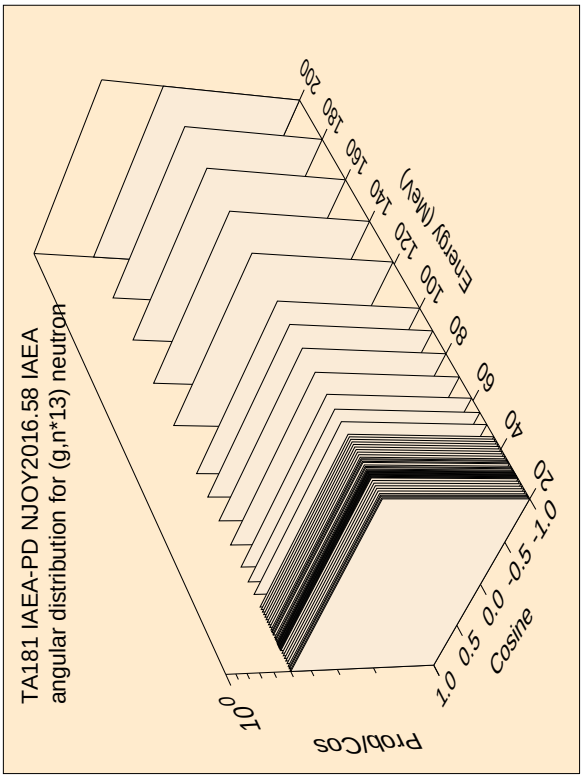
TA181 IAEA-PD NJOY2016.58 IAEA
angular distribution for (g,n*13) neutron
Prob/Cos
Cosine
Energy (MeV)

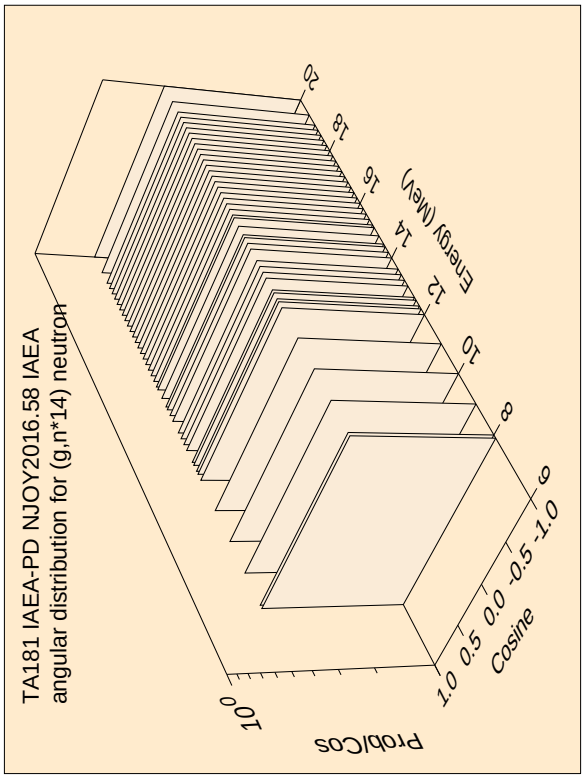
TA181 IAEA-PD NJOY2016.58 IAEA
angular distribution for (g,n*14) neutron
Prob/Cos
Cosine
Energy (MeV)

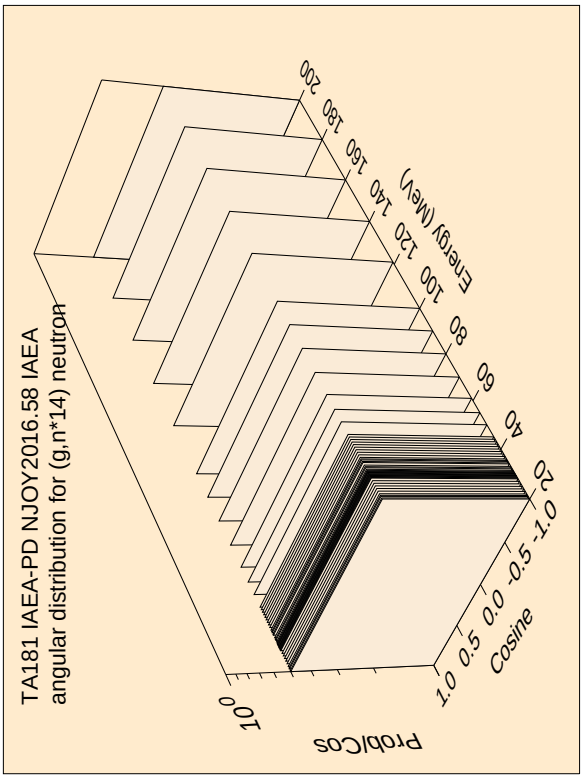
TA181 IAEA-PD NJOY2016.58 IAEA
angular distribution for (g,n*14) neutron
Prob/Cos
Cosine
Energy (MeV)

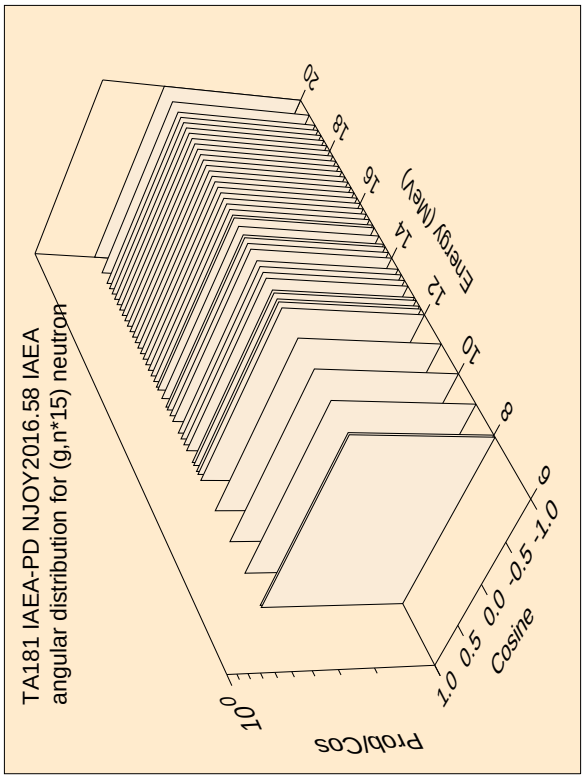
TA181 IAEA-PD NJOY2016.58 IAEA
angular distribution for (g,n*15) neutron
Prob/Cos
Cosine
Energy (MeV)

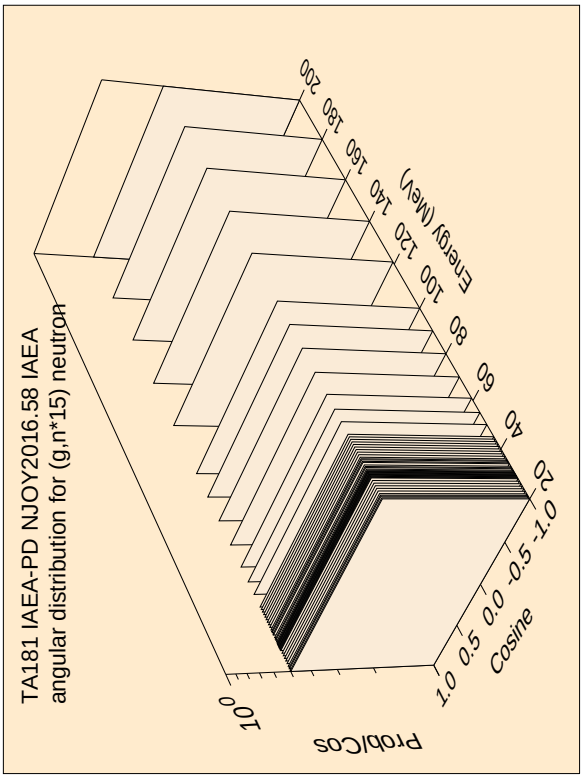
TA181 IAEA-PD NJOY2016.58 IAEA
angular distribution for (g,n*15) neutron
Prob/Cos
Cosine
Energy (MeV)

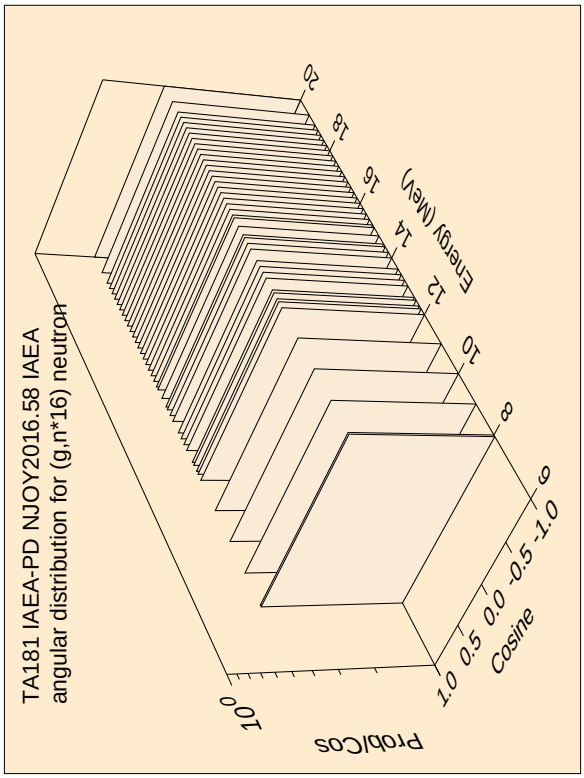
TA181 IAEA-PD NJOY2016.58 IAEA
angular distribution for (g,n*16) neutron
Prob/Cos
Cosine
Energy (MeV)

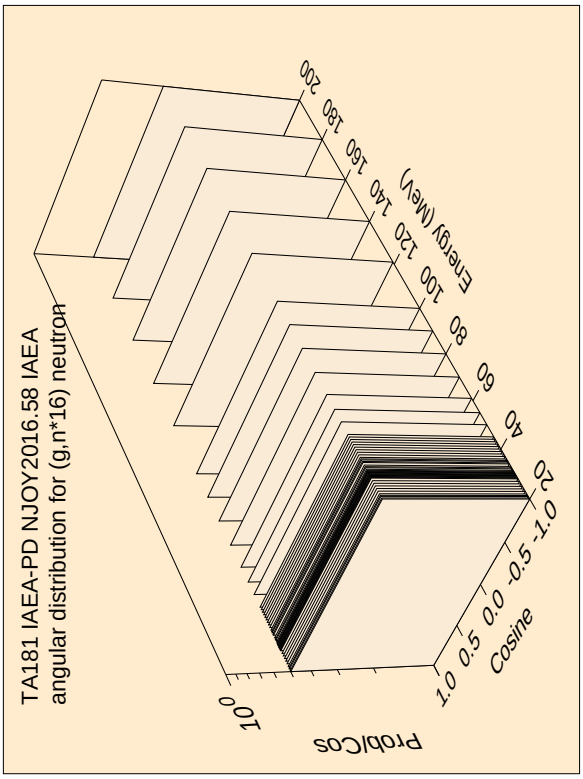
TA181 IAEA-PD NJOY2016.58 IAEA
angular distribution for (g,n*16) neutron
Prob/Cos
Cosine
Energy (MeV)

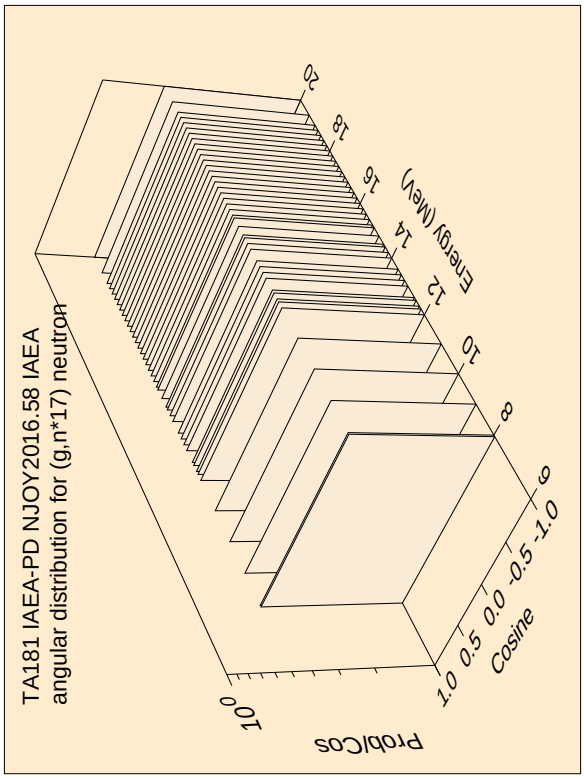
TA181 IAEA-PD NJOY2016.58 IAEA
angular distribution for (g,n*17) neutron
Prob/Cos
Cosine
Energy (MeV)

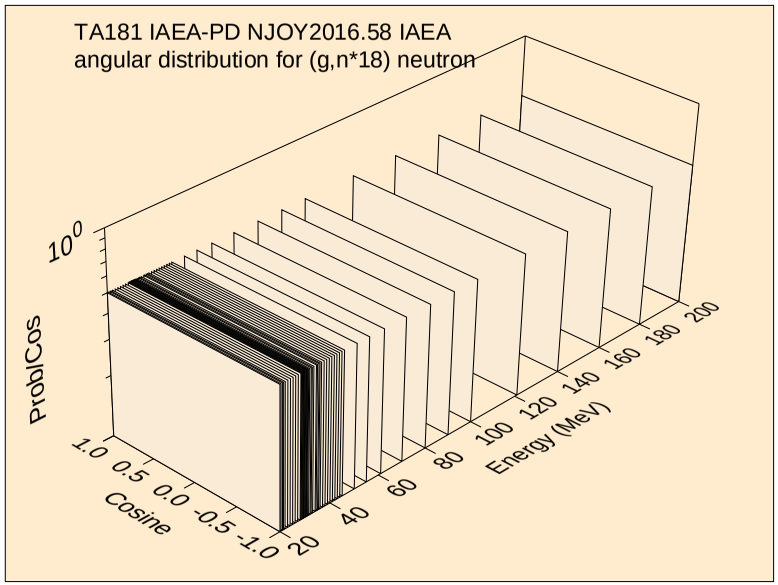
TA181 IAEA-PD NJOY2016.58 IAEA
angular distribution for (g,n*18) neutron
ProbICos
10^0
Cosine
1.0 0.5 0.0 -0.5 -1.0
Energy (MeV)
20 40 60 80 100 120 140 160 180 200

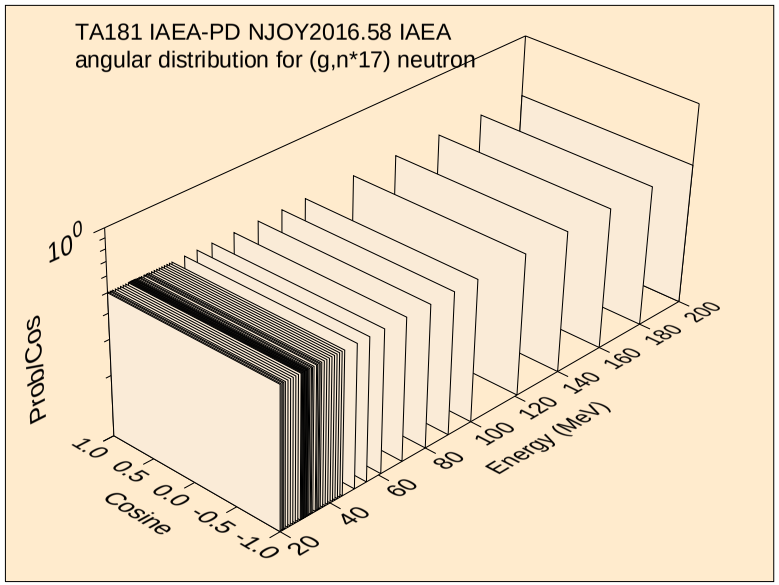
TA181 IAEA-PD NJOY2016.58 IAEA
angular distribution for (g,n*17) neutron
ProbICos
10^0
Cosine
1.0 0.5 0.0 -0.5 -1.0
Energy (MeV)
20 40 60 80 100 120 140 160 180 200

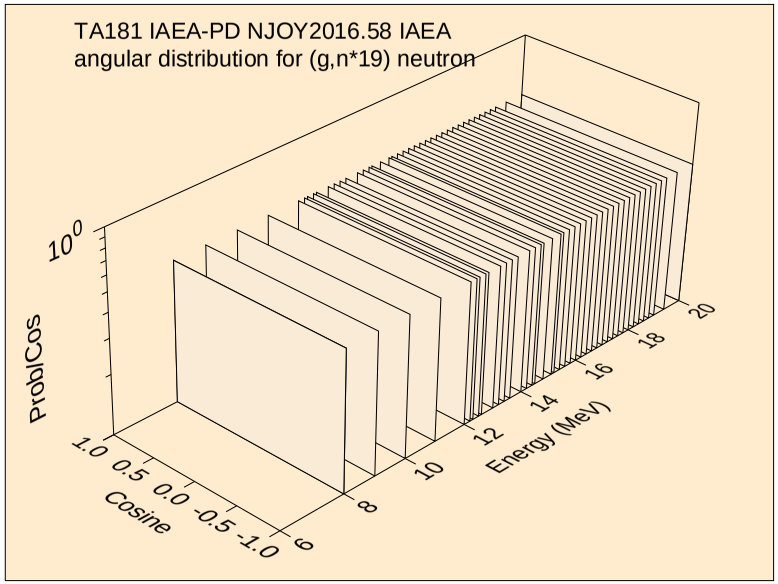
TA181 IAEA-PD NJOY2016.58 IAEA
angular distribution for (g,n*19) neutron
ProbICos
10^0
Cosine
1.0 0.5 0.0 -0.5 -1.0
Energy (MeV)
6 8 10 12 14 16 18 20

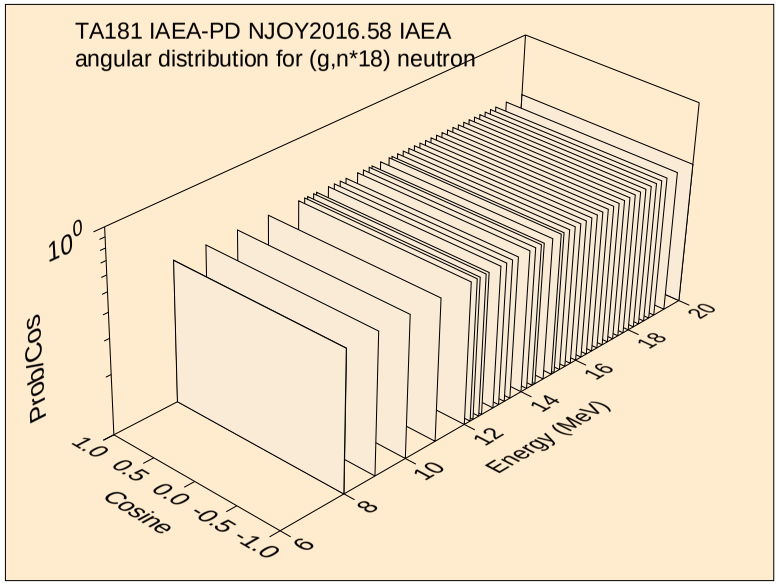
TA181 IAEA-PD NJOY2016.58 IAEA
angular distribution for (g,n*18) neutron
ProbICos
10^0
Cosine
1.0 0.5 0.0 -0.5 -1.0
Energy (MeV)
6 8 10 12 14 16 18 20

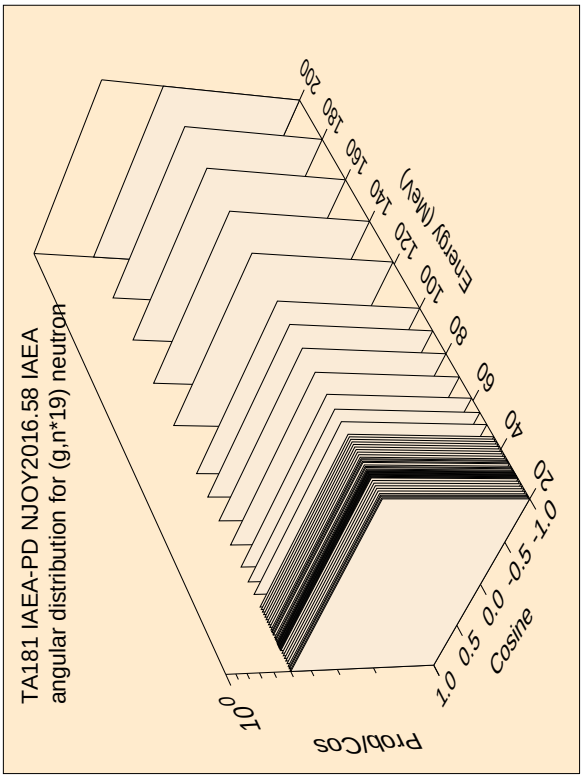
TA181 IAEA-PD NJOY2016.58 IAEA
angular distribution for (g,n*19) neutron
Prob/Cos
Cosine
Energy (MeV)

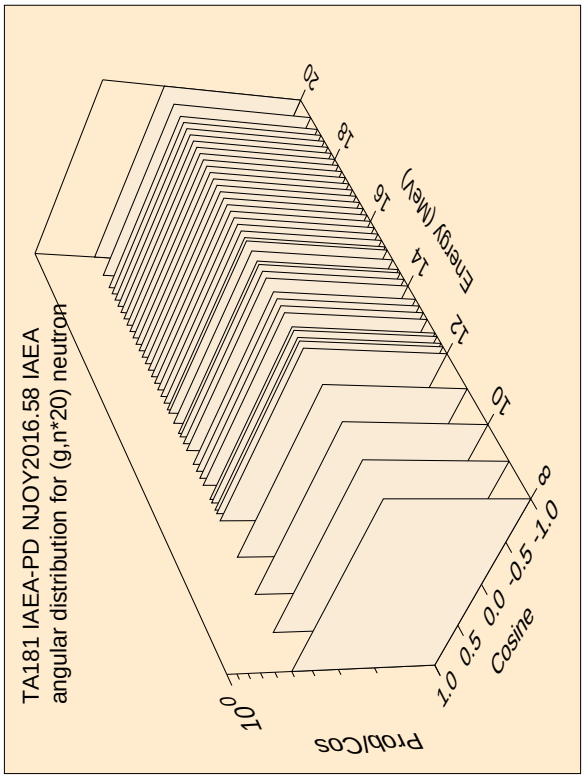
TA181 IAEA-PD NJOY2016.58 IAEA
angular distribution for (g,n*20) neutron
Prob/Cos
Cosine
Energy (MeV)

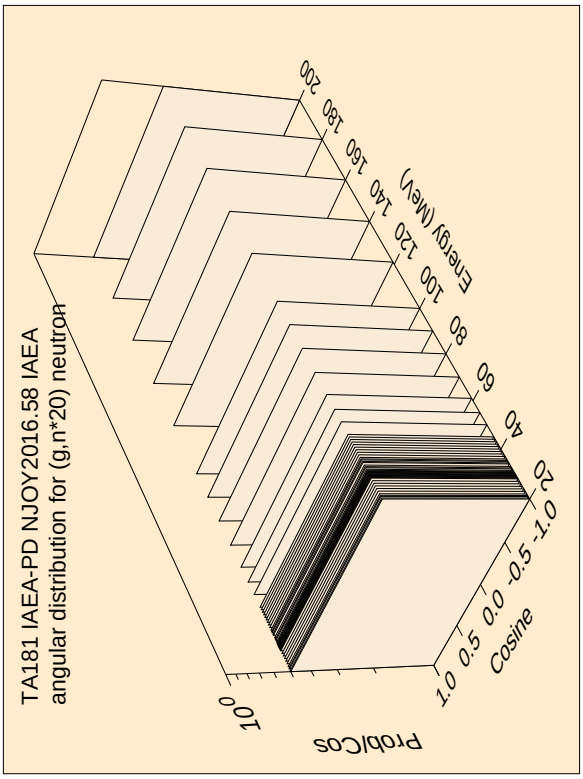
TA181 IAEA-PD NJOY2016.58 IAEA
angular distribution for (g,n*20) neutron
Prob/Cos
Cosine
Energy (MeV)

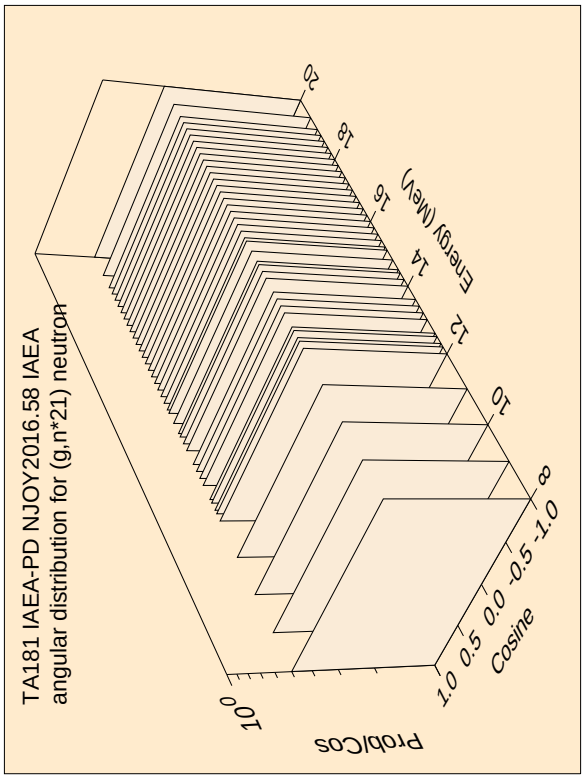
TA181 IAEA-PD NJOY2016.58 IAEA
angular distribution for (g,n*21) neutron
Prob/Cos
Cosine
Energy (MeV)

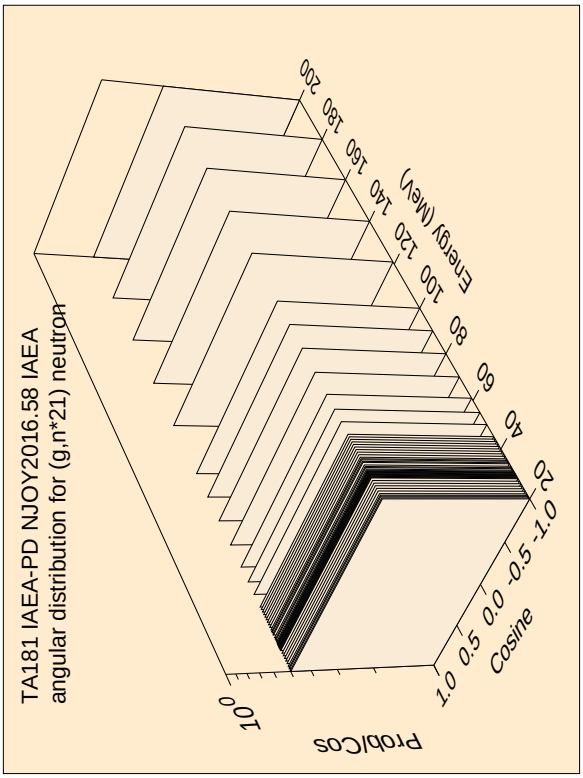
TA181 IAEA-PD NJOY2016.58 IAEA
angular distribution for (g,n*21) neutron
Prob/Cos
Cosine
Energy (MeV)

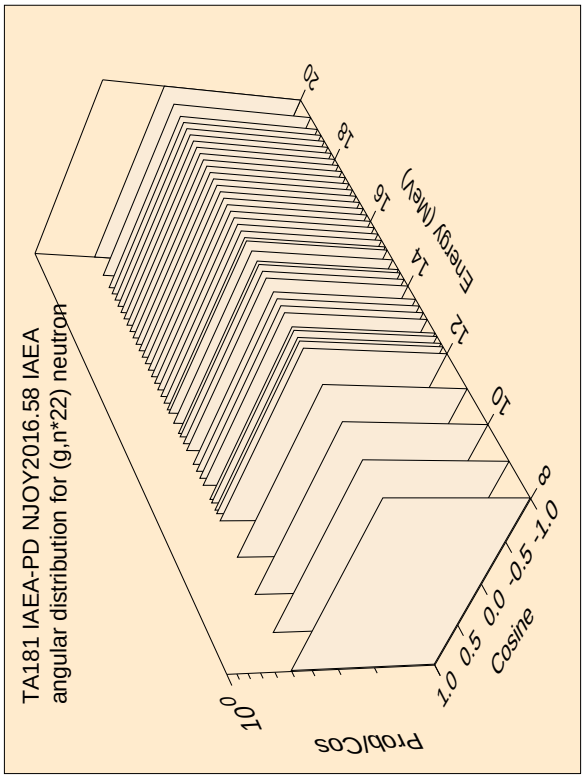
TA181 IAEA-PD NJOY2016.58 IAEA
angular distribution for (g,n*22) neutron
Prob/Cos
Cosine
Energy (MeV)

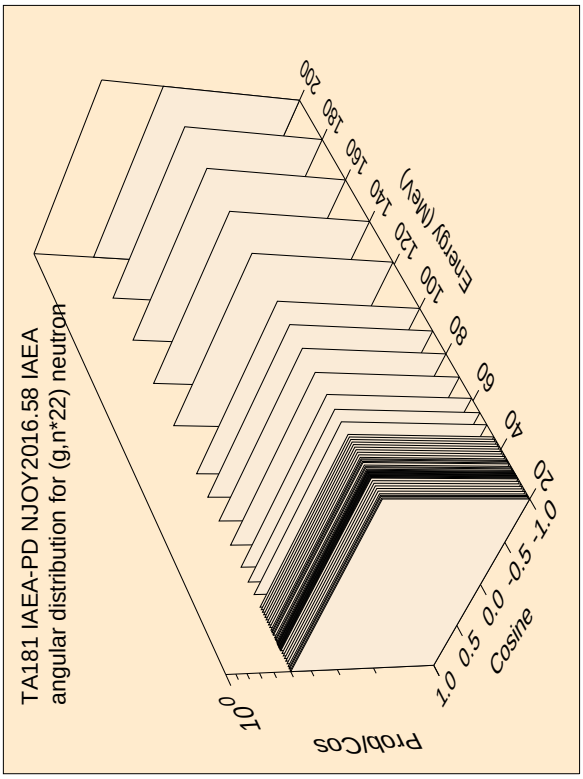
TA181 IAEA-PD NJOY2016.58 IAEA
angular distribution for (g,n*22) neutron
Prob/Cos
Cosine
Energy (MeV)

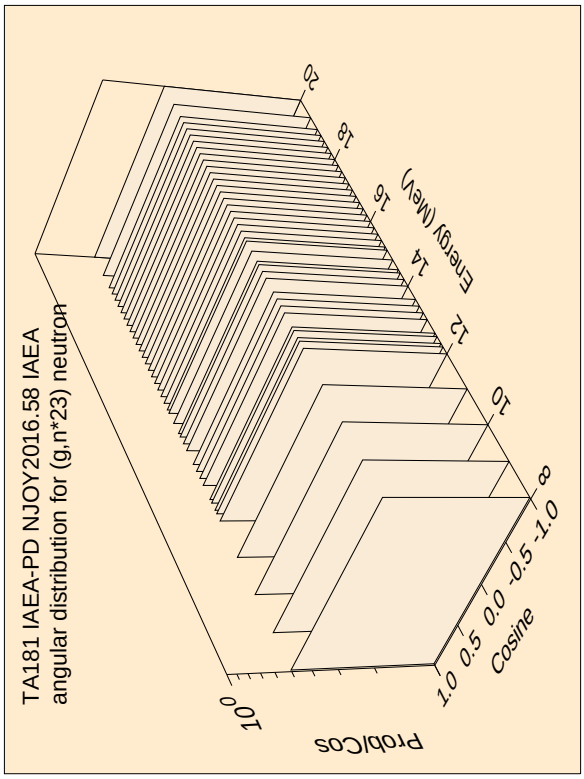
TA181 IAEA-PD NJOY2016.58 IAEA
angular distribution for (g,n*23) neutron
Prob/Cos
Cosine
Energy (MeV)

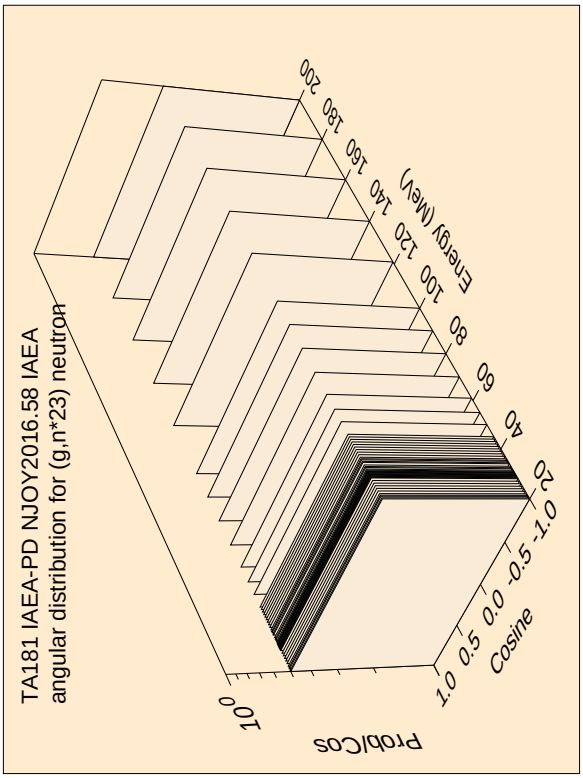
TA181 IAEA-PD NJOY2016.58 IAEA
angular distribution for (g,n*23) neutron
Prob/Cos
Cosine
Energy (MeV)

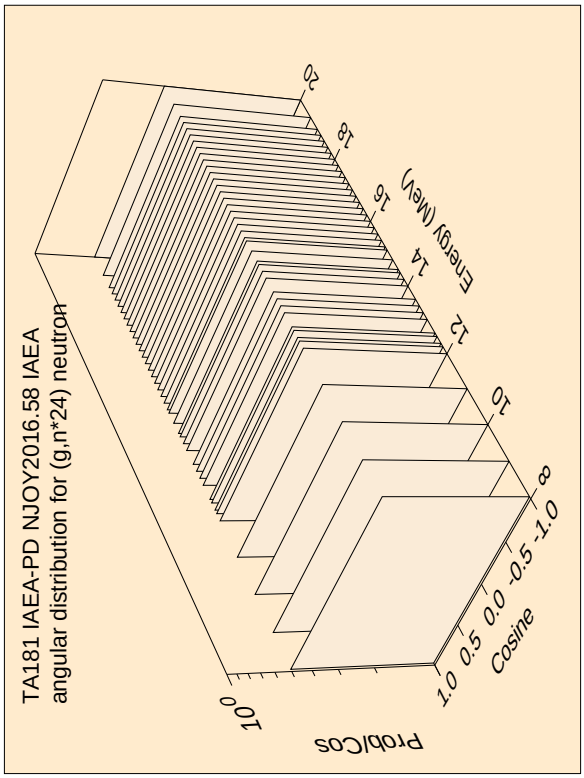
TA181 IAEA-PD NJOY2016.58 IAEA
angular distribution for (g,n*24) neutron
Prob/Cos
Cosine
Energy (MeV)

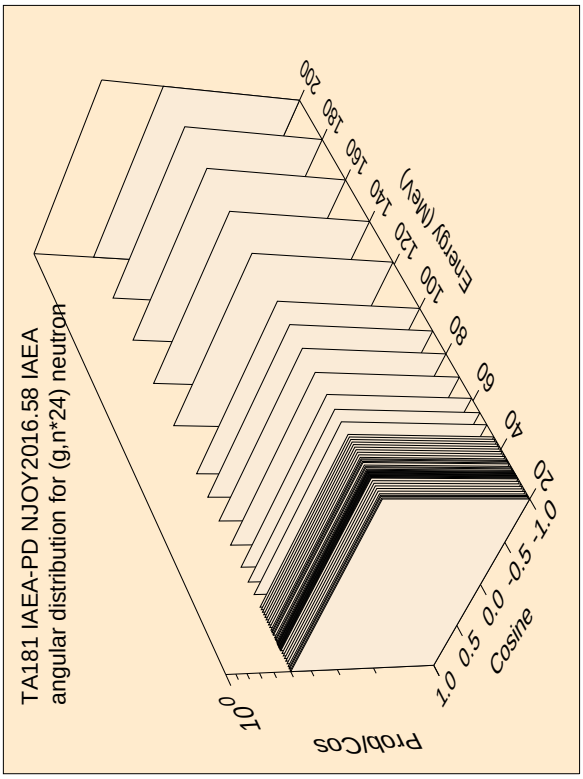
TA181 IAEA-PD NJOY2016.58 IAEA
angular distribution for (g,n*24) neutron
Prob/Cos
Cosine
Energy (MeV)

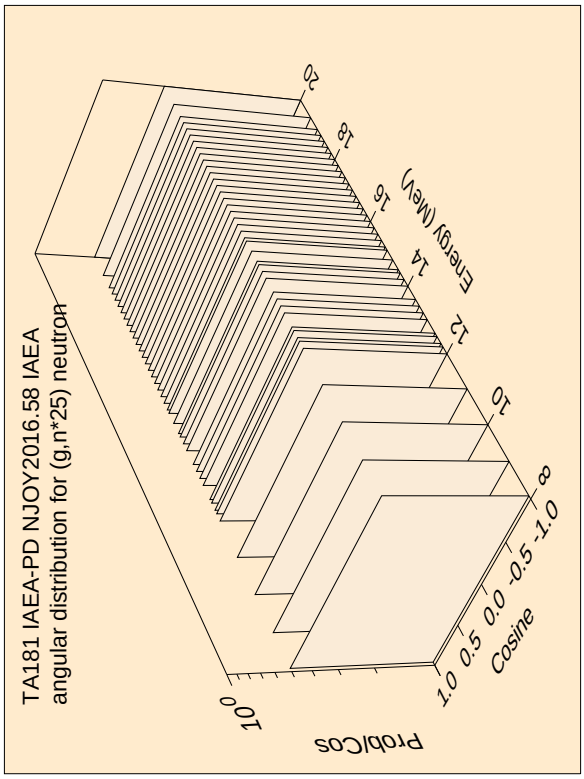
TA181 IAEA-PD NJOY2016.58 IAEA
angular distribution for (g,n*25) neutron
Prob/Cos
Cosine
Energy (MeV)

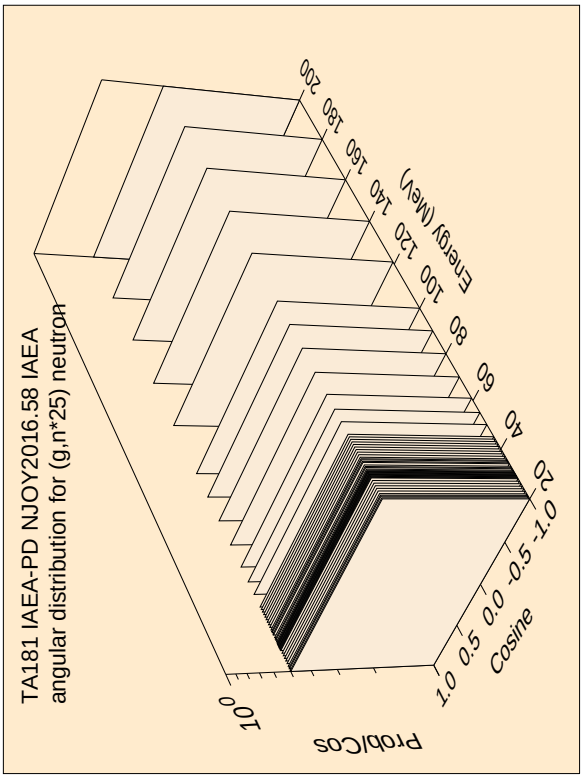
TA181 IAEA-PD NJOY2016.58 IAEA
angular distribution for (g,n*25) neutron
Prob/Cos
Cosine
Energy (MeV)

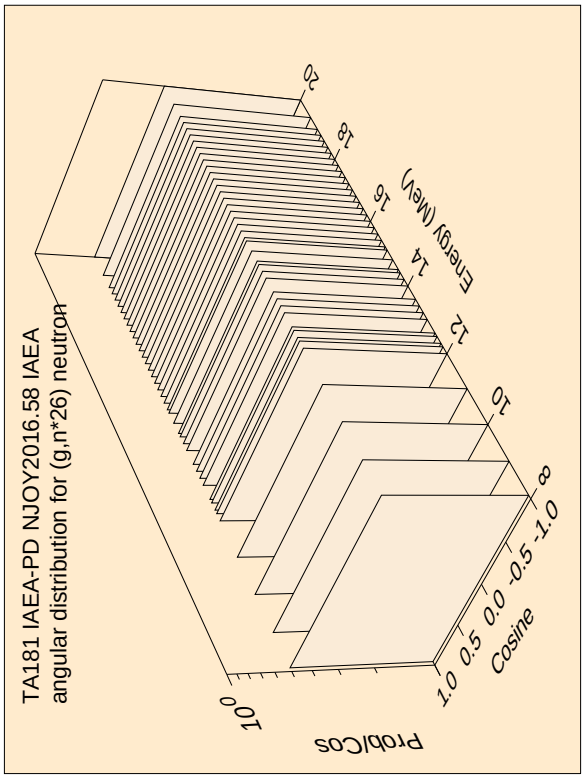
TA181 IAEA-PD NJOY2016.58 IAEA
angular distribution for (g,n*26) neutron
Prob/Cos
Cosine
Energy (MeV)

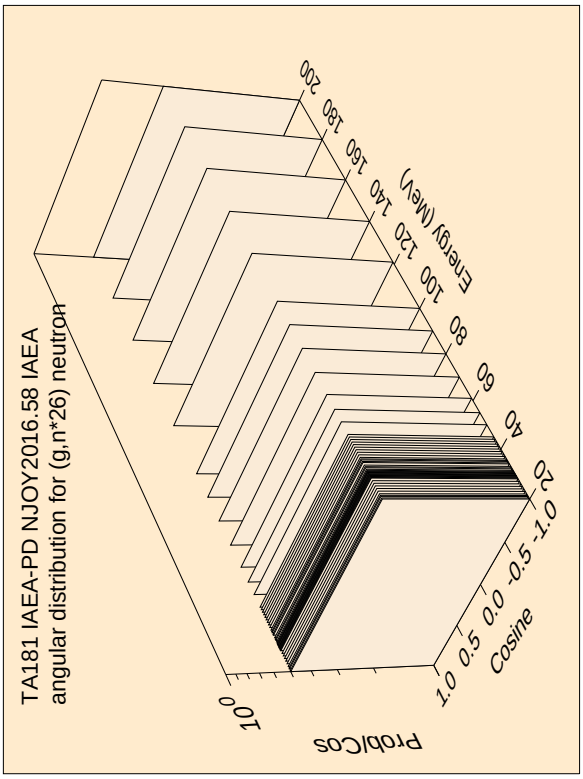
TA181 IAEA-PD NJOY2016.58 IAEA
angular distribution for (g,n*26) neutron
Prob/Cos
Cosine
Energy (MeV)

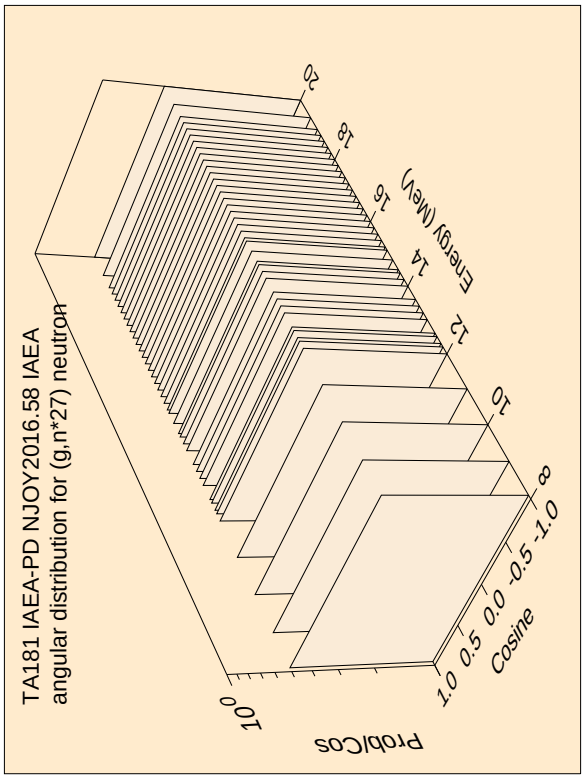
TA181 IAEA-PD NJOY2016.58 IAEA
angular distribution for (g,n*27) neutron
Prob/Cos
Cosine
Energy (MeV)

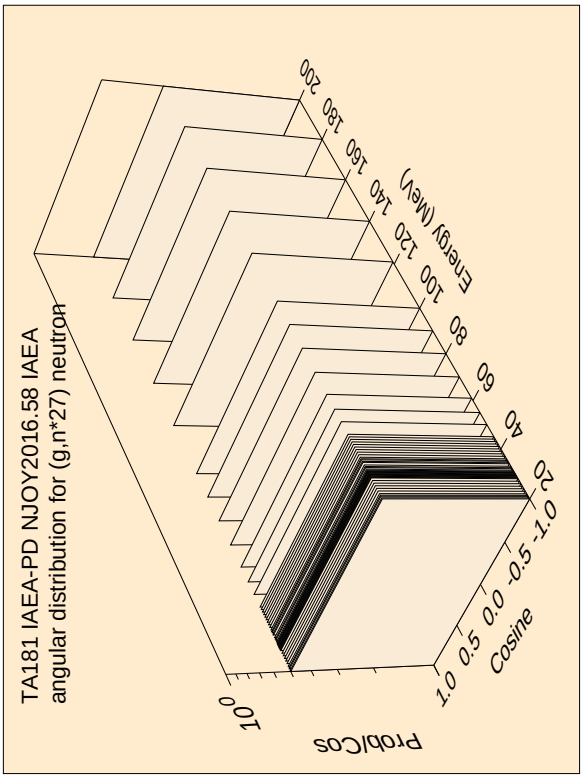
TA181 IAEA-PD NJOY2016.58 IAEA
angular distribution for (g,n*27) neutron
Prob/Cos
Cosine
Energy (MeV)

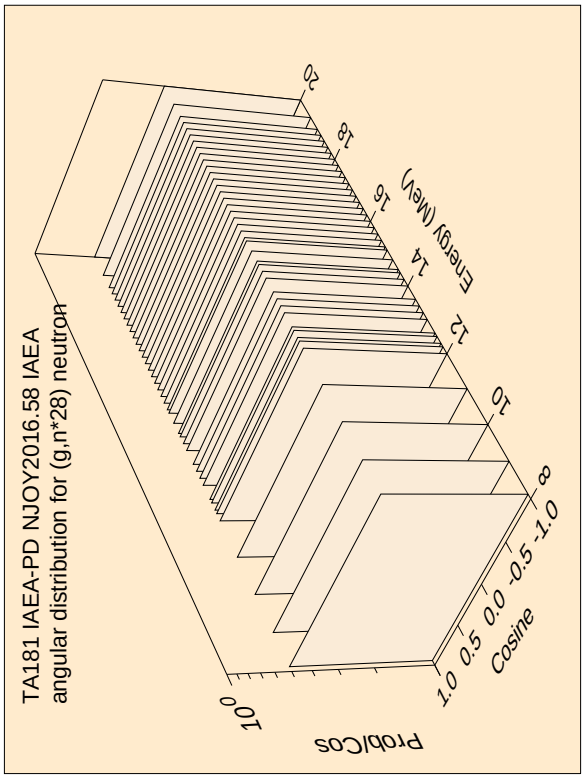
TA181 IAEA-PD NJOY2016.58 IAEA
angular distribution for (g,n*28) neutron
Prob/Cos
Cosine
Energy (MeV)

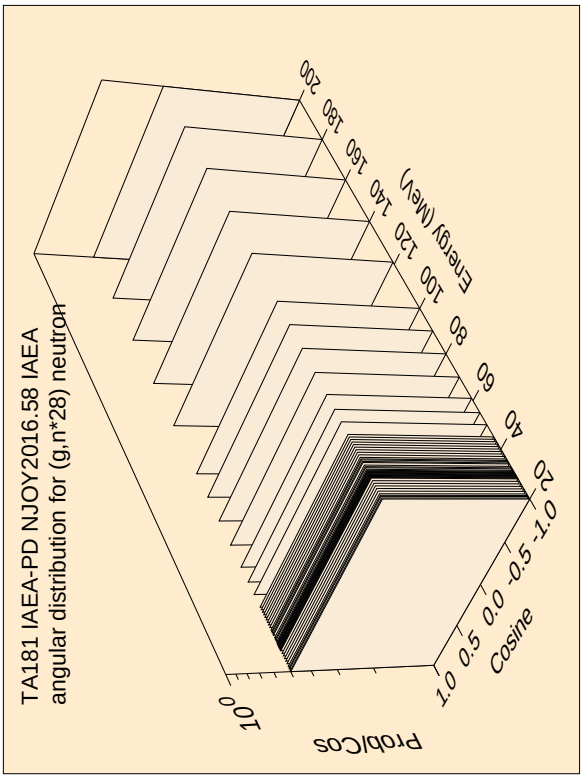
TA181 IAEA-PD NJOY2016.58 IAEA
angular distribution for (g,n*28) neutron
Prob/Cos
Cosine
Energy (MeV)

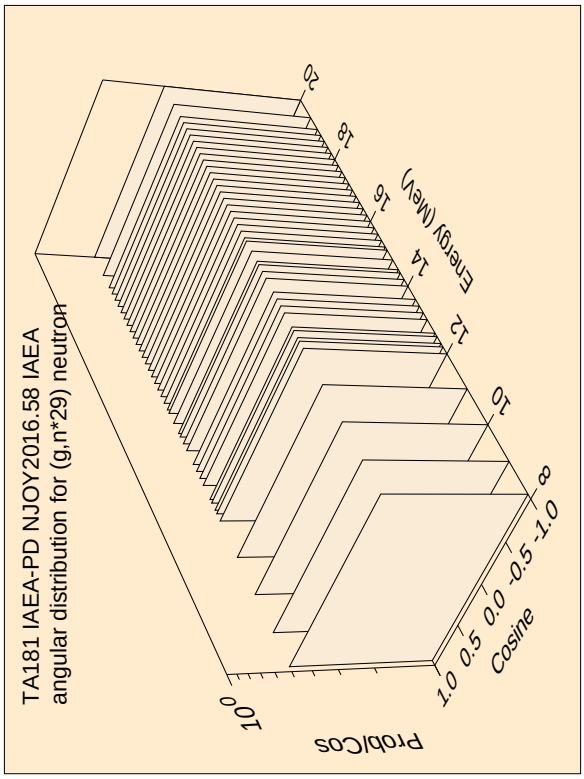
TA181 IAEA-PD NJOY2016.58 IAEA
angular distribution for (g,n*29) neutron
Prob/Cos
Cosine
Energy (MeV)

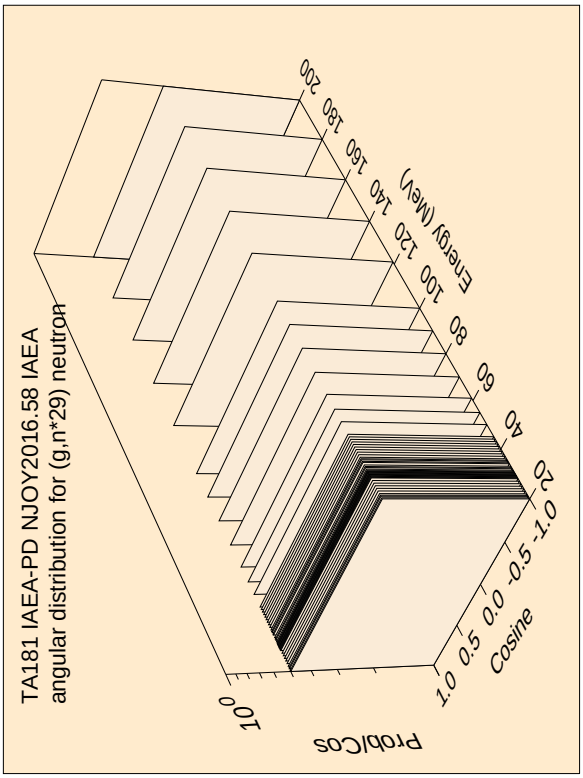
TA181 IAEA-PD NJOY2016.58 IAEA
angular distribution for (g,n*29) neutron
Prob/Cos
Cosine
Energy (MeV)

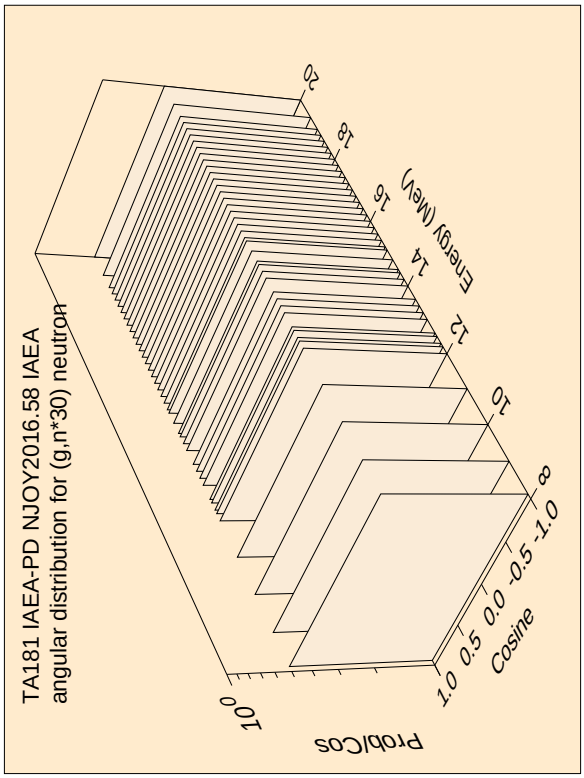
TA181 IAEA-PD NJOY2016.58 IAEA
angular distribution for (g,n*30) neutron
Prob/Cos
Cosine
Energy (MeV)

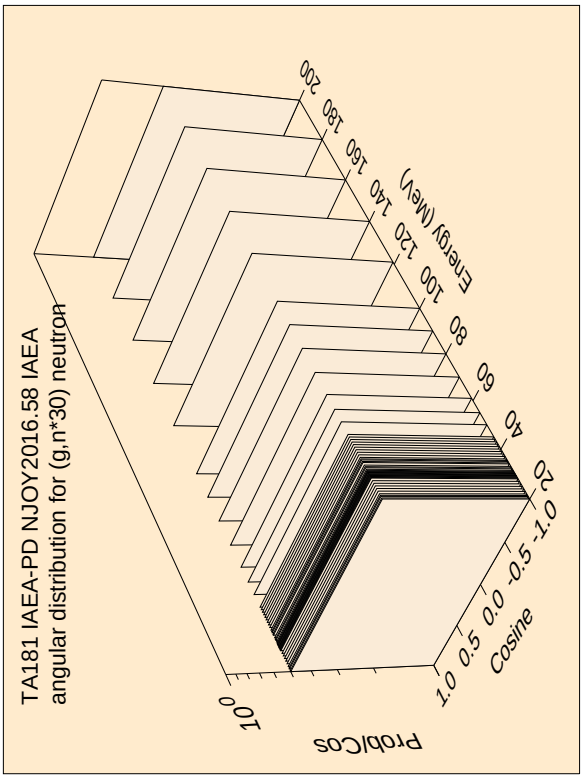
TA181 IAEA-PD NJOY2016.58 IAEA
angular distribution for (g,n*30) neutron
Prob/Cos
Cosine
Energy (MeV)

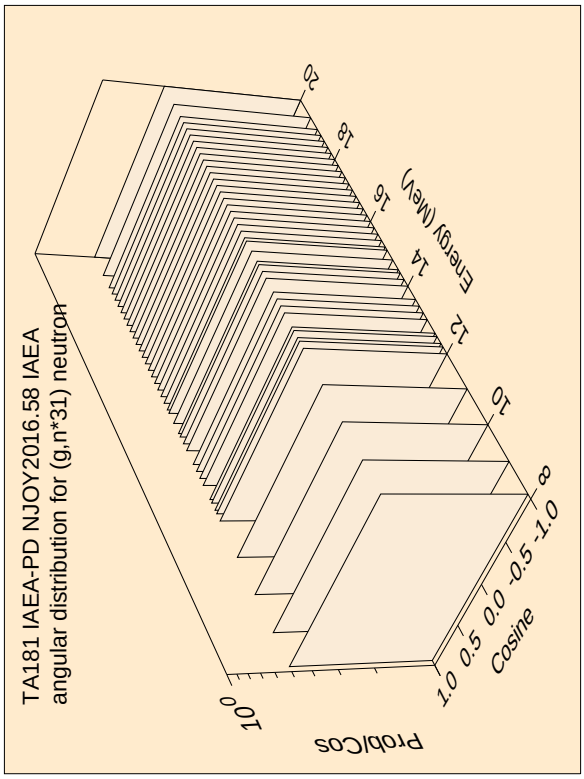
TA181 IAEA-PD NJOY2016.58 IAEA
angular distribution for (g,n*31) neutron
Prob/Cos
Cosine
Energy (MeV)

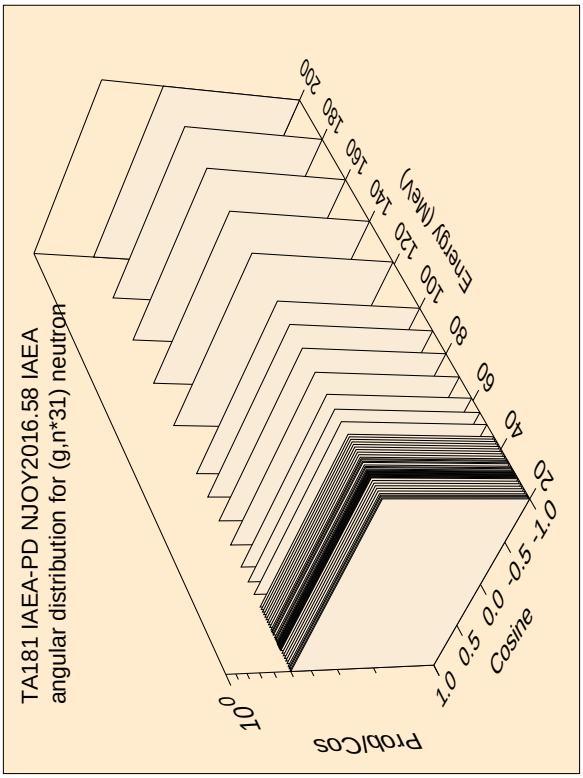
TA181 IAEA-PD NJOY2016.58 IAEA
angular distribution for (g,n*31) neutron
Prob/Cos
Cosine
Energy (MeV)

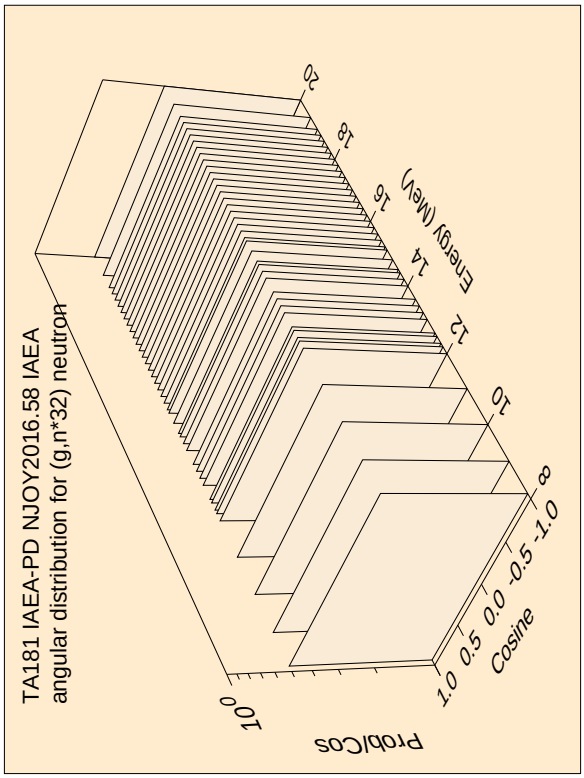
TA181 IAEA-PD NJOY2016.58 IAEA
angular distribution for (g,n*32) neutron
Prob/Cos
Cosine
Energy (MeV)

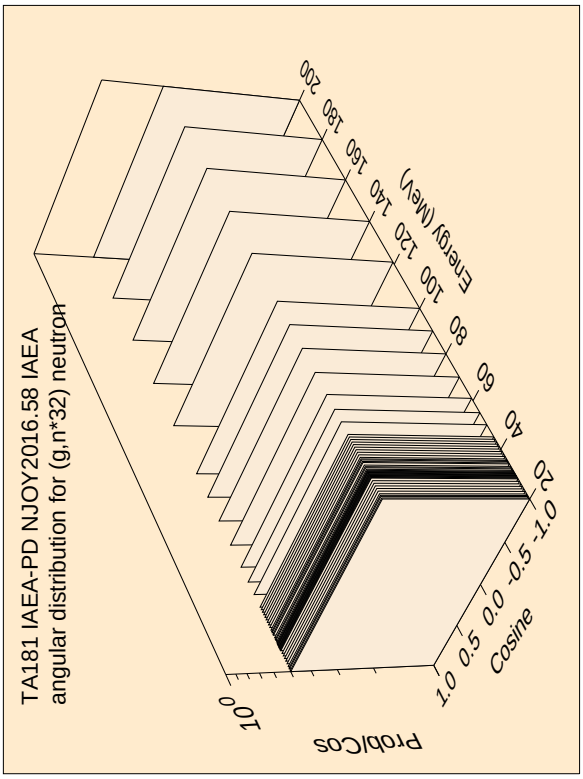
TA181 IAEA-PD NJOY2016.58 IAEA
angular distribution for (g,n*32) neutron
Prob/Cos
Cosine
Energy (MeV)

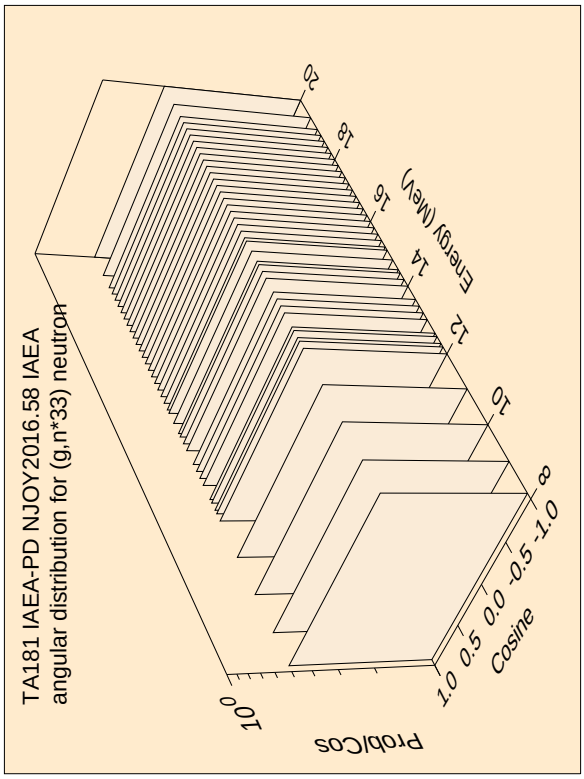
TA181 IAEA-PD NJOY2016.58 IAEA
angular distribution for (g,n*33) neutron
Prob/Cos
Cosine
Energy (MeV)

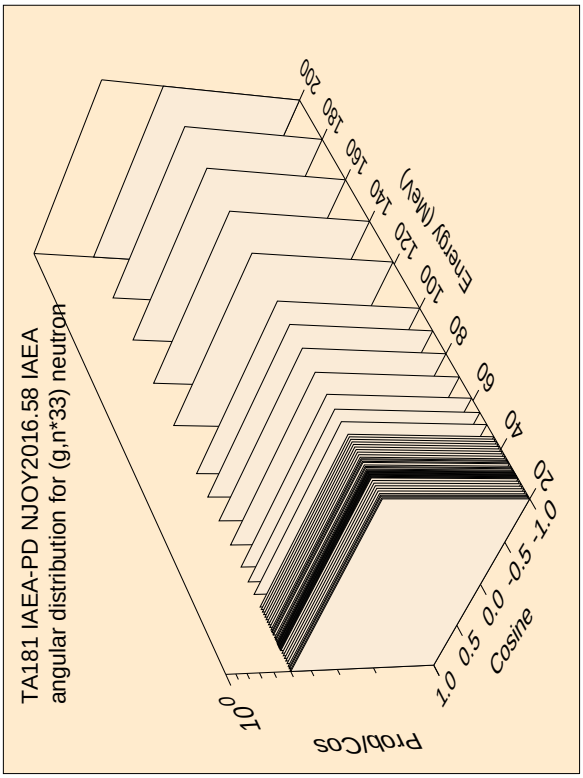
TA181 IAEA-PD NJOY2016.58 IAEA
angular distribution for (g,n*33) neutron
Prob/Cos
Cosine
Energy (MeV)

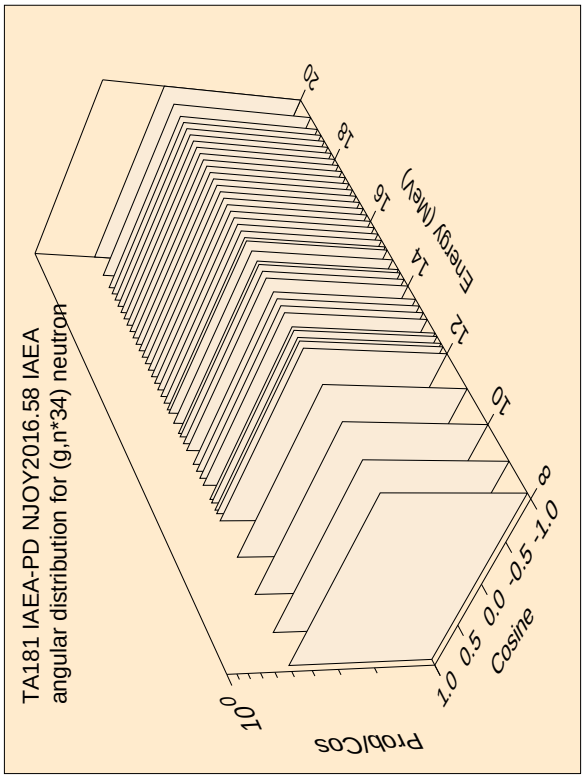
TA181 IAEA-PD NJOY2016.58 IAEA
angular distribution for (g,n*34) neutron
Prob/Cos
Cosine
Energy (MeV)

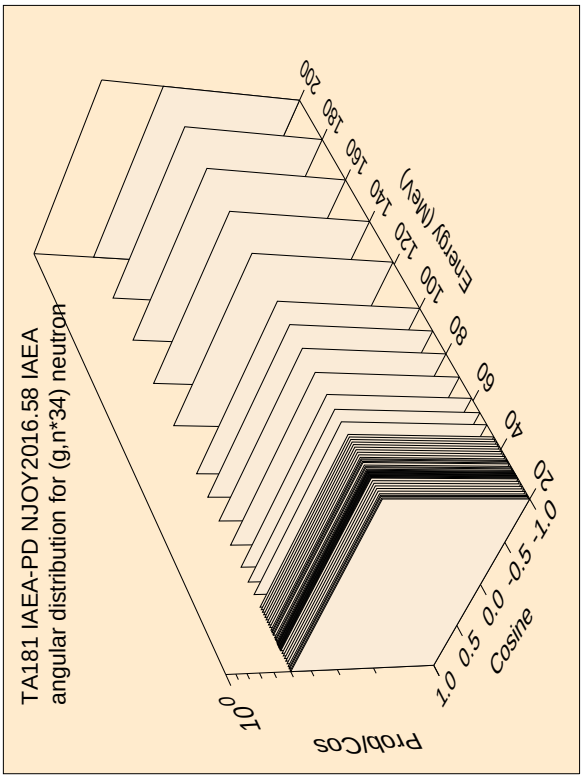
TA181 IAEA-PD NJOY2016.58 IAEA
angular distribution for (g,n*34) neutron
Prob/Cos
Cosine
Energy (MeV)

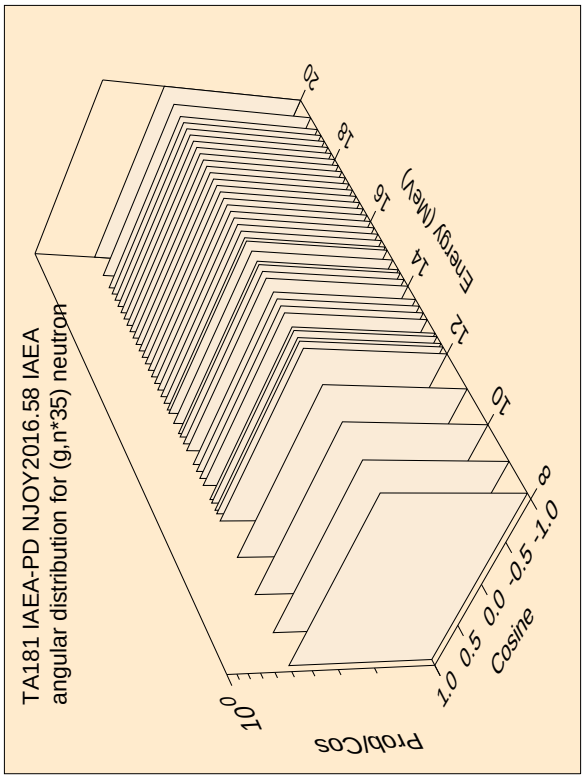
TA181 IAEA-PD NJOY2016.58 IAEA
angular distribution for (g,n*35) neutron
Prob/Cos
Cosine
Energy (MeV)

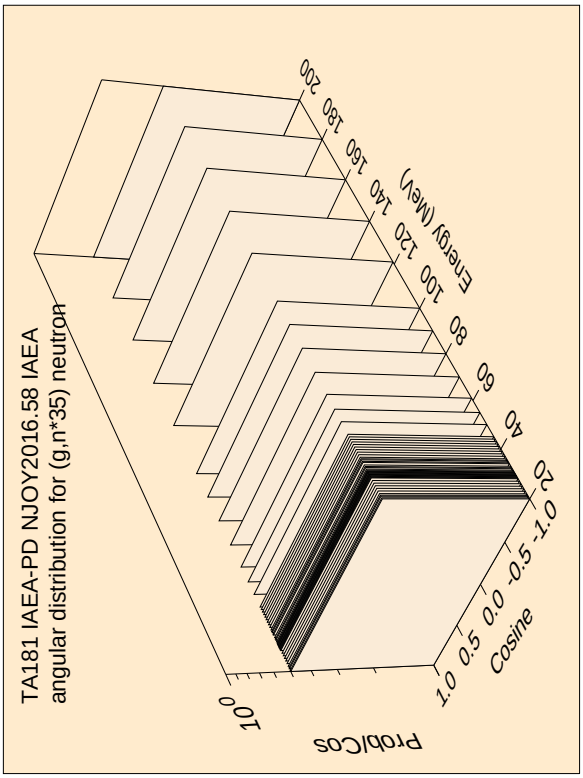
TA181 IAEA-PD NJOY2016.58 IAEA
angular distribution for (g,n*35) neutron
Prob/Cos
Cosine
Energy (MeV)

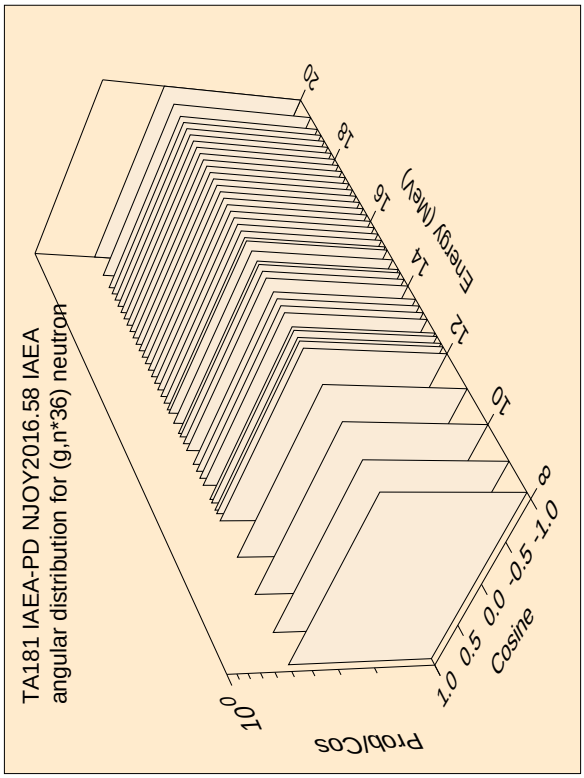
TA181 IAEA-PD NJOY2016.58 IAEA
angular distribution for (g,n*36) neutron
Prob/Cos
Cosine
Energy (MeV)

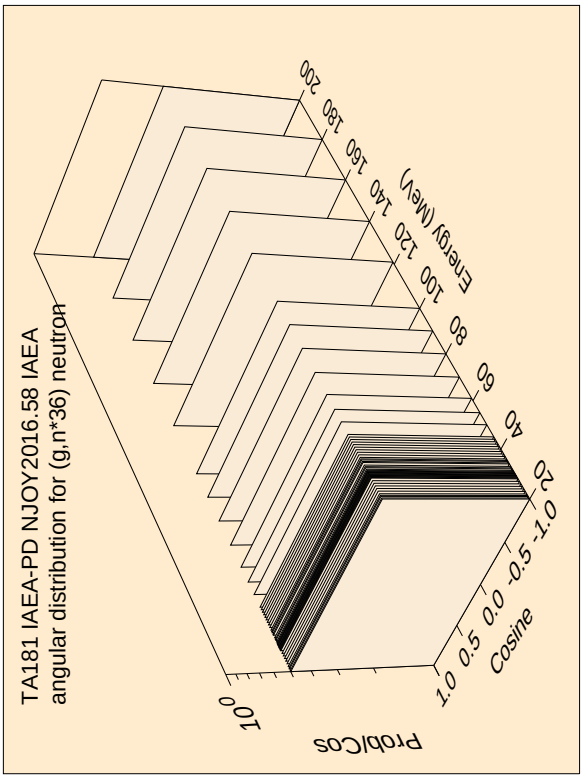
TA181 IAEA-PD NJOY2016.58 IAEA
angular distribution for (g,n*36) neutron
Prob/Cos
Cosine
Energy (MeV)

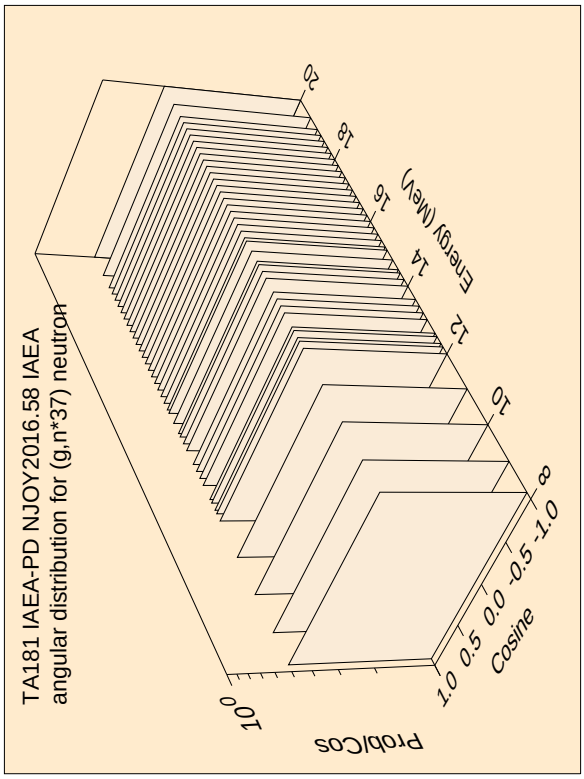
TA181 IAEA-PD NJOY2016.58 IAEA
angular distribution for (g,n*37) neutron
Prob/Cos
Cosine
Energy (MeV)

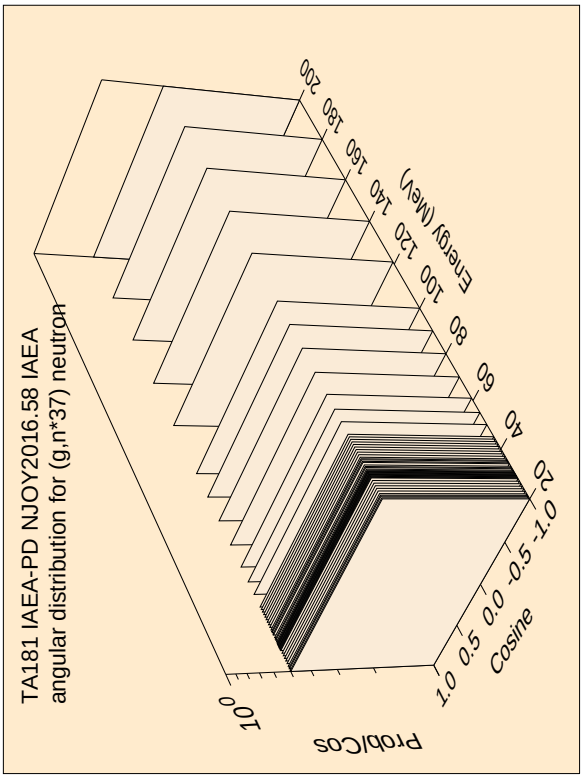
TA181 IAEA-PD NJOY2016.58 IAEA
angular distribution for (g,n*37) neutron
Prob/Cos
Cosine
Energy (MeV)

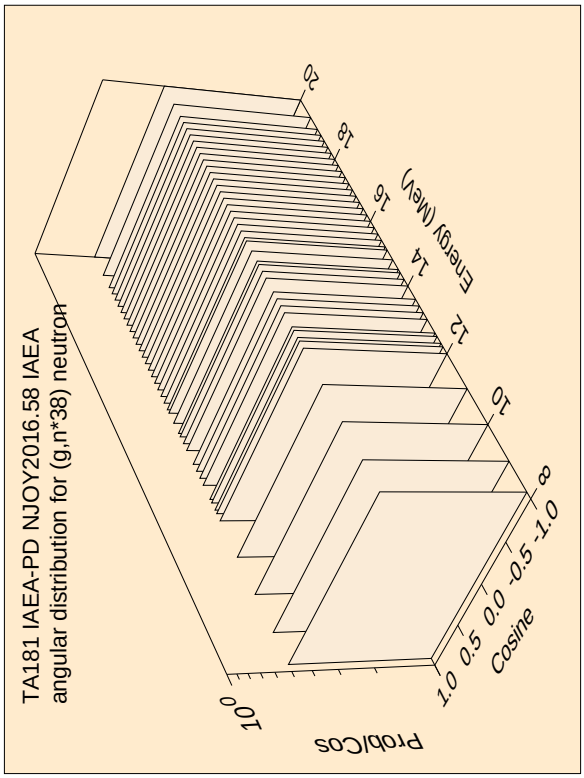
TA181 IAEA-PD NJOY2016.58 IAEA
angular distribution for (g,n*38) neutron
Prob/Cos
Cosine
Energy (MeV)

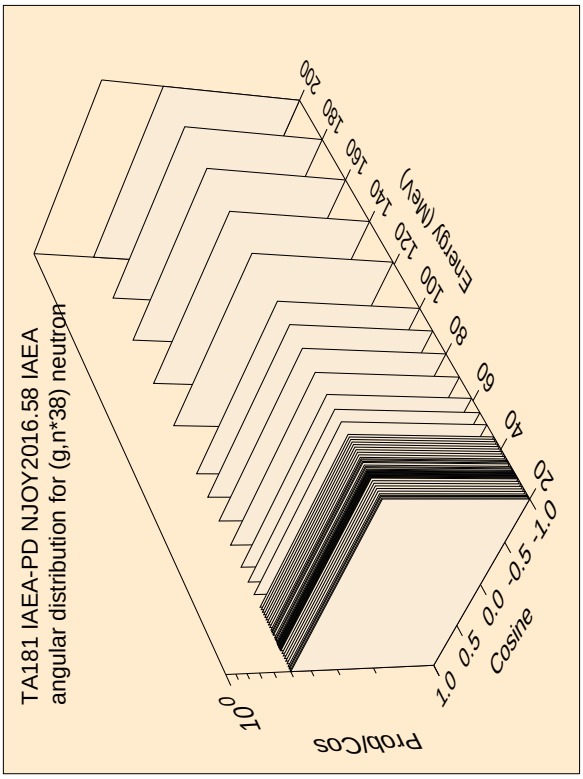
TA181 IAEA-PD NJOY2016.58 IAEA
angular distribution for (g,n*38) neutron
Prob/Cos
Cosine
Energy (MeV)

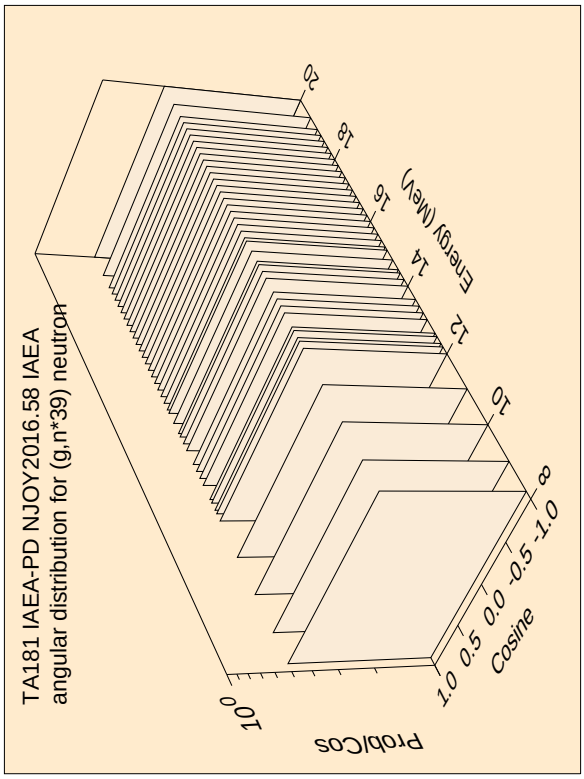
TA181 IAEA-PD NJOY2016.58 IAEA
angular distribution for (g,n*39) neutron
Prob/Cos
Cosine
Energy (MeV)

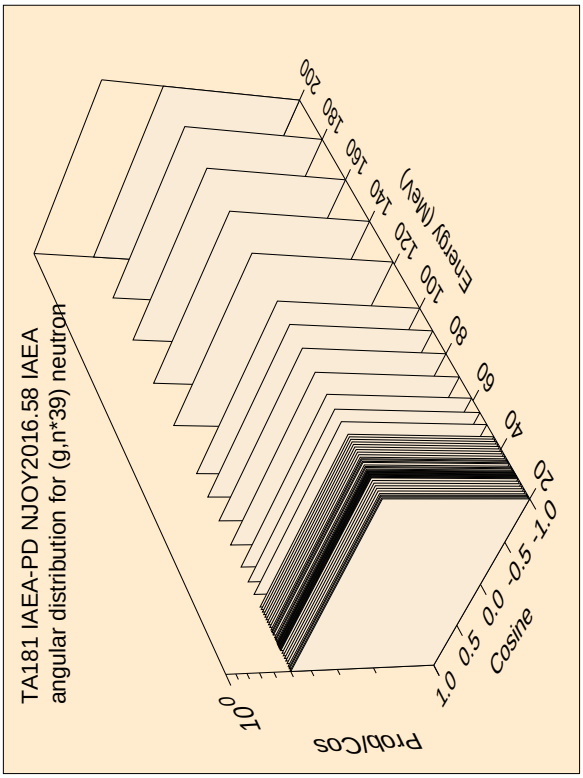
TA181 IAEA-PD NJOY2016.58 IAEA
angular distribution for (g,n*39) neutron
Prob/Cos
Cosine
Energy (Mev)

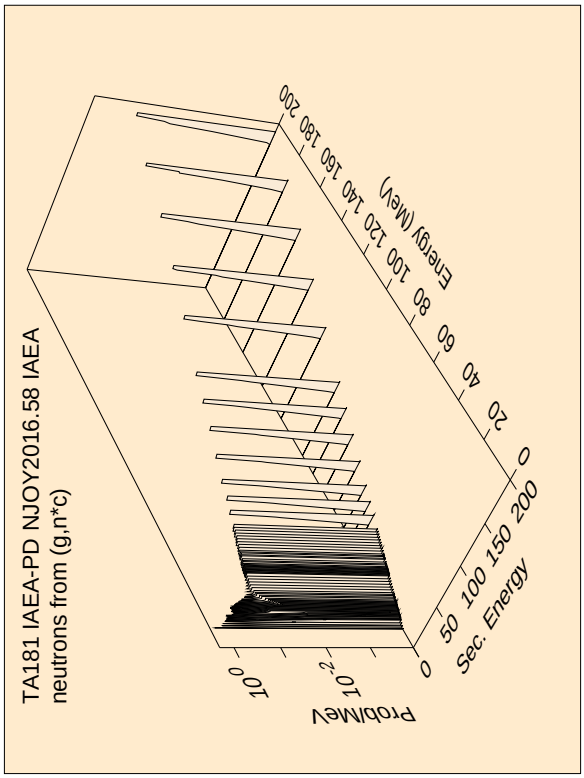
TA181 IAEA-PD NJOY2016.58 IAEA
neutrons from (g,n*c)
Prob/MeV
Sec. Energy
Energy (Mev)

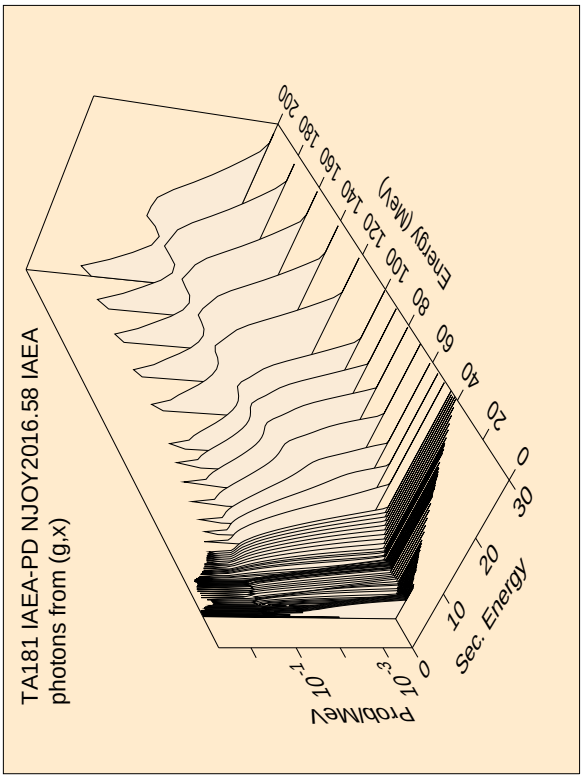
TA181 IAEA-PD NJOY2016.58 IAEA
photons from (g,x)
Prob/MeV
Sec. Energy
Energy (Mev)

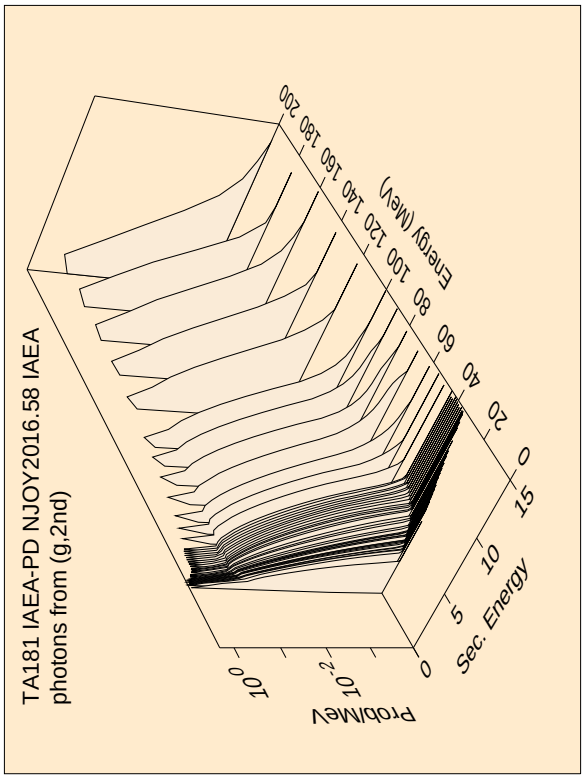
TA181 IAEA-PD NJOY2016.58 IAEA
photons from (g,2nd)
Prob/MeV
Sec. Energy
Energy (Mev)

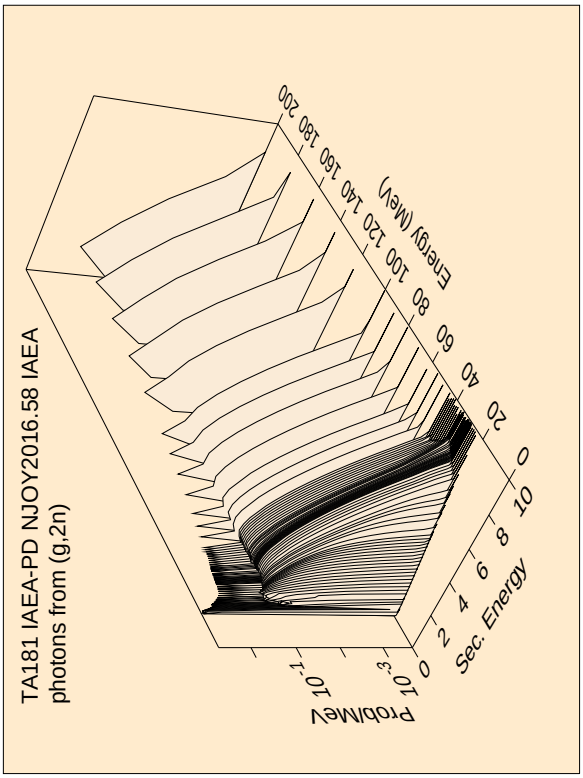
TA181 IAEA-PD NJOY2016.58 IAEA
photons from (g,2n)
Prob/MeV
Energy (Mev)
Sec. Energy

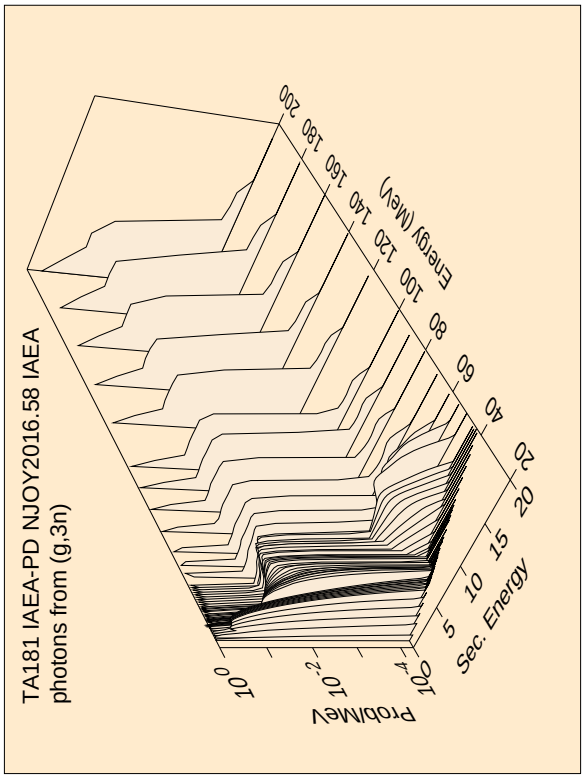
TA181 IAEA-PD NJOY2016.58 IAEA
photons from (g,3n)
Prob/MeV
Energy (Mev)
Sec. Energy

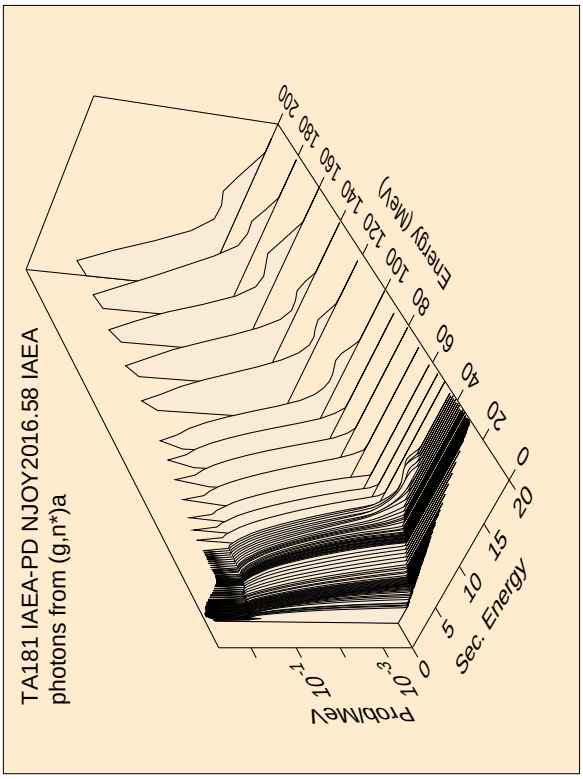
TA181 IAEA-PD NJOY2016.58 IAEA
photons from (g,n*)a
Prob/MeV
Energy (Mev)
Sec. Energy

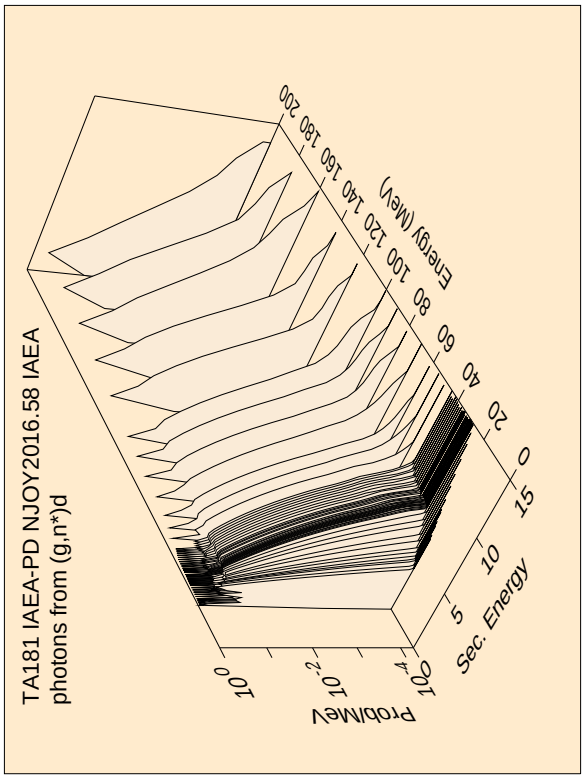
TA181 IAEA-PD NJOY2016.58 IAEA
photons from (g,n*)d
Prob/MeV
Energy (Mev)
Sec. Energy

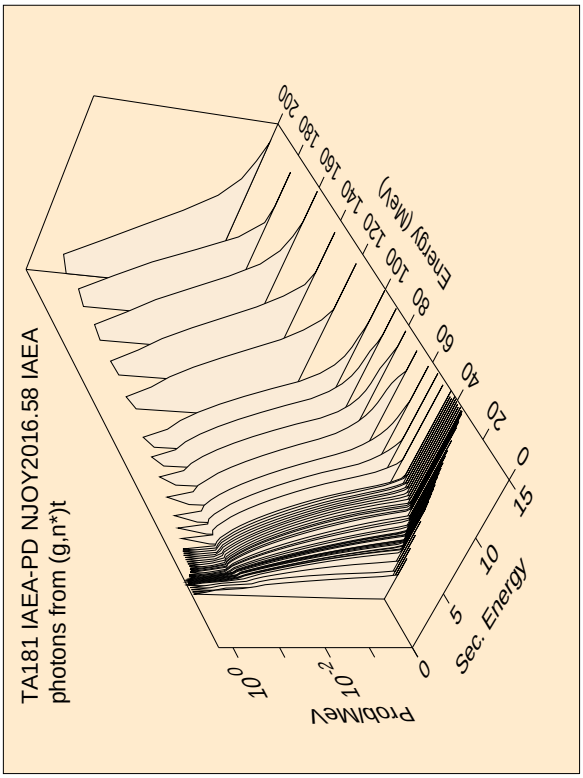
TA181 IAEA-PD NJOY2016.58 IAEA
photons from (g,n*)t
Prob/MeV
Sec. Energy
Energy (Mev)

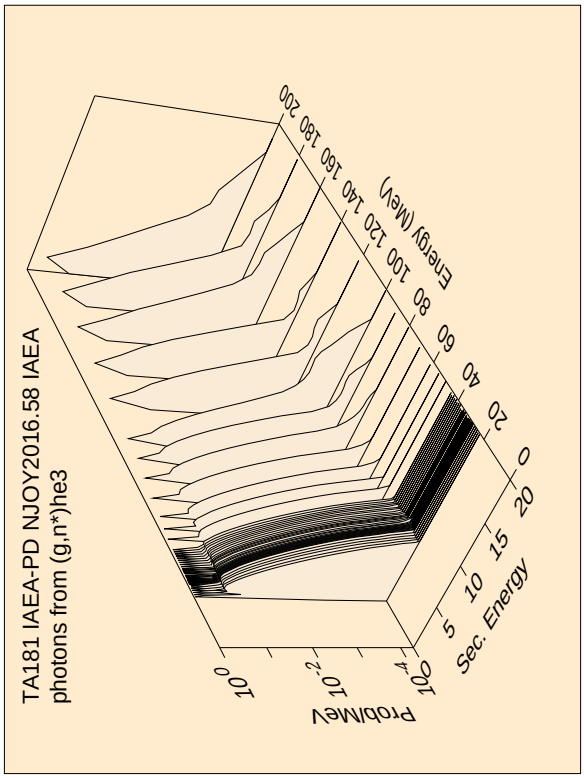
TA181 IAEA-PD NJOY2016.58 IAEA
photons from (g,n*)he3
Prob/MeV
Sec. Energy
Energy (Mev)

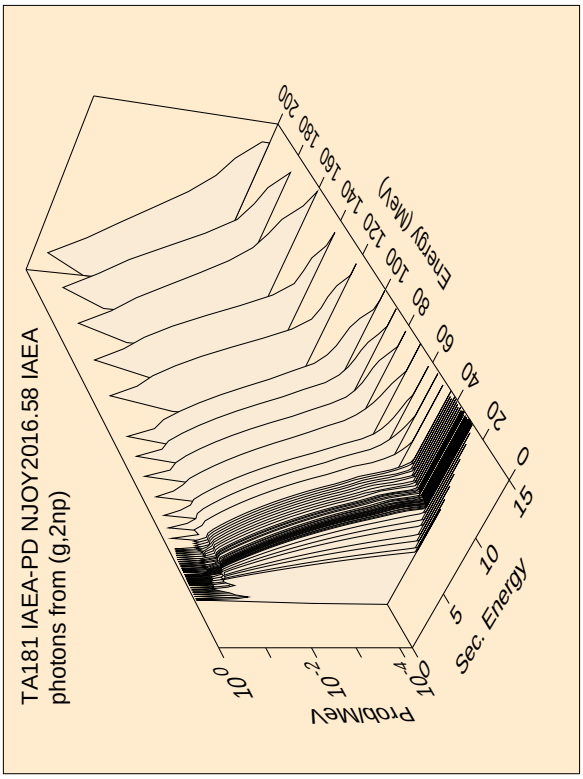
TA181 IAEA-PD NJOY2016.58 IAEA
photons from (g,2np)
Prob/MeV
Sec. Energy
Energy (Mev)

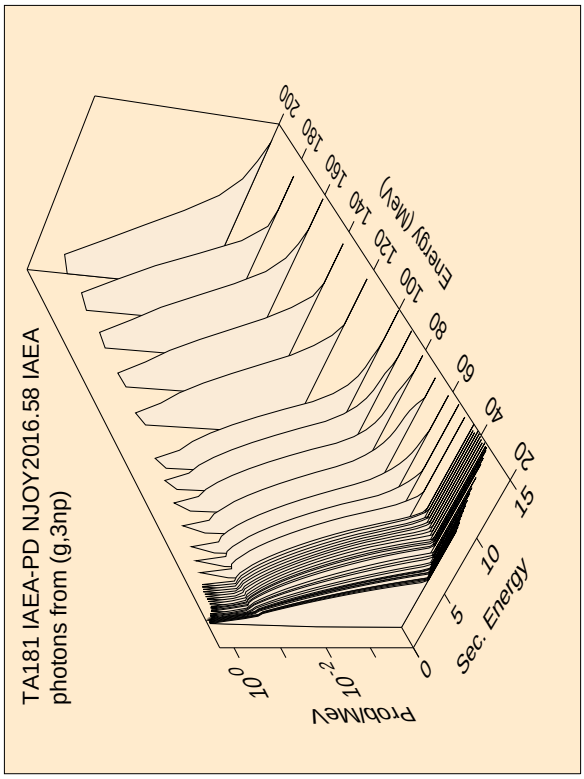
TA181 IAEA-PD NJOY2016.58 IAEA
photons from (g,3np)
Prob/MeV
Sec. Energy
Energy (Mev)

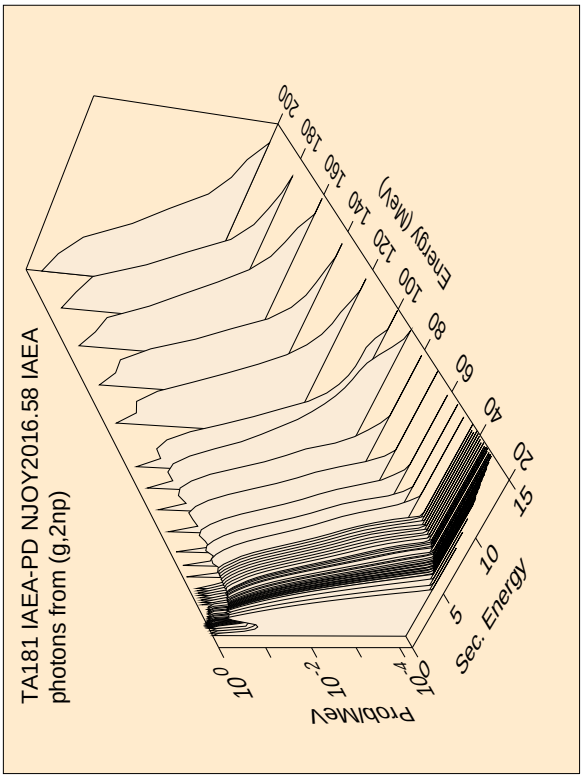
TA181 IAEA-PD NJOY2016.58 IAEA
photons from (g,2np)
Prob/MeV
Energy (Mev)
Sec. Energy

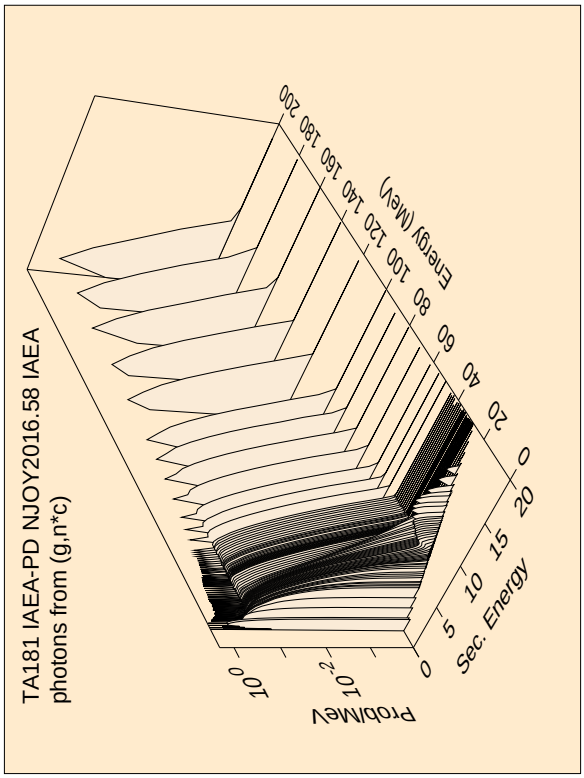
TA181 IAEA-PD NJOY2016.58 IAEA
photons from (g,n*c)
Prob/MeV
Energy (Mev)
Sec. Energy

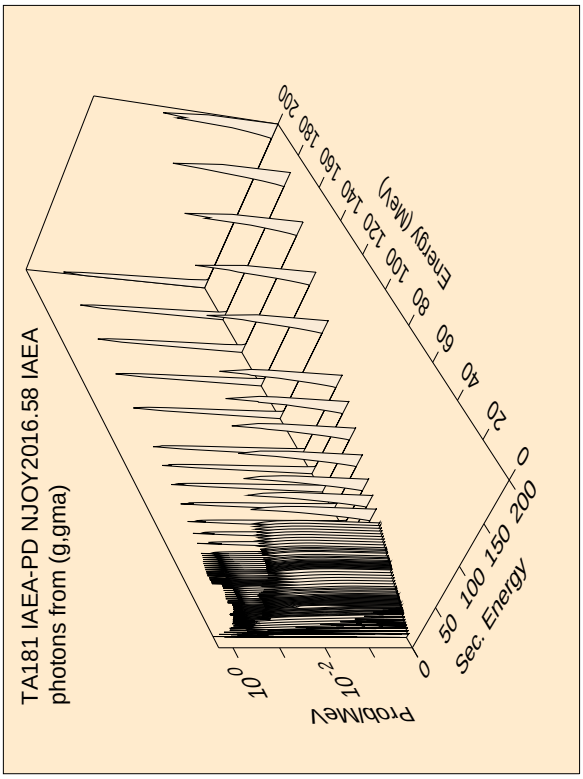
TA181 IAEA-PD NJOY2016.58 IAEA
photons from (g,gma)
Prob/MeV
Energy (Mev)
Sec. Energy

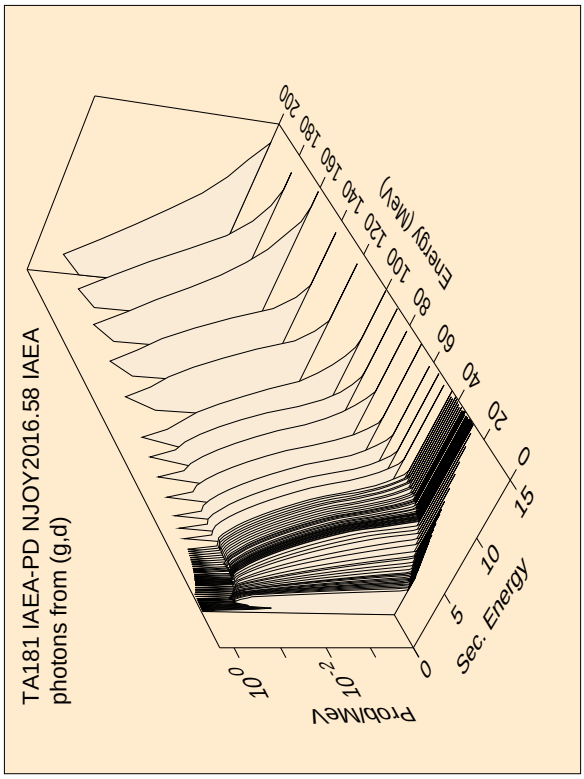
TA181 IAEA-PD NJOY2016.58 IAEA
photons from (g,d)
Prob/MeV
Energy (Mev)
Sec. Energy

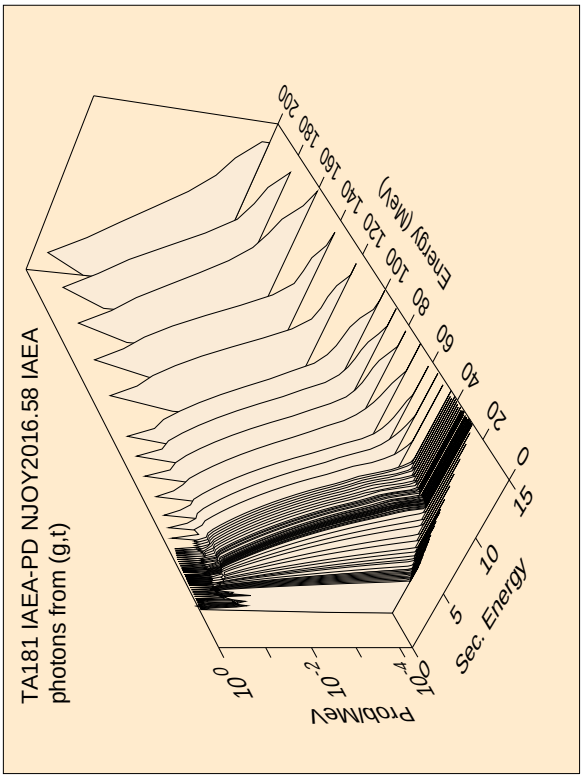
TA181 IAEA-PD NJOY2016.58 IAEA
photons from (g,t)
Prob/MeV
Energy (Mev)
Sec. Energy

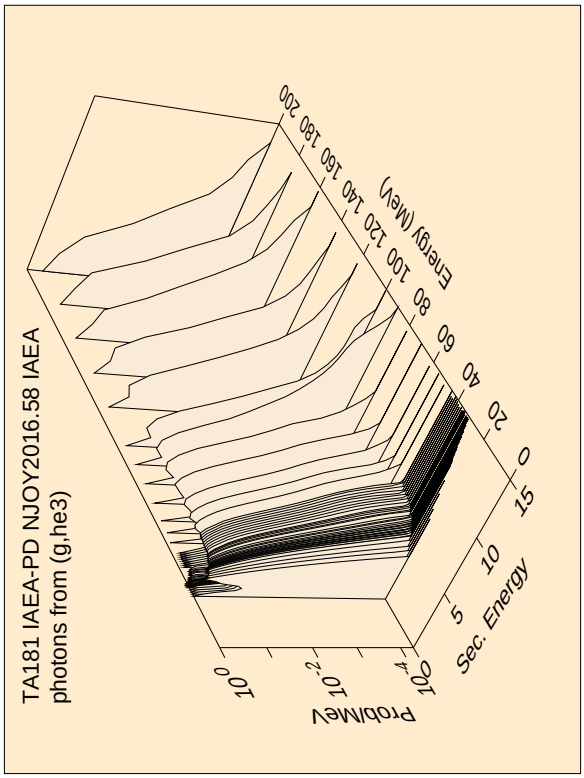
TA181 IAEA-PD NJOY2016.58 IAEA
photons from (g,he3)
Prob/MeV
Energy (Mev)
Sec. Energy

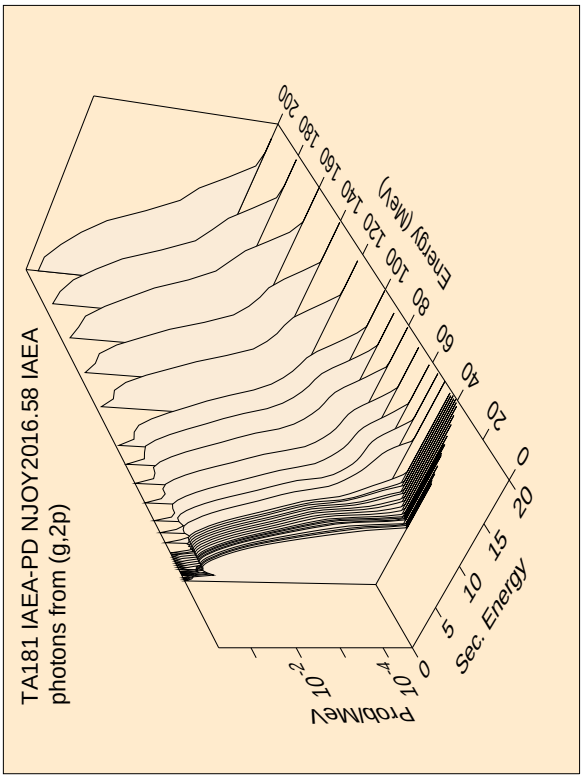
TA181 IAEA-PD NJOY2016.58 IAEA
photons from (g,2p)
Prob/MeV
Energy (Mev)
Sec. Energy

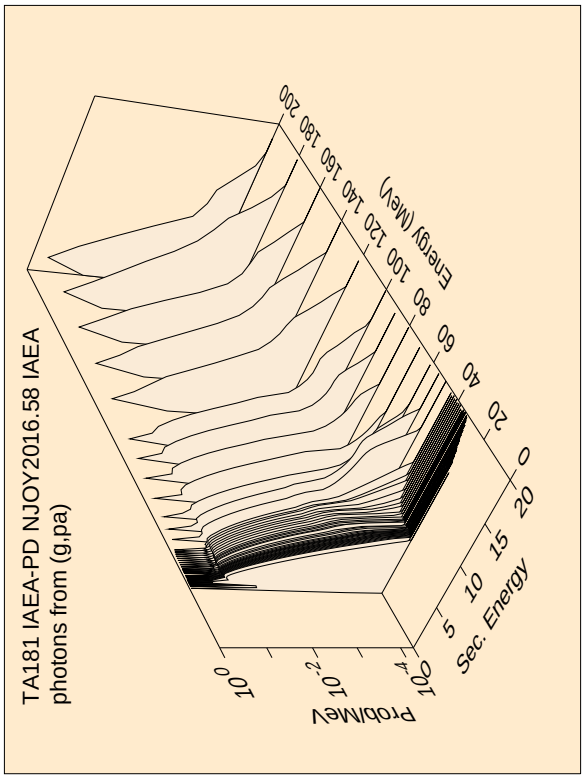
TA181 IAEA-PD NJOY2016.58 IAEA
photons from (g,pa)
Prob/MeV
Energy (Mev)
Sec. Energy

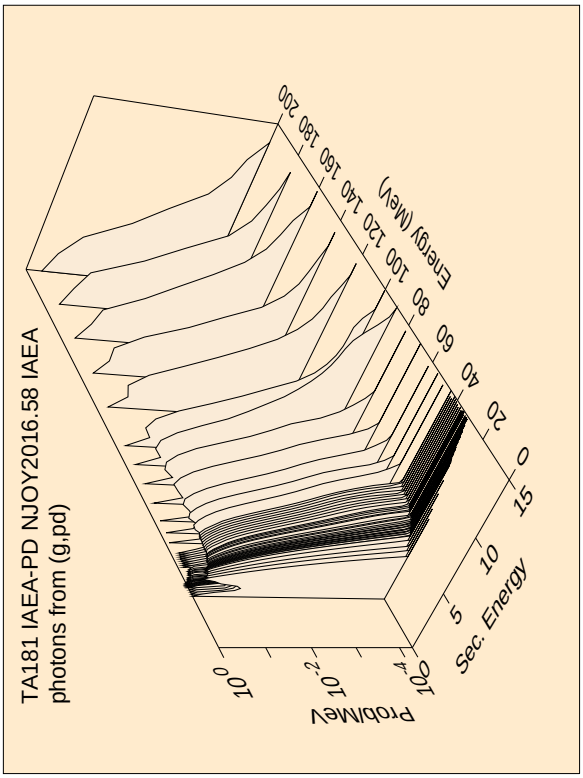
TA181 IAEA-PD NJOY2016.58 IAEA
photons from (g,pd)
Prob/MeV
Energy (MeV)
Sec. Energy

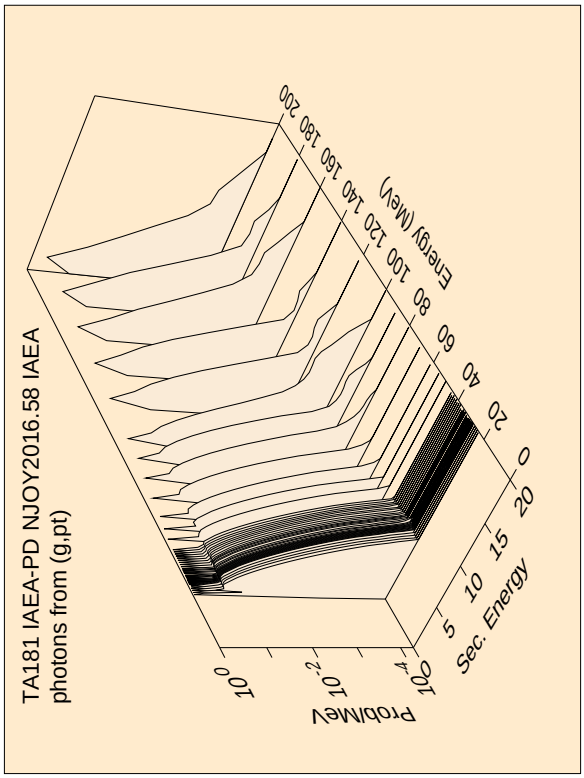
TA181 IAEA-PD NJOY2016.58 IAEA
photons from (g,pt)
Prob/MeV
Energy (MeV)
Sec. Energy

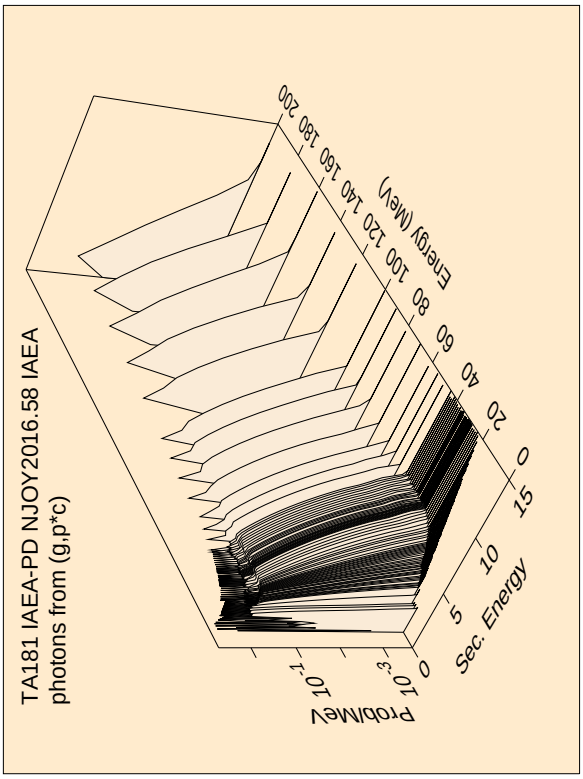
TA181 IAEA-PD NJOY2016.58 IAEA
photons from (g,p*c)
Prob/MeV
Energy (MeV)
Sec. Energy

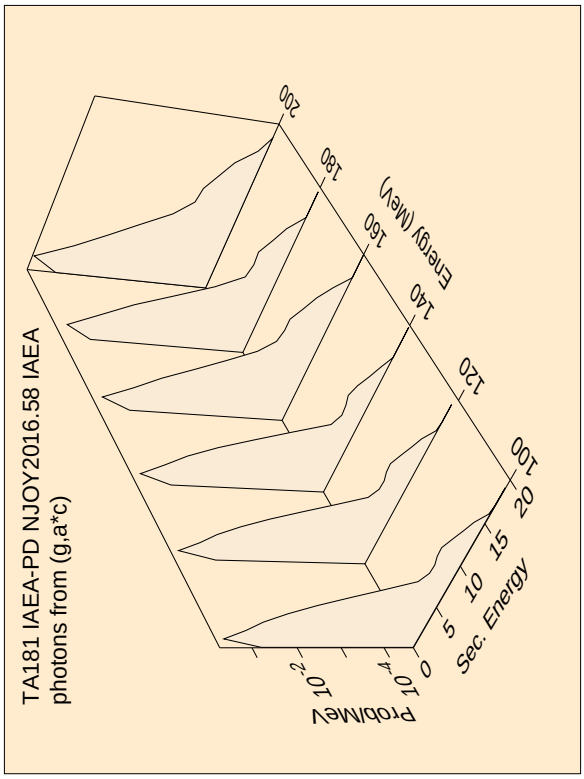
TA181 IAEA-PD NJOY2016.58 IAEA
photons from (g,a*c)
Prob/MeV
Energy (MeV)
Sec. Energy

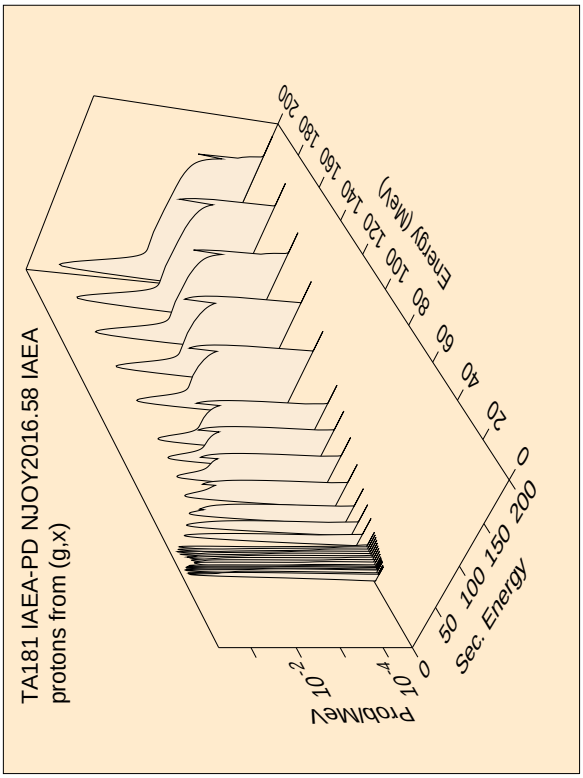
TA181 IAEA-PD NJOY2016.58 IAEA
protons from (g,x)
Prob/MeV
Energy (Mev)
Sec. Energy

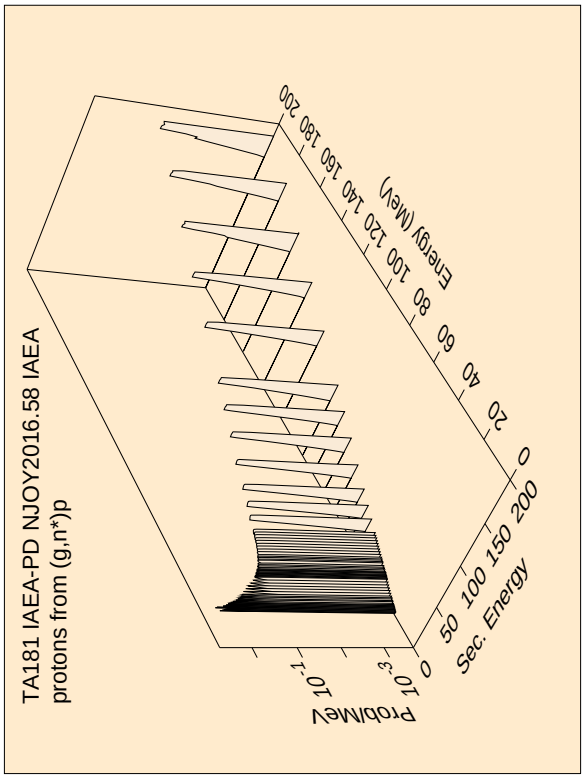
TA181 IAEA-PD NJOY2016.58 IAEA
protons from (g,n*)p
Prob/MeV
Energy (Mev)
Sec. Energy

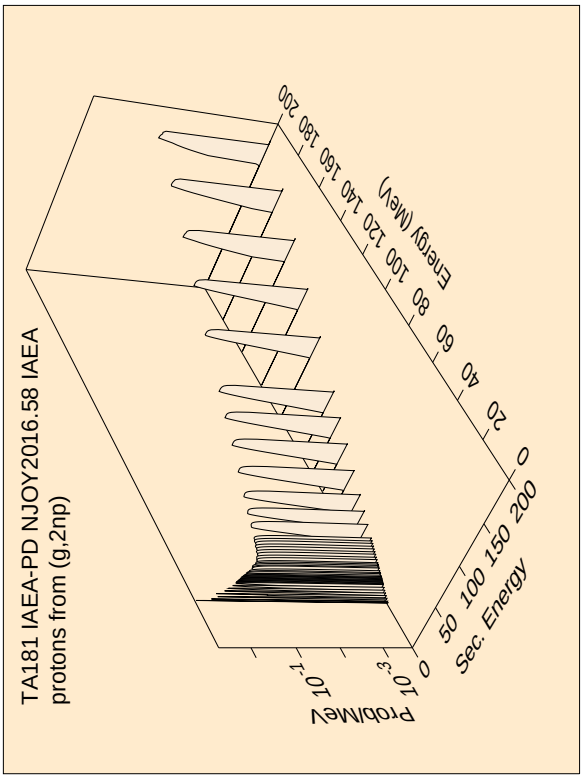
TA181 IAEA-PD NJOY2016.58 IAEA
protons from (g,2np)
Prob/MeV
Energy (Mev)
Sec. Energy

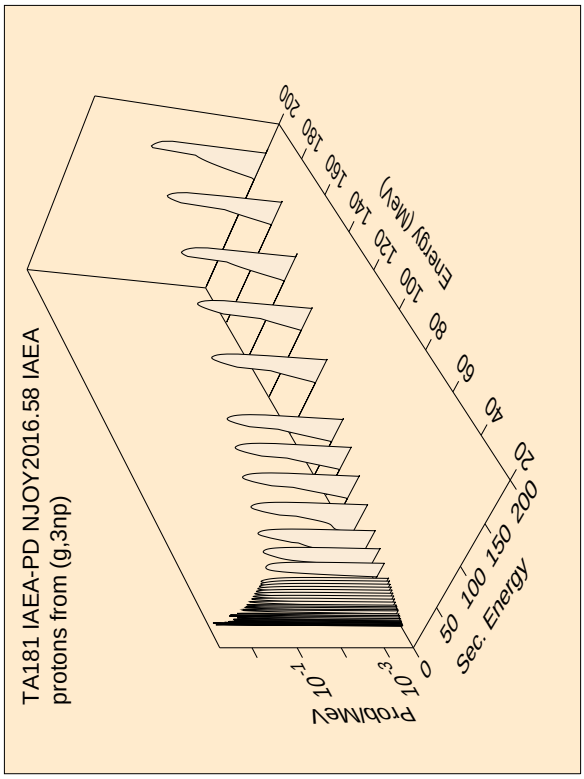
TA181 IAEA-PD NJOY2016.58 IAEA
protons from (g,3np)
Prob/MeV
Energy (Mev)
Sec. Energy

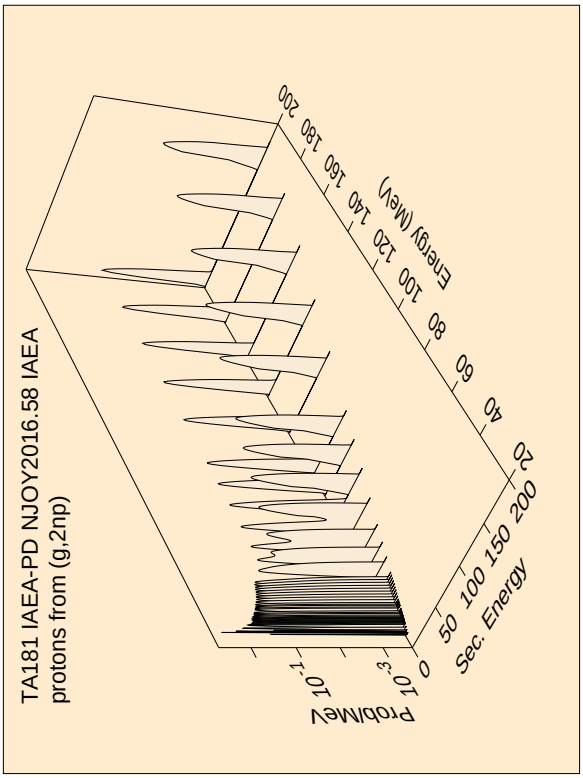
TA181 IAEA-PD NJOY2016.58 IAEA
protons from (g,2np)
Prob/MeV
Energy (Mev)
Sec. Energy

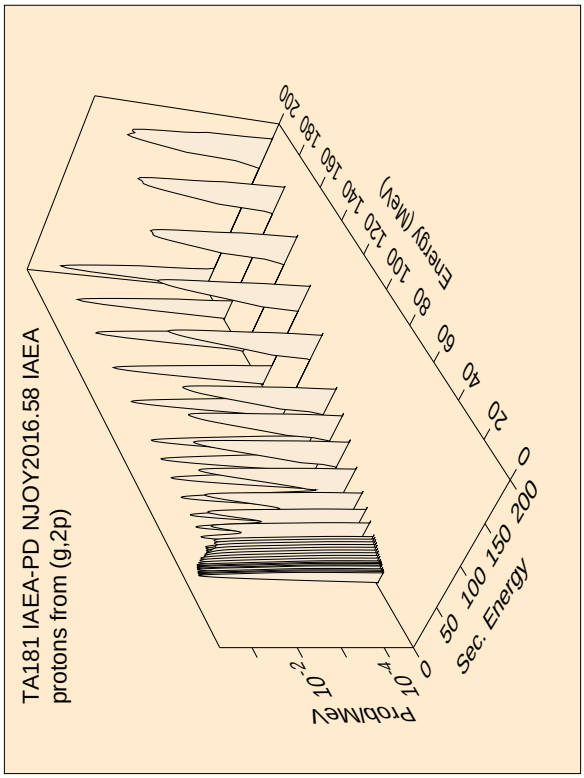
TA181 IAEA-PD NJOY2016.58 IAEA
protons from (g,2p)
Prob/MeV
Energy (Mev)
Sec. Energy

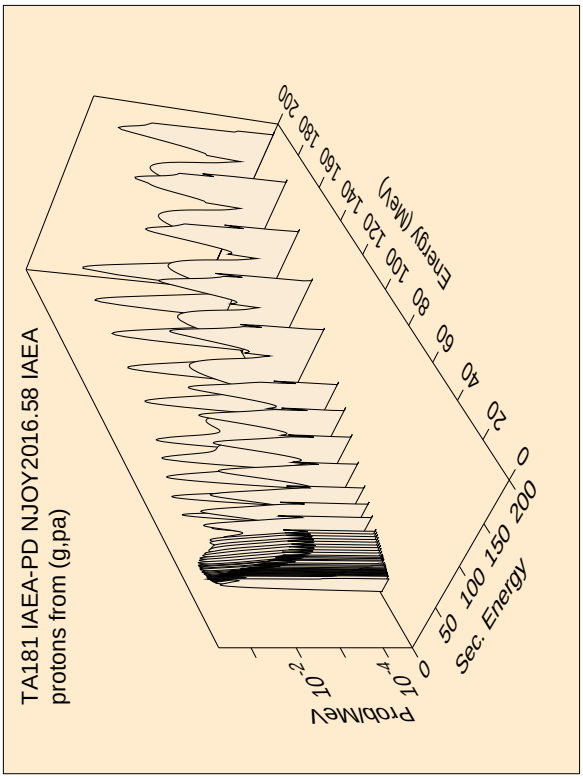
TA181 IAEA-PD NJOY2016.58 IAEA
protons from (g,pa)
Prob/MeV
Energy (Mev)
Sec. Energy

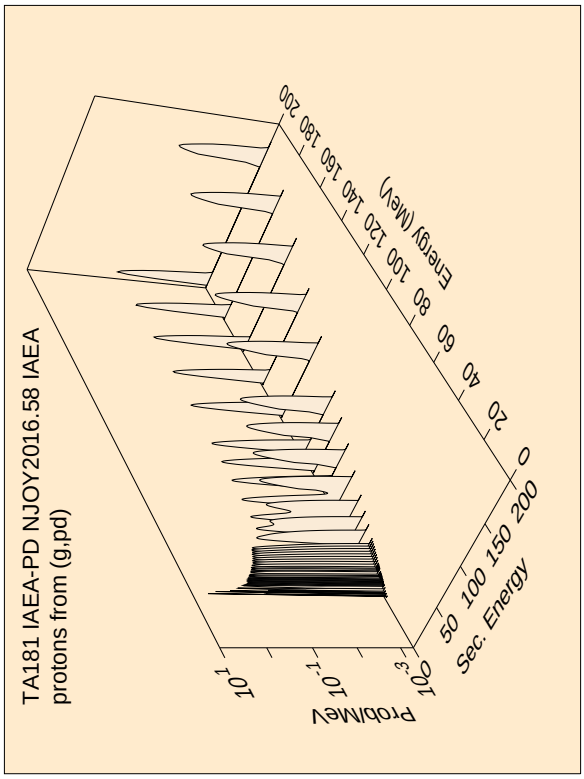
TA181 IAEA-PD NJOY2016.58 IAEA
protons from (g,pd)
Prob/MeV
Energy (Mev)
Sec. Energy

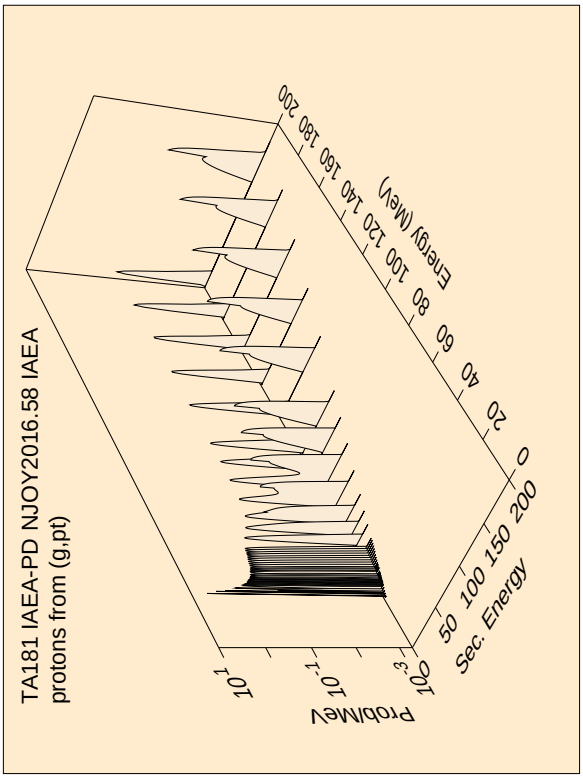
TA181 IAEA-PD NJOY2016.58 IAEA
protons from (g,pt)
Prob/MeV
Energy (Mev)
Sec. Energy

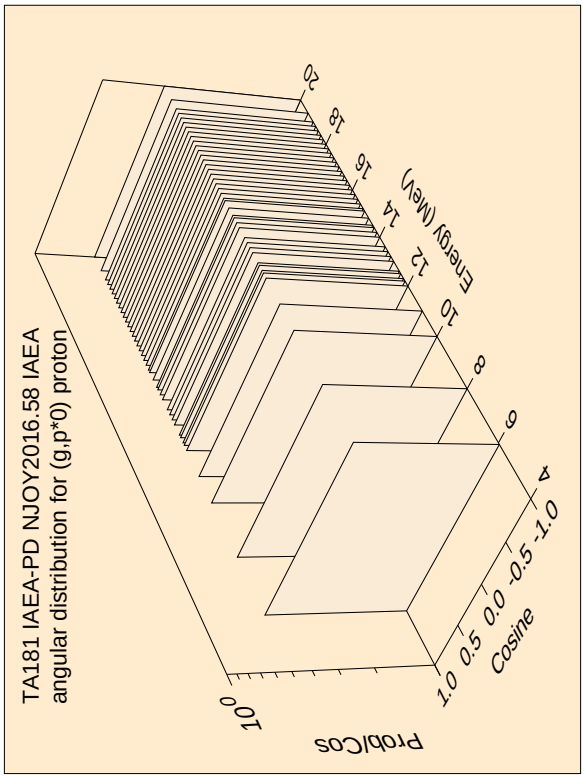
TA181 IAEA-PD NJOY2016.58 IAEA
angular distribution for (g,p*0) proton
Prob/Cos
Energy (Mev)
Cosine

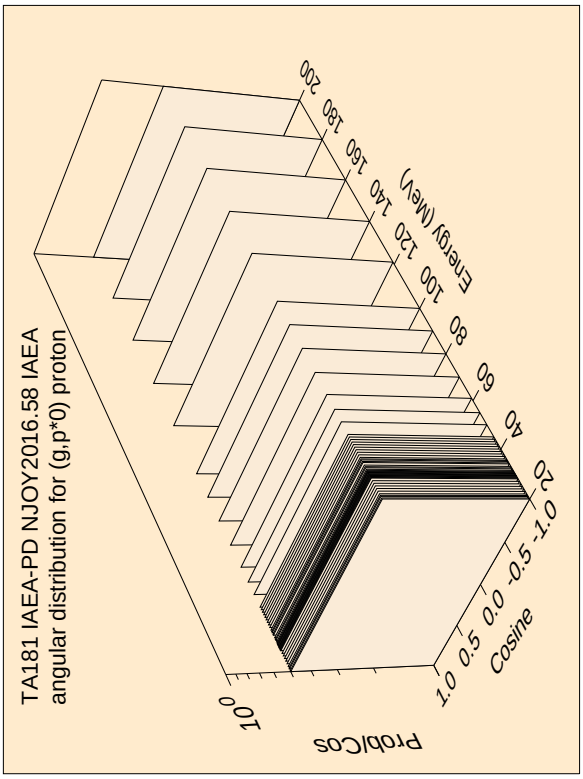
TA181 IAEA-PD NJOY2016.58 IAEA
angular distribution for (g,p*0) proton
Prob/Cos
Energy (Mev)
Cosine

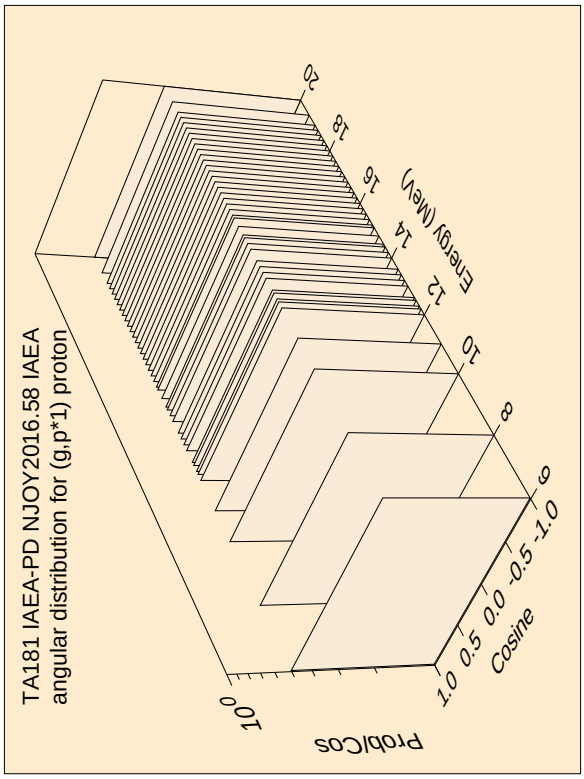
TA181 IAEA-PD NJOY2016.58 IAEA
angular distribution for (g,p*1) proton
Prob/Cos
Energy (Mev)
Cosine

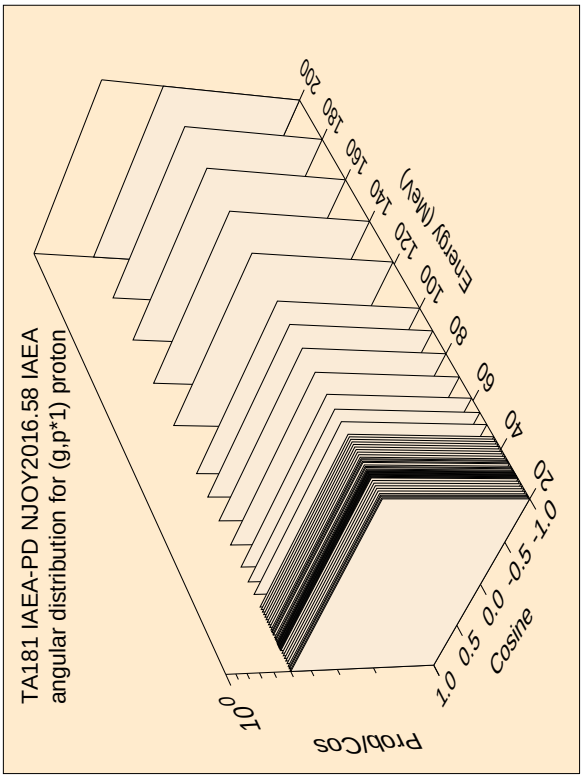
TA181 IAEA-PD NJOY2016.58 IAEA
angular distribution for (g,p*1) proton
Prob/Cos
Cosine
Energy (MeV)

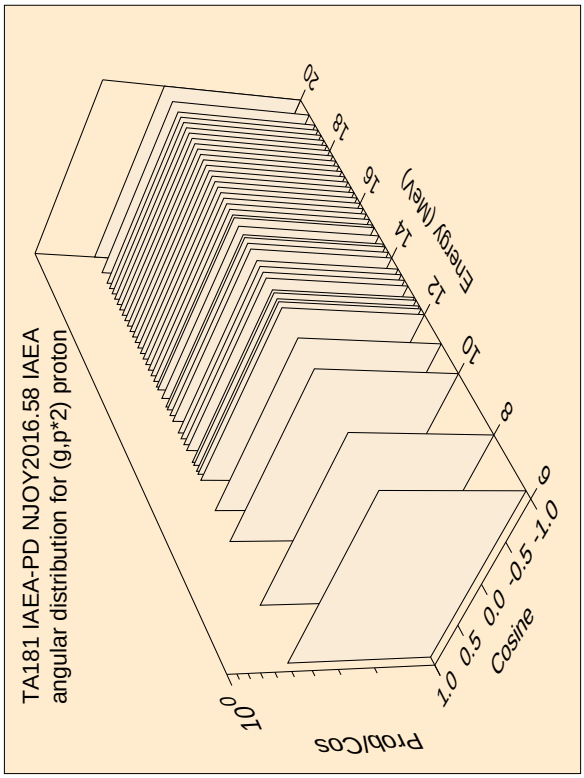
TA181 IAEA-PD NJOY2016.58 IAEA
angular distribution for (g,p*2) proton
Prob/Cos
Cosine
Energy (MeV)

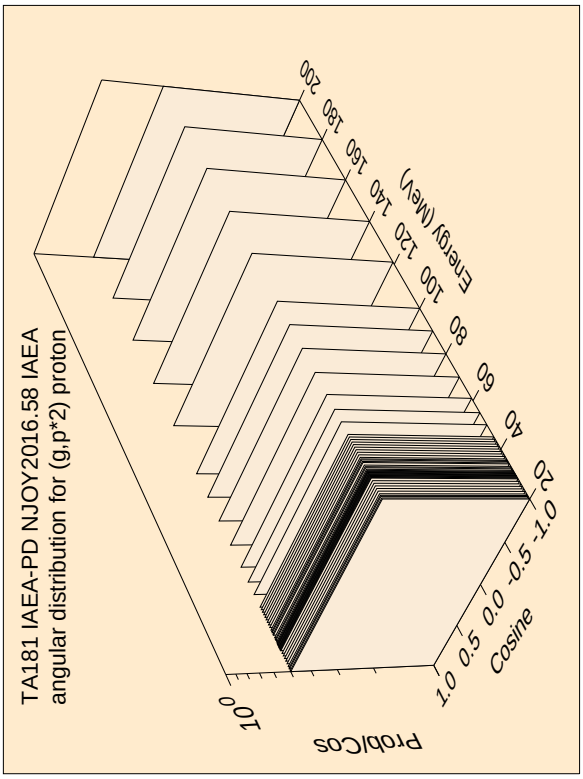
TA181 IAEA-PD NJOY2016.58 IAEA
angular distribution for (g,p*2) proton
Prob/Cos
Cosine
Energy (MeV)

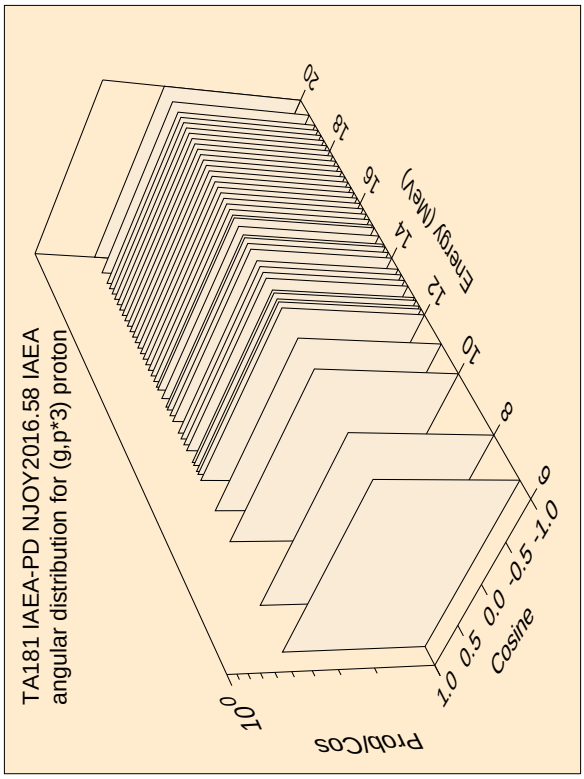
TA181 IAEA-PD NJOY2016.58 IAEA
angular distribution for (g,p*3) proton
Prob/Cos
Cosine
Energy (MeV)

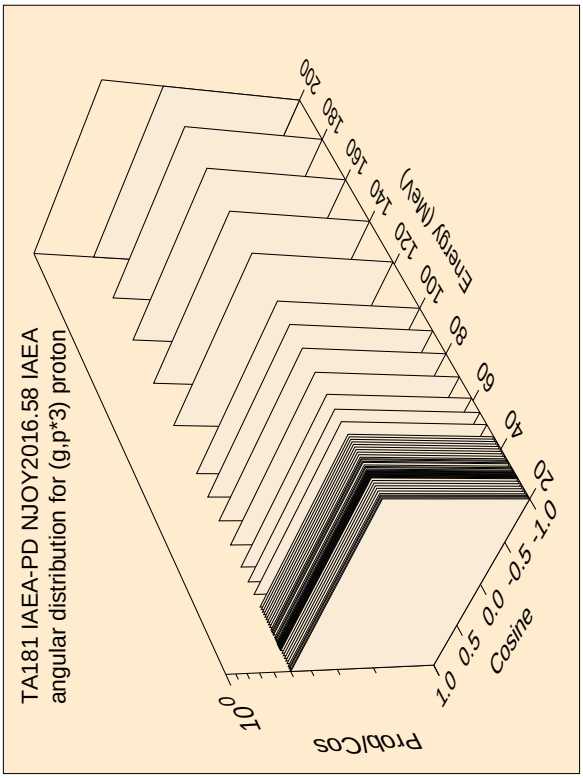
TA181 IAEA-PD NJOY2016.58 IAEA
angular distribution for (g,p*3) proton
Prob/Cos
Cosine
Energy (MeV)

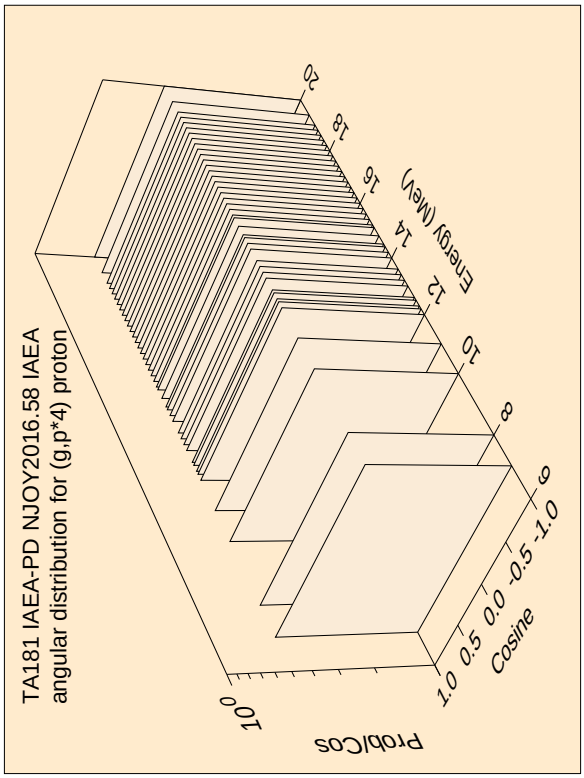
TA181 IAEA-PD NJOY2016.58 IAEA
angular distribution for (g,p*4) proton
Prob/Cos
Cosine
Energy (MeV)

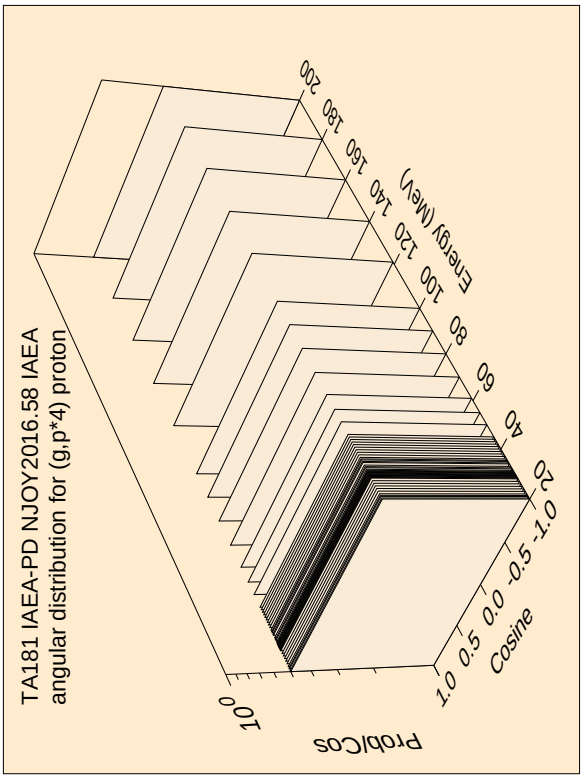
TA181 IAEA-PD NJOY2016.58 IAEA
angular distribution for (g,p*4) proton
Prob/Cos
Cosine
Energy (MeV)

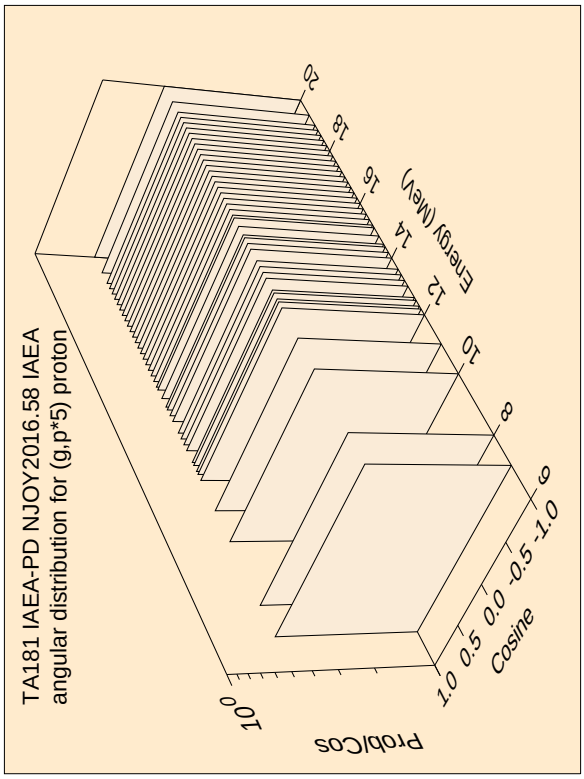
TA181 IAEA-PD NJOY2016.58 IAEA
angular distribution for (g,p*5) proton
Prob/Cos
Cosine
Energy (MeV)

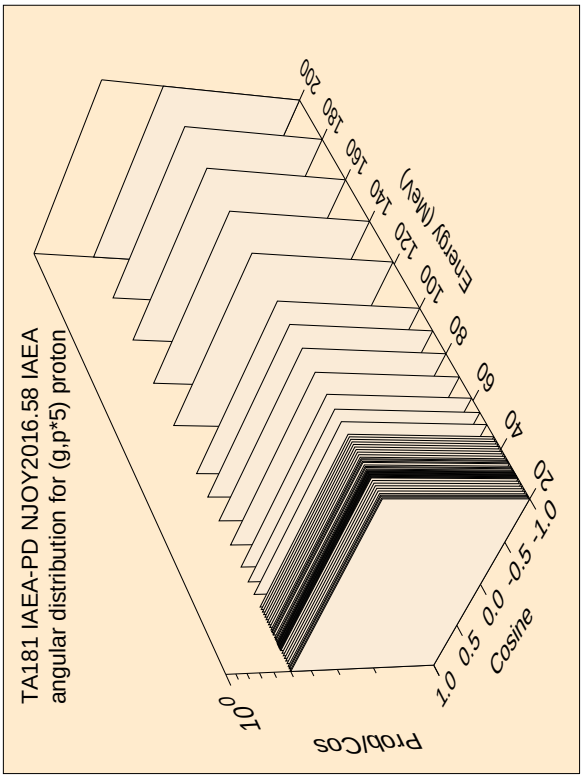
TA181 IAEA-PD NJOY2016.58 IAEA
angular distribution for (g,p*5) proton
Prob/Cos
Energy (MeV)
Cosine

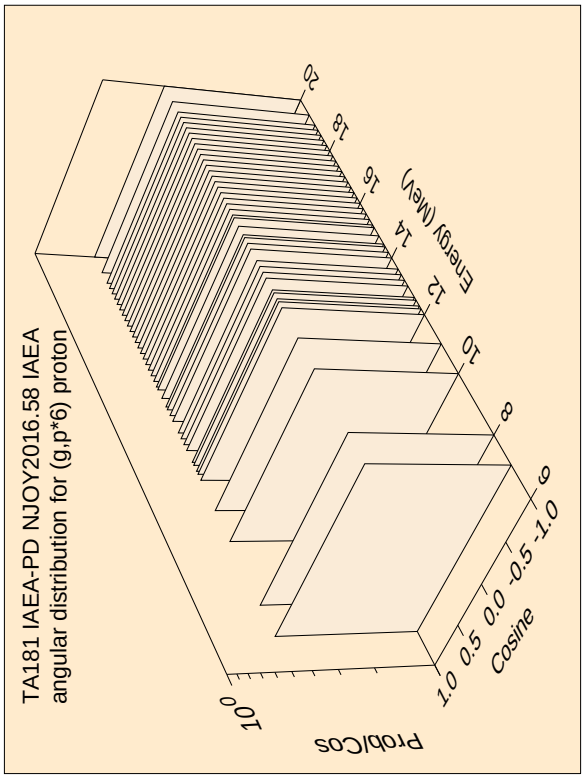
TA181 IAEA-PD NJOY2016.58 IAEA
angular distribution for (g,p*6) proton
Prob/Cos
Energy (MeV)
Cosine

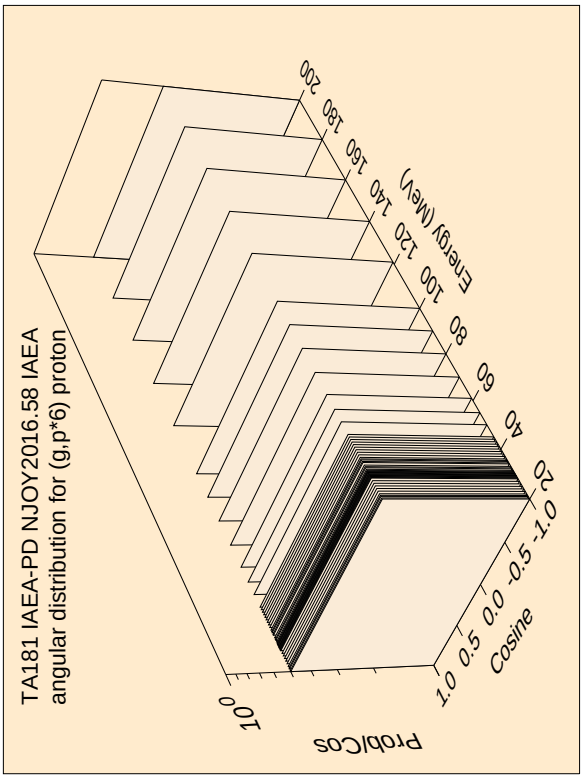
TA181 IAEA-PD NJOY2016.58 IAEA
angular distribution for (g,p*6) proton
Prob/Cos
Energy (MeV)
Cosine

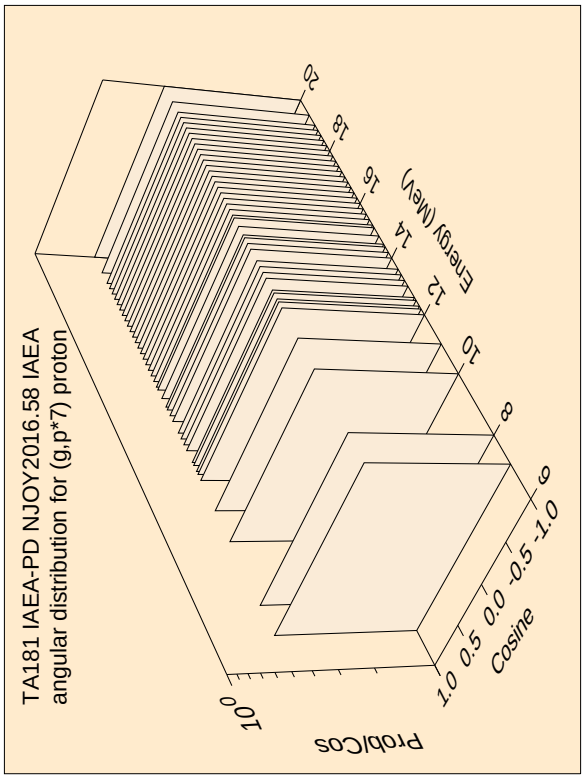
TA181 IAEA-PD NJOY2016.58 IAEA
angular distribution for (g,p*7) proton
Prob/Cos
Energy (MeV)
Cosine

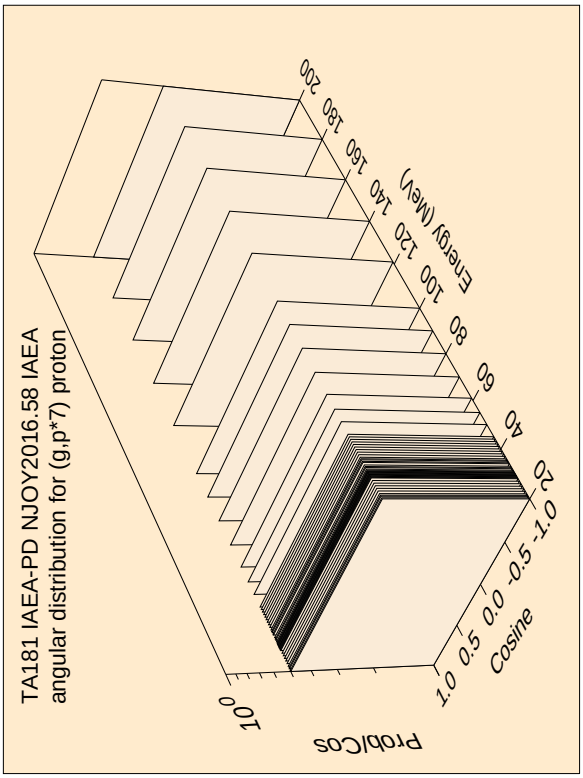
TA181 IAEA-PD NJOY2016.58 IAEA
angular distribution for (g,p*7) proton
Prob/Cos
Energy (MeV)
Cosine

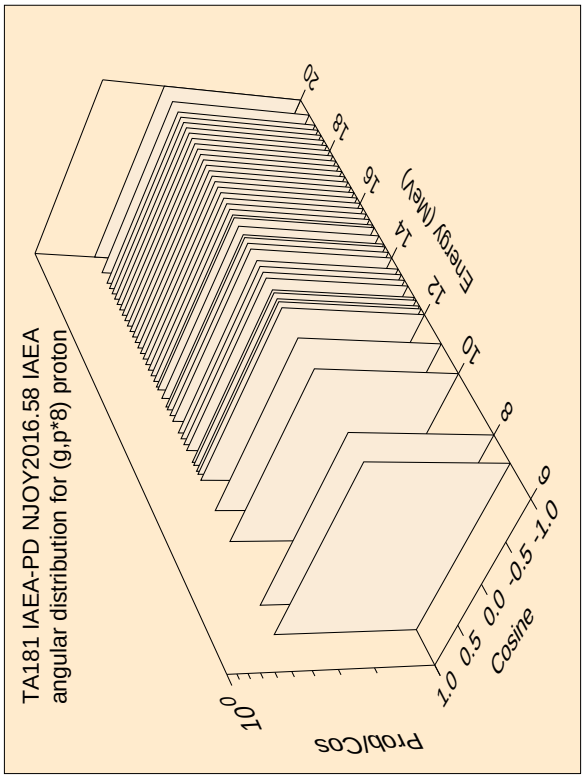
TA181 IAEA-PD NJOY2016.58 IAEA
angular distribution for (g,p*8) proton
Prob/Cos
Energy (MeV)
Cosine

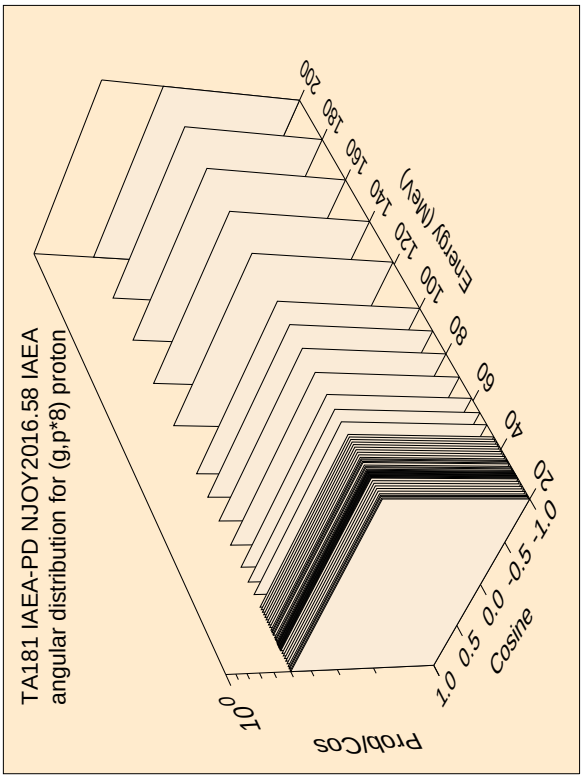
TA181 IAEA-PD NJOY2016.58 IAEA
angular distribution for (g,p*8) proton
Prob/Cos
Energy (MeV)
Cosine

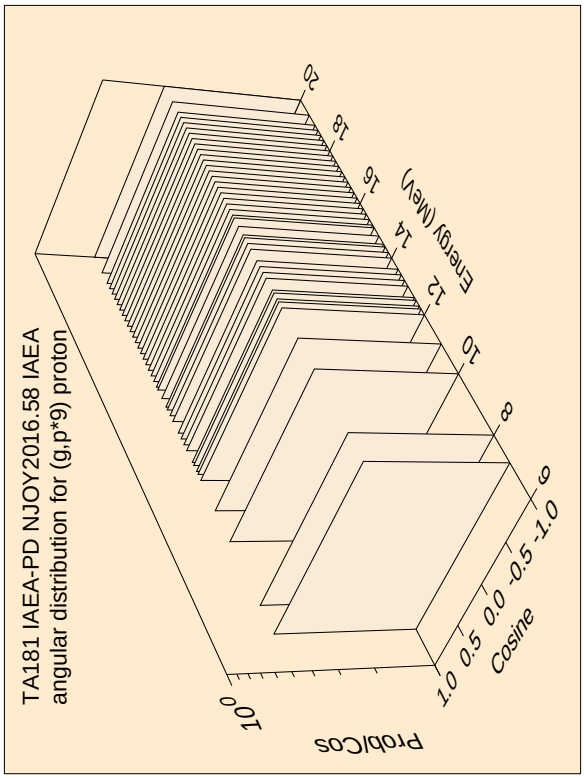
TA181 IAEA-PD NJOY2016.58 IAEA
angular distribution for (g,p*9) proton
Prob/Cos
Energy (MeV)
Cosine

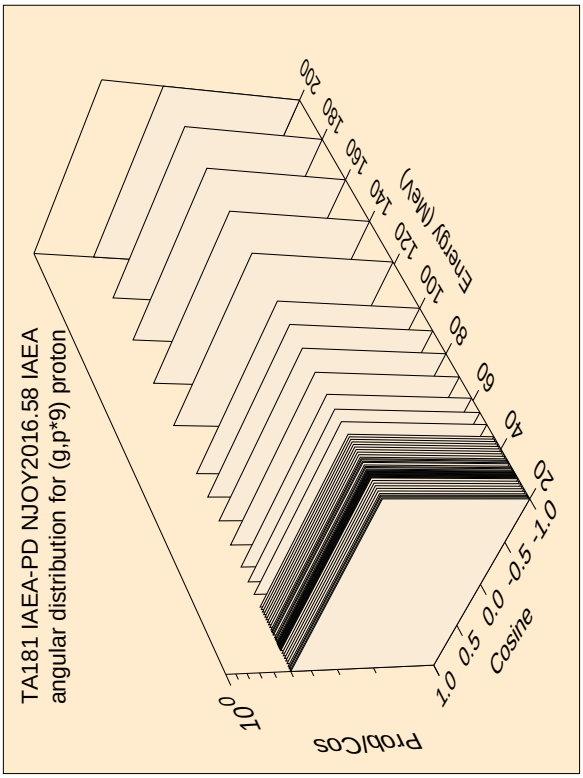
TA181 IAEA-PD NJOY2016.58 IAEA
angular distribution for (g,p*9) proton
Prob/Cos
Energy (MeV)
Cosine

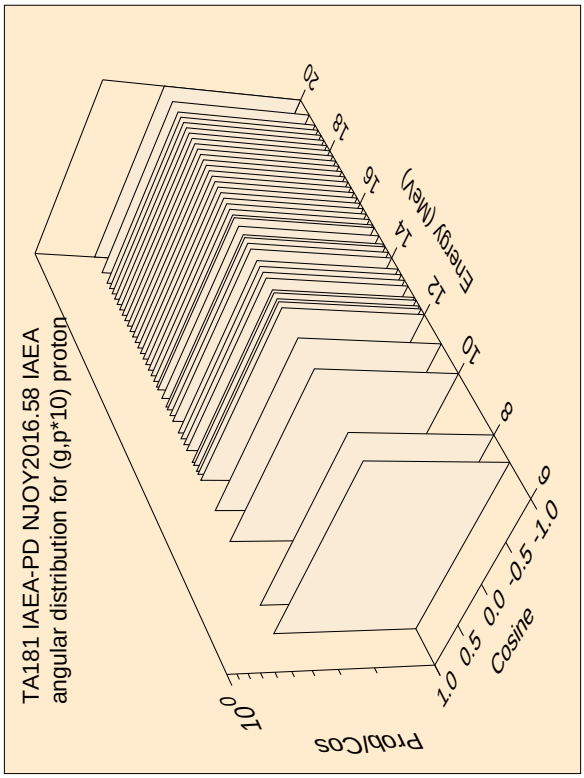
TA181 IAEA-PD NJOY2016.58 IAEA
angular distribution for (g,p*10) proton
Prob/Cos
Energy (MeV)
Cosine

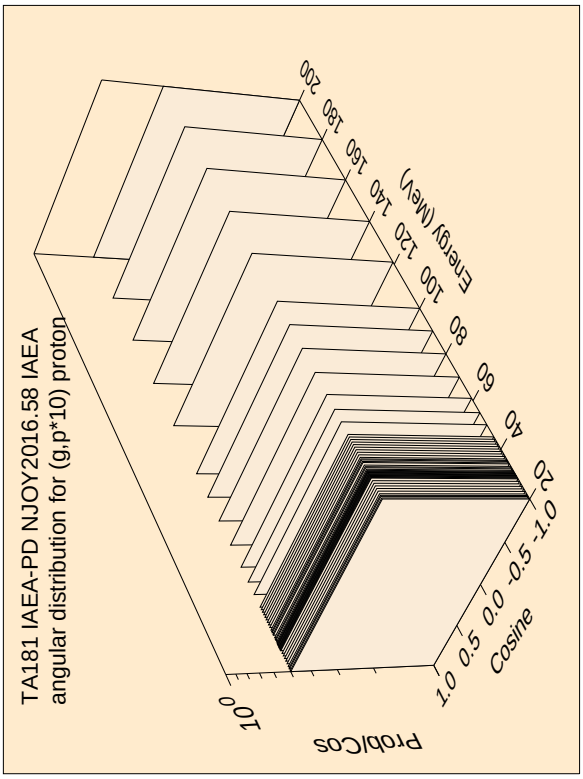
TA181 IAEA-PD NJOY2016.58 IAEA
angular distribution for (g,p*10) proton
Prob/Cos
Energy (MeV)
Cosine

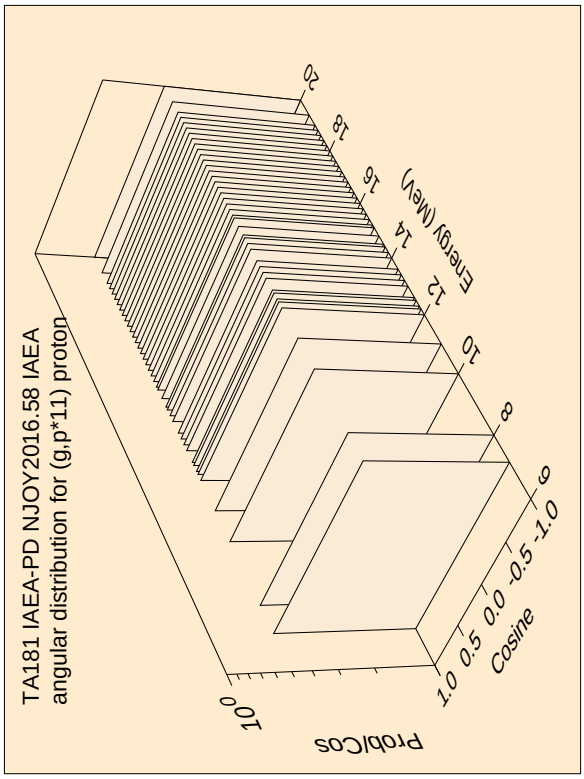
TA181 IAEA-PD NJOY2016.58 IAEA
angular distribution for (g,p*11) proton
Prob/Cos
Energy (MeV)
Cosine

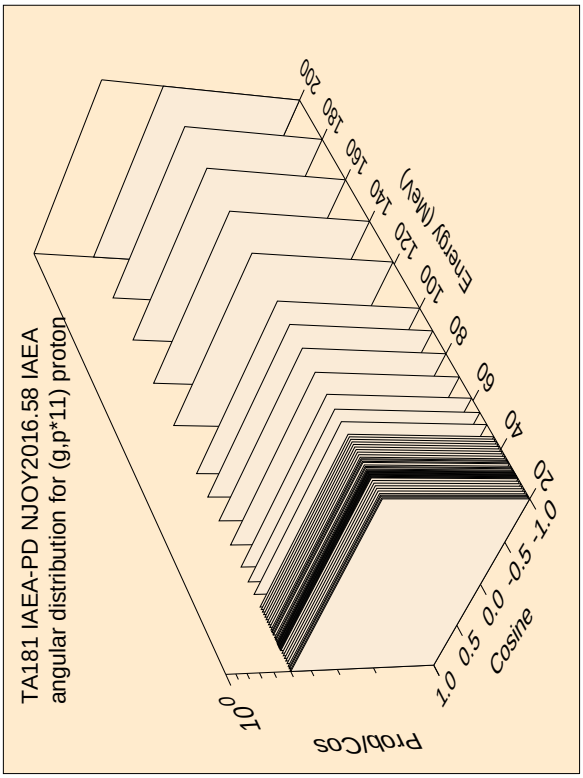
TA181 IAEA-PD NJOY2016.58 IAEA
angular distribution for (g,p*11) proton
Prob/Cos
Energy (MeV)
Cosine

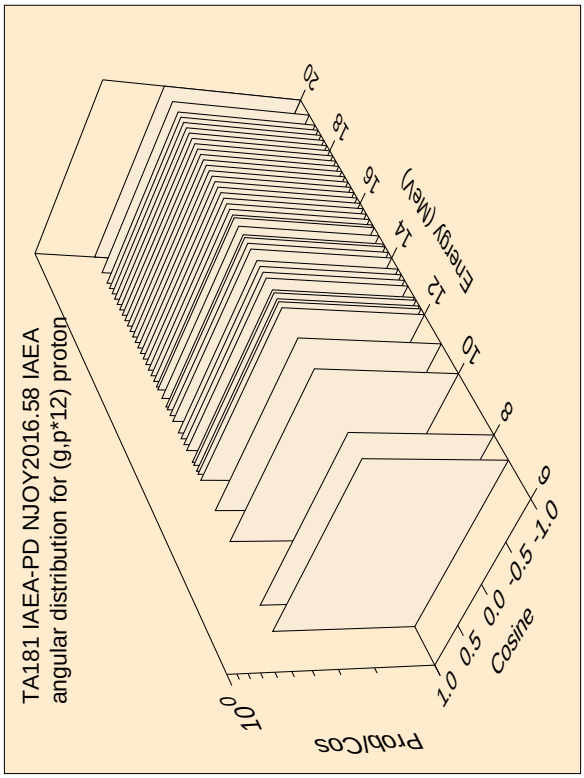
TA181 IAEA-PD NJOY2016.58 IAEA
angular distribution for (g,p*12) proton
Prob/Cos
Energy (MeV)
Cosine

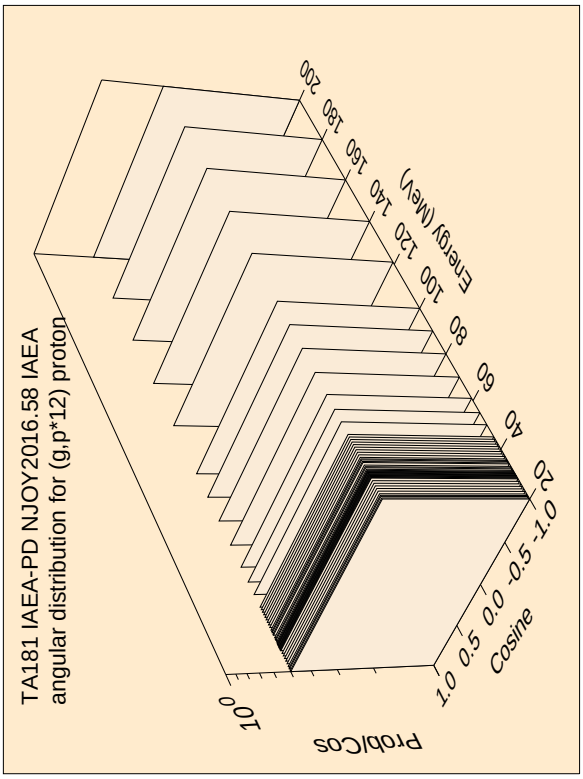
TA181 IAEA-PD NJOY2016.58 IAEA
angular distribution for (g,p*12) proton
Prob/Cos
Energy (MeV)
Cosine

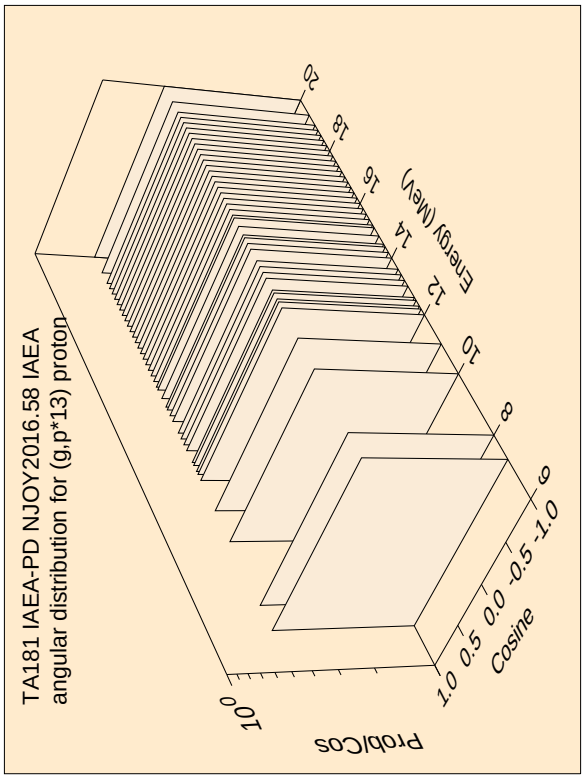
TA181 IAEA-PD NJOY2016.58 IAEA
angular distribution for (g,p*13) proton
Prob/Cos
Energy (MeV)
Cosine

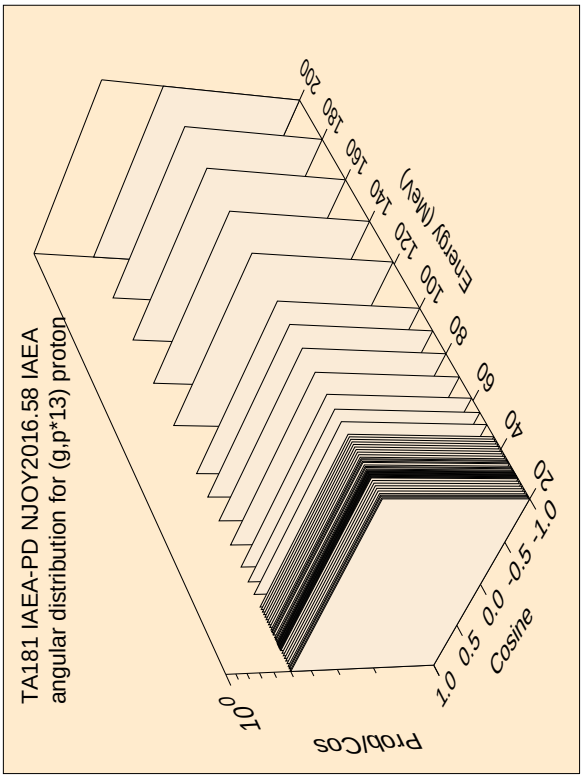
TA181 IAEA-PD NJOY2016.58 IAEA
angular distribution for (g,p*13) proton
Prob/Cos
Energy (MeV)
Cosine

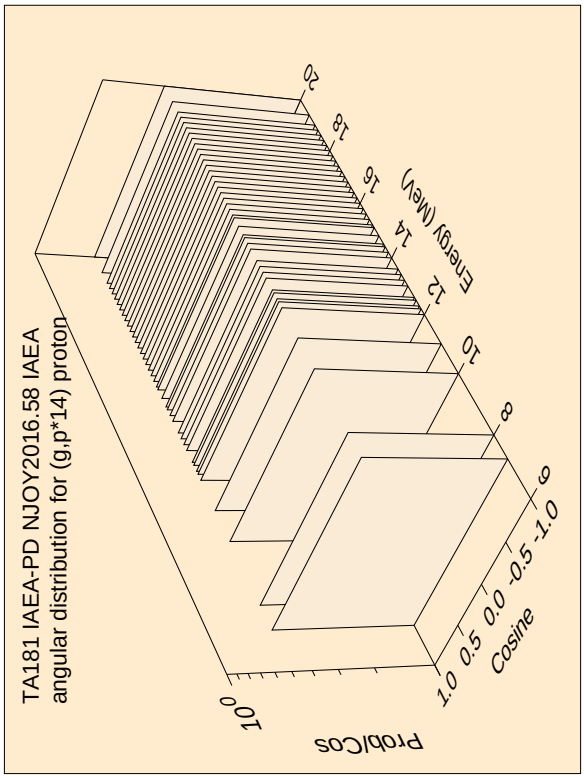
TA181 IAEA-PD NJOY2016.58 IAEA
angular distribution for (g,p*14) proton
Prob/Cos
Energy (MeV)
Cosine

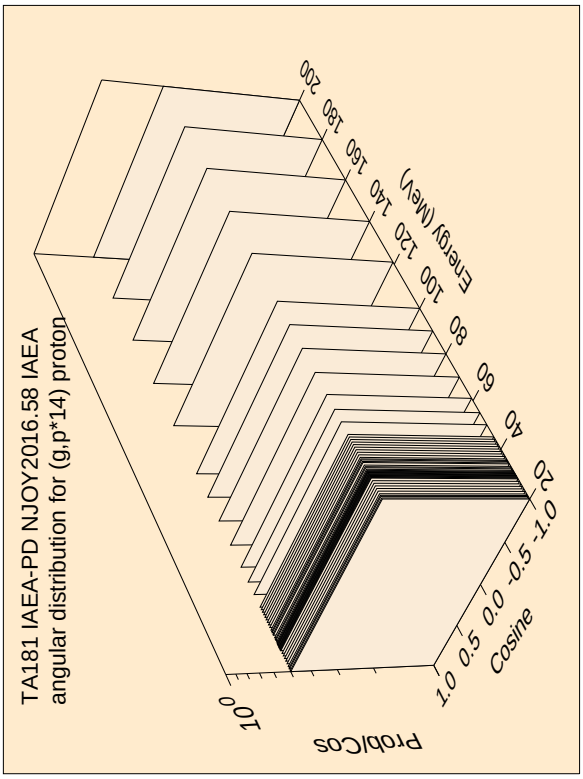
TA181 IAEA-PD NJOY2016.58 IAEA
angular distribution for (g,p*14) proton
Prob/Cos
Energy (MeV)
Cosine

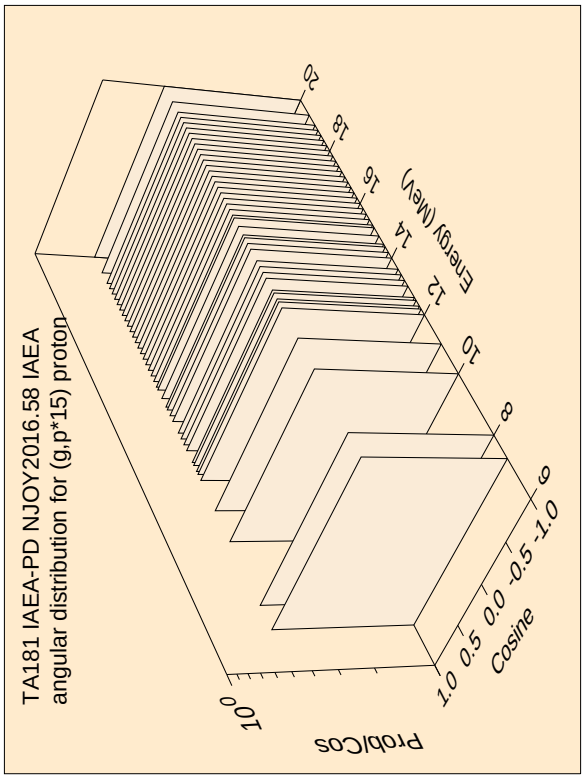
TA181 IAEA-PD NJOY2016.58 IAEA
angular distribution for (g,p*15) proton
Prob/Cos
Energy (MeV)
Cosine

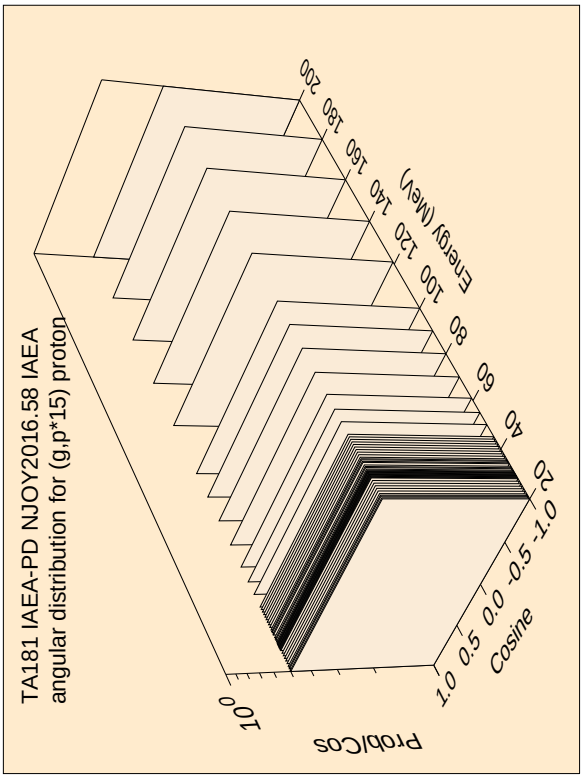
TA181 IAEA-PD NJOY2016.58 IAEA
angular distribution for (g,p*15) proton
Prob/Cos
Cosine
Energy (MeV)

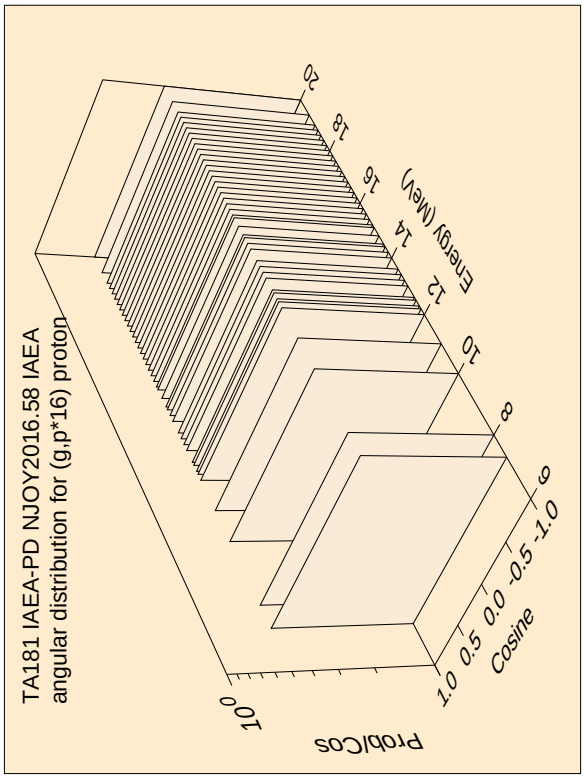
TA181 IAEA-PD NJOY2016.58 IAEA
angular distribution for (g,p*16) proton
Prob/Cos
Cosine
Energy (MeV)

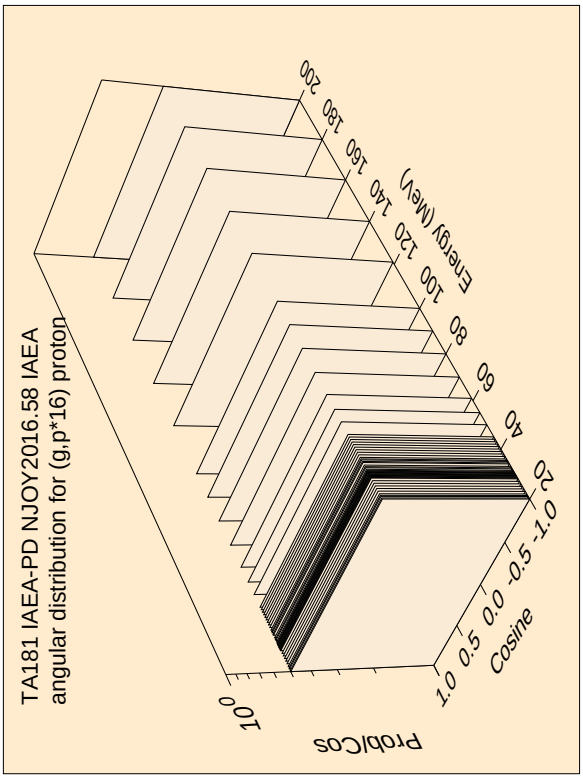
TA181 IAEA-PD NJOY2016.58 IAEA
angular distribution for (g,p*16) proton
Prob/Cos
Cosine
Energy (MeV)

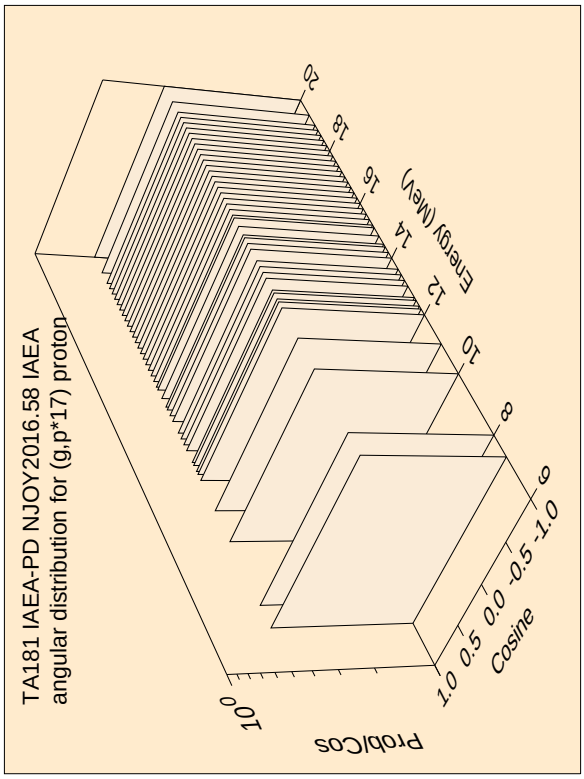
TA181 IAEA-PD NJOY2016.58 IAEA
angular distribution for (g,p*17) proton
Prob/Cos
Cosine
Energy (MeV)

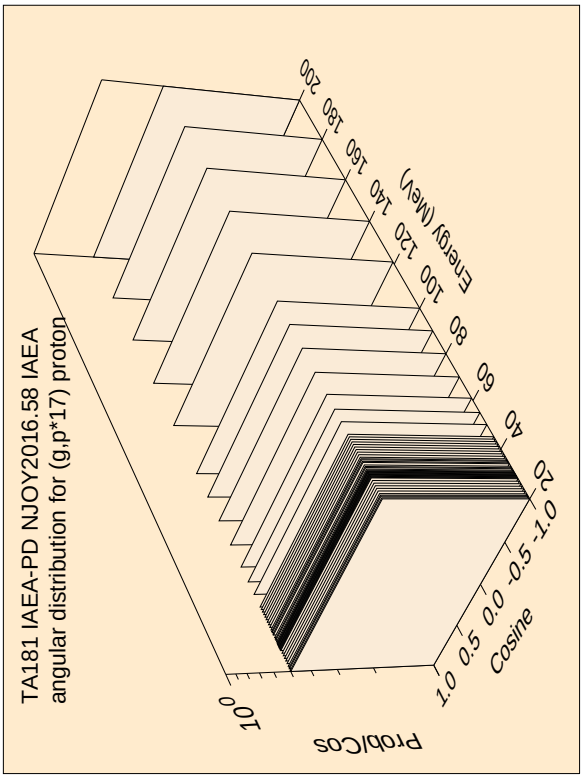
TA181 IAEA-PD NJOY2016.58 IAEA
angular distribution for (g,p*17) proton
Prob/Cos
Energy (MeV)
Cosine

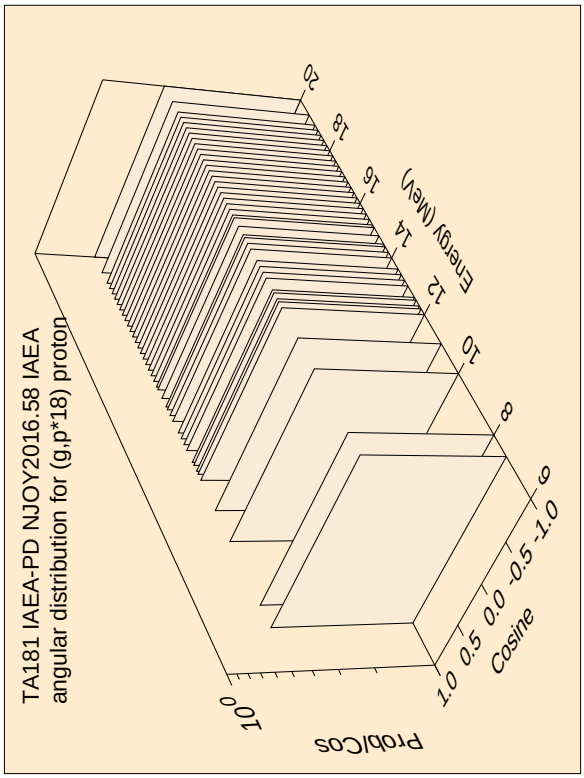
TA181 IAEA-PD NJOY2016.58 IAEA
angular distribution for (g,p*18) proton
Prob/Cos
Energy (MeV)
Cosine

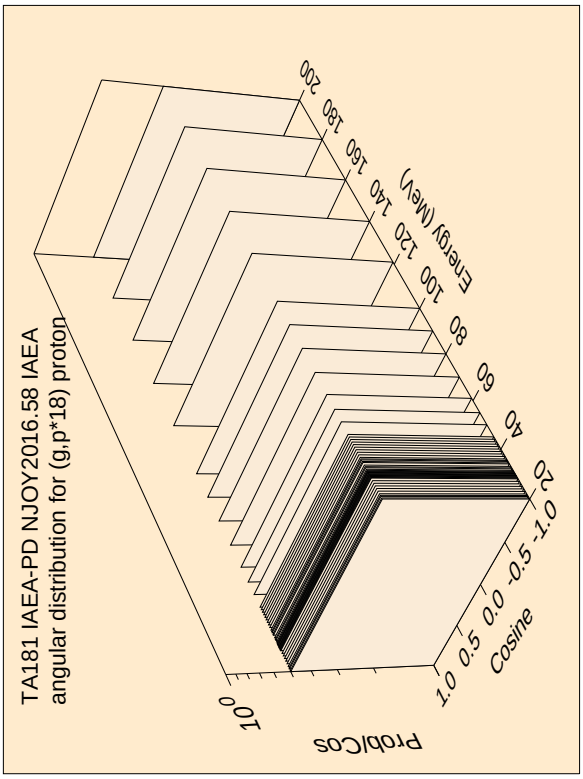
TA181 IAEA-PD NJOY2016.58 IAEA
angular distribution for (g,p*18) proton
Prob/Cos
Energy (MeV)
Cosine

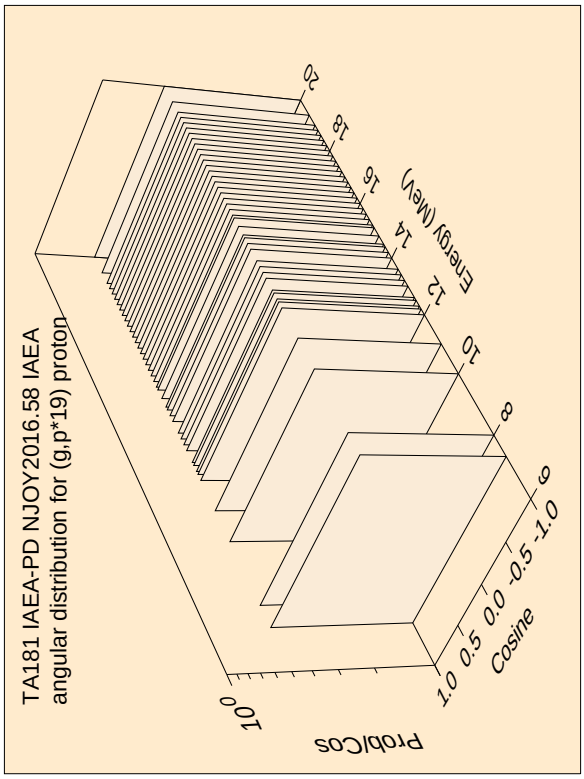
TA181 IAEA-PD NJOY2016.58 IAEA
angular distribution for (g,p*19) proton
Prob/Cos
Energy (MeV)
Cosine

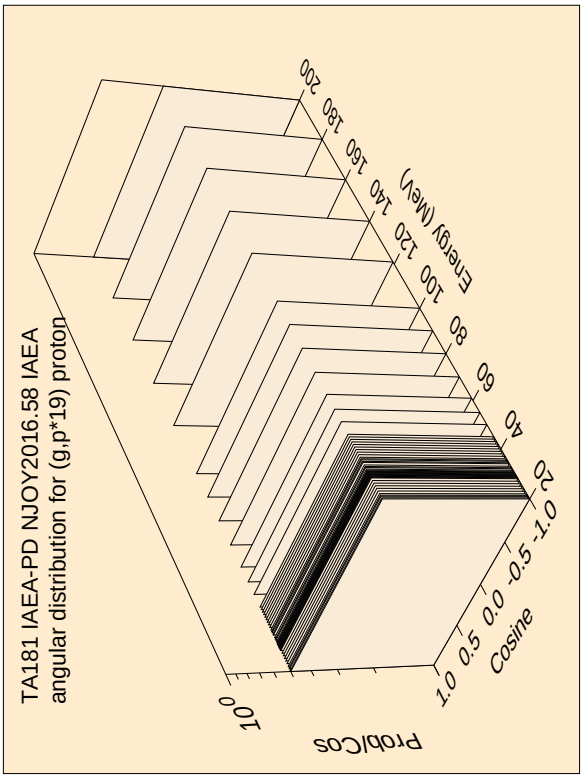
TA181 IAEA-PD NJOY2016.58 IAEA
angular distribution for (g,p*19) proton
Prob/Cos
Cosine
Energy (MeV)

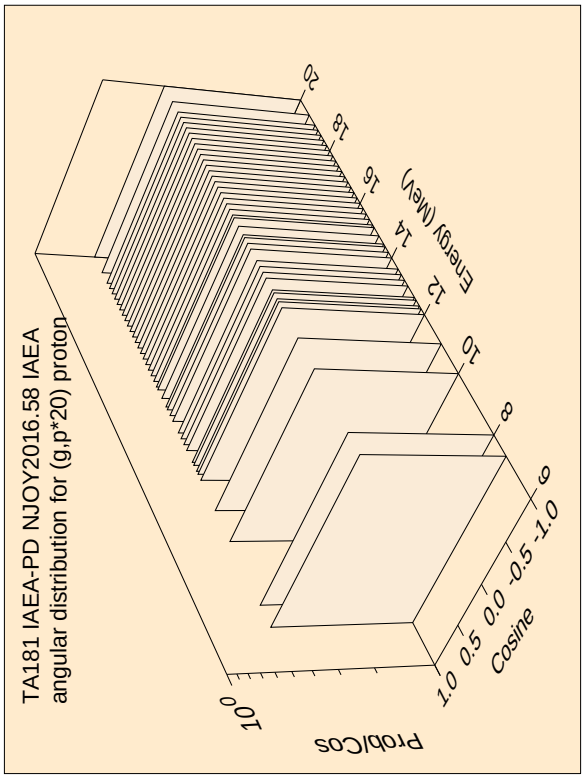
TA181 IAEA-PD NJOY2016.58 IAEA
angular distribution for (g,p*20) proton
Prob/Cos
Cosine
Energy (MeV)

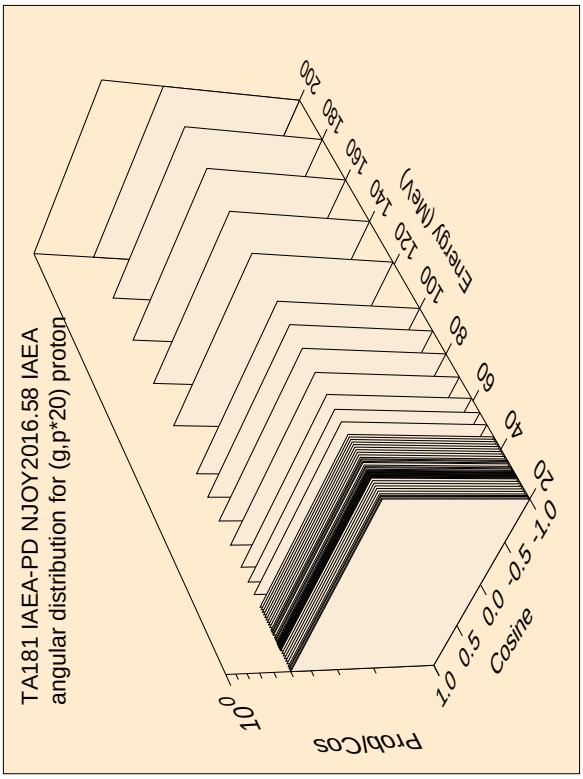
TA181 IAEA-PD NJOY2016.58 IAEA
angular distribution for (g,p*20) proton
Prob/Cos
Cosine
Energy (MeV)

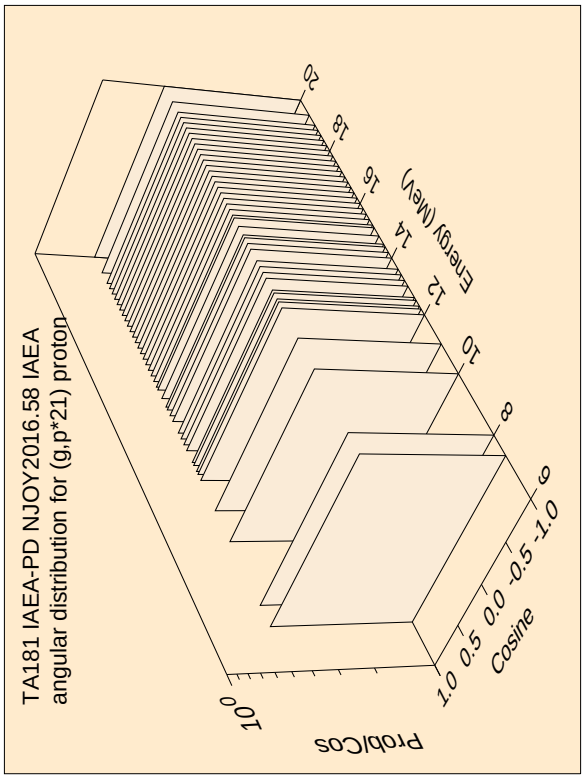
TA181 IAEA-PD NJOY2016.58 IAEA
angular distribution for (g,p*21) proton
Prob/Cos
Cosine
Energy (MeV)

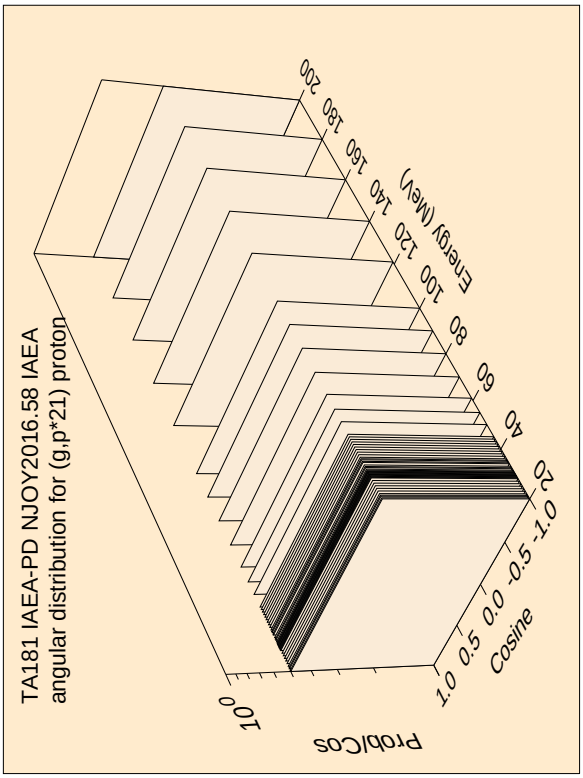
TA181 IAEA-PD NJOY2016.58 IAEA
angular distribution for (g,p*21) proton
Prob/Cos
Energy (MeV)
Cosine

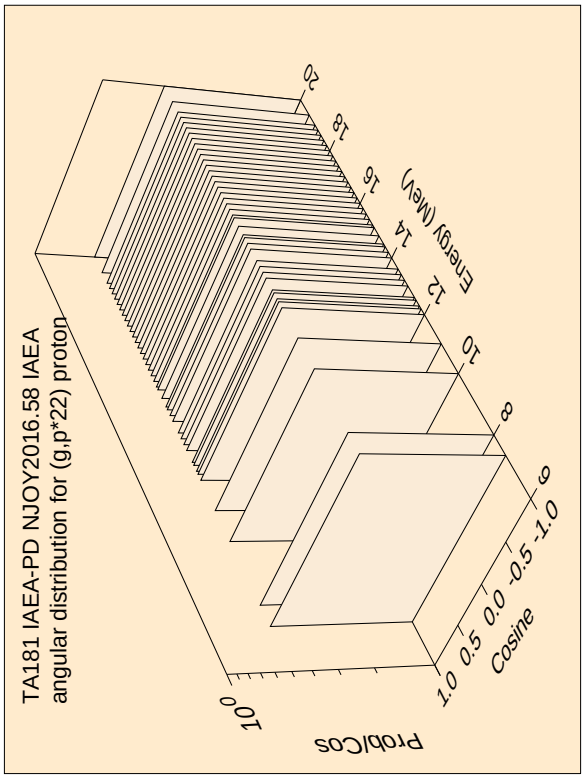
TA181 IAEA-PD NJOY2016.58 IAEA
angular distribution for (g,p*22) proton
Prob/Cos
Energy (MeV)
Cosine

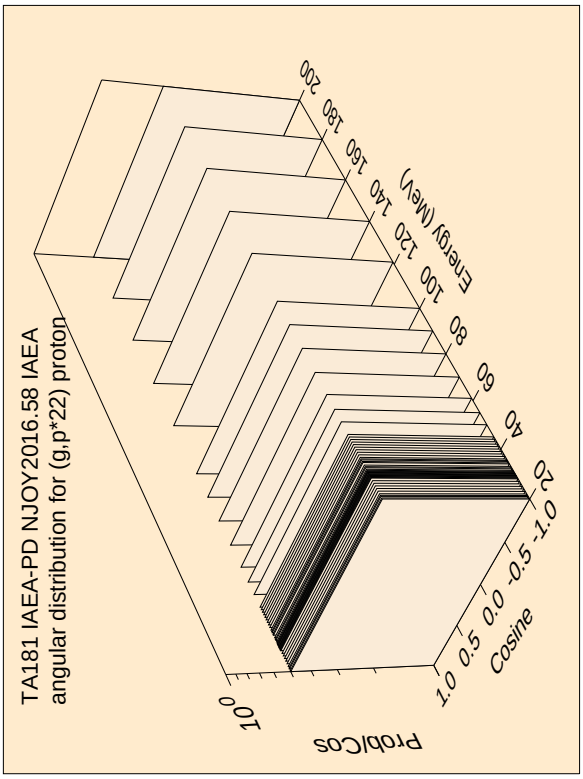
TA181 IAEA-PD NJOY2016.58 IAEA
angular distribution for (g,p*22) proton
Prob/Cos
Energy (MeV)
Cosine

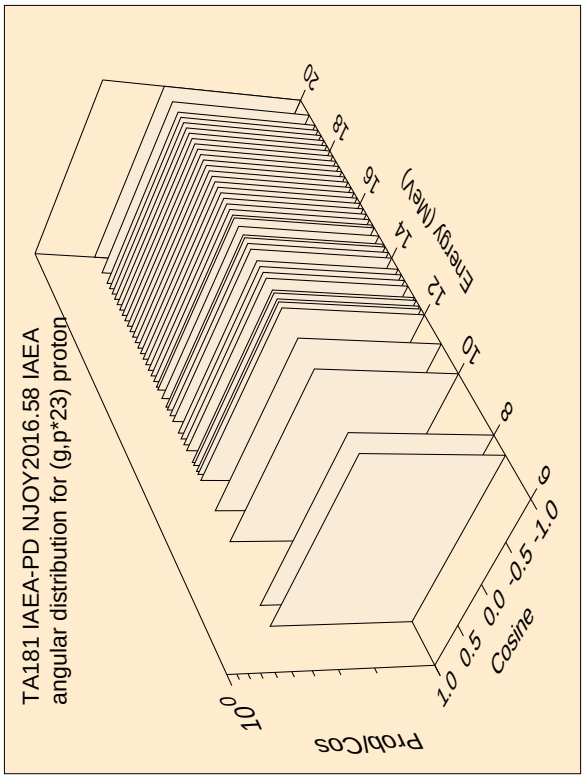
TA181 IAEA-PD NJOY2016.58 IAEA
angular distribution for (g,p*23) proton
Prob/Cos
Energy (MeV)
Cosine

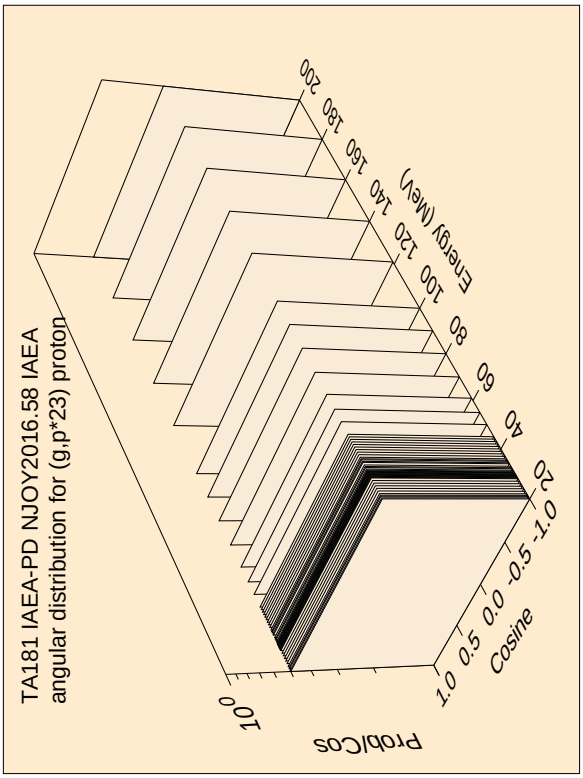
TA181 IAEA-PD NJOY2016.58 IAEA
angular distribution for (g,p*23) proton
Prob/Cos
Energy (MeV)
Cosine

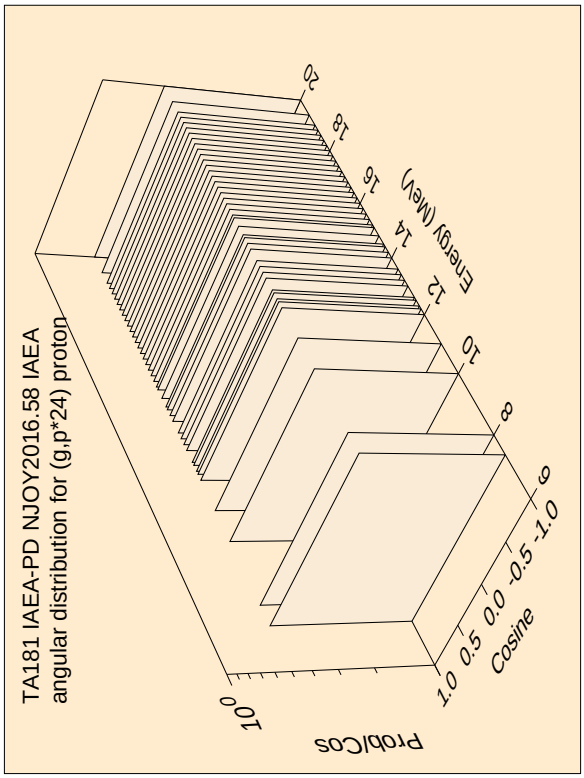
TA181 IAEA-PD NJOY2016.58 IAEA
angular distribution for (g,p*24) proton
Prob/Cos
Energy (MeV)
Cosine

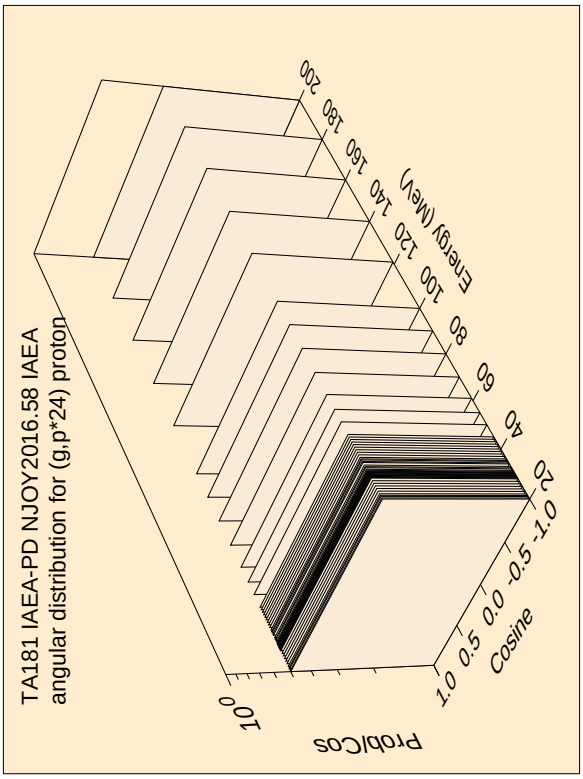
TA181 IAEA-PD NJOY2016.58 IAEA
angular distribution for (g,p*24) proton
Prob/Cos
Energy (MeV)
Cosine

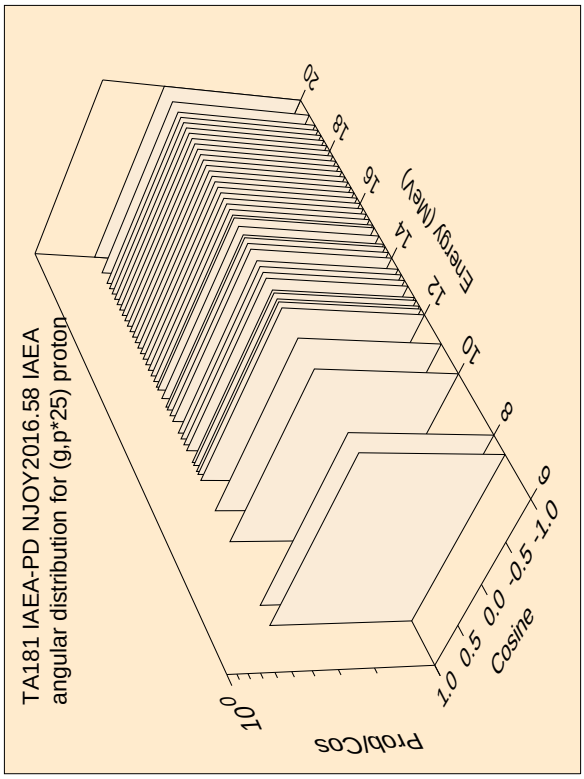
TA181 IAEA-PD NJOY2016.58 IAEA
angular distribution for (g,p*25) proton
Prob/Cos
Energy (MeV)
Cosine

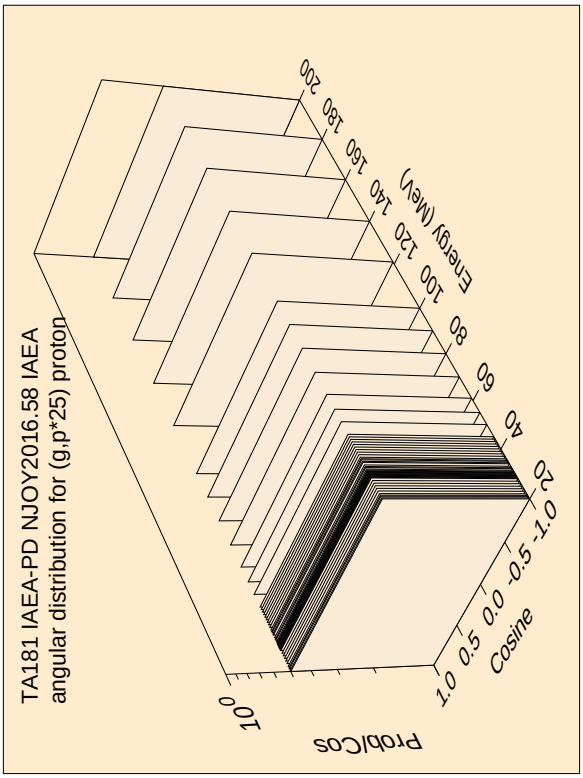
TA181 IAEA-PD NJOY2016.58 IAEA
angular distribution for (g,p*25) proton
Prob/Cos
Energy (MeV)
Cosine

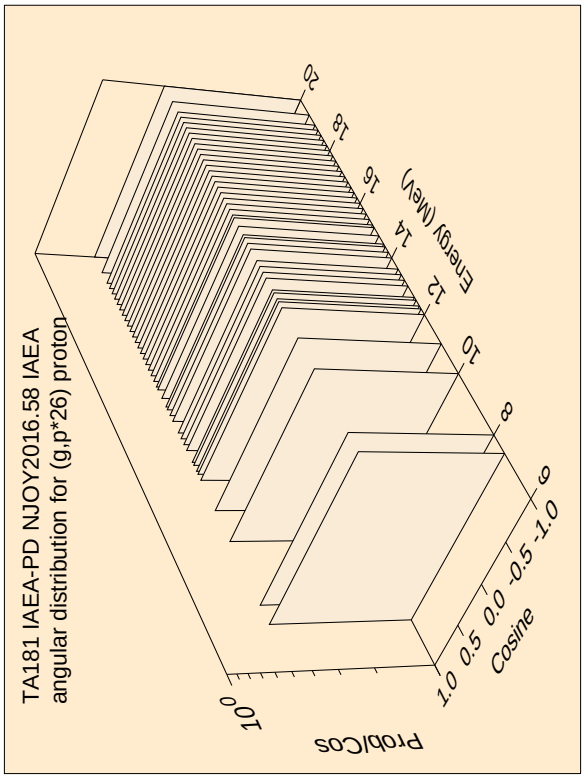
TA181 IAEA-PD NJOY2016.58 IAEA
angular distribution for (g,p*26) proton
Prob/Cos
Energy (MeV)
Cosine

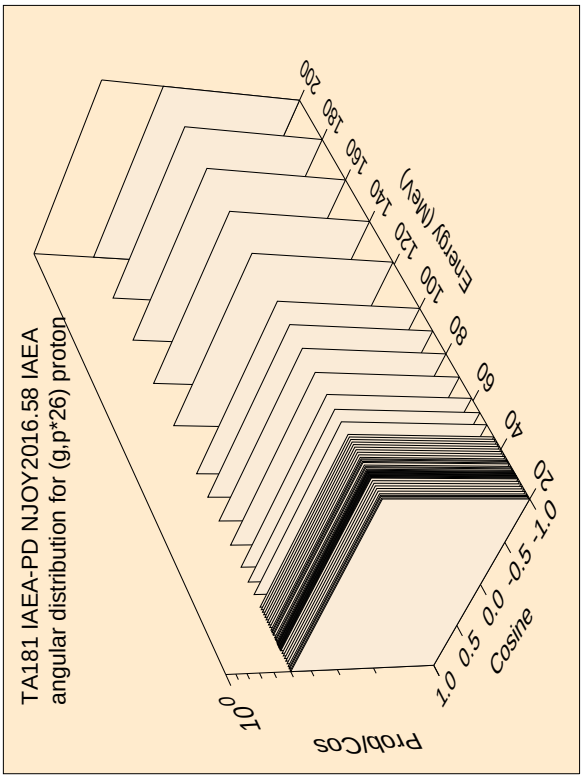
TA181 IAEA-PD NJOY2016.58 IAEA
angular distribution for (g,p*26) proton
Prob/Cos
Energy (MeV)
Cosine

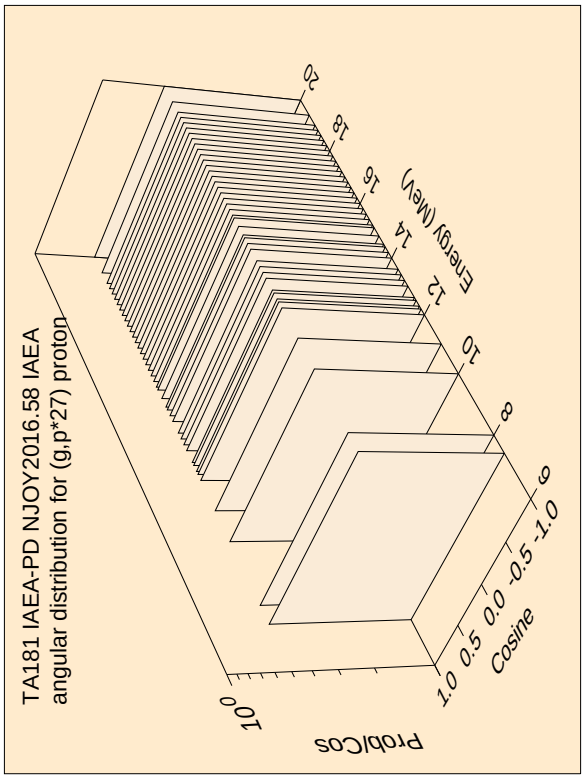
TA181 IAEA-PD NJOY2016.58 IAEA
angular distribution for (g,p*27) proton
Prob/Cos
Energy (MeV)
Cosine

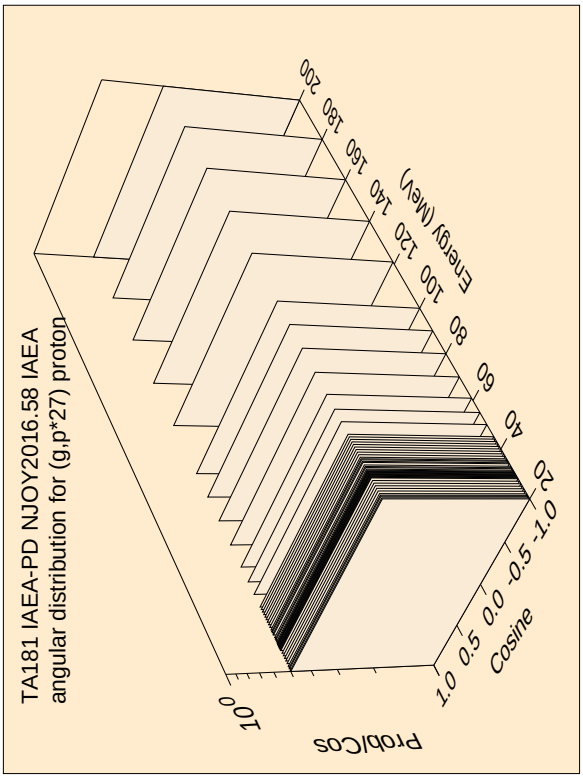
TA181 IAEA-PD NJOY2016.58 IAEA
angular distribution for (g,p*27) proton
Prob/Cos
Energy (MeV)
Cosine

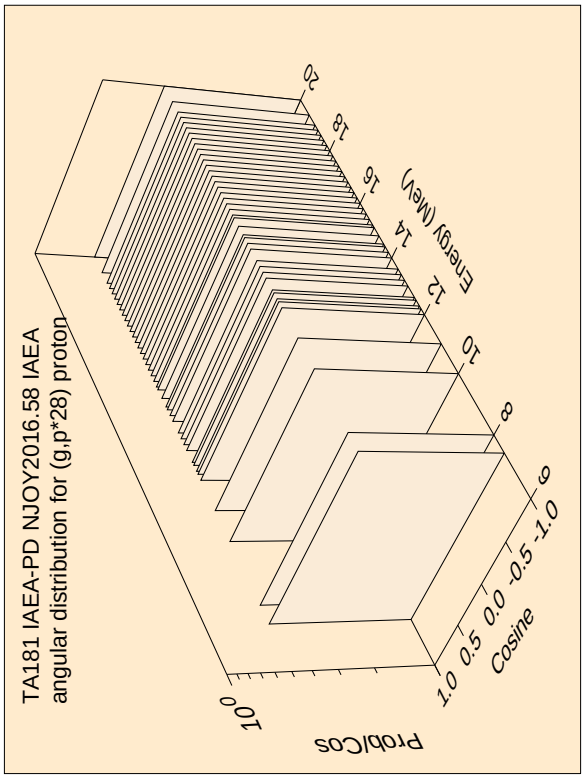
TA181 IAEA-PD NJOY2016.58 IAEA
angular distribution for (g,p*28) proton
Prob/Cos
Energy (MeV)
Cosine

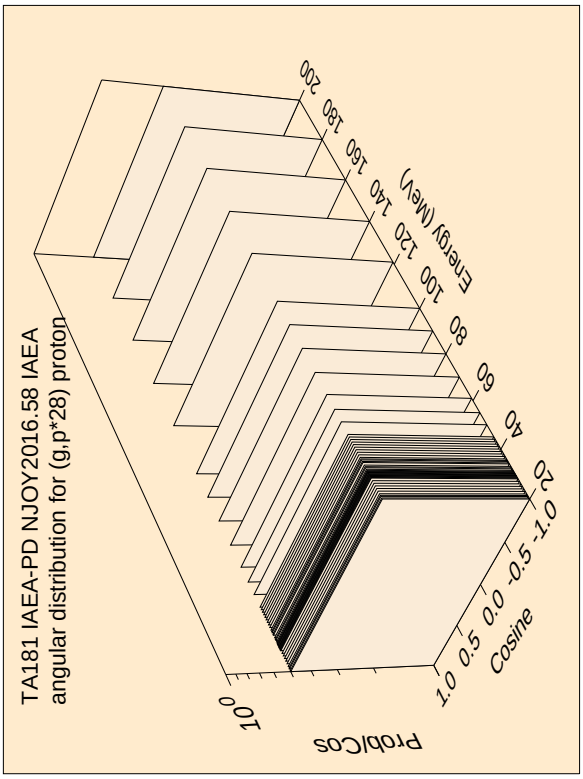
TA181 IAEA-PD NJOY2016.58 IAEA
angular distribution for (g,p*28) proton
Prob/Cos
Energy (MeV)
Cosine

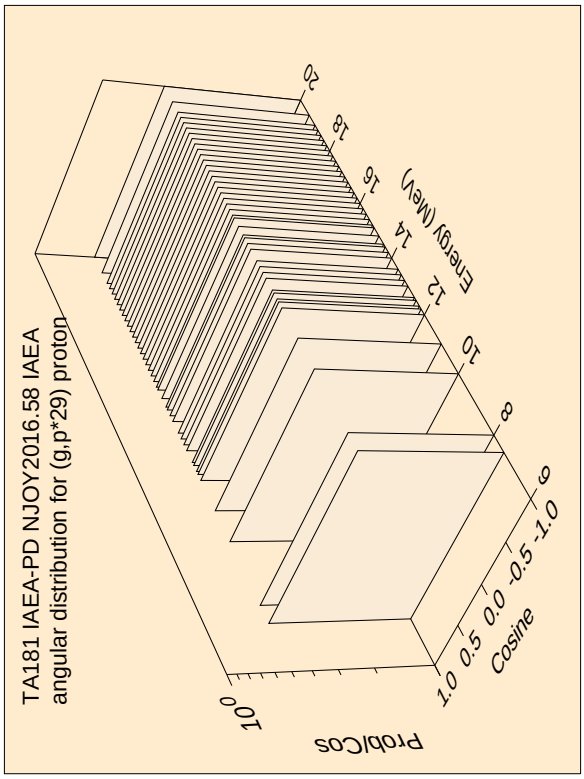
TA181 IAEA-PD NJOY2016.58 IAEA
angular distribution for (g,p*29) proton
Prob/Cos
Energy (MeV)
Cosine

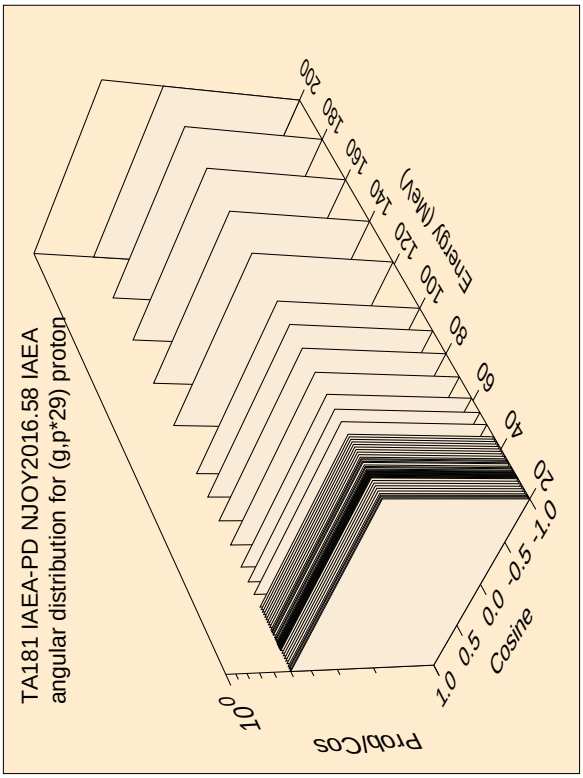
TA181 IAEA-PD NJOY2016.58 IAEA
angular distribution for (g,p*29) proton
Prob/Cos
Energy (MeV)
Cosine

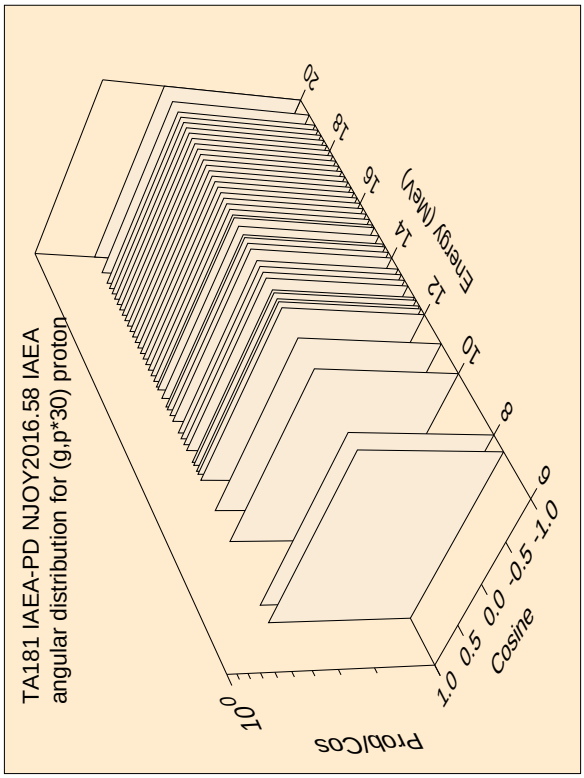
TA181 IAEA-PD NJOY2016.58 IAEA
angular distribution for (g,p*30) proton
Prob/Cos
Energy (MeV)
Cosine

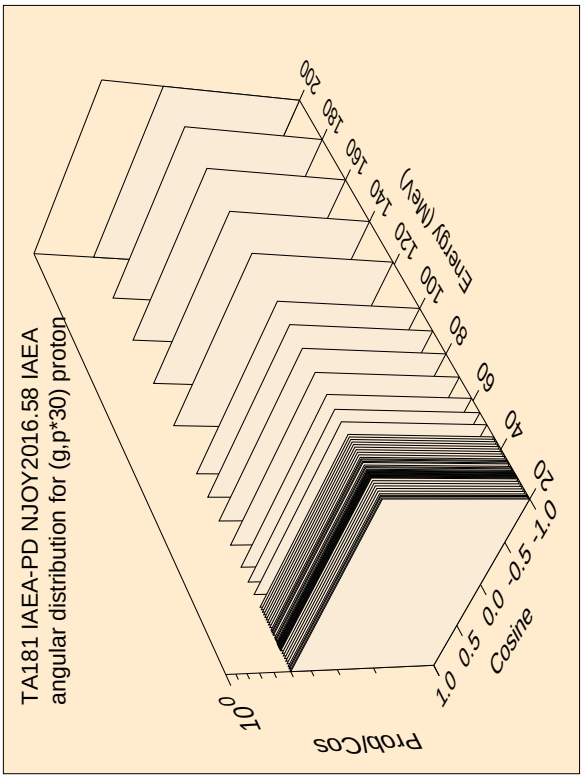
TA181 IAEA-PD NJOY2016.58 IAEA
angular distribution for (g,p*30) proton
Prob/Cos
Energy (MeV)
Cosine

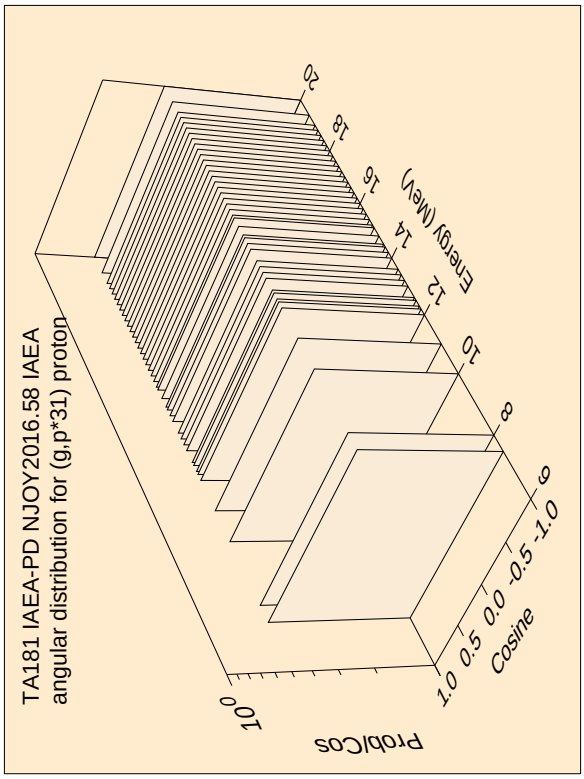
TA181 IAEA-PD NJOY2016.58 IAEA
angular distribution for (g,p*31) proton
Prob/Cos
Energy (MeV)
Cosine

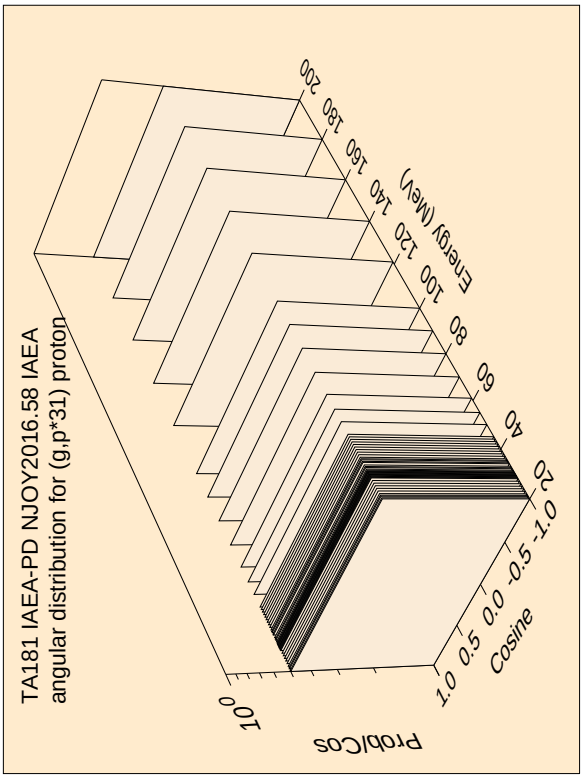
TA181 IAEA-PD NJOY2016.58 IAEA
angular distribution for (g,p*31) proton
Prob/Cos
Energy (MeV)
Cosine

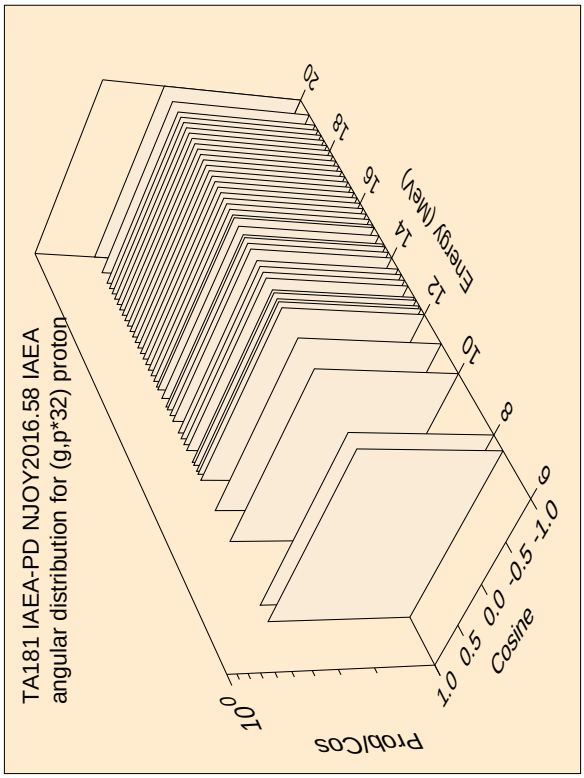
TA181 IAEA-PD NJOY2016.58 IAEA
angular distribution for (g,p*32) proton
Prob/Cos
Energy (MeV)
Cosine

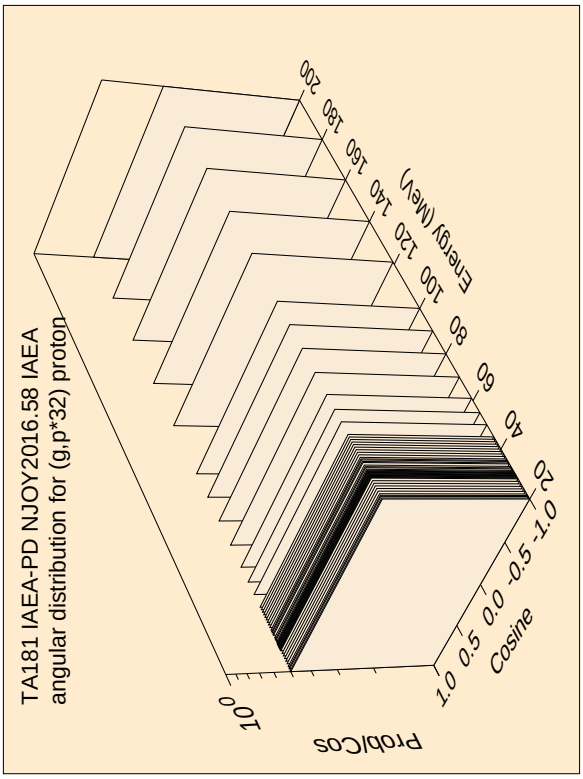
TA181 IAEA-PD NJOY2016.58 IAEA
angular distribution for (g,p*32) proton
Prob/Cos
Energy (MeV)
Cosine

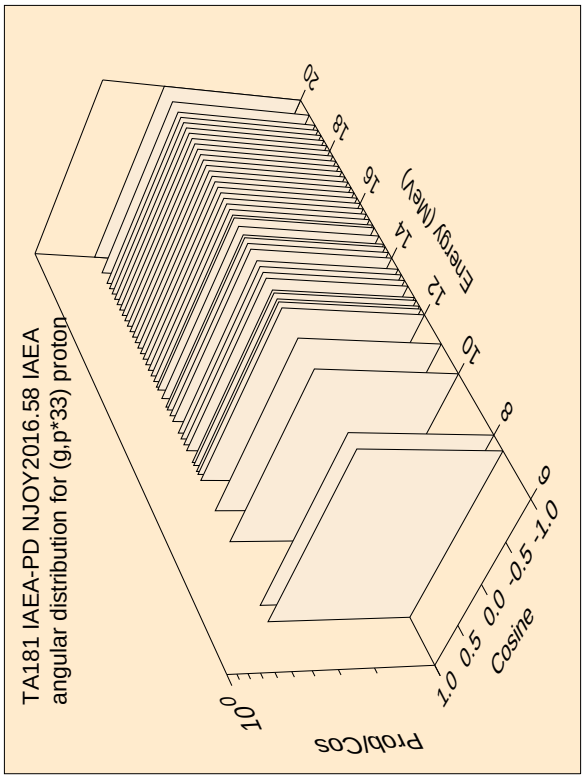
TA181 IAEA-PD NJOY2016.58 IAEA
angular distribution for (g,p*33) proton
Prob/Cos
Energy (MeV)
Cosine

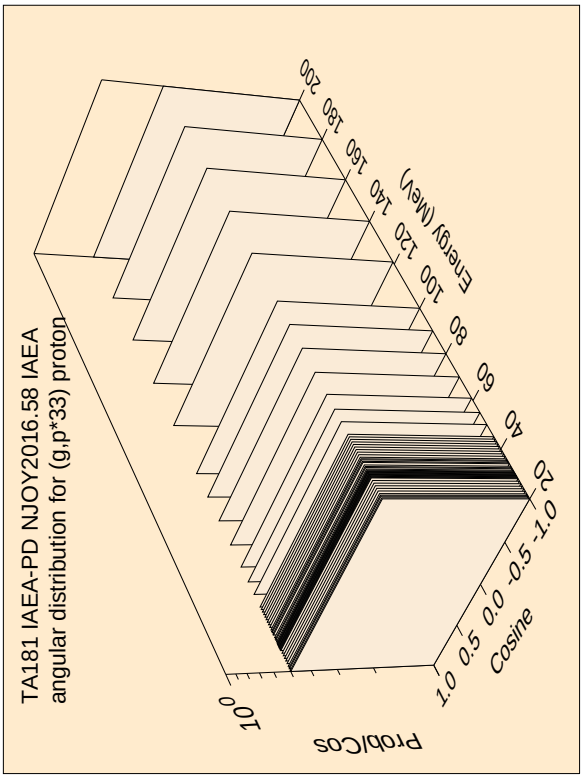
TA181 IAEA-PD NJOY2016.58 IAEA
angular distribution for (g,p*33) proton
Prob/Cos
Energy (MeV)
Cosine

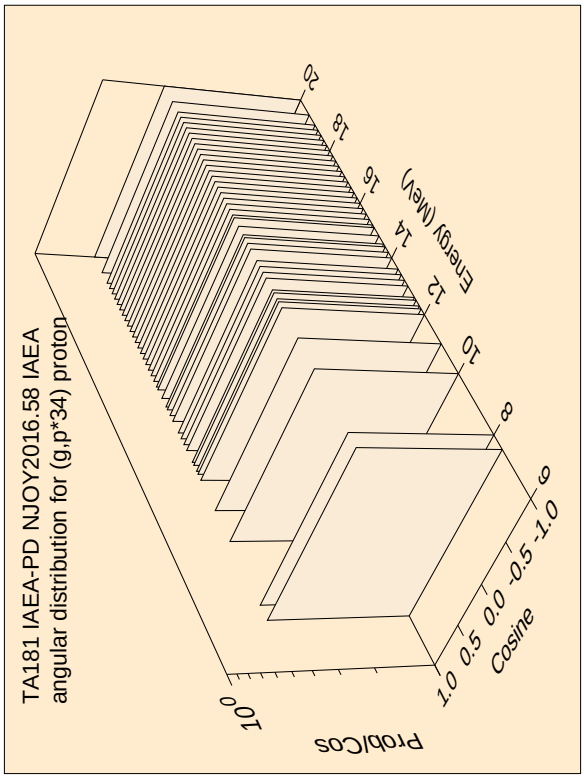
TA181 IAEA-PD NJOY2016.58 IAEA
angular distribution for (g,p*34) proton
Prob/Cos
Energy (MeV)
Cosine

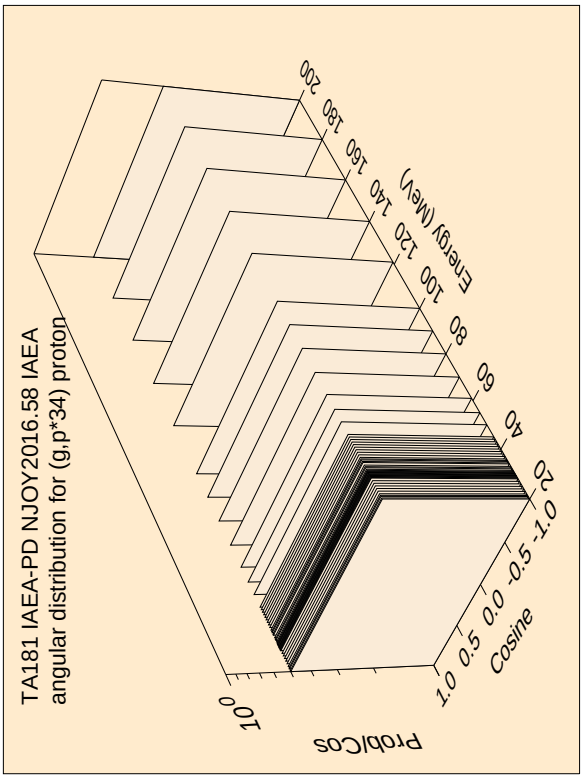
TA181 IAEA-PD NJOY2016.58 IAEA
angular distribution for (g,p*34) proton
Prob/Cos
Energy (MeV)
Cosine

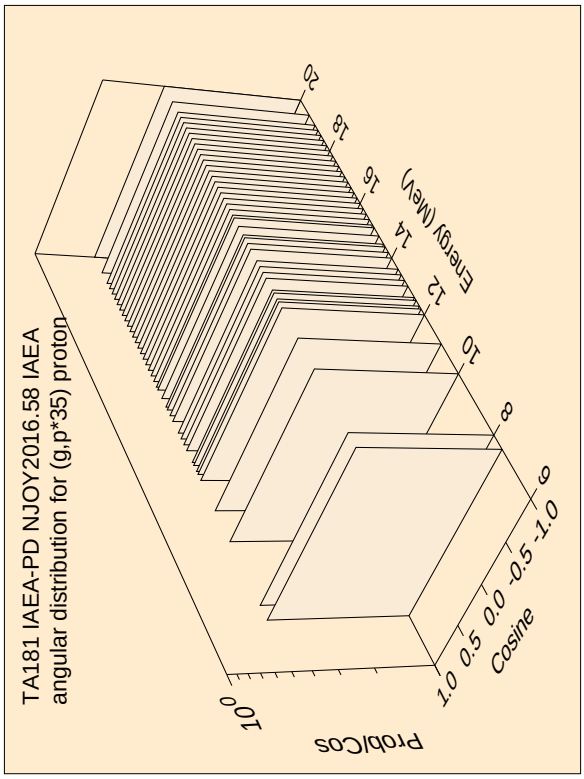
TA181 IAEA-PD NJOY2016.58 IAEA
angular distribution for (g,p*35) proton
Prob/Cos
Energy (MeV)
Cosine

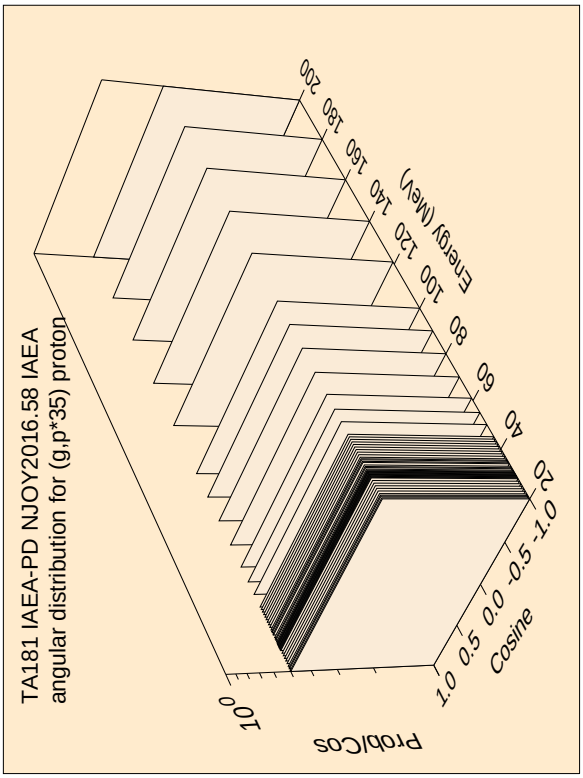
TA181 IAEA-PD NJOY2016.58 IAEA
angular distribution for (g,p*35) proton
Prob/Cos
Energy (MeV)
Cosine

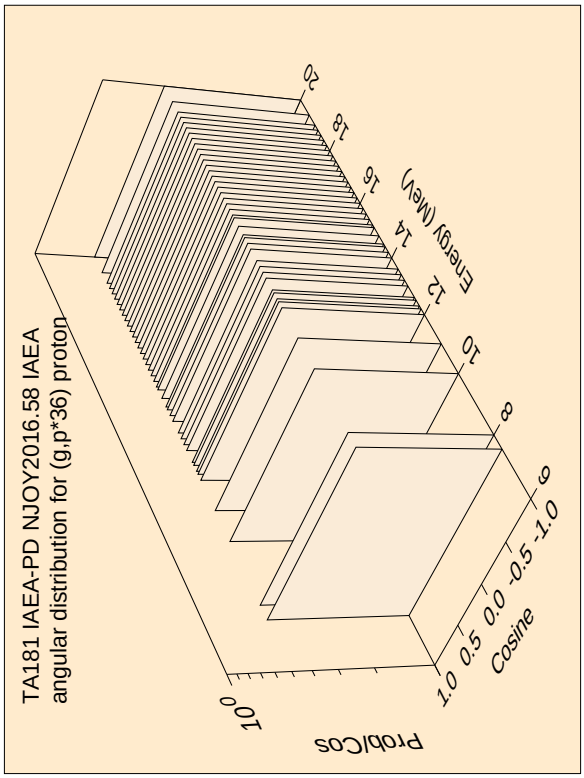
TA181 IAEA-PD NJOY2016.58 IAEA
angular distribution for (g,p*36) proton
Prob/Cos
Energy (MeV)
Cosine

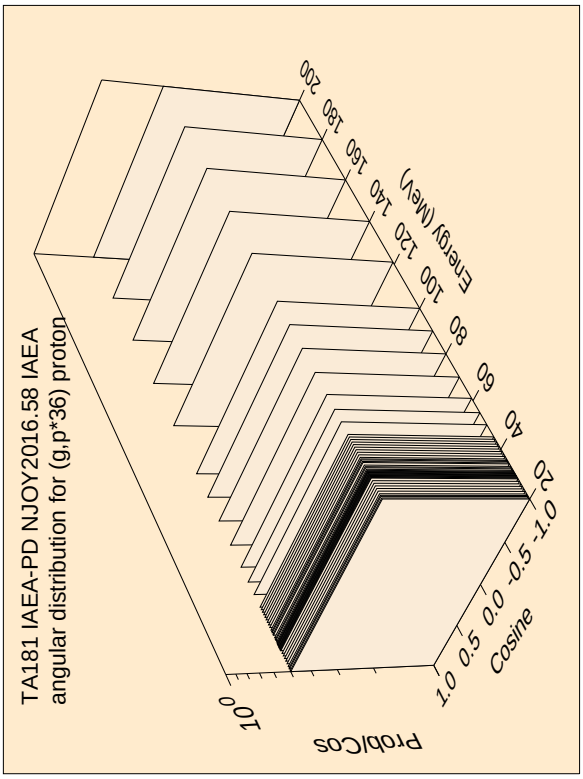
TA181 IAEA-PD NJOY2016.58 IAEA
angular distribution for (g,p*36) proton
Prob/Cos
Energy (MeV)
Cosine

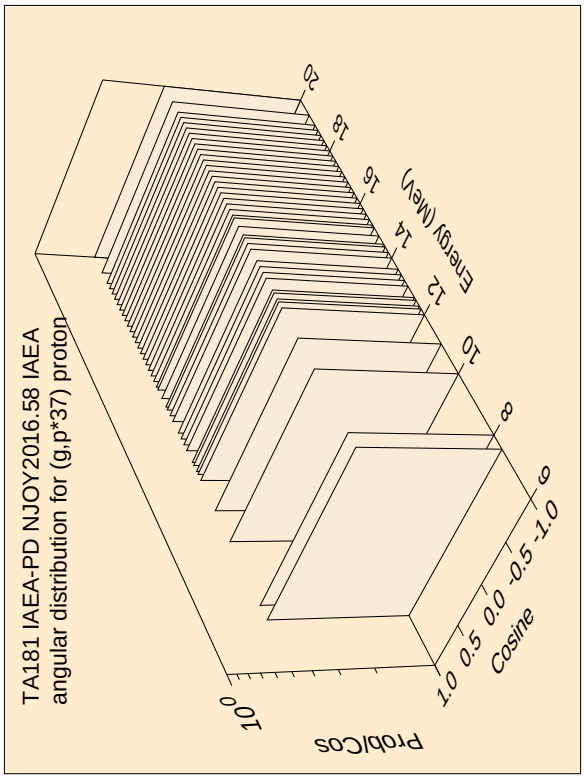
TA181 IAEA-PD NJOY2016.58 IAEA
angular distribution for (g,p*37) proton
Prob/Cos
Energy (MeV)
Cosine

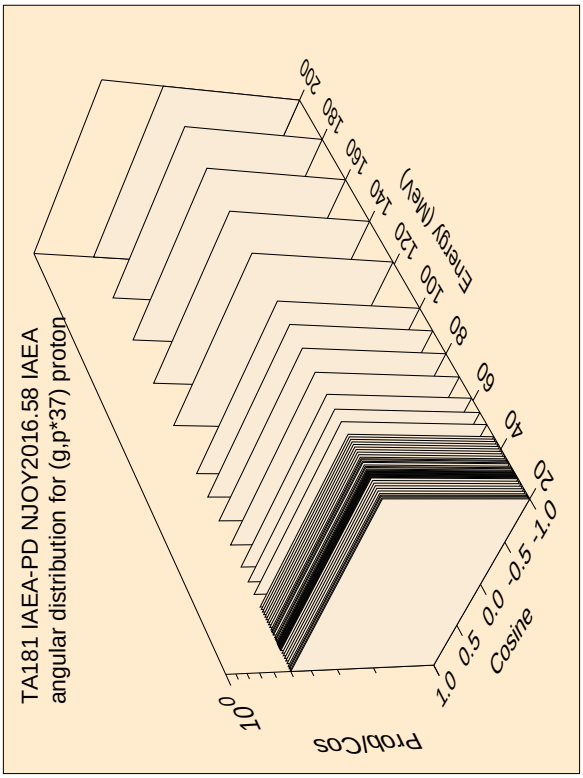
TA181 IAEA-PD NJOY2016.58 IAEA
angular distribution for (g,p*37) proton
Prob/Cos
Energy (MeV)
Cosine

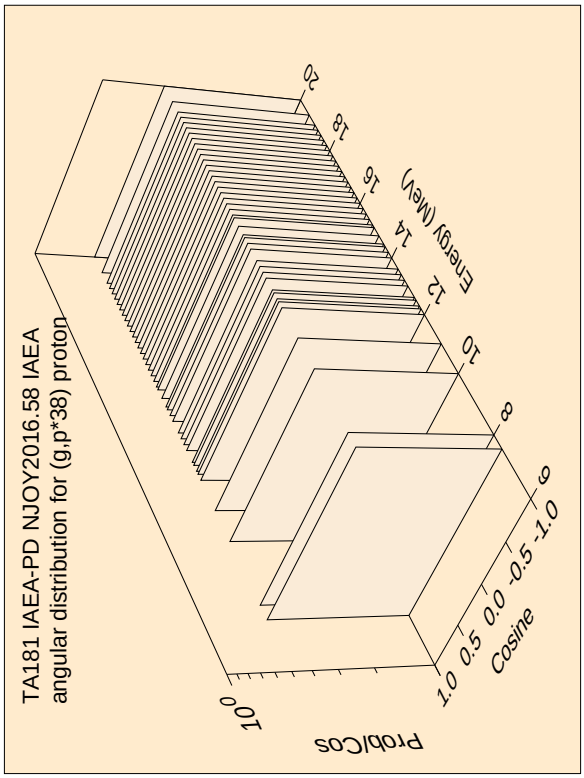
TA181 IAEA-PD NJOY2016.58 IAEA
angular distribution for (g,p*38) proton
Prob/Cos
Energy (MeV)
Cosine

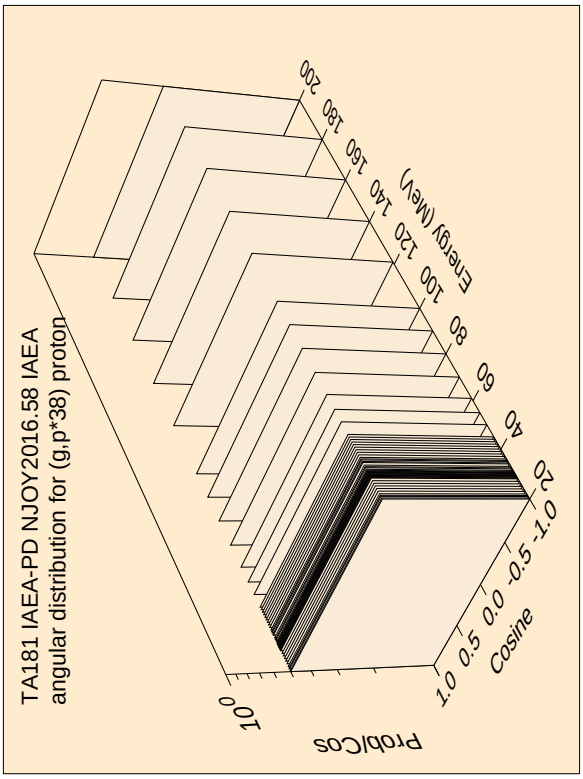
TA181 IAEA-PD NJOY2016.58 IAEA
angular distribution for (g,p*38) proton
Prob/Cos
Energy (MeV)
Cosine

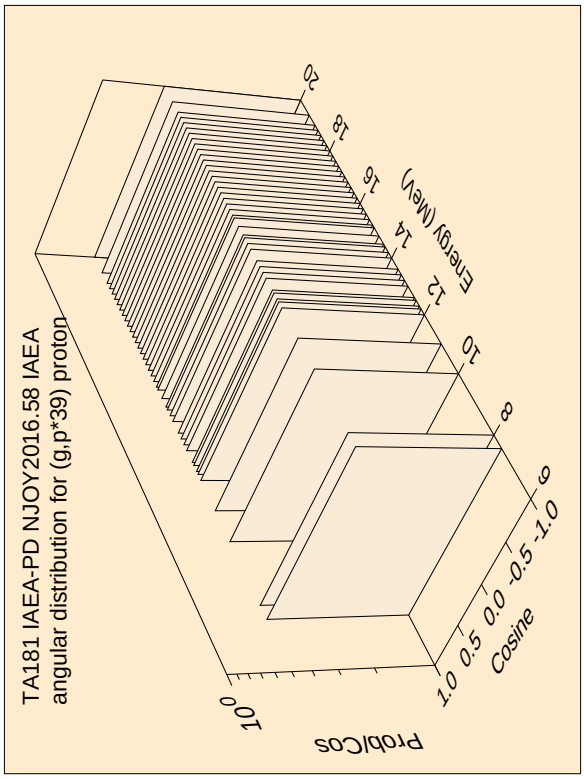
TA181 IAEA-PD NJOY2016.58 IAEA
angular distribution for (g,p*39) proton
Prob/Cos
Energy (MeV)
Cosine

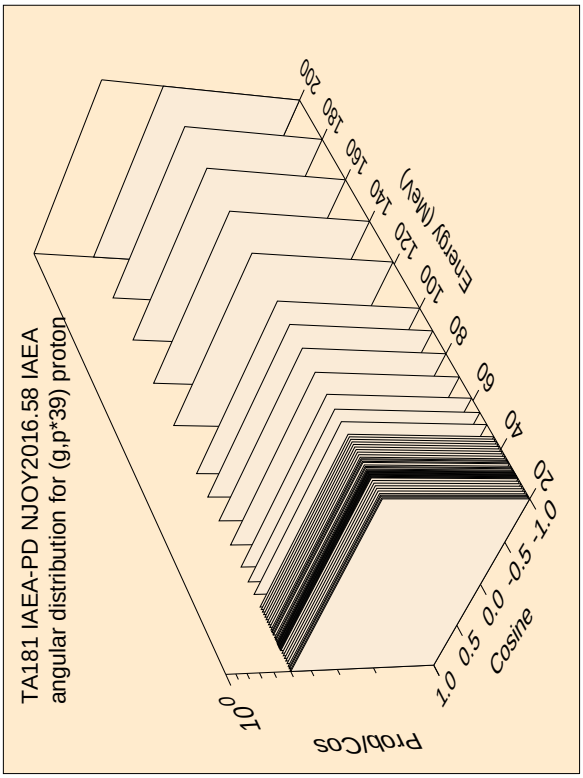
TA181 IAEA-PD NJOY2016.58 IAEA
angular distribution for (g,p*39) proton
Prob/Cos
Cosine
Energy (Mev)

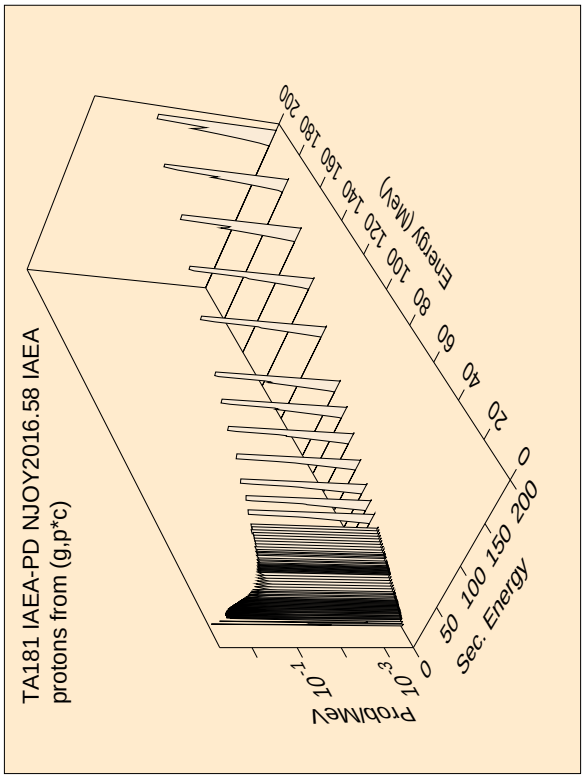
TA181 IAEA-PD NJOY2016.58 IAEA
protons from (g,p*c)
Prob/MeV
Sec. Energy
Energy (Mev)

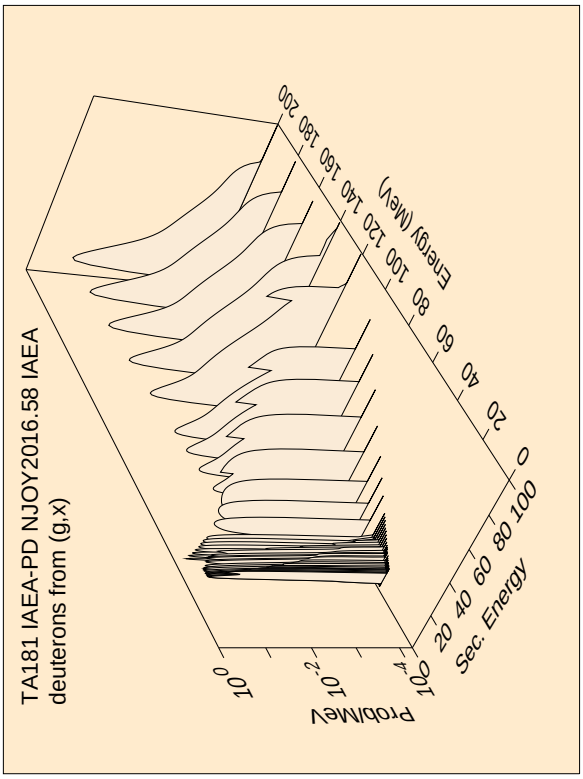
TA181 IAEA-PD NJOY2016.58 IAEA
deuterons from (g,x)
Prob/MeV
Sec. Energy
Energy (Mev)

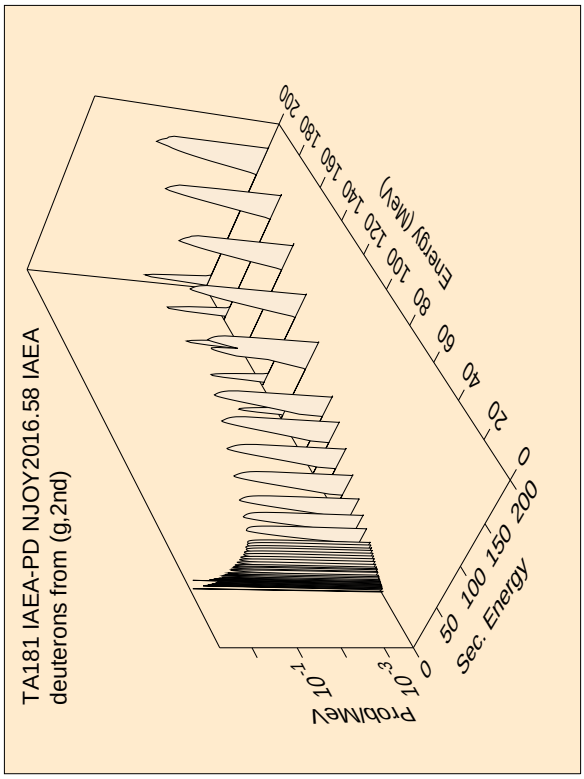
TA181 IAEA-PD NJOY2016.58 IAEA
deuterons from (g,2nd)
Prob/MeV
Sec. Energy
Energy (Mev)

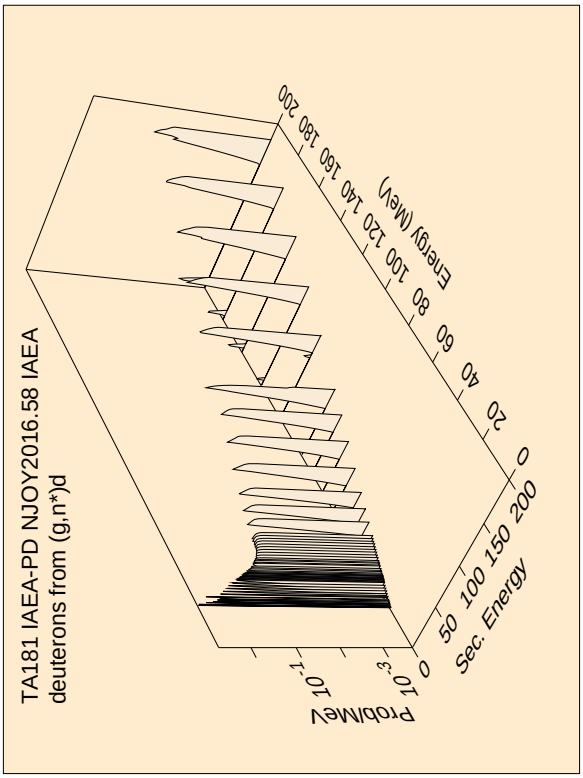
TA181 IAEA-PD NJOY2016.58 IAEA
deuterons from (g,n*)d
Prob/MeV
Energy (Mev)
Sec. Energy

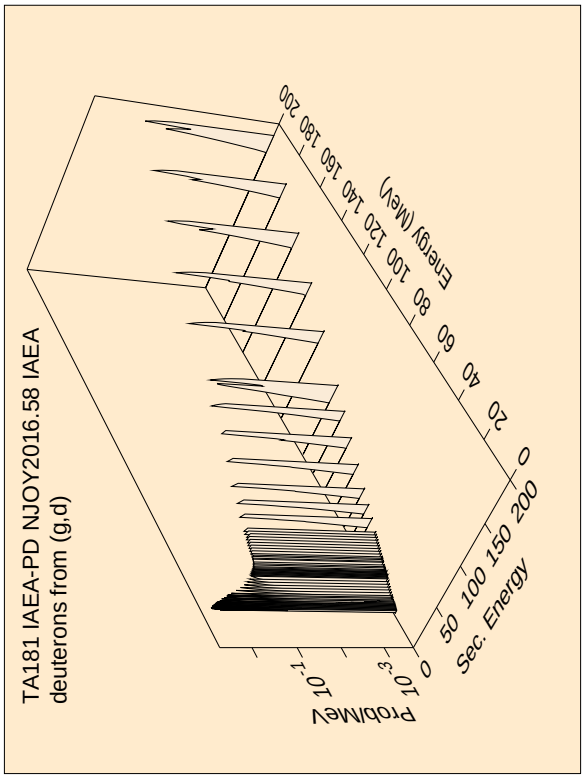
TA181 IAEA-PD NJOY2016.58 IAEA
deuterons from (g,d)
Prob/MeV
Energy (Mev)
Sec. Energy

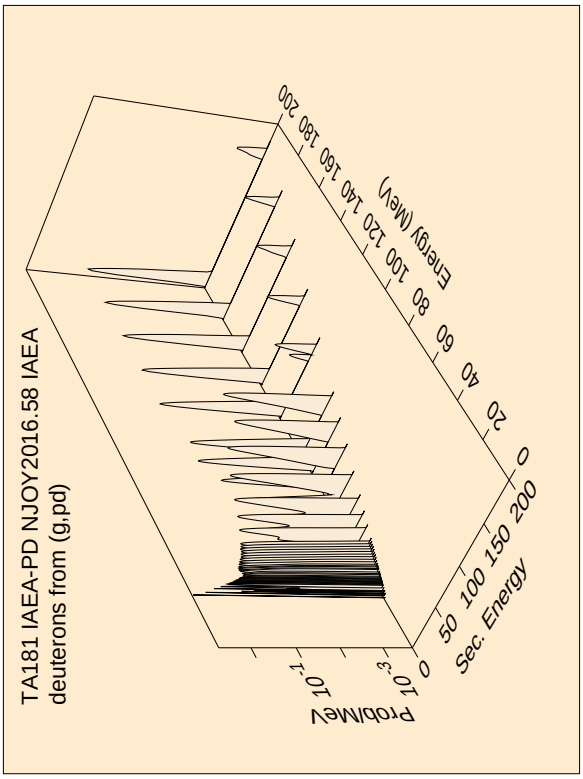
TA181 IAEA-PD NJOY2016.58 IAEA
deuterons from (g,pd)
Prob/MeV
Energy (Mev)
Sec. Energy

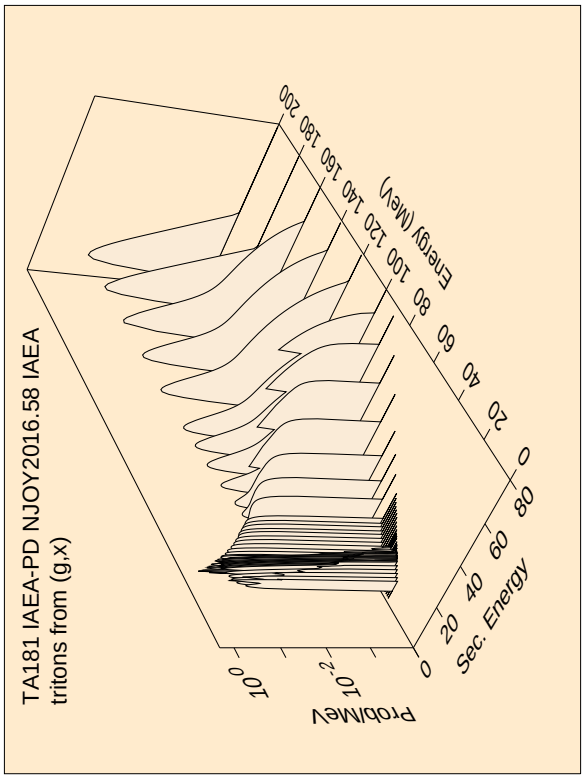
TA181 IAEA-PD NJOY2016.58 IAEA
tritons from (g,x)
Prob/MeV
Energy (Mev)
Sec. Energy

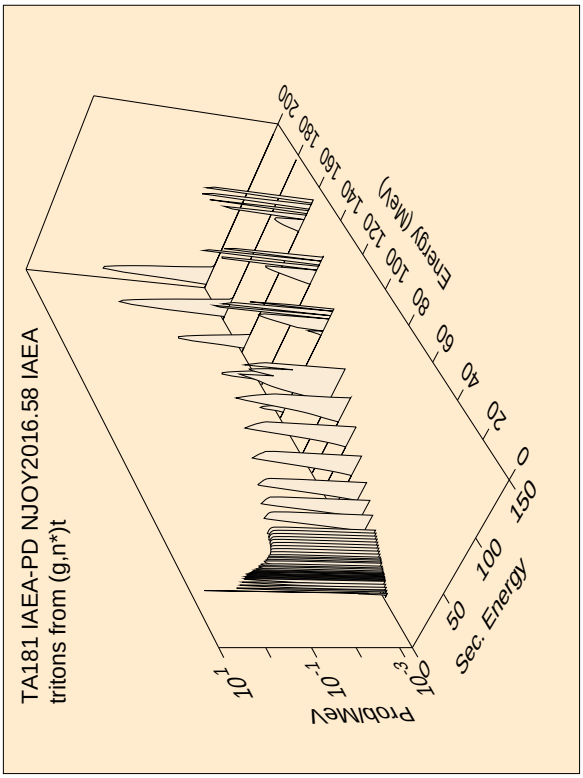
TA181 IAEA-PD NJOY2016.58 IAEA
tritons from (g,n*)t
Prob/MeV
Energy (Mev)
Sec. Energy

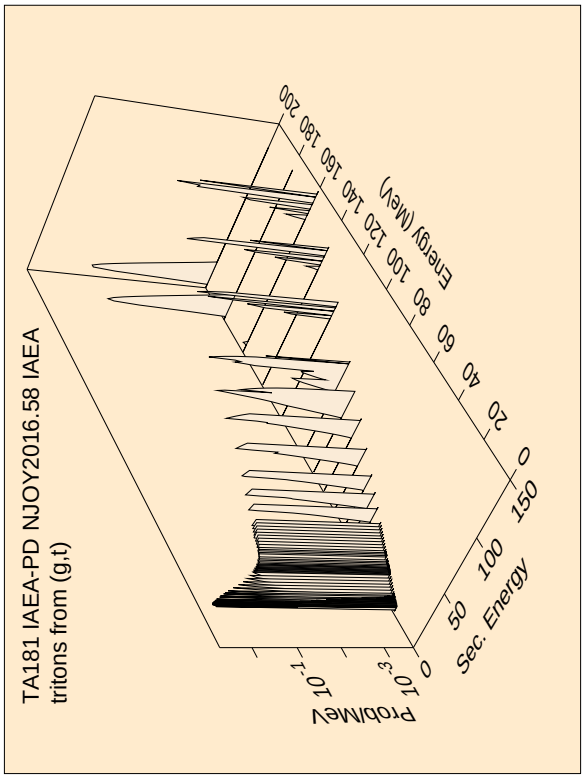
TA181 IAEA-PD NJOY2016.58 IAEA
tritons from (g,t)
Prob/MeV
Energy (Mev)
Sec. Energy

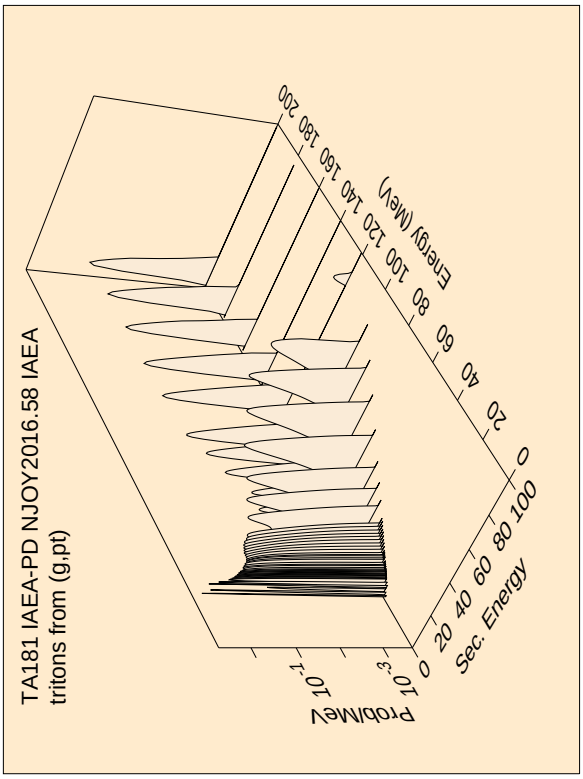
TA181 IAEA-PD NJOY2016.58 IAEA
tritons from (g,pt)
Prob/MeV
Energy (Mev)
Sec. Energy

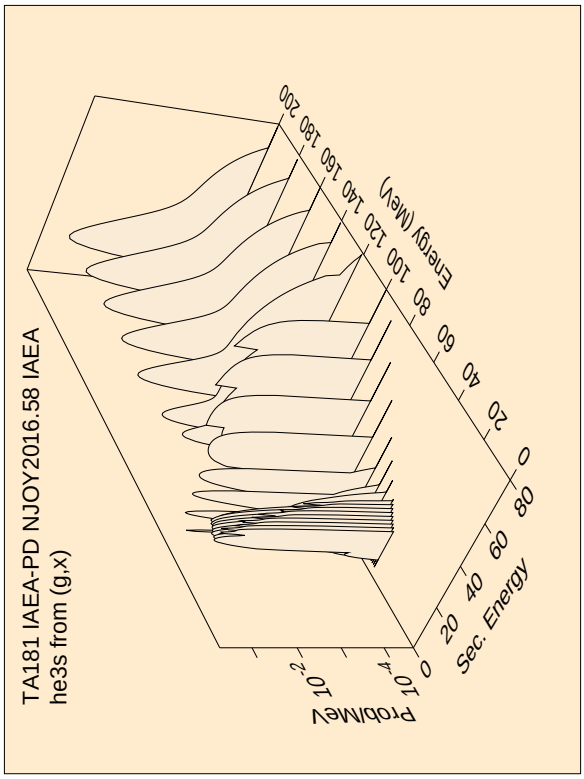
TA181 IAEA-PD NJOY2016.58 IAEA
he3s from (g,x)
Prob/MeV
Energy (Mev)
Sec. Energy

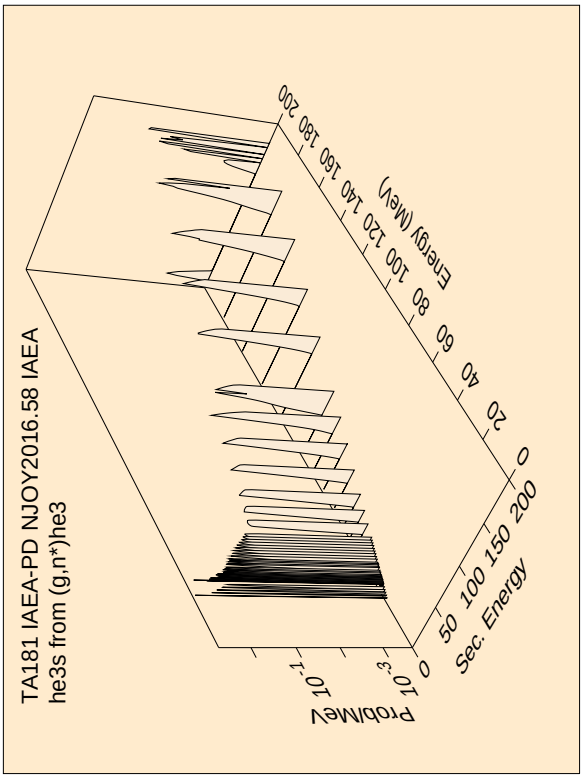
TA181 IAEA-PD NJOY2016.58 IAEA
he3s from (g,n*)he3
Prob/MeV
Energy (Mev)
Sec. Energy

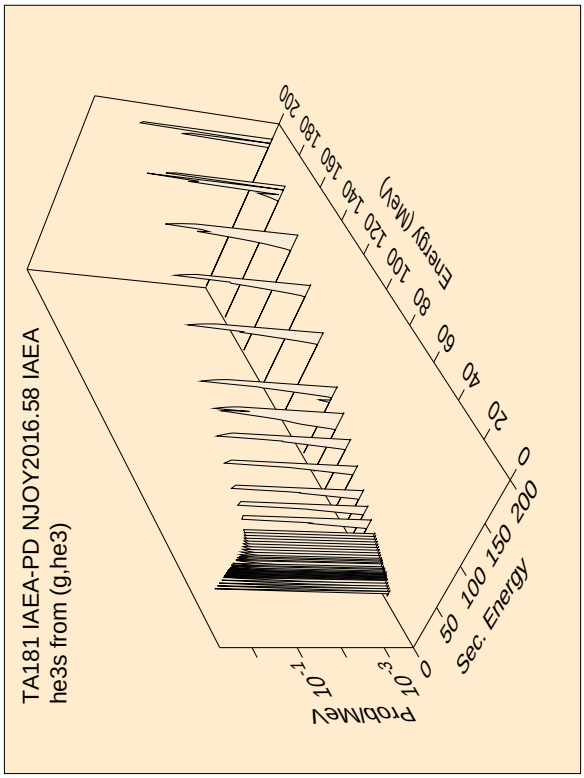
TA181 IAEA-PD NJOY2016.58 IAEA
he3s from (g,he3)
Prob/MeV
Energy (Mev)
Sec. Energy

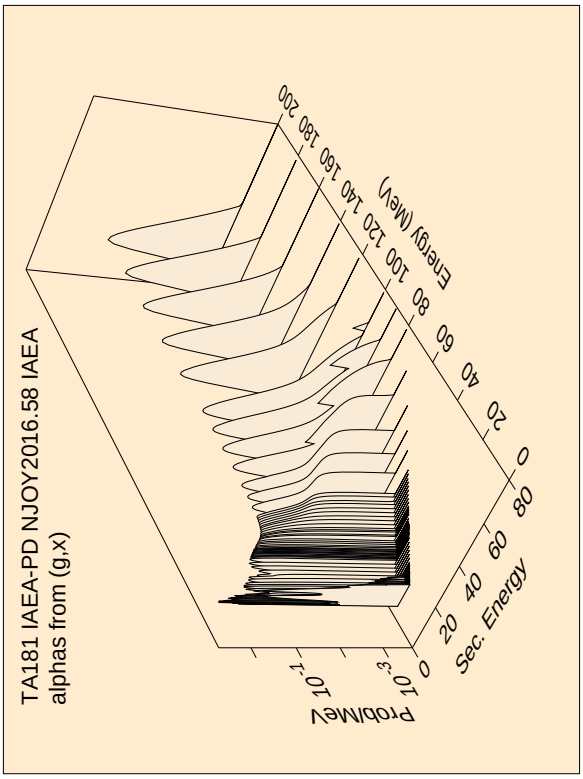
TA181 IAEA-PD NJOY2016.58 IAEA
alphas from (g,x)
Prob/MeV
Energy (Mev)
Sec. Energy

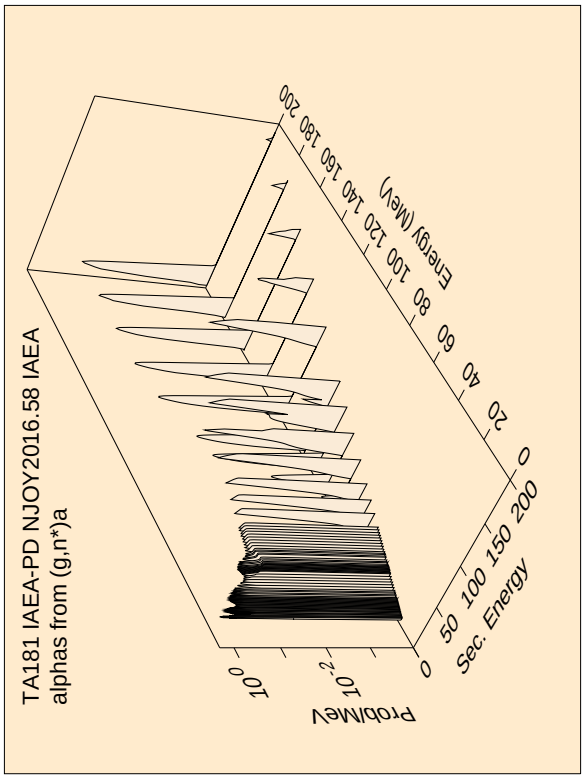
TA181 IAEA-PD NJOY2016.58 IAEA
alphas from (g,n*)a
Prob/MeV
Energy (Mev)
Sec. Energy

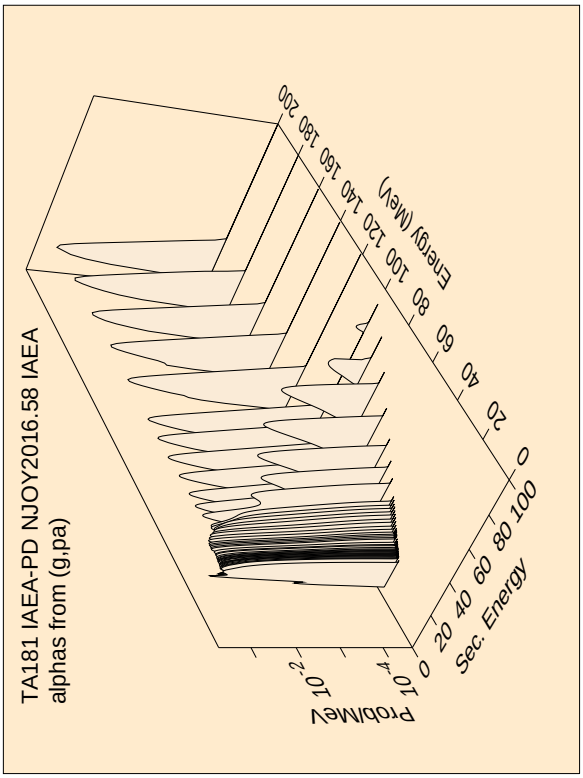
TA181 IAEA-PD NJOY2016.58 IAEA
alphas from (g,pa)
Prob/MeV
Sec. Energy
Energy (Mev)

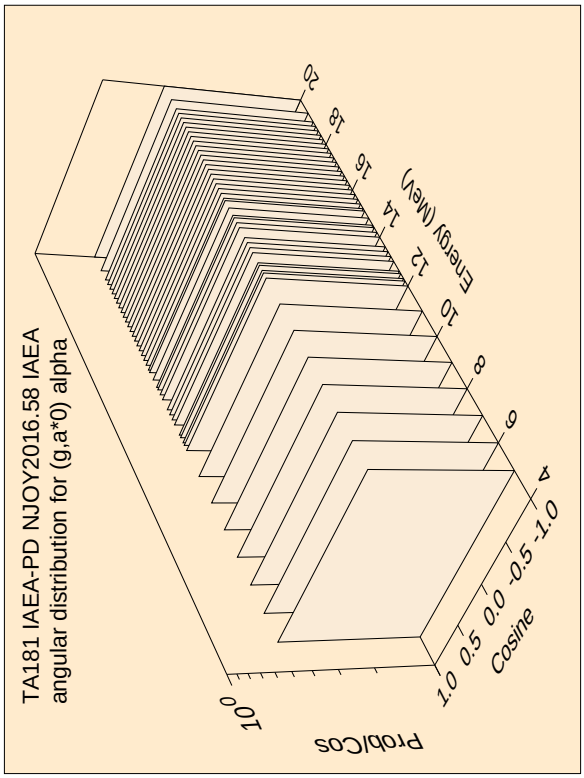
TA181 IAEA-PD NJOY2016.58 IAEA
angular distribution for (g,a*0) alpha
Prob/Cos
Cosine
Energy (Mev)

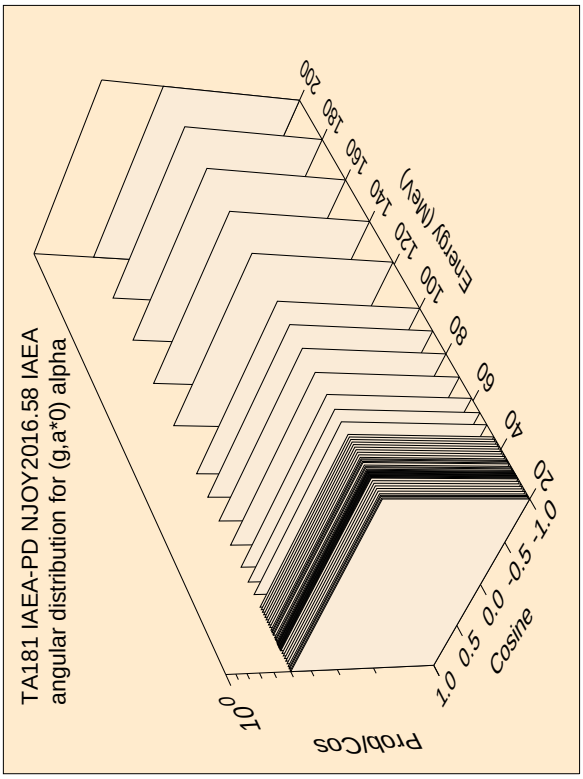
TA181 IAEA-PD NJOY2016.58 IAEA
angular distribution for (g,a*0) alpha
Prob/Cos
Cosine
Energy (Mev)

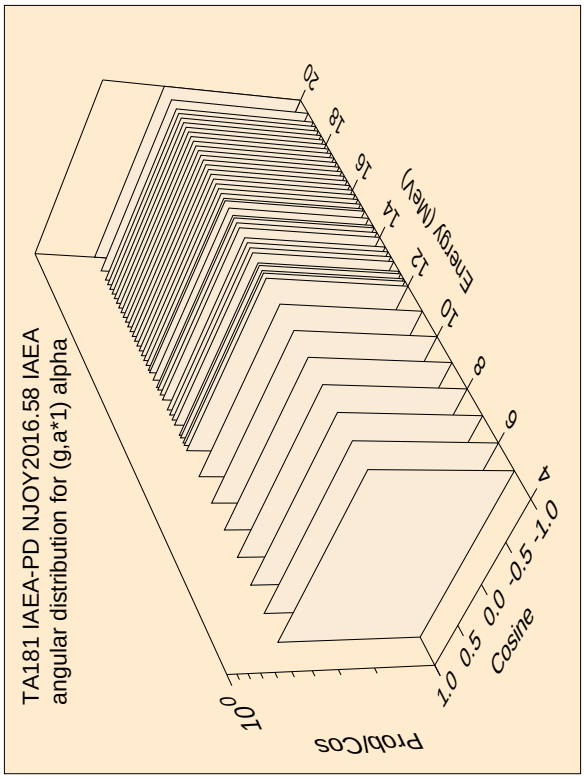
TA181 IAEA-PD NJOY2016.58 IAEA
angular distribution for (g,a*1) alpha
Prob/Cos
Cosine
Energy (Mev)

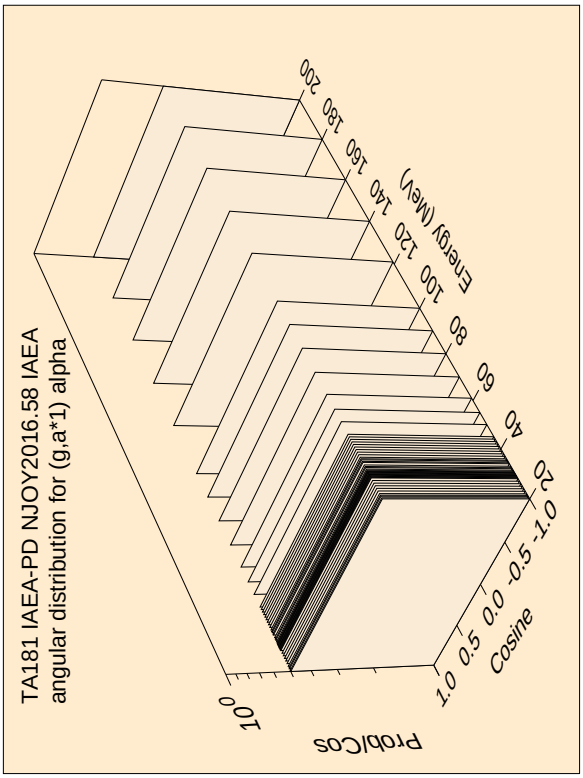
TA181 IAEA-PD NJOY2016.58 IAEA
angular distribution for (g,a*1) alpha
Prob/Cos
Cosine
Energy (MeV)

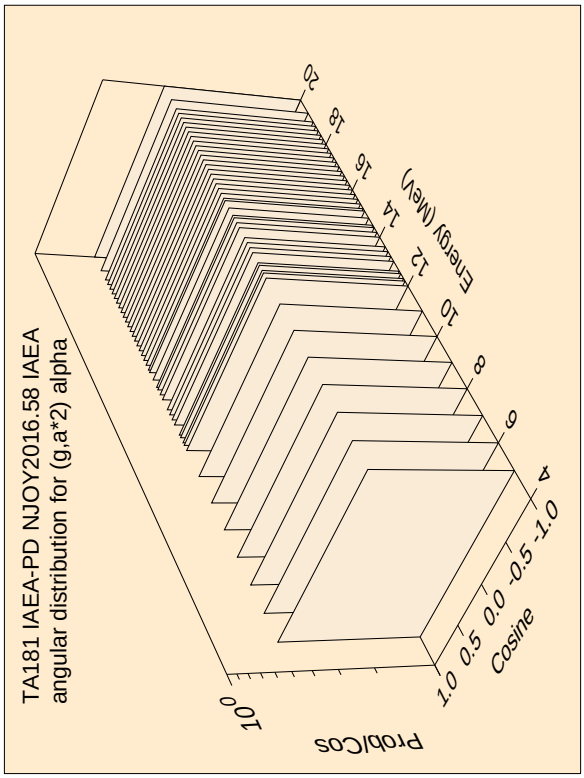
TA181 IAEA-PD NJOY2016.58 IAEA
angular distribution for (g,a*2) alpha
Prob/Cos
Cosine
Energy (MeV)

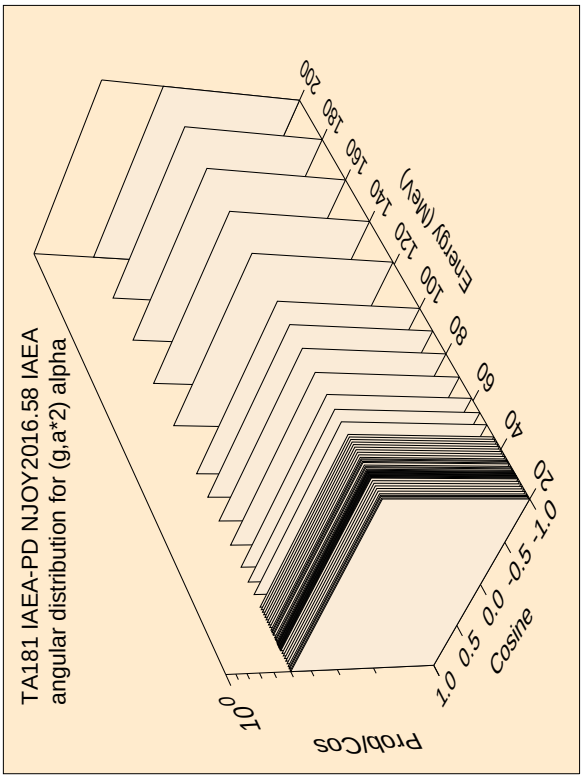
TA181 IAEA-PD NJOY2016.58 IAEA
angular distribution for (g,a*2) alpha
Prob/Cos
Cosine
Energy (MeV)

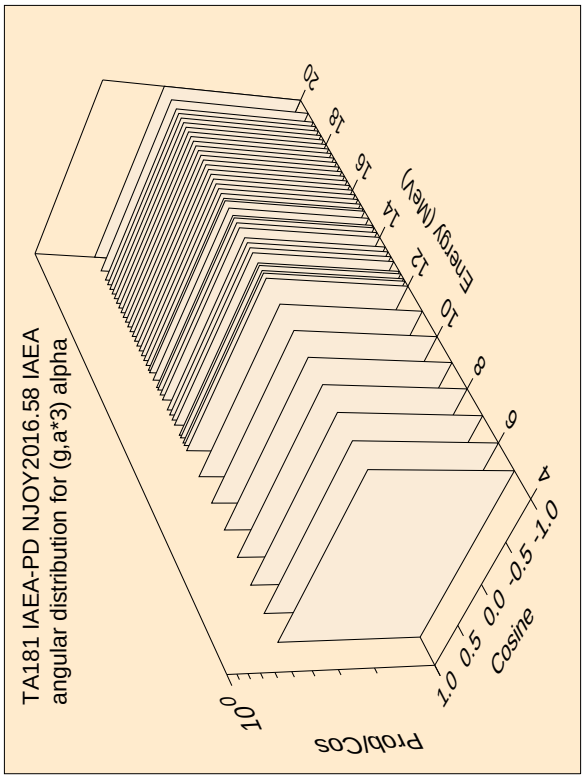
TA181 IAEA-PD NJOY2016.58 IAEA
angular distribution for (g,a*3) alpha
Prob/Cos
Cosine
Energy (MeV)

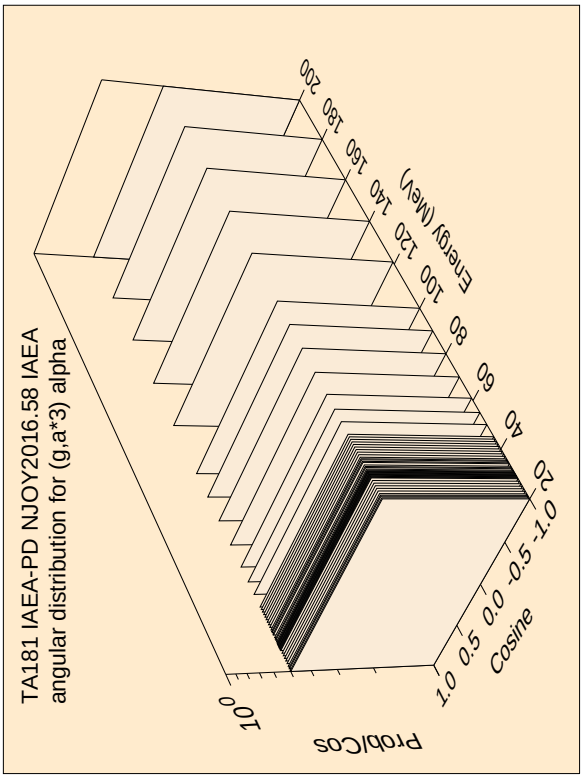
TA181 IAEA-PD NJOY2016.58 IAEA
angular distribution for (g,a*3) alpha
Prob/Cos
Cosine
Energy (MeV)

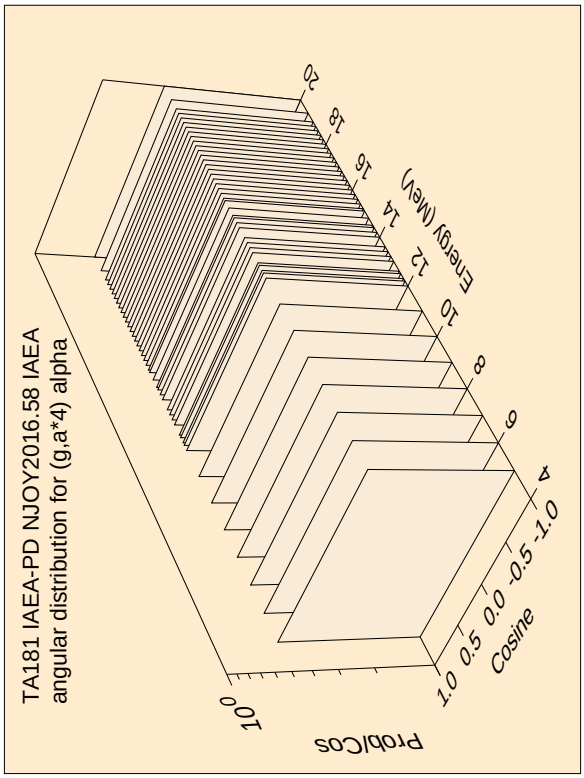
TA181 IAEA-PD NJOY2016.58 IAEA
angular distribution for (g,a*4) alpha
Prob/Cos
Cosine
Energy (MeV)

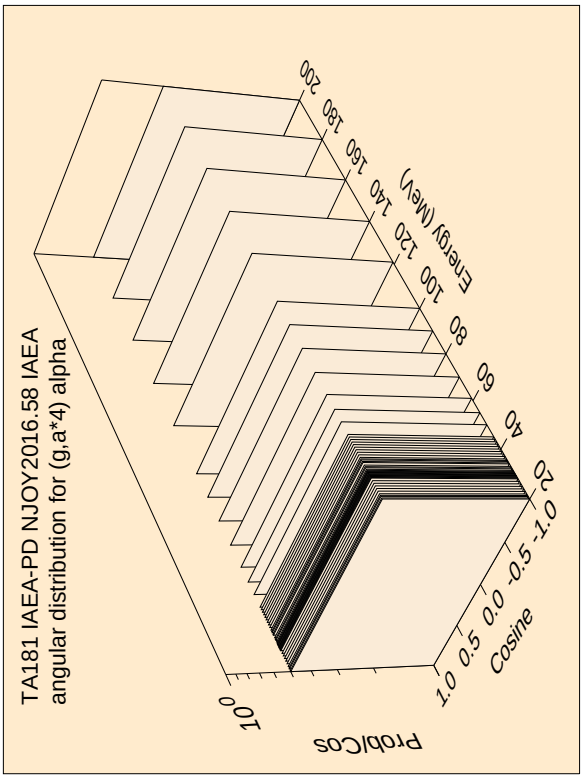
TA181 IAEA-PD NJOY2016.58 IAEA
angular distribution for (g,a*4) alpha
Prob/Cos
Cosine
Energy (MeV)

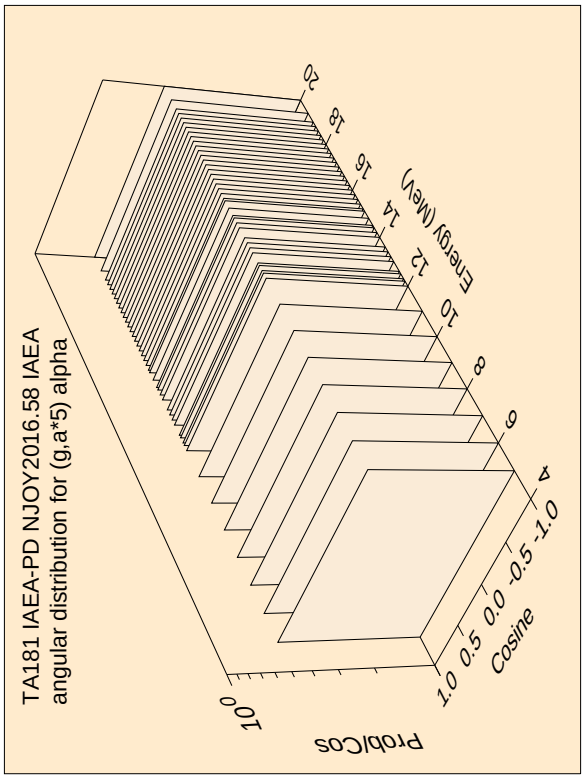
TA181 IAEA-PD NJOY2016.58 IAEA
angular distribution for (g,a*5) alpha
Prob/Cos
Cosine
Energy (MeV)

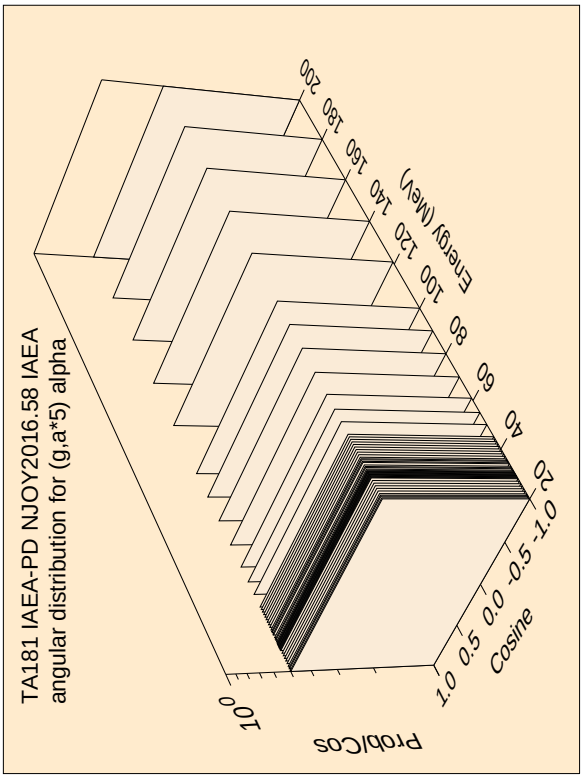
TA181 IAEA-PD NJOY2016.58 IAEA
angular distribution for (g,a*5) alpha
Prob/Cos
Cosine
Energy (MeV)

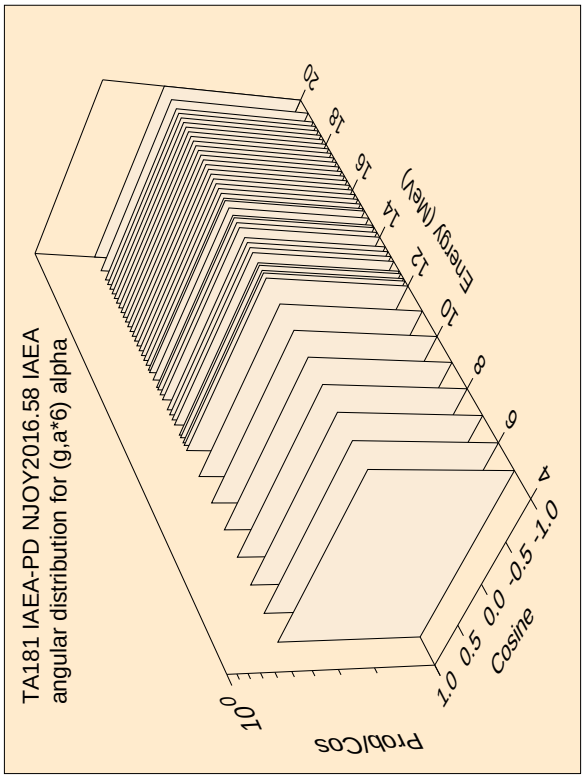
TA181 IAEA-PD NJOY2016.58 IAEA
angular distribution for (g,a*6) alpha
Prob/Cos
Cosine
Energy (MeV)

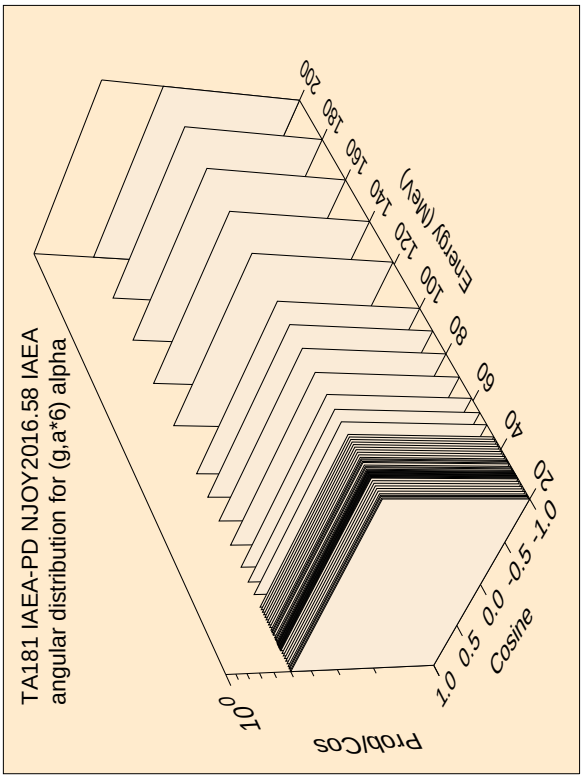
TA181 IAEA-PD NJOY2016.58 IAEA
angular distribution for (g,a*6) alpha
Prob/Cos
Cosine
Energy (MeV)

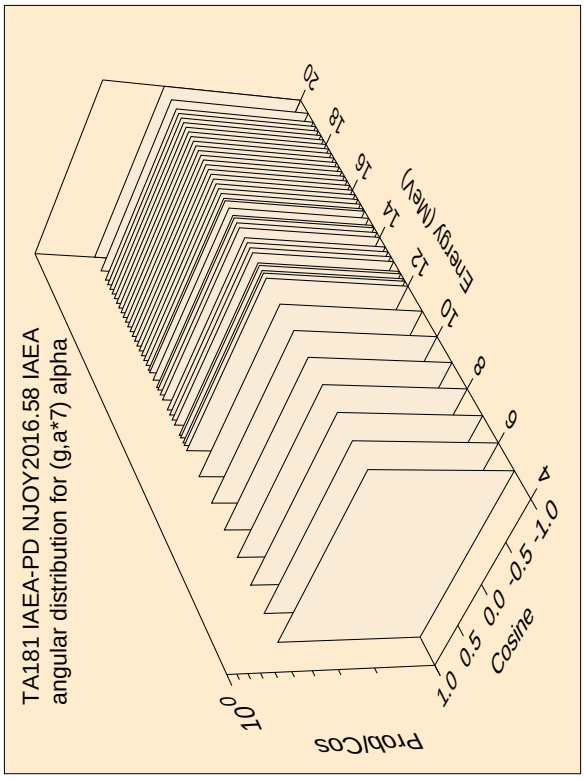
TA181 IAEA-PD NJOY2016.58 IAEA
angular distribution for (g,a*7) alpha
Prob/Cos
Cosine
Energy (MeV)

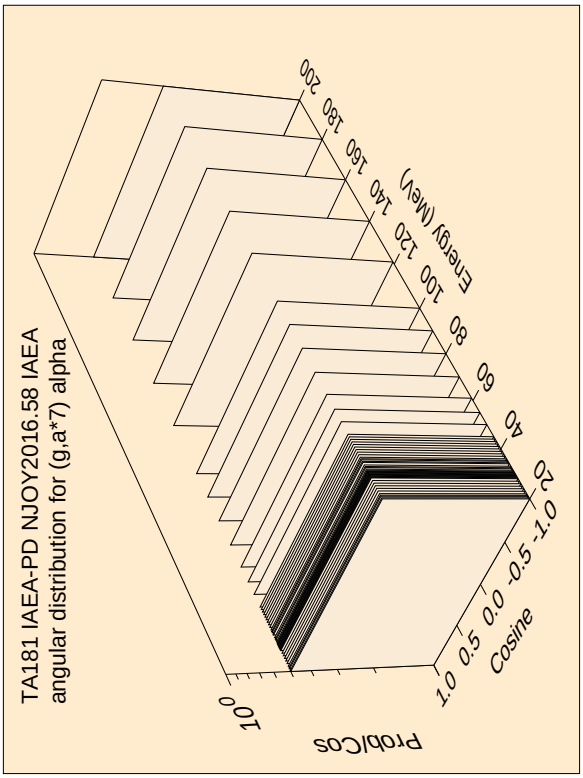
TA181 IAEA-PD NJOY2016.58 IAEA
angular distribution for (g,a*7) alpha
Prob/Cos
Cosine
Energy (MeV)

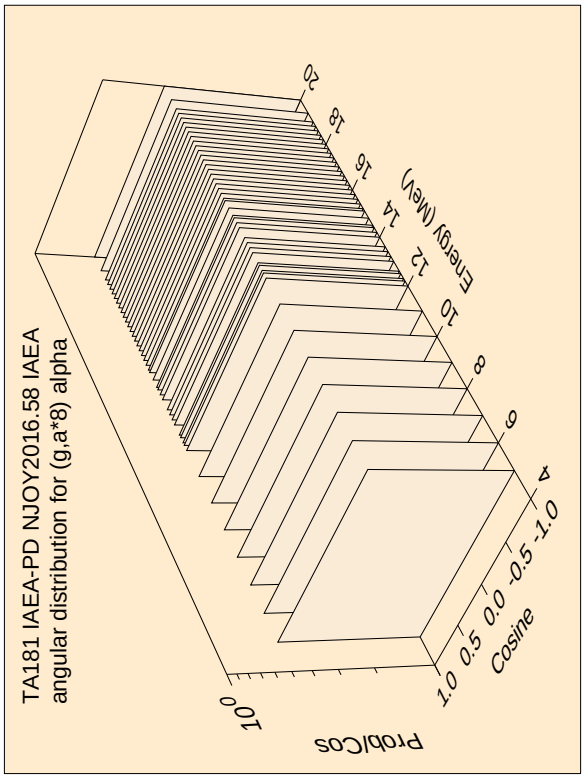
TA181 IAEA-PD NJOY2016.58 IAEA
angular distribution for (g,a*8) alpha
Prob/Cos
Cosine
Energy (MeV)

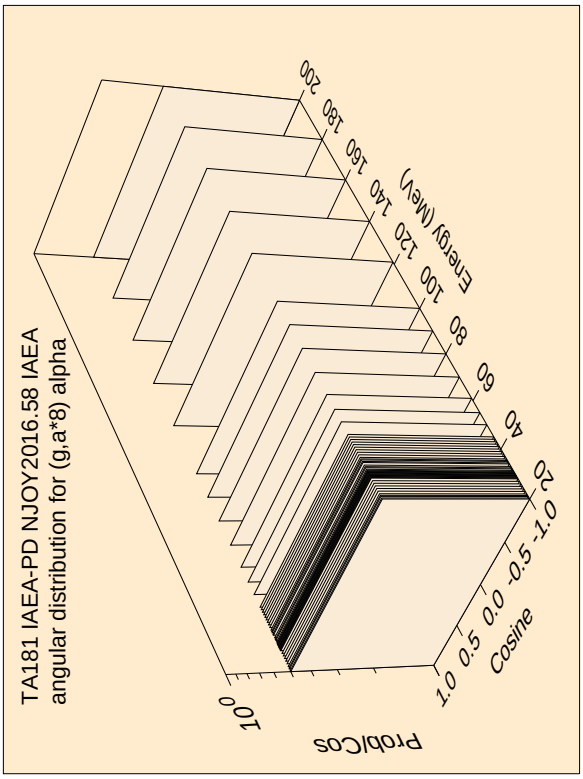
TA181 IAEA-PD NJOY2016.58 IAEA
angular distribution for (g,a*8) alpha
Prob/Cos
Cosine
Energy (MeV)

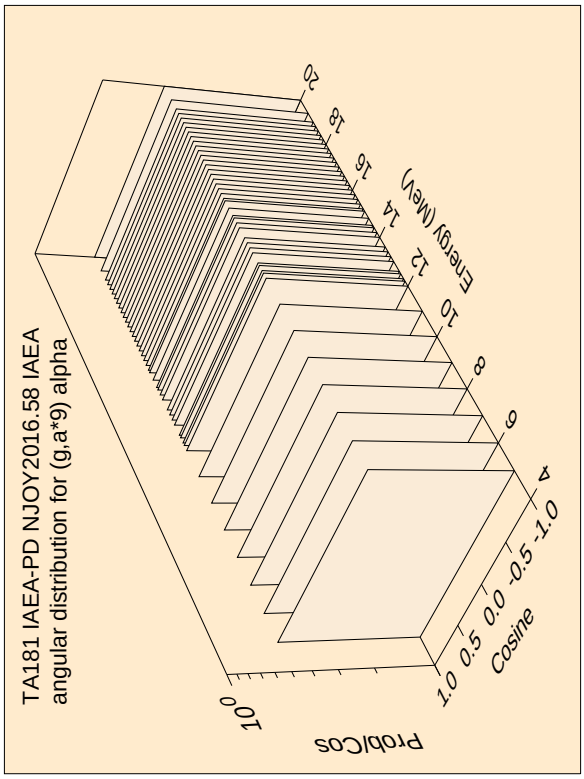
TA181 IAEA-PD NJOY2016.58 IAEA
angular distribution for (g,a*9) alpha
Prob/Cos
Cosine
Energy (MeV)

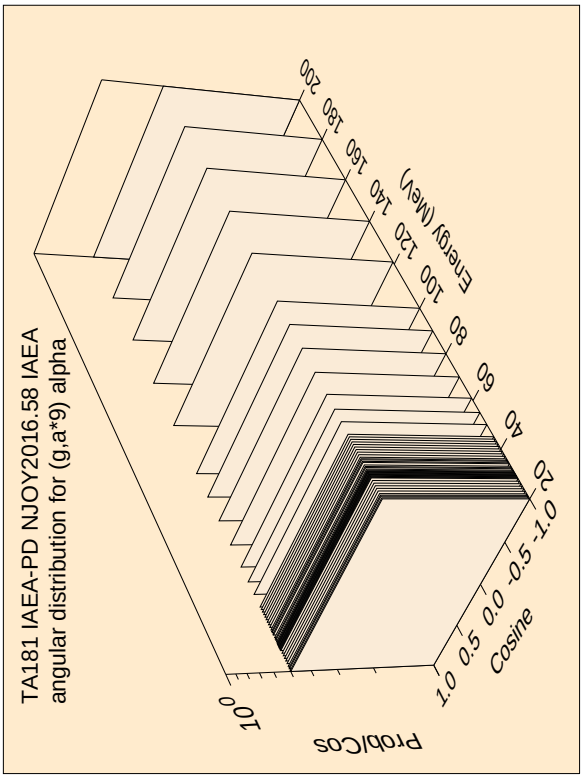
TA181 IAEA-PD NJOY2016.58 IAEA
angular distribution for (g,a*9) alpha
Prob/Cos
Cosine
Energy (MeV)

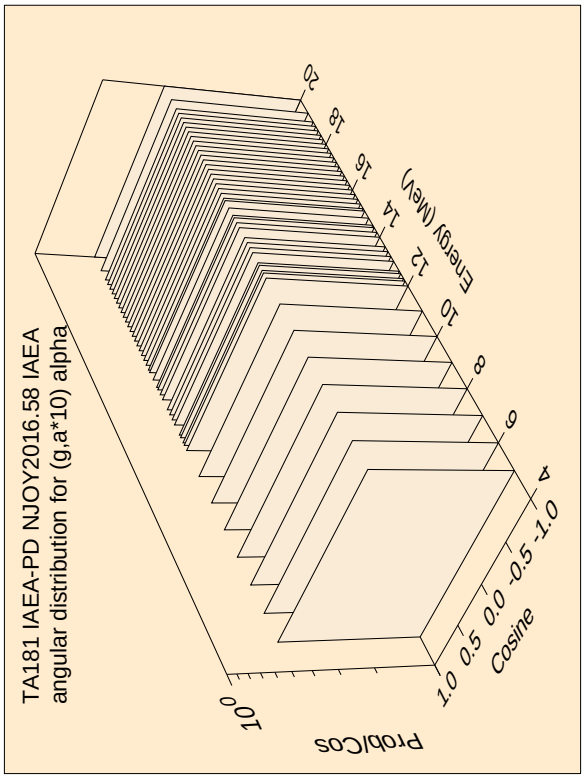
TA181 IAEA-PD NJOY2016.58 IAEA
angular distribution for (g,a*10) alpha
Prob/Cos
Cosine
Energy (MeV)

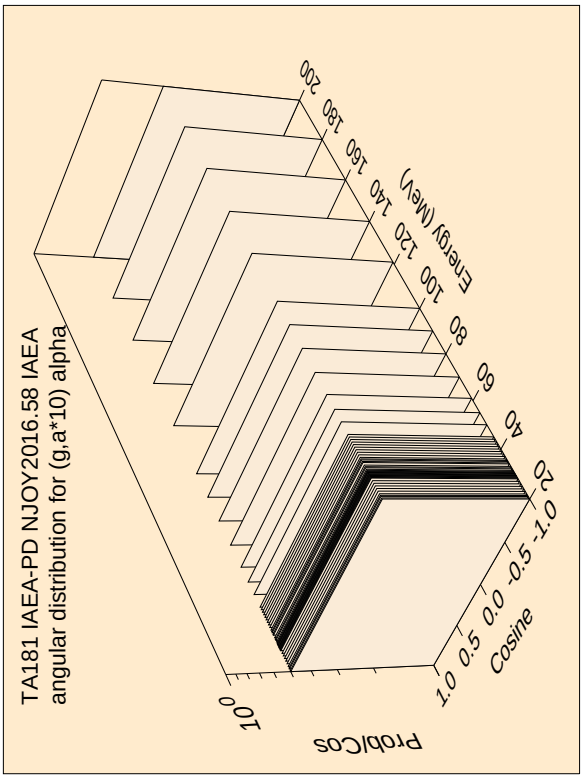
TA181 IAEA-PD NJOY2016.58 IAEA
angular distribution for (g,a*10) alpha
Prob/Cos
Cosine
Energy (MeV)

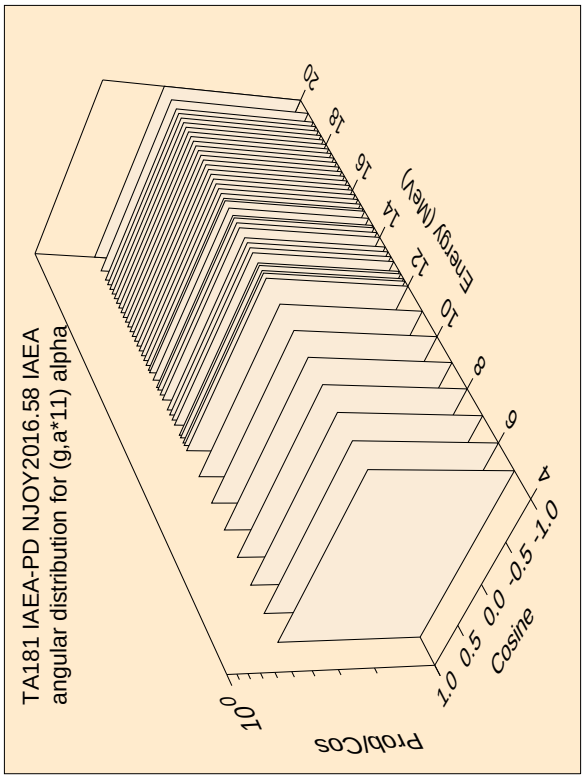
TA181 IAEA-PD NJOY2016.58 IAEA
angular distribution for (g,a*11) alpha
Prob/Cos
Cosine
Energy (MeV)

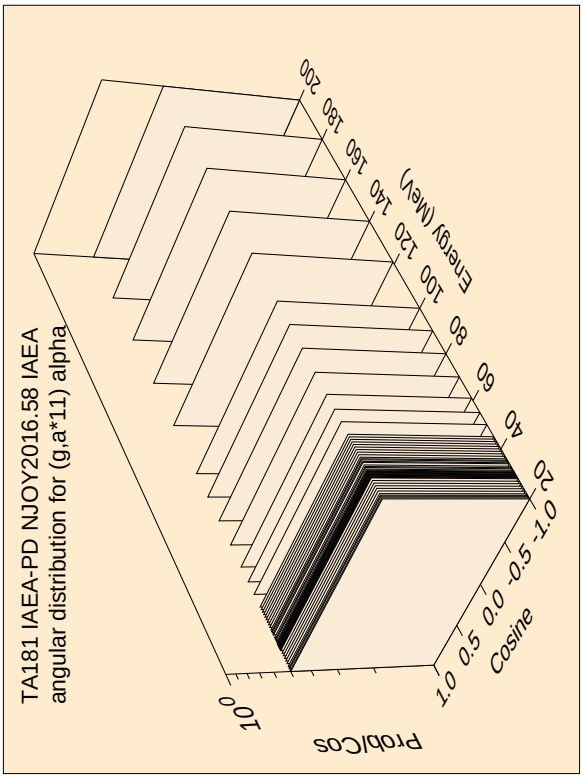
TA181 IAEA-PD NJOY2016.58 IAEA
angular distribution for (g,a*11) alpha
Prob/Cos
Cosine
Energy (MeV)

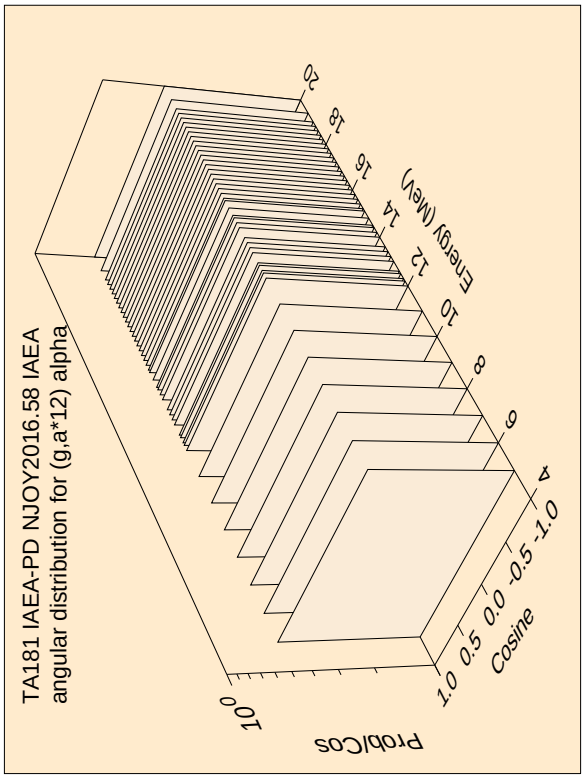
TA181 IAEA-PD NJOY2016.58 IAEA
angular distribution for (g,a*12) alpha
Prob/Cos
Cosine
Energy (MeV)

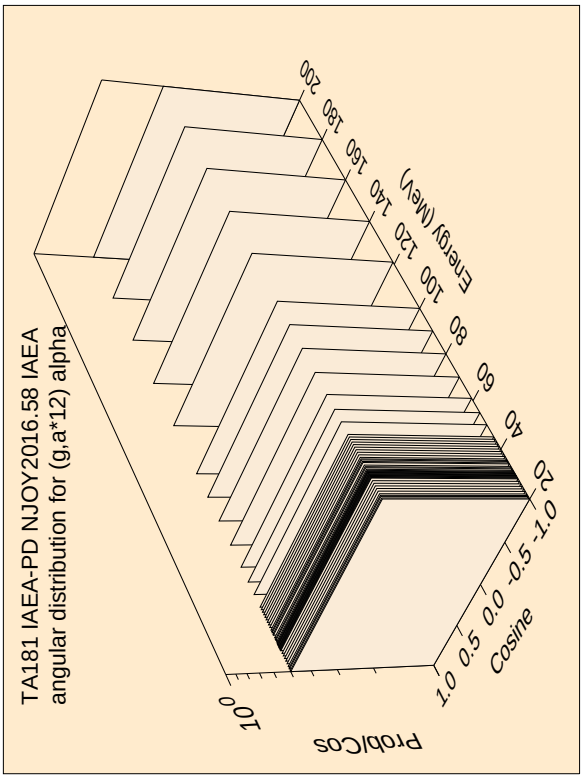
TA181 IAEA-PD NJOY2016.58 IAEA
angular distribution for (g,a*12) alpha
Prob/Cos
Cosine
Energy (MeV)

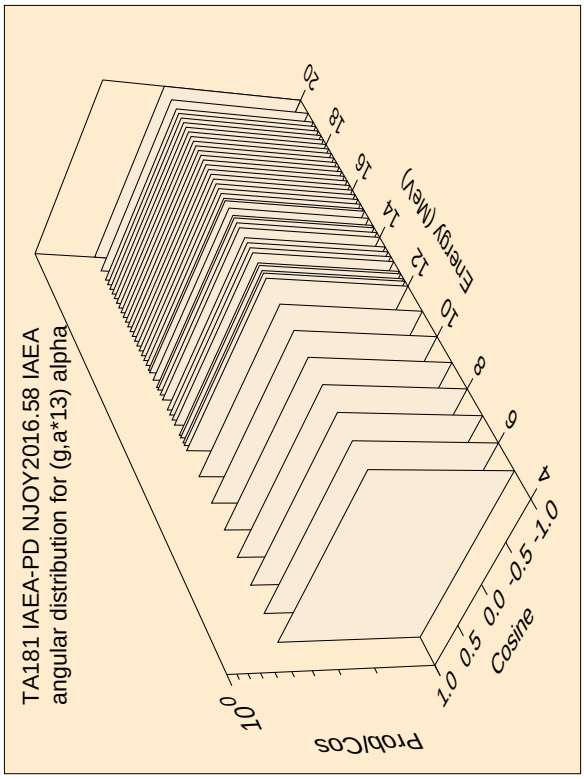
TA181 IAEA-PD NJOY2016.58 IAEA
angular distribution for (g,a*13) alpha
Prob/Cos
Cosine
Energy (MeV)

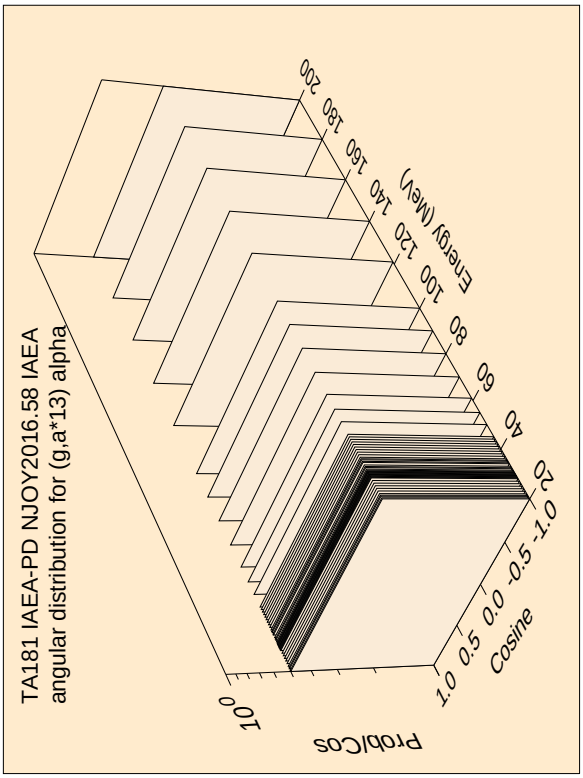
TA181 IAEA-PD NJOY2016.58 IAEA
angular distribution for (g,a*13) alpha
Prob/Cos
Cosine
Energy (MeV)

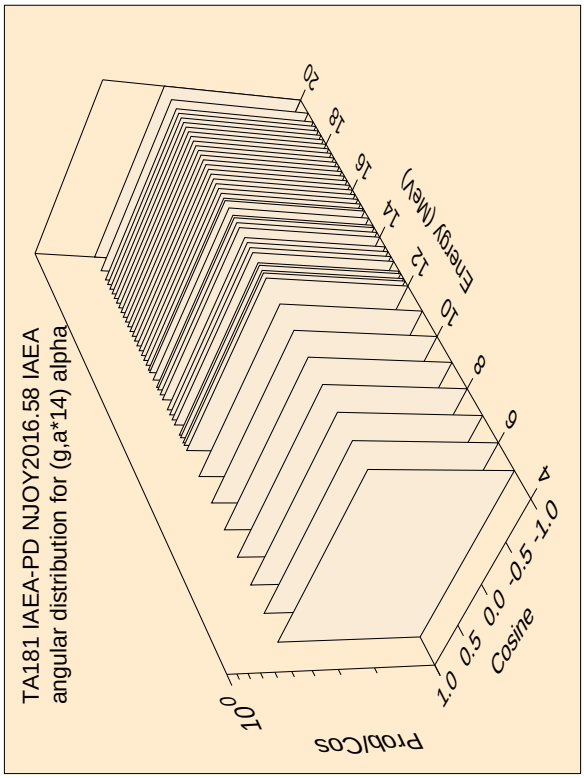
TA181 IAEA-PD NJOY2016.58 IAEA
angular distribution for (g,a*14) alpha
Prob/Cos
Cosine
Energy (MeV)

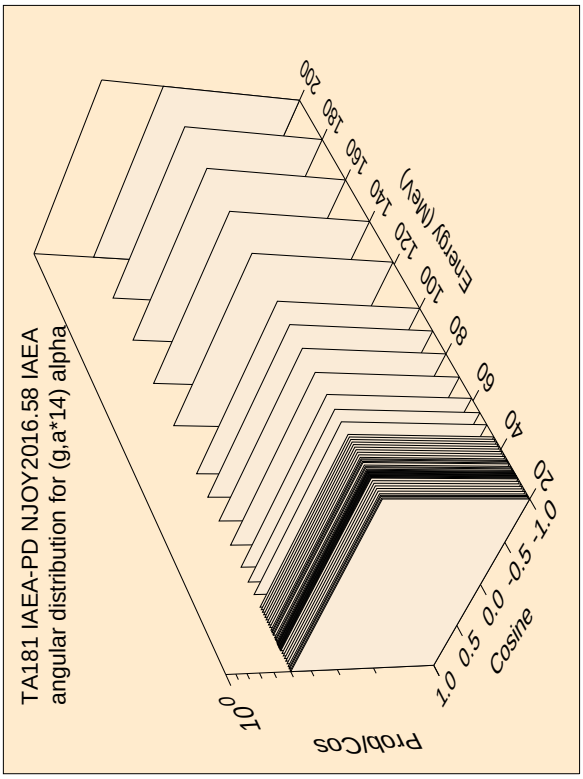
TA181 IAEA-PD NJOY2016.58 IAEA
angular distribution for (g,a*14) alpha
Prob/Cos
Cosine
Energy (MeV)

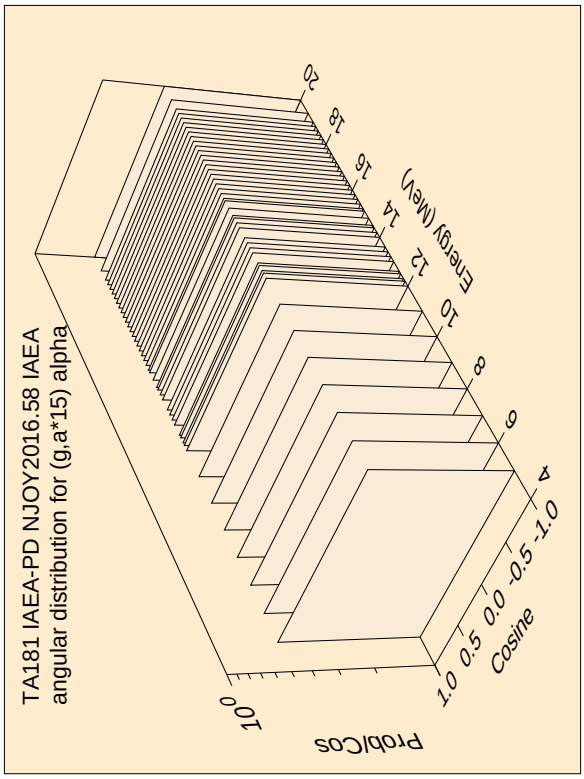
TA181 IAEA-PD NJOY2016.58 IAEA
angular distribution for (g,a*15) alpha
Prob/Cos
Cosine
Energy (MeV)

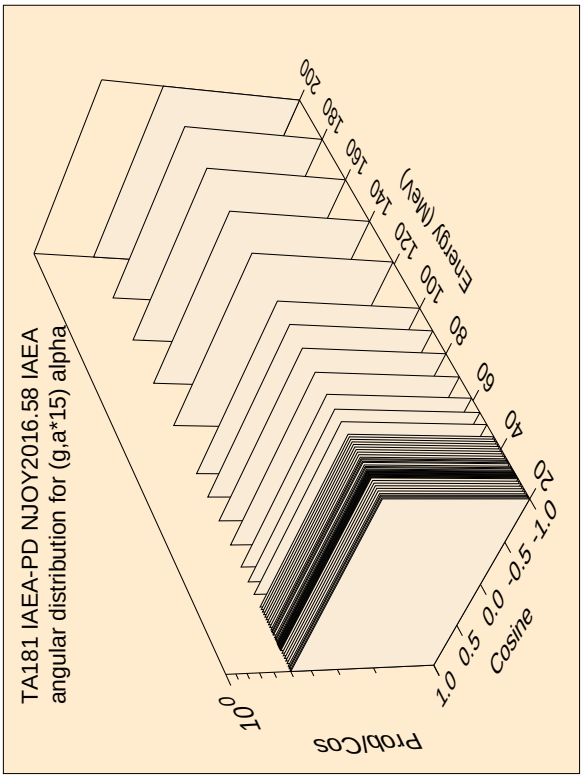
TA181 IAEA-PD NJOY2016.58 IAEA
angular distribution for (g,a*15) alpha
Prob/Cos
Cosine
Energy (MeV)

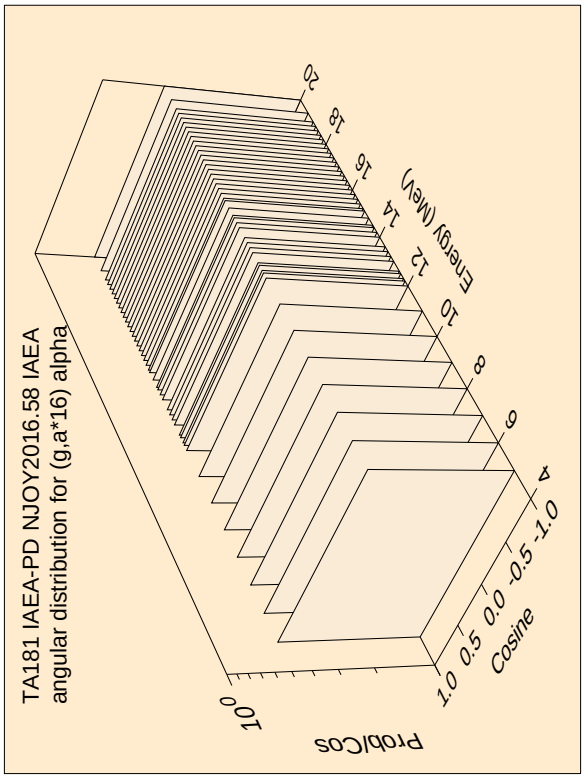
TA181 IAEA-PD NJOY2016.58 IAEA
angular distribution for (g,a*16) alpha
Prob/Cos
Cosine
Energy (MeV)

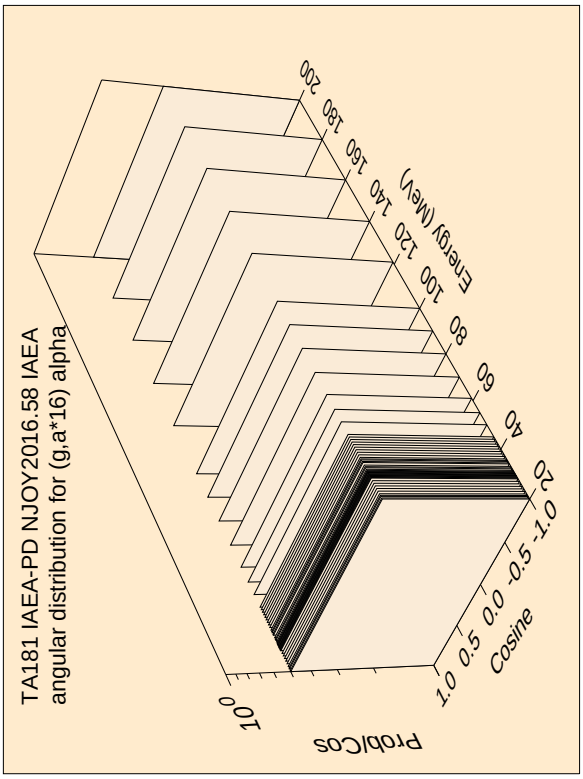
TA181 IAEA-PD NJOY2016.58 IAEA
angular distribution for (g,a*16) alpha
Prob/Cos
Cosine
Energy (MeV)

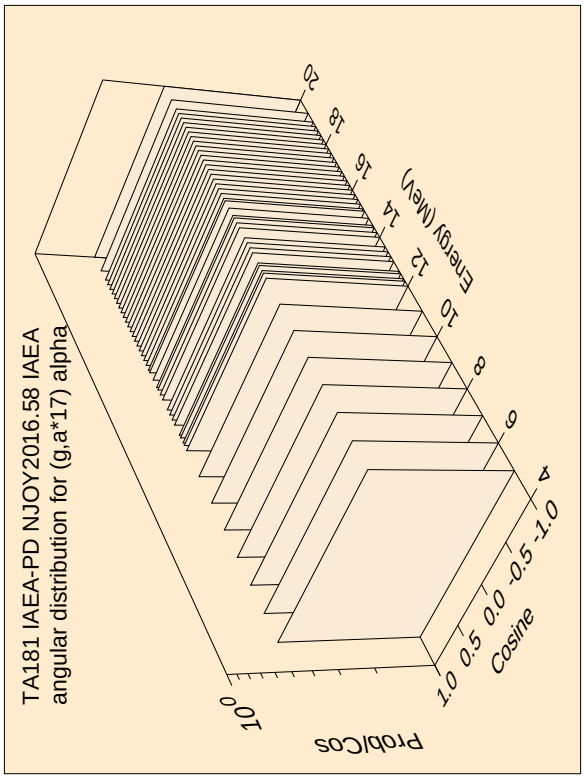
TA181 IAEA-PD NJOY2016.58 IAEA
angular distribution for (g,a*17) alpha
Prob/Cos
Cosine
Energy (MeV)

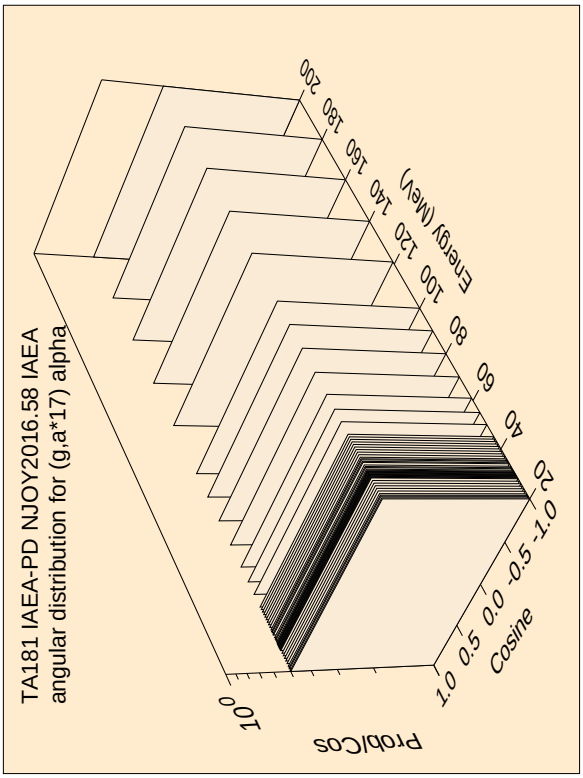
TA181 IAEA-PD NJOY2016.58 IAEA
angular distribution for (g,a*17) alpha
Prob/Cos
Cosine
Energy (MeV)

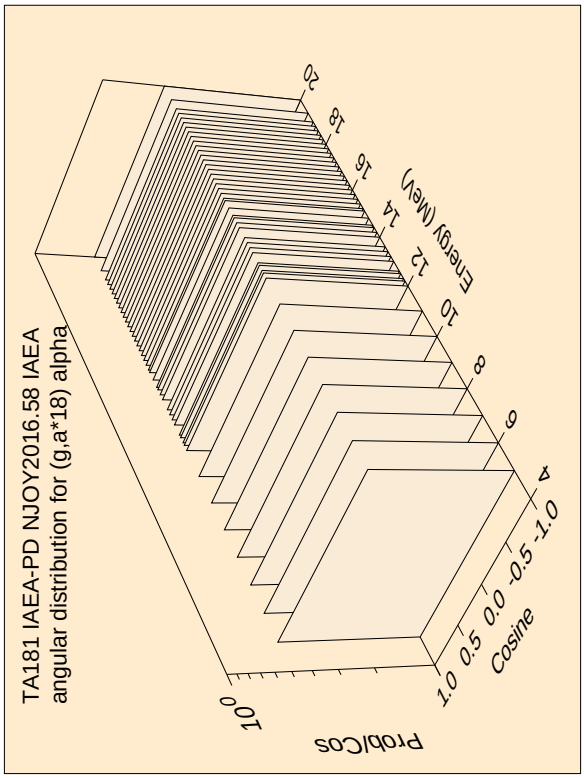
TA181 IAEA-PD NJOY2016.58 IAEA
angular distribution for (g,a*18) alpha
Prob/Cos
Cosine
Energy (MeV)

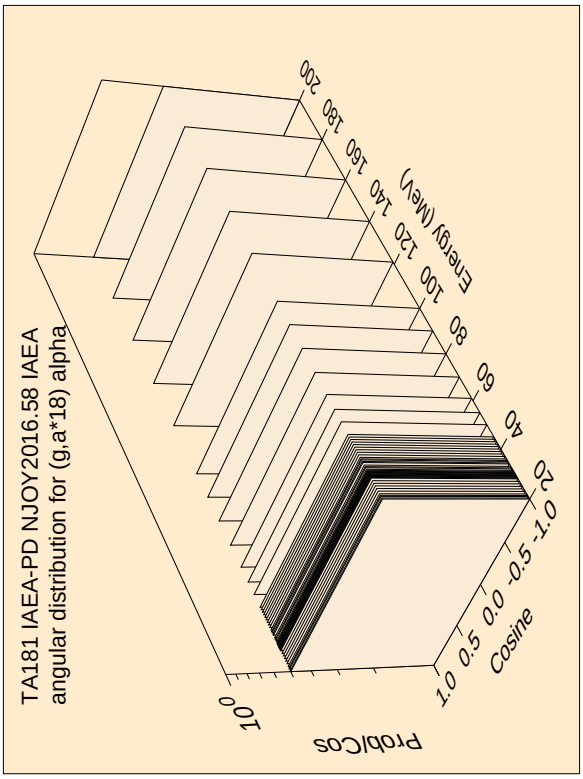
TA181 IAEA-PD NJOY2016.58 IAEA
angular distribution for (g,a*18) alpha
Prob/Cos
Cosine
Energy (MeV)

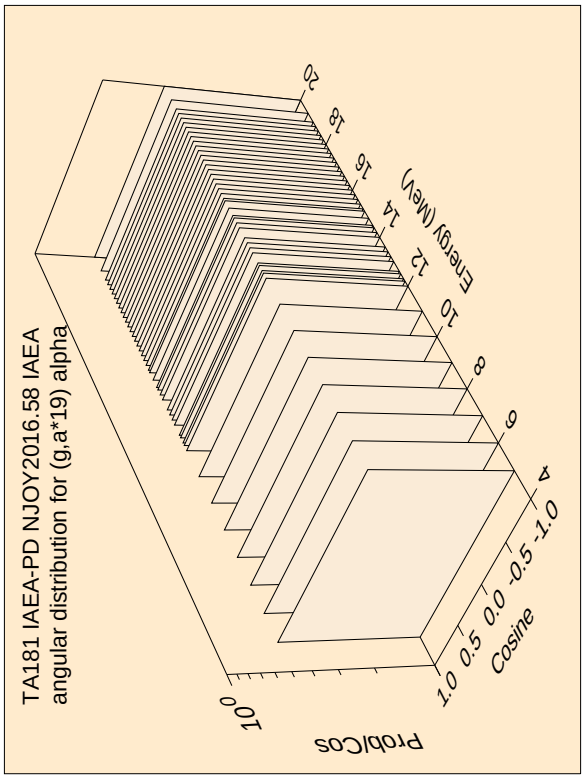
TA181 IAEA-PD NJOY2016.58 IAEA
angular distribution for (g,a*19) alpha
Prob/Cos
Cosine
Energy (MeV)

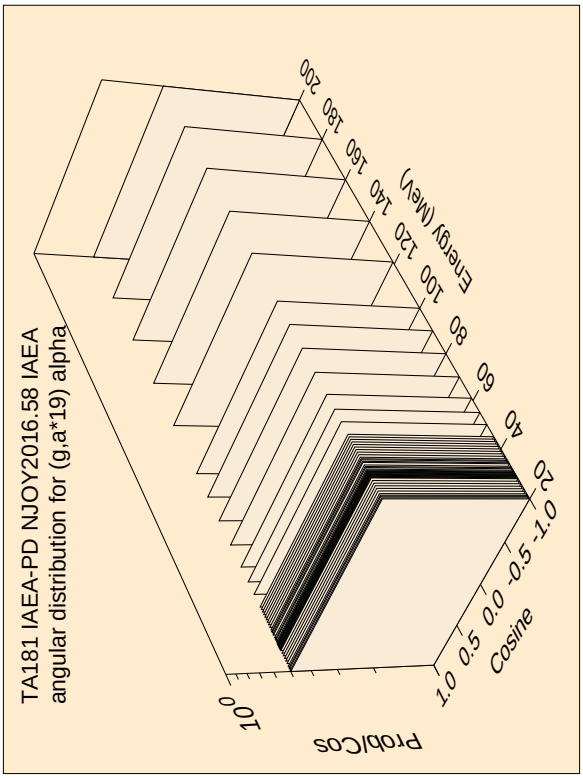
TA181 IAEA-PD NJOY2016.58 IAEA
angular distribution for (g,a*19) alpha
Prob/Cos
Cosine
Energy (MeV)

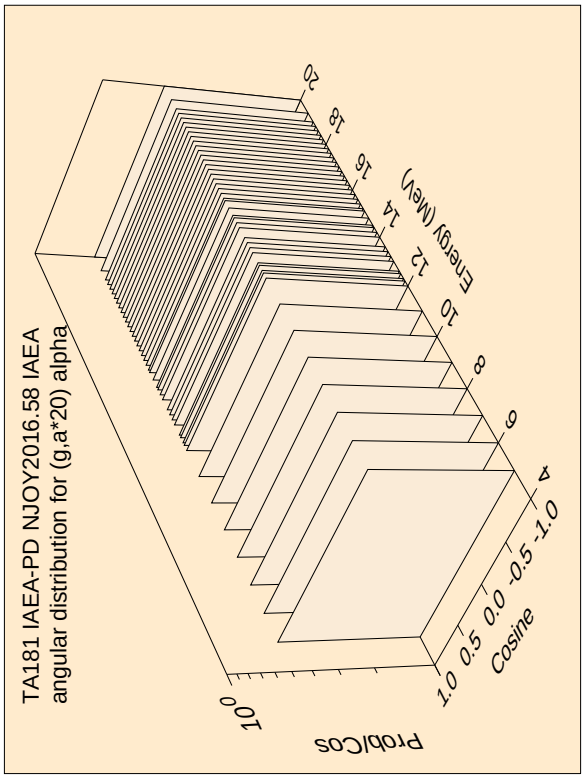
TA181 IAEA-PD NJOY2016.58 IAEA
angular distribution for (g,a*20) alpha
Prob/Cos
Cosine
Energy (MeV)

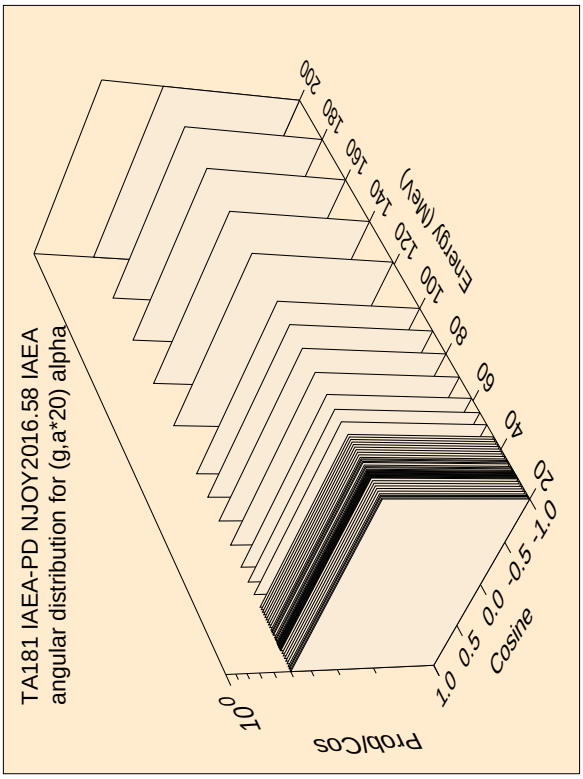
TA181 IAEA-PD NJOY2016.58 IAEA
angular distribution for (g,a*20) alpha
Prob/Cos
Cosine
Energy (MeV)

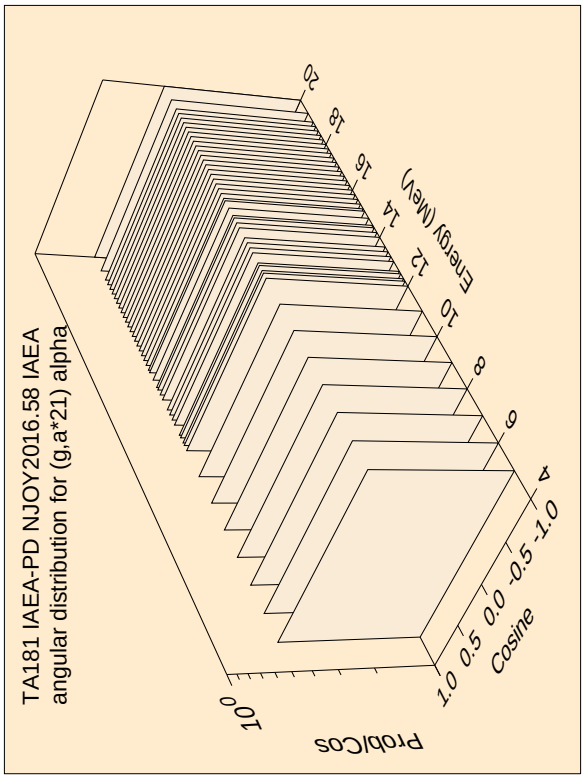
TA181 IAEA-PD NJOY2016.58 IAEA
angular distribution for (g,a*21) alpha
Prob/Cos
Cosine
Energy (MeV)

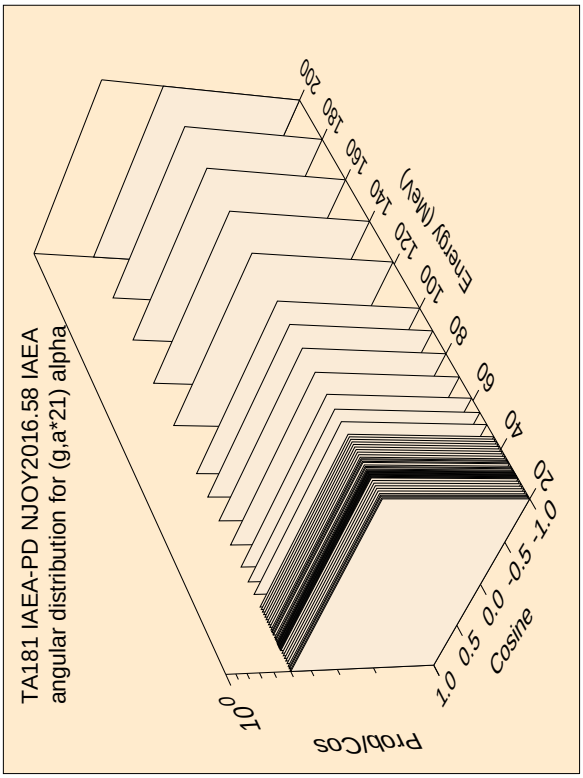
TA181 IAEA-PD NJOY2016.58 IAEA
angular distribution for (g,a*21) alpha
Prob/Cos
Cosine
Energy (MeV)

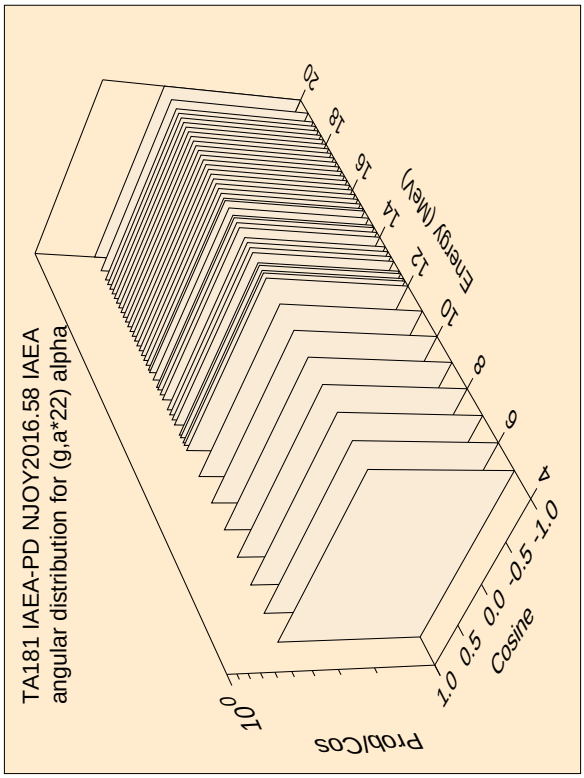
TA181 IAEA-PD NJOY2016.58 IAEA
angular distribution for (g,a*22) alpha
Prob/Cos
Cosine
Energy (MeV)

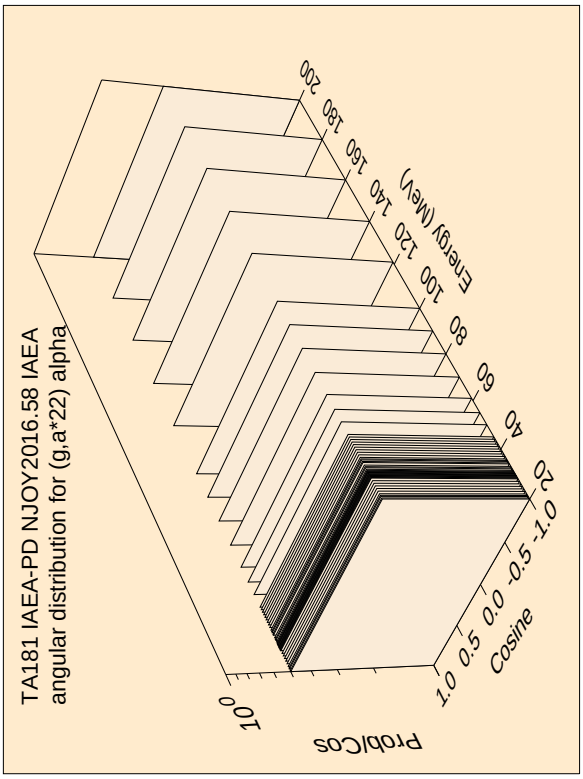
TA181 IAEA-PD NJOY2016.58 IAEA
angular distribution for (g,a*22) alpha
Prob/Cos
Cosine
Energy (MeV)

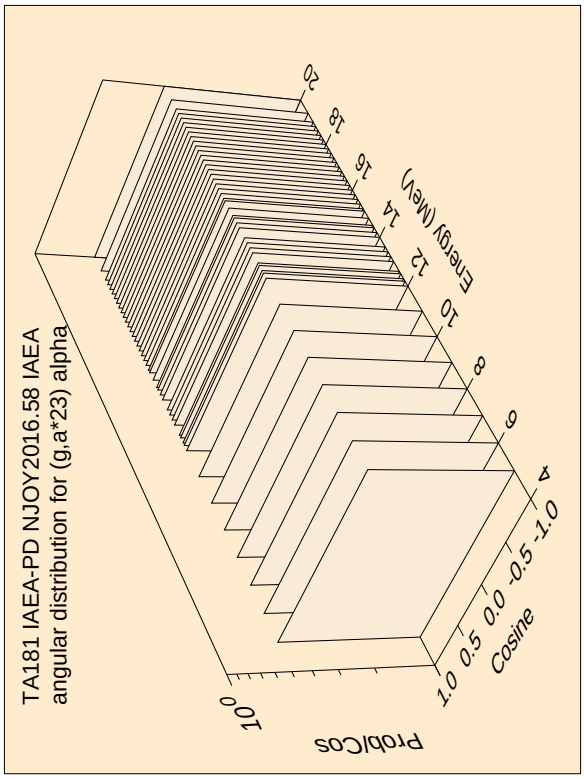
TA181 IAEA-PD NJOY2016.58 IAEA
angular distribution for (g,a*23) alpha
Prob/Cos
Cosine
Energy (MeV)

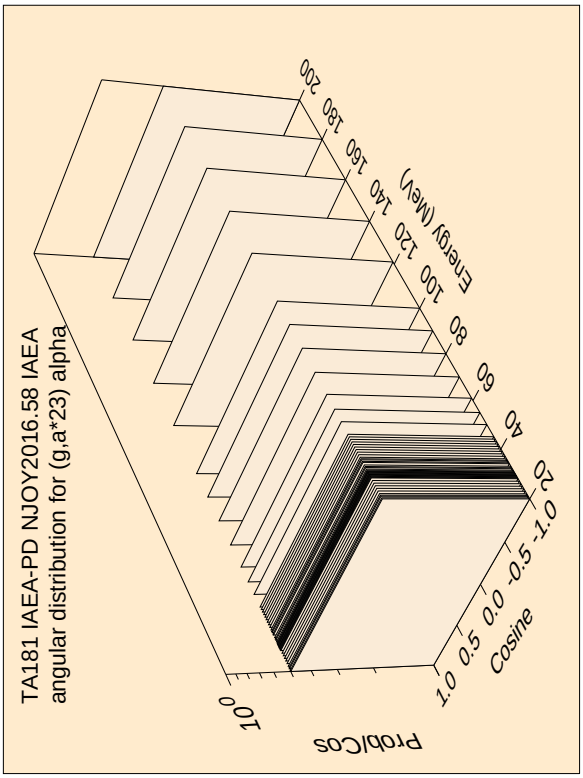
TA181 IAEA-PD NJOY2016.58 IAEA
angular distribution for (g,a*23) alpha
Prob/Cos
Cosine
Energy (MeV)

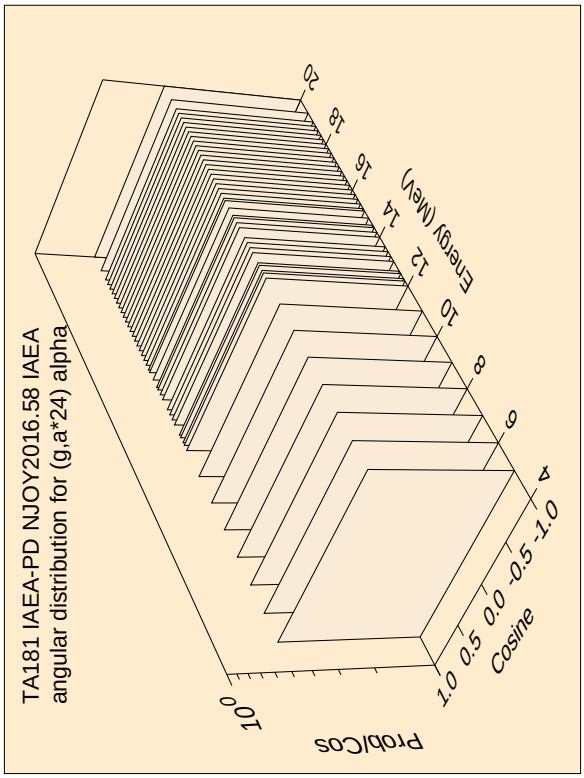
TA181 IAEA-PD NJOY2016.58 IAEA
angular distribution for (g,a*24) alpha
Prob/Cos
Cosine
Energy (MeV)

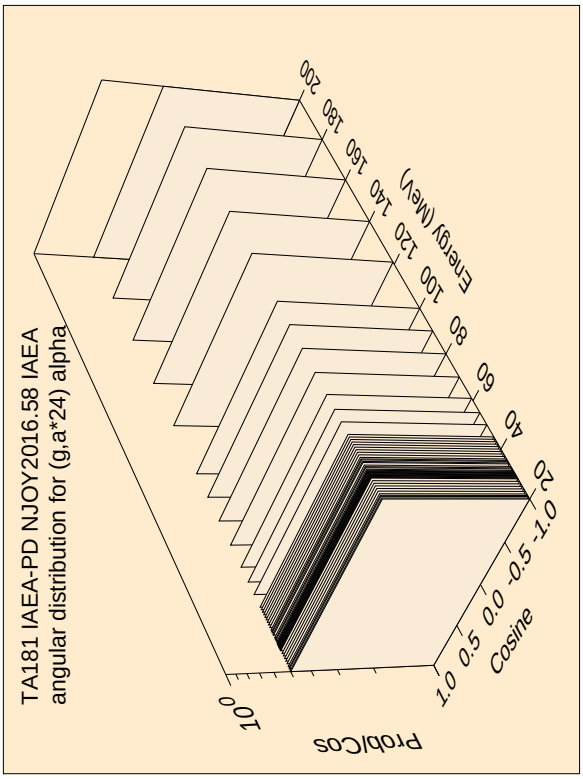
TA181 IAEA-PD NJOY2016.58 IAEA
angular distribution for (g,a*24) alpha
Prob/Cos
Cosine
Energy (MeV)

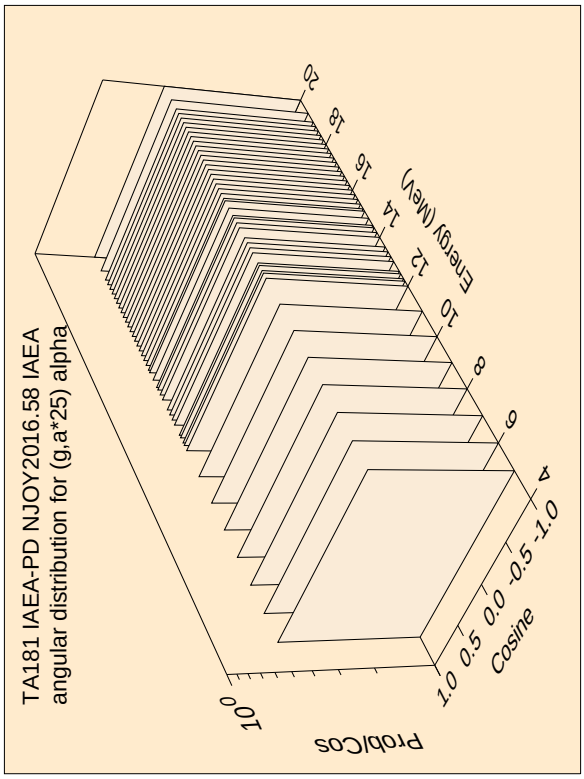
TA181 IAEA-PD NJOY2016.58 IAEA
angular distribution for (g,a*25) alpha
Prob/Cos
Cosine
Energy (MeV)

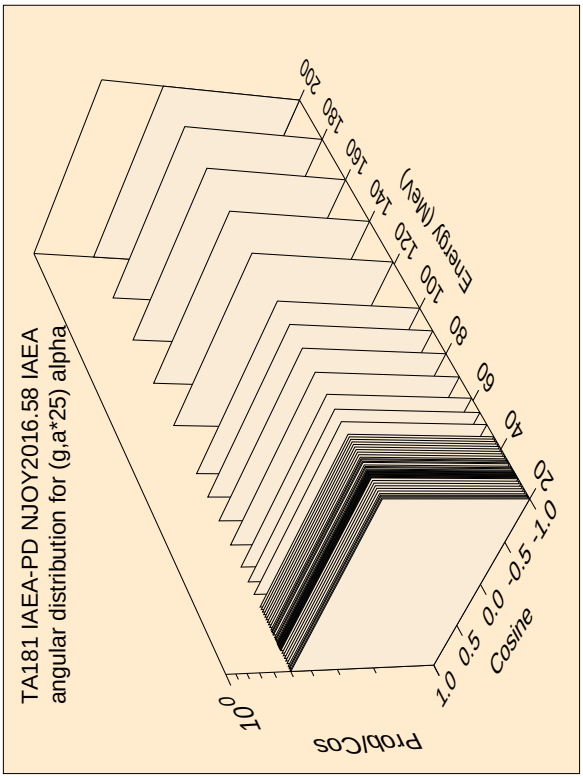
TA181 IAEA-PD NJOY2016.58 IAEA
angular distribution for (g,a*25) alpha
Prob/Cos
Cosine
Energy (MeV)

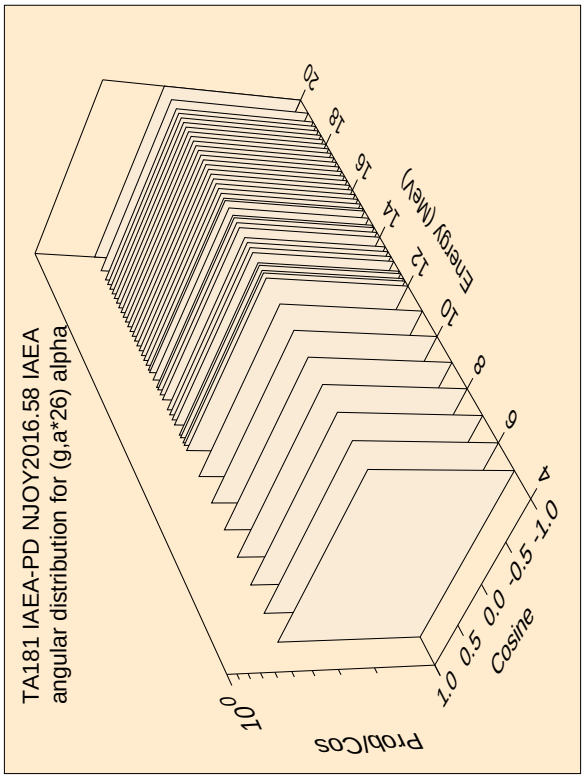
TA181 IAEA-PD NJOY2016.58 IAEA
angular distribution for (g,a*26) alpha
Prob/Cos
Cosine
Energy (MeV)

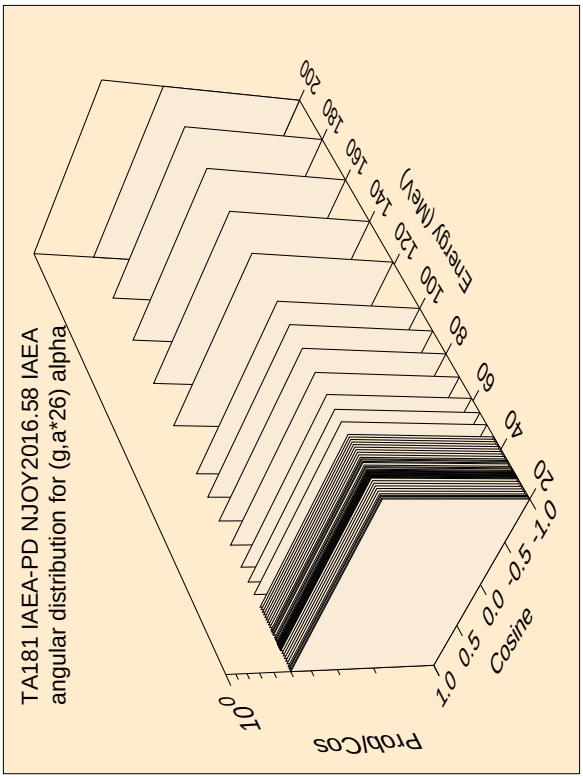
TA181 IAEA-PD NJOY2016.58 IAEA
angular distribution for (g,a*26) alpha
Prob/Cos
Cosine
Energy (MeV)

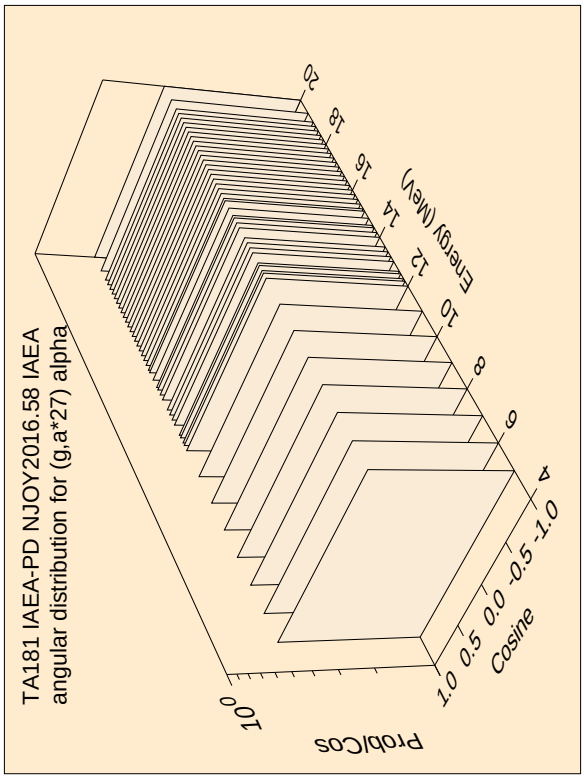
TA181 IAEA-PD NJOY2016.58 IAEA
angular distribution for (g,a*27) alpha
Prob/Cos
Cosine
Energy (MeV)

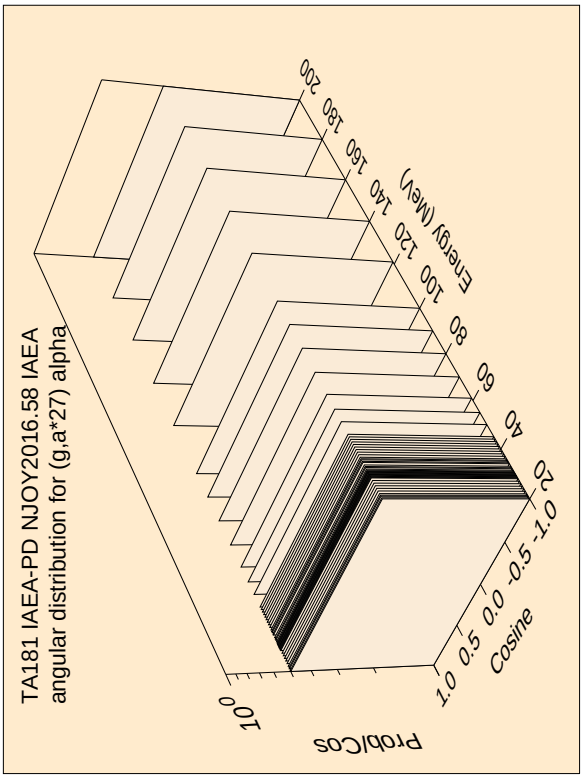
TA181 IAEA-PD NJOY2016.58 IAEA
angular distribution for (g,a*27) alpha
Prob/Cos
Cosine
Energy (MeV)

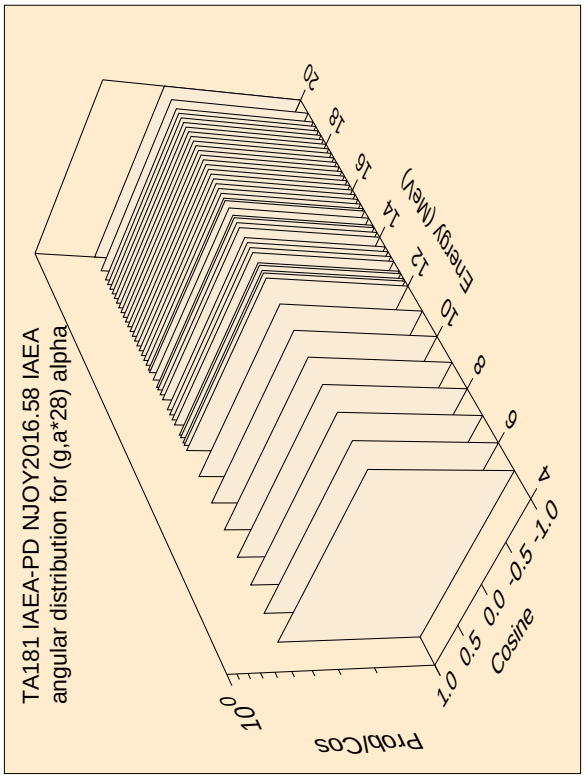
TA181 IAEA-PD NJOY2016.58 IAEA
angular distribution for (g,a*28) alpha
Prob/Cos
Cosine
Energy (MeV)

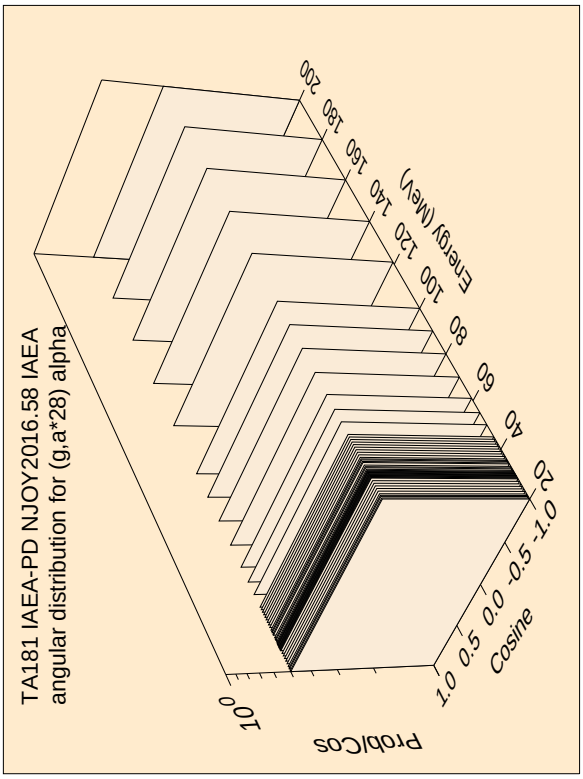
TA181 IAEA-PD NJOY2016.58 IAEA
angular distribution for (g,a*28) alpha
Prob/Cos
Cosine
Energy (MeV)

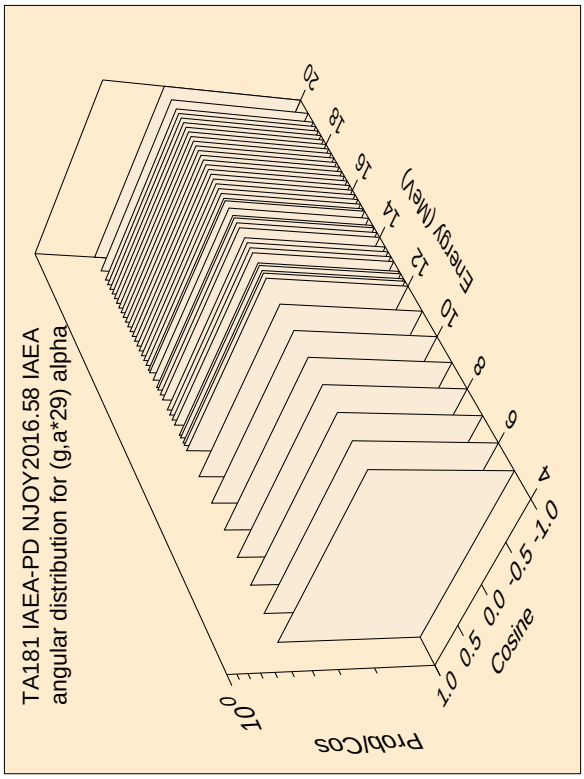
TA181 IAEA-PD NJOY2016.58 IAEA
angular distribution for (g,a*29) alpha
Prob/Cos
Cosine
Energy (MeV)

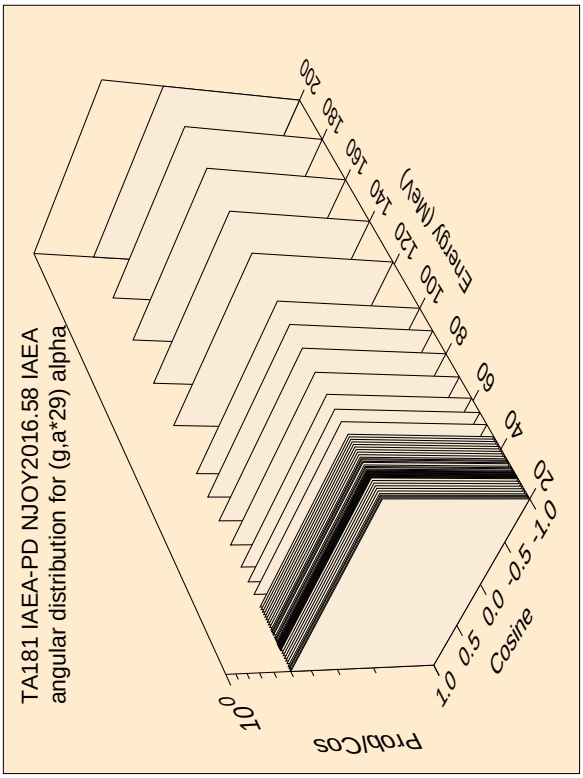
TA181 IAEA-PD NJOY2016.58 IAEA
angular distribution for (g,a*29) alpha
Prob/Cos
Cosine
Energy (MeV)

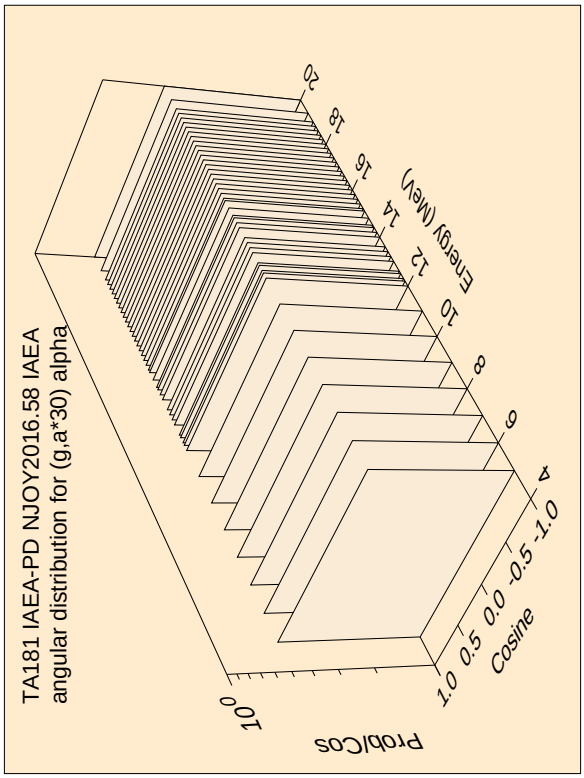
TA181 IAEA-PD NJOY2016.58 IAEA
angular distribution for (g,a*30) alpha
Prob/Cos
Cosine
Energy (MeV)

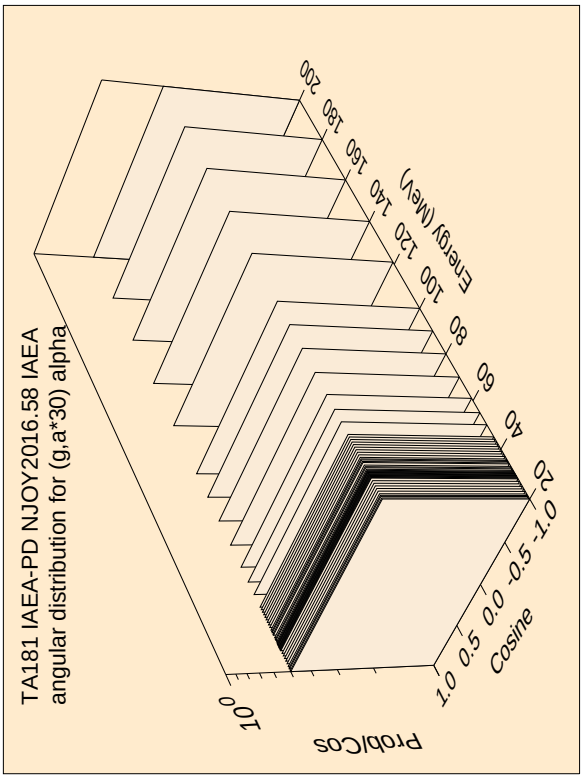
TA181 IAEA-PD NJOY2016.58 IAEA
angular distribution for (g,a*30) alpha
Prob/Cos
Cosine
Energy (MeV)

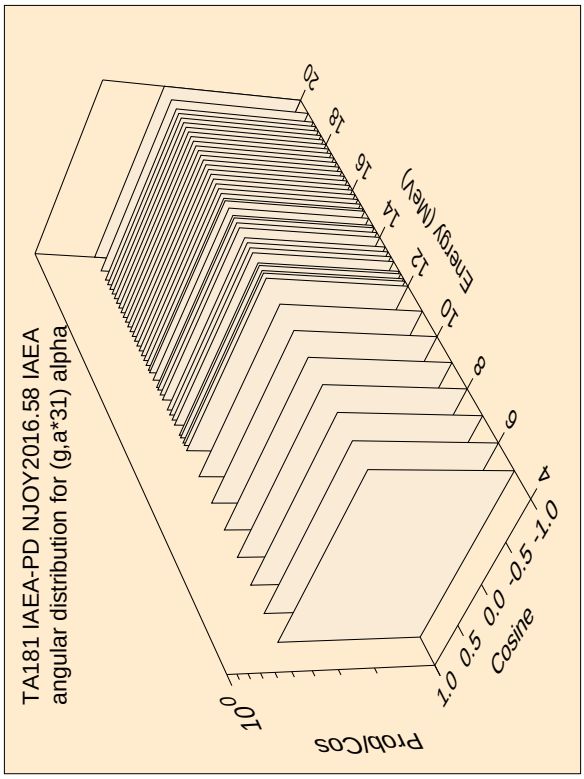
TA181 IAEA-PD NJOY2016.58 IAEA
angular distribution for (g,a*31) alpha
Prob/Cos
Cosine
Energy (MeV)

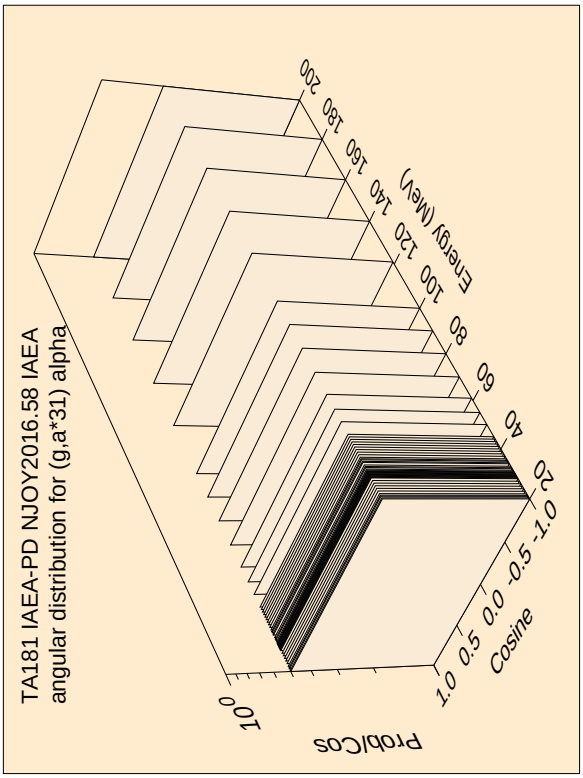
TA181 IAEA-PD NJOY2016.58 IAEA
angular distribution for (g,a*31) alpha
Prob/Cos
Cosine
Energy (MeV)

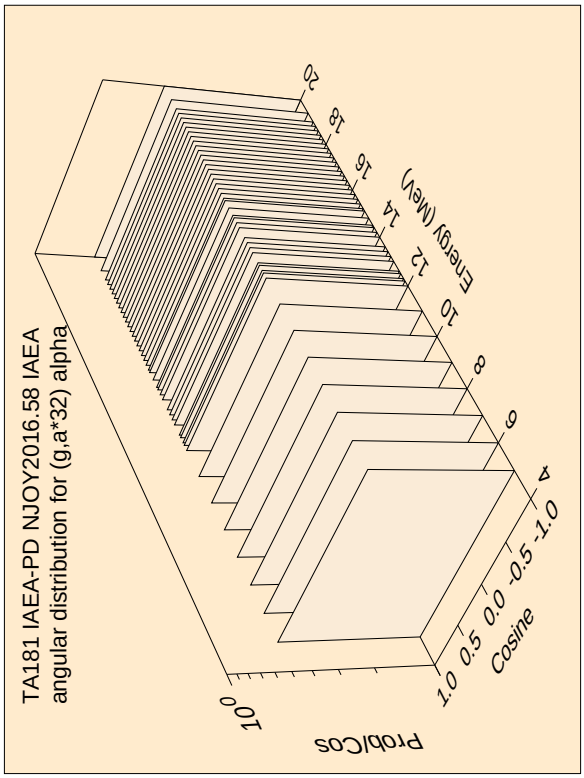
TA181 IAEA-PD NJOY2016.58 IAEA
angular distribution for (g,a*32) alpha
Prob/Cos
Cosine
Energy (MeV)

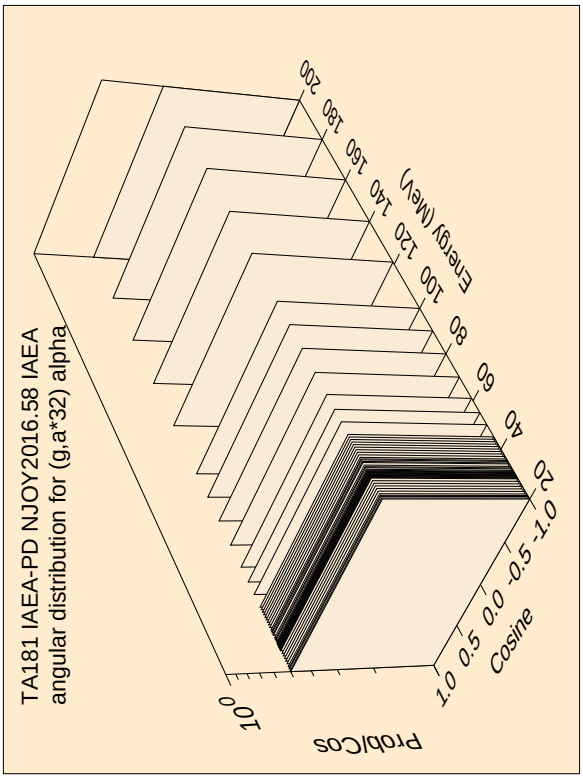
TA181 IAEA-PD NJOY2016.58 IAEA
angular distribution for (g,a*32) alpha
Prob/Cos
Cosine
Energy (MeV)

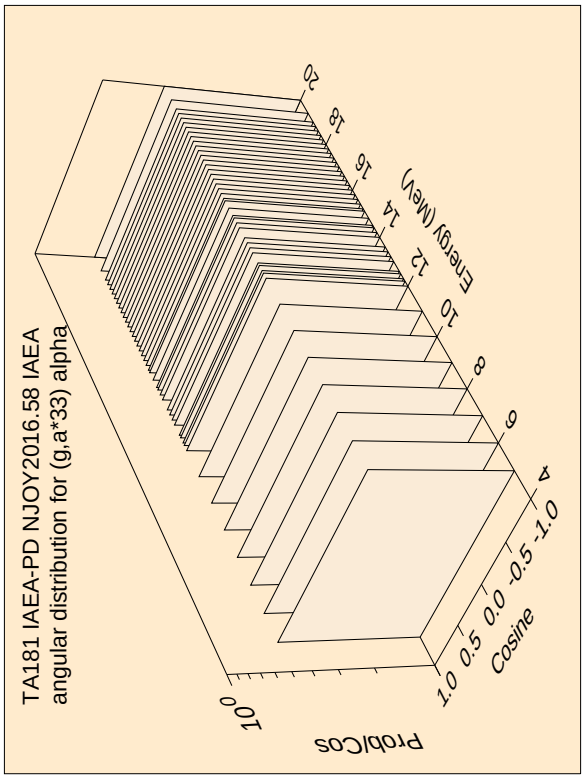
TA181 IAEA-PD NJOY2016.58 IAEA
angular distribution for (g,a*33) alpha
Prob/Cos
Cosine
Energy (MeV)

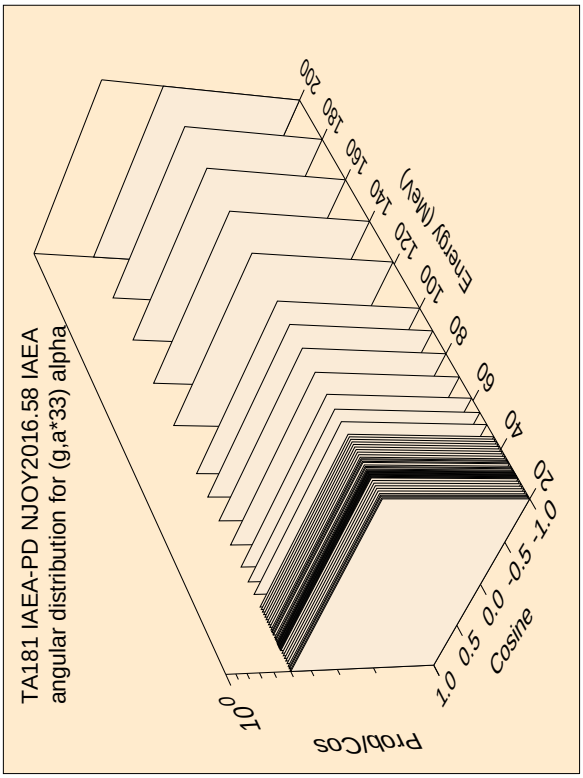
TA181 IAEA-PD NJOY2016.58 IAEA
angular distribution for (g,a*33) alpha
Prob/Cos
Cosine
Energy (MeV)

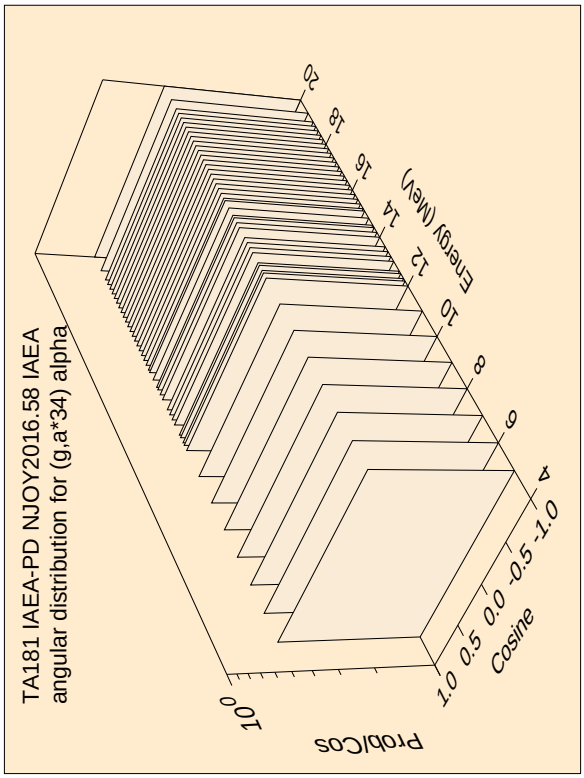
TA181 IAEA-PD NJOY2016.58 IAEA
angular distribution for (g,a*34) alpha
Prob/Cos
Cosine
Energy (MeV)

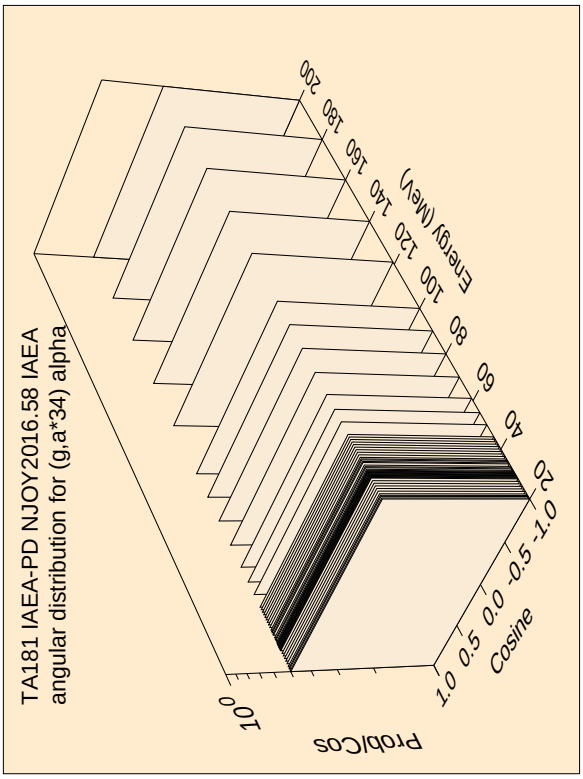
TA181 IAEA-PD NJOY2016.58 IAEA
angular distribution for (g,a*34) alpha
Prob/Cos
Cosine
Energy (MeV)

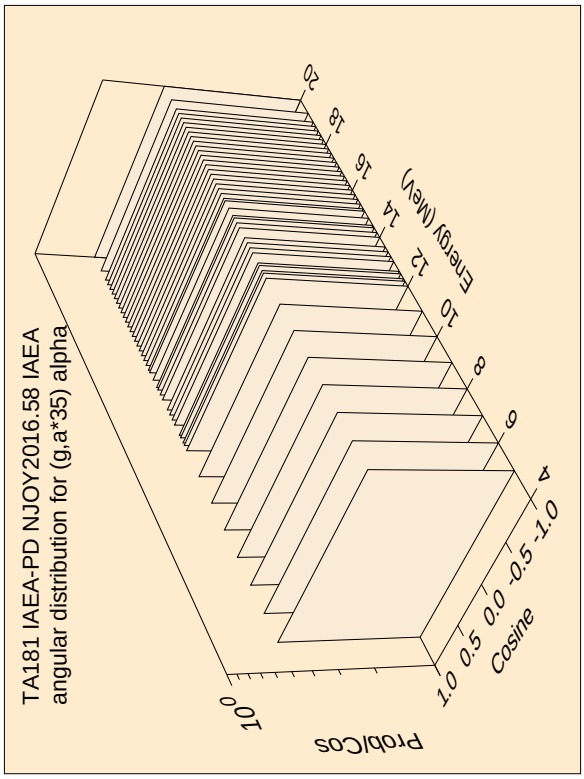
TA181 IAEA-PD NJOY2016.58 IAEA
angular distribution for (g,a*35) alpha
Prob/Cos
Cosine
Energy (MeV)

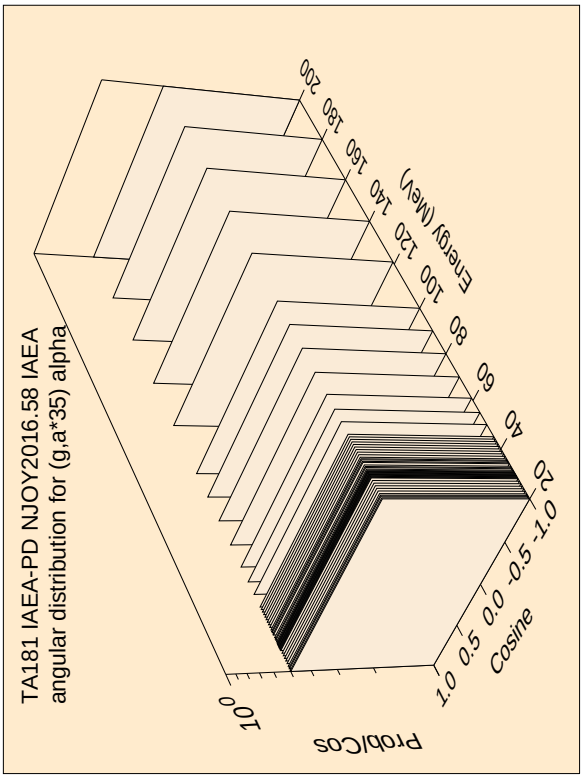
TA181 IAEA-PD NJOY2016.58 IAEA
angular distribution for (g,a*35) alpha
Prob/Cos
Energy (MeV)
Cosine

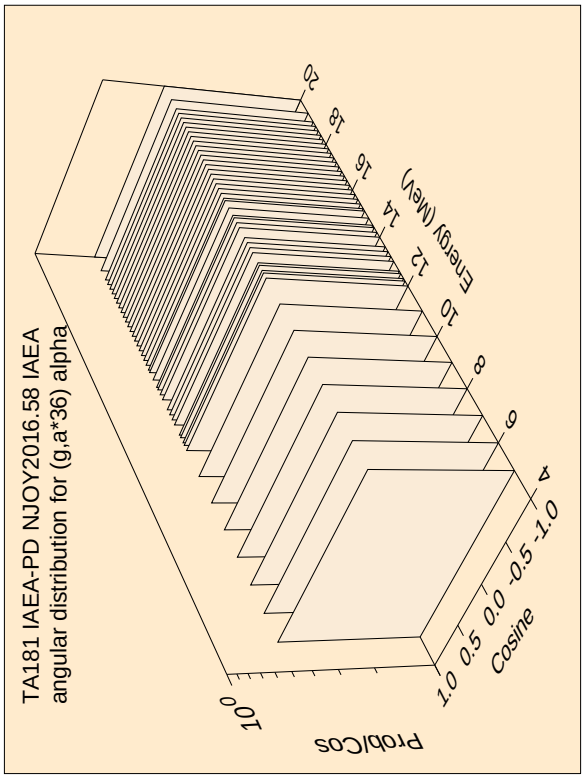
TA181 IAEA-PD NJOY2016.58 IAEA
angular distribution for (g,a*36) alpha
Prob/Cos
Energy (MeV)
Cosine

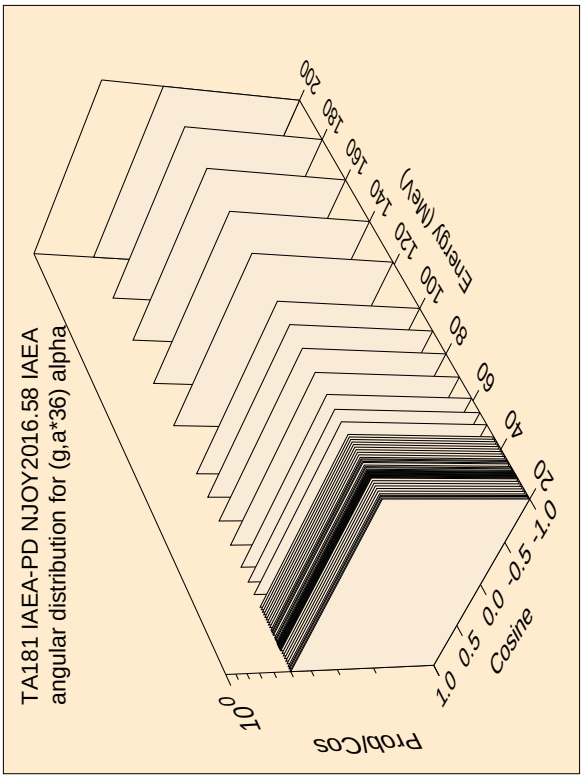
TA181 IAEA-PD NJOY2016.58 IAEA
angular distribution for (g,a*36) alpha
Prob/Cos
Energy (MeV)
Cosine

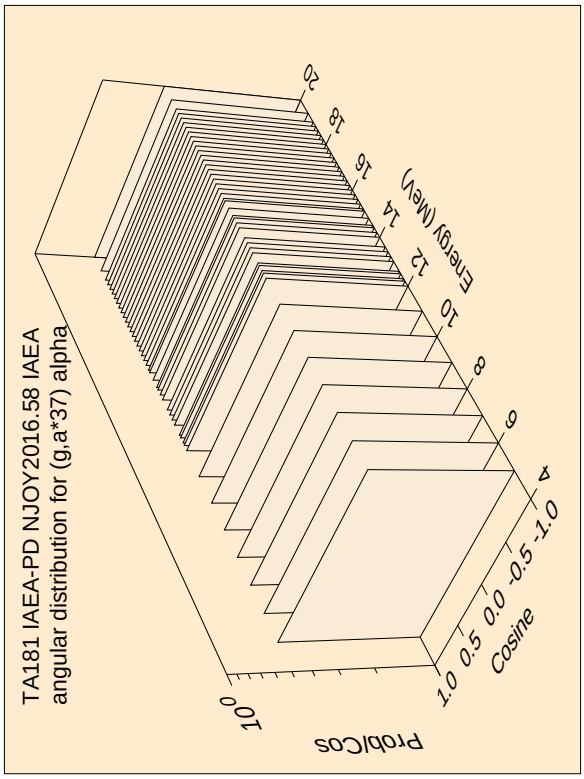
TA181 IAEA-PD NJOY2016.58 IAEA
angular distribution for (g,a*37) alpha
Prob/Cos
Energy (MeV)
Cosine

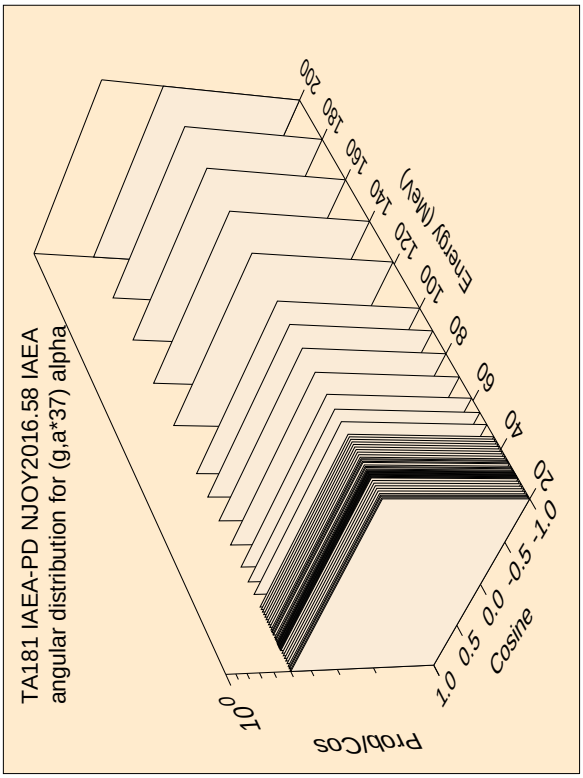
TA181 IAEA-PD NJOY2016.58 IAEA
angular distribution for (g,a*37) alpha
Prob/Cos
Cosine
Energy (MeV)

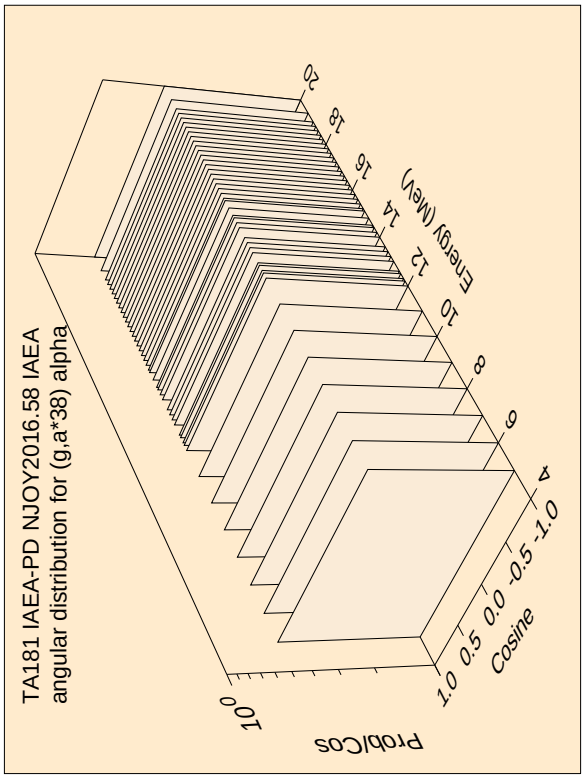
TA181 IAEA-PD NJOY2016.58 IAEA
angular distribution for (g,a*38) alpha
Prob/Cos
Cosine
Energy (MeV)

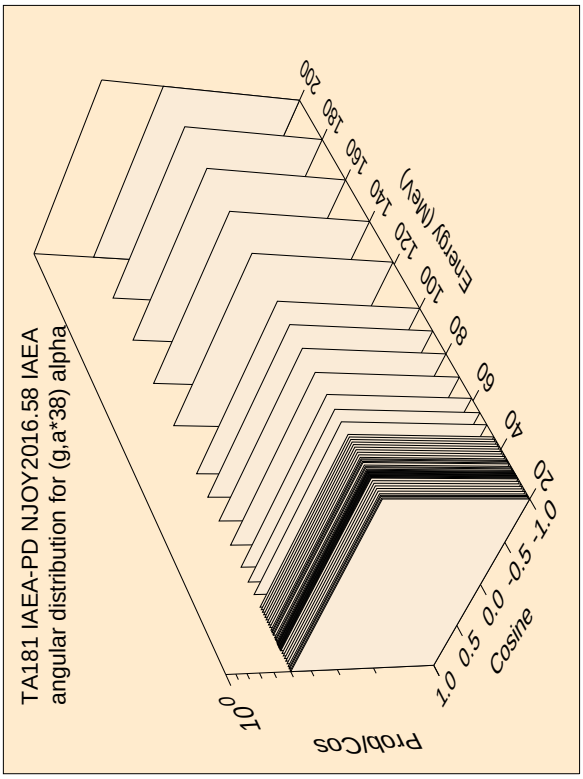
TA181 IAEA-PD NJOY2016.58 IAEA
angular distribution for (g,a*38) alpha
Prob/Cos
Cosine
Energy (MeV)

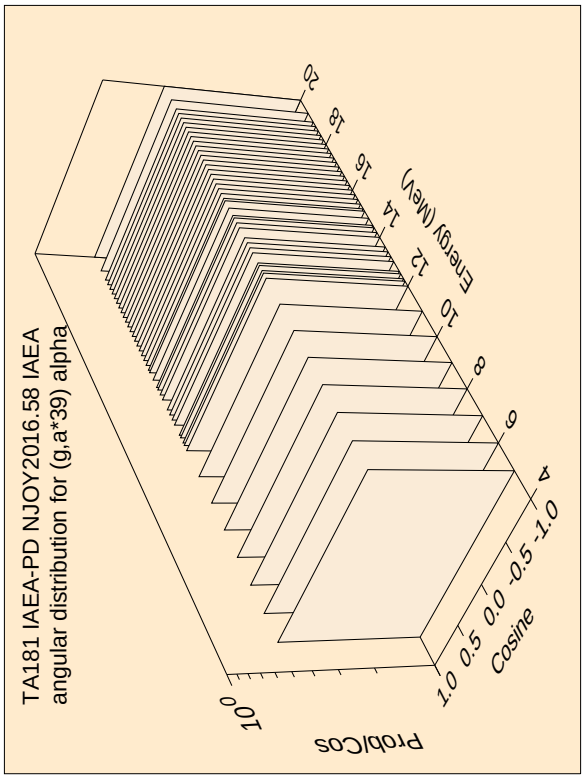
TA181 IAEA-PD NJOY2016.58 IAEA
angular distribution for (g,a*39) alpha
Prob/Cos
Cosine
Energy (MeV)

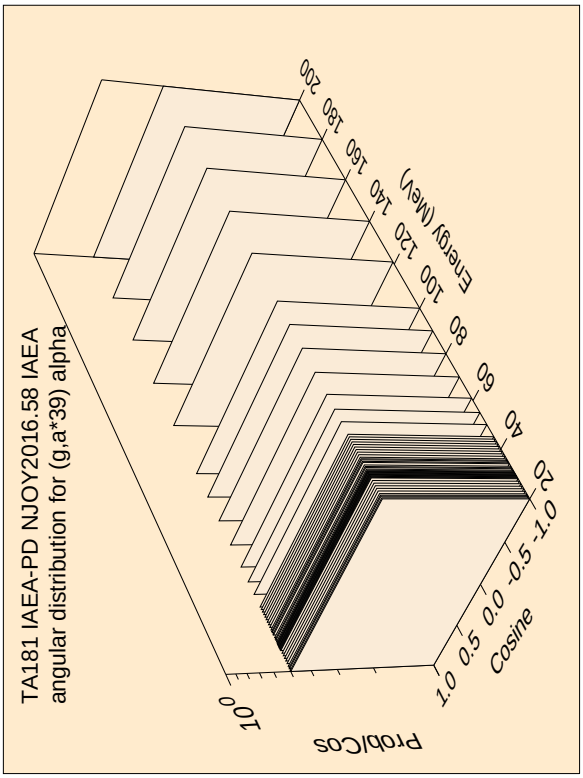
TA181 IAEA-PD NJOY2016.58 IAEA
angular distribution for (g,a*39) alpha
Prob/Cos
Cosine
Energy (MeV)

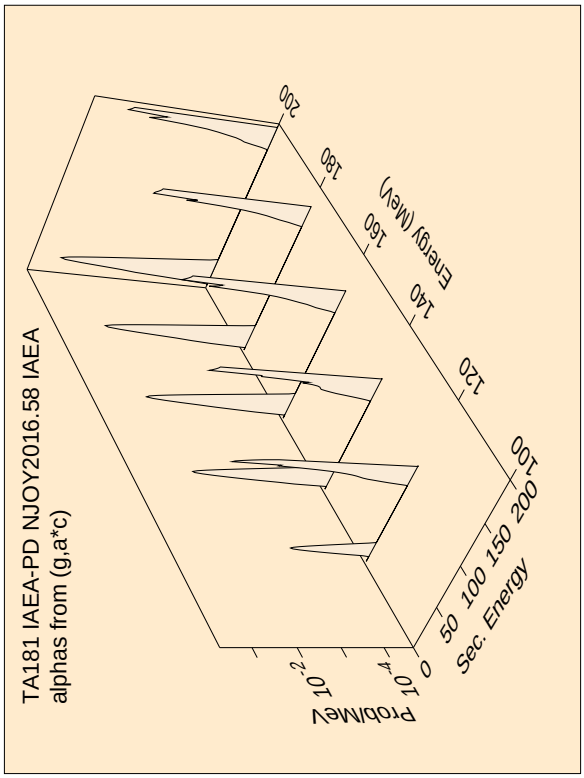
TA181 IAEA-PD NJOY2016.58 IAEA
alphas from (g,a*c)
Prob/MeV
Sec. Energy
Energy (MeV)

A.6.2 Activation Library

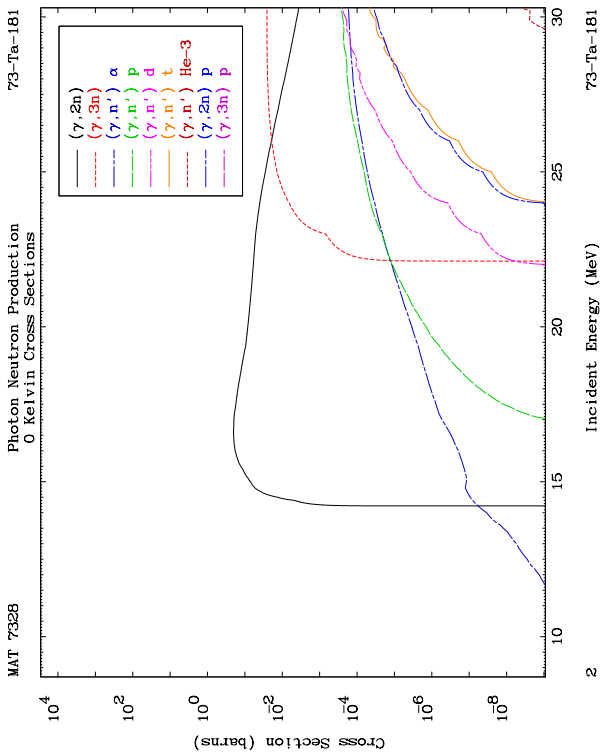

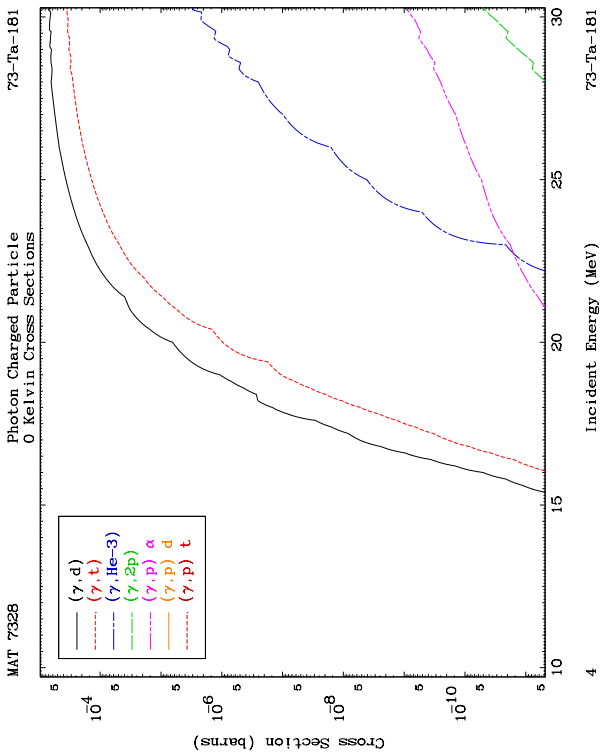

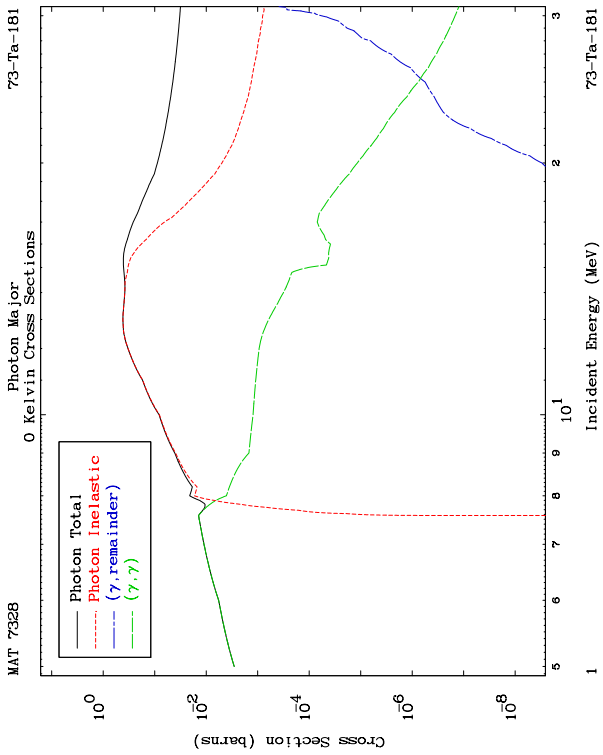

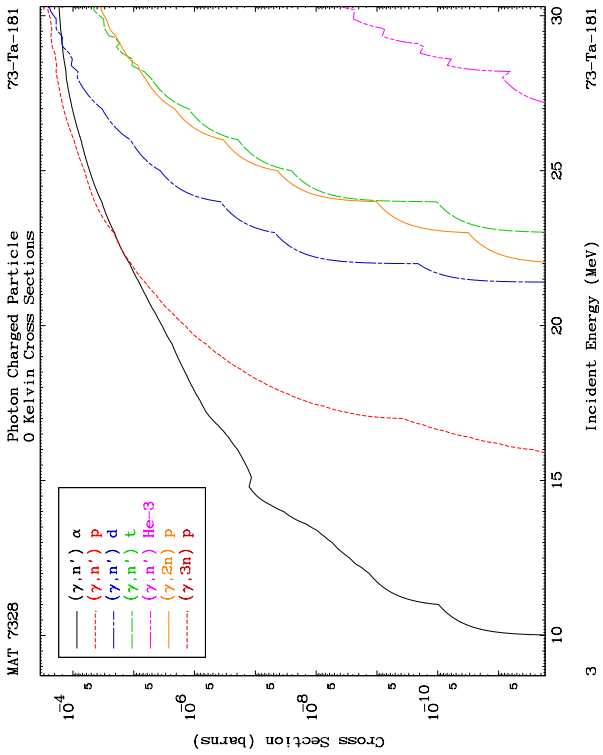

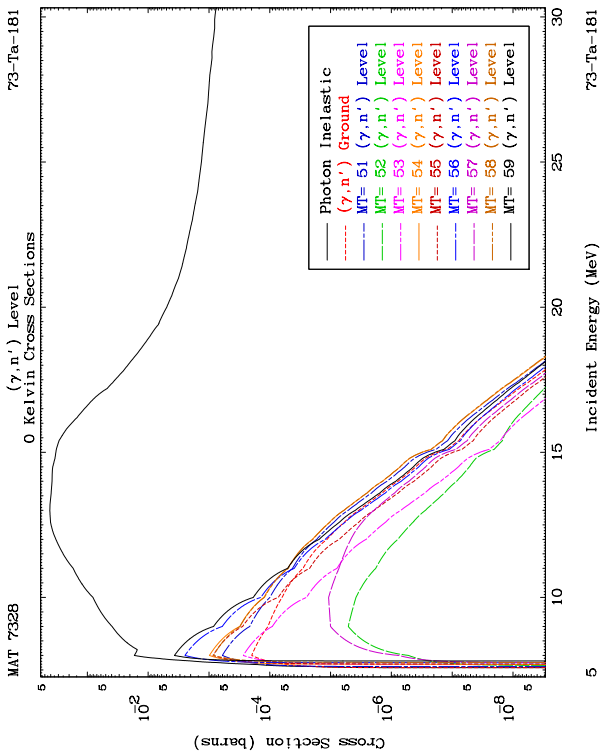
MAT 7328
(γ,n') Level
0 Kelvin Cross Sections
73-Ta-181
Photon Inelastic
(γ,n') Ground
MT= 51 (γ,n') Level
MT= 52 (γ,n') Level
MT= 53 (γ,n') Level
MT= 54 (γ,n') Level
MT= 55 (γ,n') Level
MT= 56 (γ,n') Level
MT= 57 (γ,n') Level
MT= 58 (γ,n') Level
MT= 59 (γ,n') Level
Cross Section (barns)
Incident Energy (MeV)

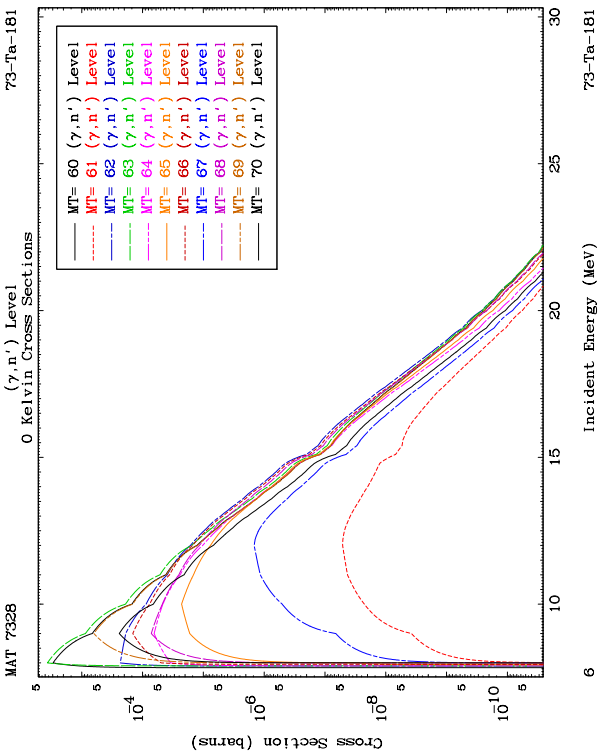
MAT 7328
(γ,n') Level
0 Kelvin Cross Sections
73-Ta-181
MT= 60 (γ,n') Level
MT= 61 (γ,n') Level
MT= 62 (γ,n') Level
MT= 63 (γ,n') Level
MT= 64 (γ,n') Level
MT= 65 (γ,n') Level
MT= 66 (γ,n') Level
MT= 67 (γ,n') Level
MT= 68 (γ,n') Level
MT= 69 (γ,n') Level
MT= 70 (γ,n') Level
Cross Section (barns)
Incident Energy (MeV)

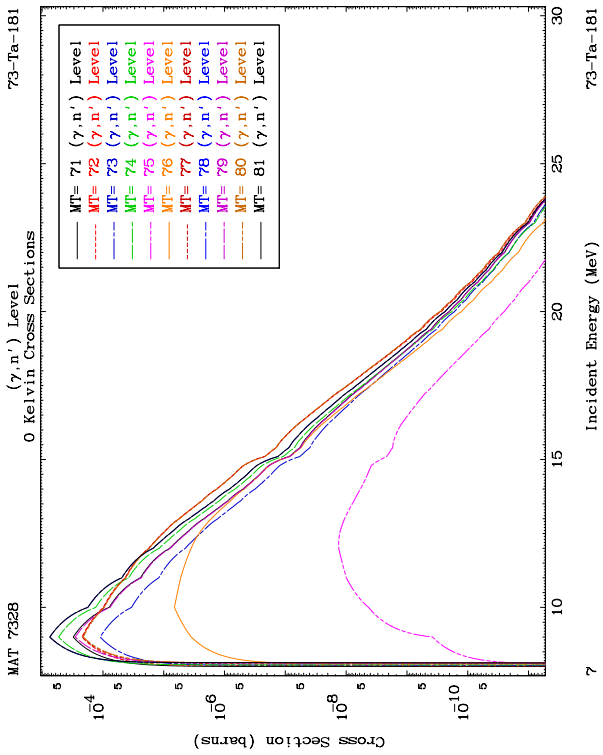
MAT 7328
(γ,n') Level
0 Kelvin Cross Sections
73-Ta-181
MT= 71 (γ,n') Level
MT= 72 (γ,n') Level
MT= 73 (γ,n') Level
MT= 74 (γ,n') Level
MT= 75 (γ,n') Level
MT= 76 (γ,n') Level
MT= 77 (γ,n') Level
MT= 78 (γ,n') Level
MT= 79 (γ,n') Level
MT= 80 (γ,n') Level
MT= 81 (γ,n') Level
Cross Section (barns)
Incident Energy (MeV)

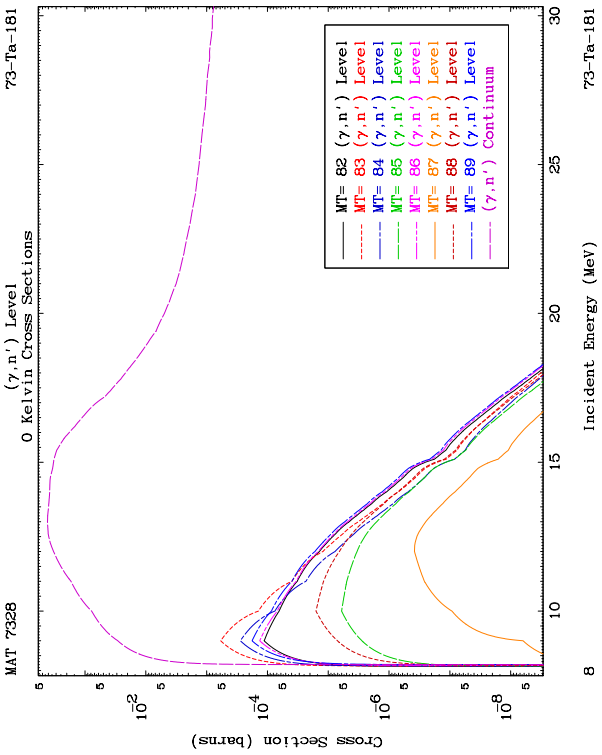
MAT 7328
(γ,n') Level
0 Kelvin Cross Sections
73-Ta-181
MT= 82 (γ,n') Level
MT= 83 (γ,n') Level
MT= 84 (γ,n') Level
MT= 85 (γ,n') Level
MT= 86 (γ,n') Level
MT= 87 (γ,n') Level
MT= 88 (γ,n') Level
MT= 89 (γ,n') Level
(γ,n') Continuum
Cross Section (barns)
Incident Energy (MeV)

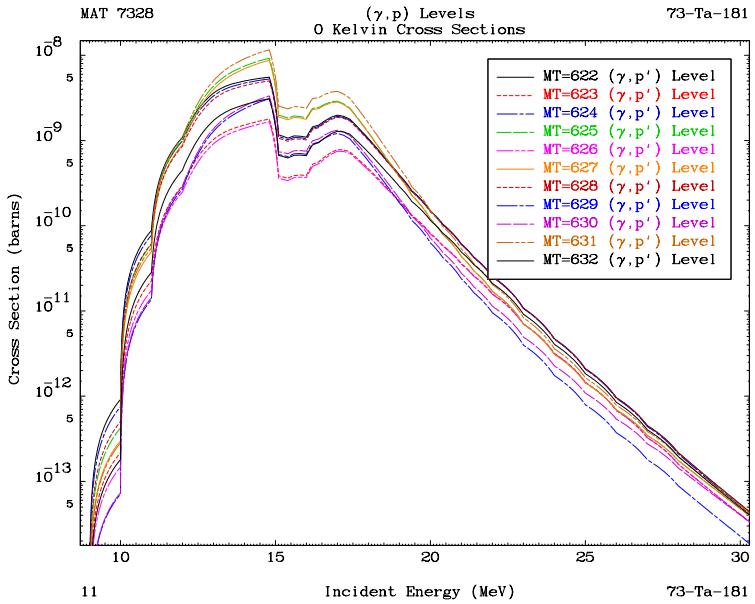
MAT 7328
(γ,p) Levels
0 Kelvin Cross Sections
73-Ta-181
MT=622 (γ,p') Level
MT=623 (γ,p') Level
MT=624 (γ,p') Level
MT=625 (γ,p') Level
MT=626 (γ,p') Level
MT=627 (γ,p') Level
MT=628 (γ,p') Level
MT=629 (γ,p') Level
MT=630 (γ,p') Level
MT=631 (γ,p') Level
MT=632 (γ,p') Level
Cross Section (barns)
Incident Energy (MeV)
11
73-Ta-181

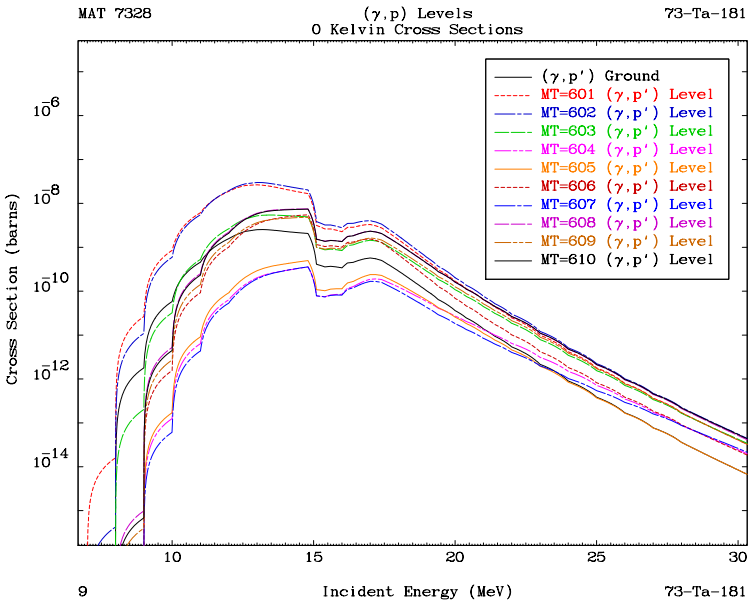
MAT 7328
(γ,p) Levels
0 Kelvin Cross Sections
73-Ta-181
(γ,p') Ground
MT=601 (γ,p') Level
MT=602 (γ,p') Level
MT=603 (γ,p') Level
MT=604 (γ,p') Level
MT=605 (γ,p') Level
MT=606 (γ,p') Level
MT=607 (γ,p') Level
MT=608 (γ,p') Level
MT=609 (γ,p') Level
MT=610 (γ,p') Level
Cross Section (barns)
Incident Energy (MeV)
9
73-Ta-181

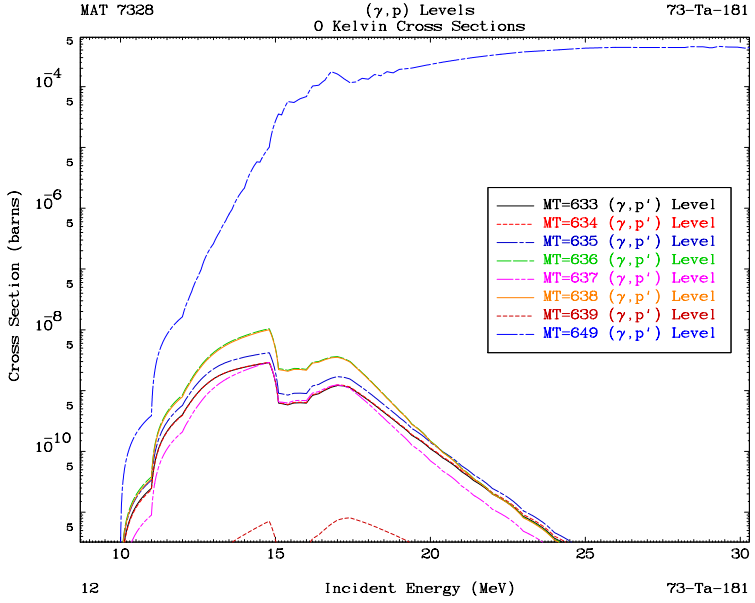
MAT 7328
(γ,p) Levels
0 Kelvin Cross Sections
73-Ta-181
MT=633 (γ,p') Level
MT=634 (γ,p') Level
MT=635 (γ,p') Level
MT=636 (γ,p') Level
MT=637 (γ,p') Level
MT=638 (γ,p') Level
MT=639 (γ,p') Level
MT=649 (γ,p') Level
Cross Section (barns)
Incident Energy (MeV)
12
73-Ta-181

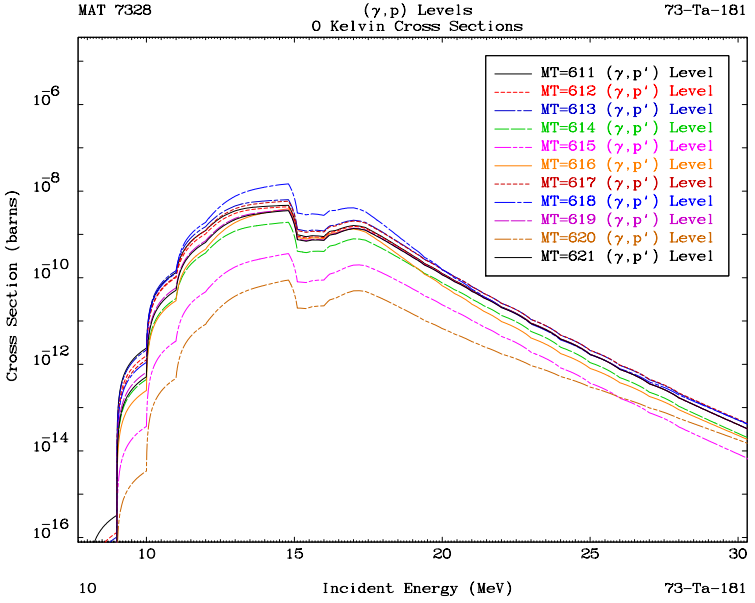
MAT 7328
(γ,p) Levels
0 Kelvin Cross Sections
73-Ta-181
MT=611 (γ,p') Level
MT=612 (γ,p') Level
MT=613 (γ,p') Level
MT=614 (γ,p') Level
MT=615 (γ,p') Level
MT=616 (γ,p') Level
MT=617 (γ,p') Level
MT=618 (γ,p') Level
MT=619 (γ,p') Level
MT=620 (γ,p') Level
MT=621 (γ,p') Level
Cross Section (barns)
Incident Energy (MeV)
10
73-Ta-181

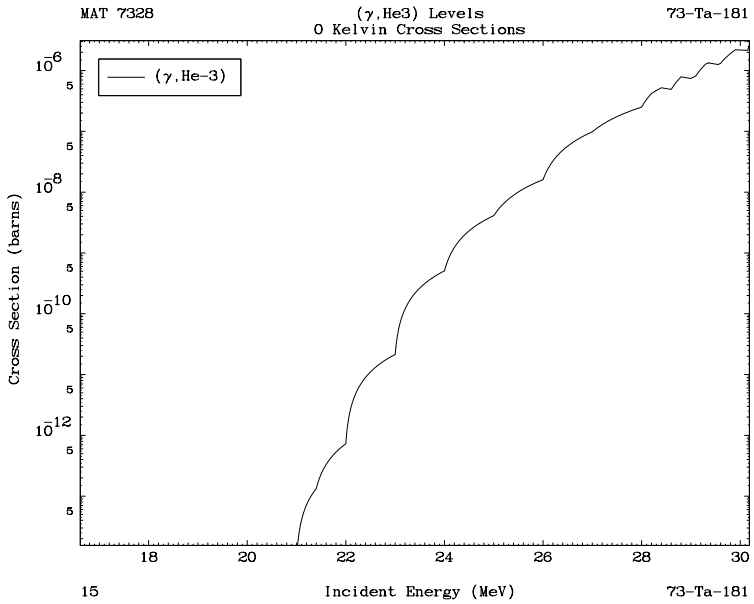
MAT 7328
(γ,He3) Levels
0 Kelvin Cross Sections
73-Ta-181
(γ,He-3)
Cross Section (barns)
Incident Energy (MeV)
15
73-Ta-181

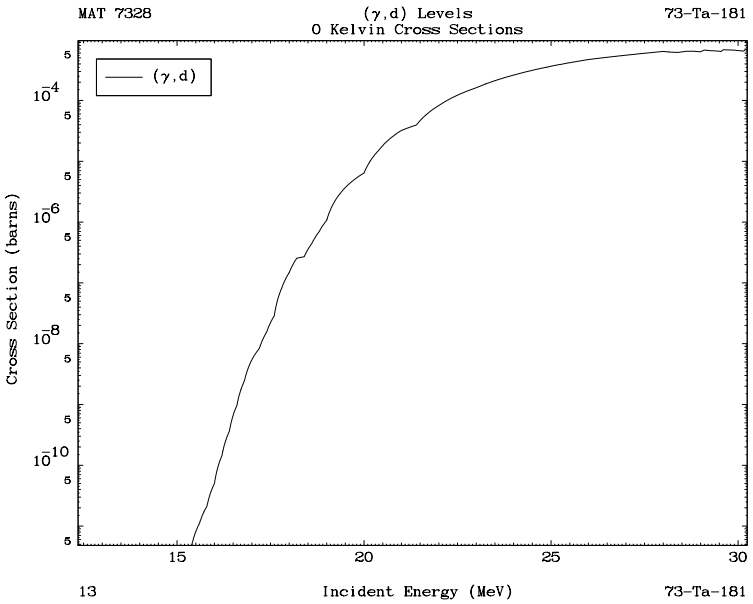
MAT 7328
(γ,d) Levels
0 Kelvin Cross Sections
73-Ta-181
(γ,d)
Cross Section (barns)
Incident Energy (MeV)
13
73-Ta-181

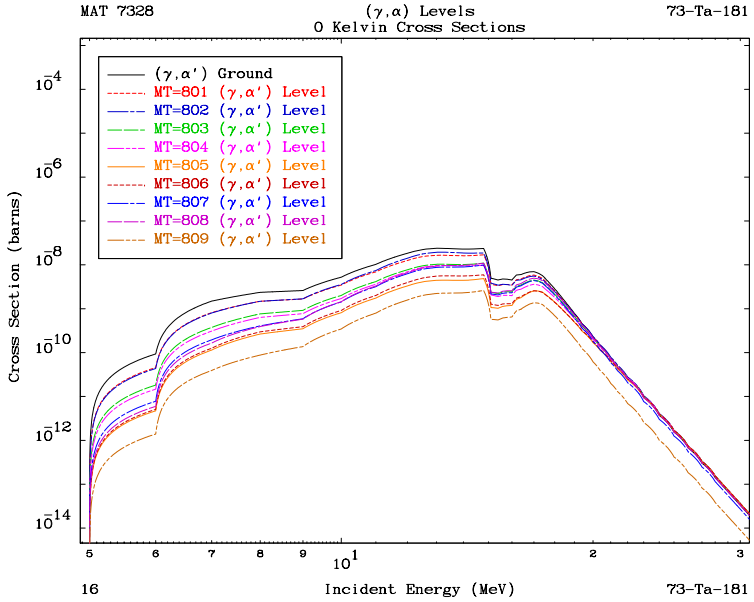
MAT 7328
(γ,α) Levels
0 Kelvin Cross Sections
73-Ta-181
(γ,α') Ground
MT=801 (γ,α') Level
MT=802 (γ,α') Level
MT=803 (γ,α') Level
MT=804 (γ,α') Level
MT=805 (γ,α') Level
MT=806 (γ,α') Level
MT=807 (γ,α') Level
MT=808 (γ,α') Level
MT=809 (γ,α') Level
Cross Section (barns)
Incident Energy (MeV)
16
73-Ta-181

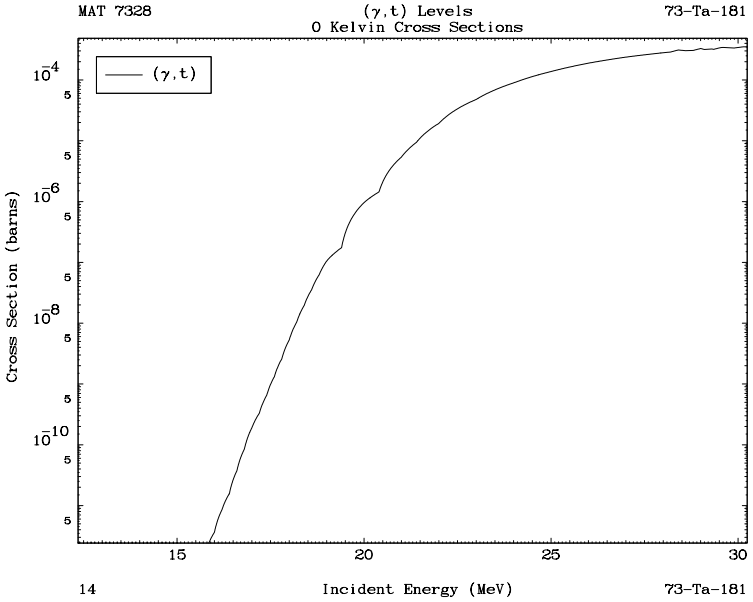
MAT 7328
(γ,t) Levels
0 Kelvin Cross Sections
73-Ta-181
(γ,t)
Cross Section (barns)
Incident Energy (MeV)
14
73-Ta-181

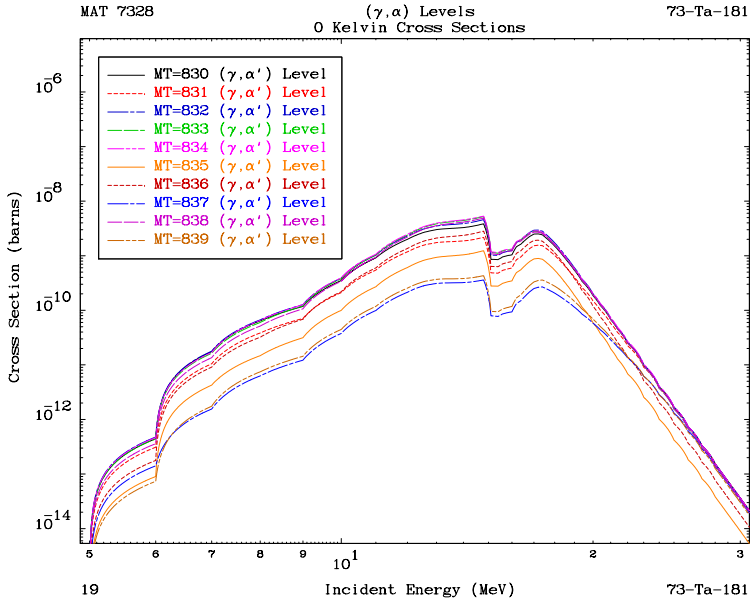
MAT 7328
(γ,α) Levels
0 Kelvin Cross Sections
73-Ta-181
MT=830 (γ,α') Level
MT=831 (γ,α') Level
MT=832 (γ,α') Level
MT=833 (γ,α') Level
MT=834 (γ,α') Level
MT=835 (γ,α') Level
MT=836 (γ,α') Level
MT=837 (γ,α') Level
MT=838 (γ,α') Level
MT=839 (γ,α') Level
Cross Section (barns)
19
Incident Energy (MeV)
73-Ta-181

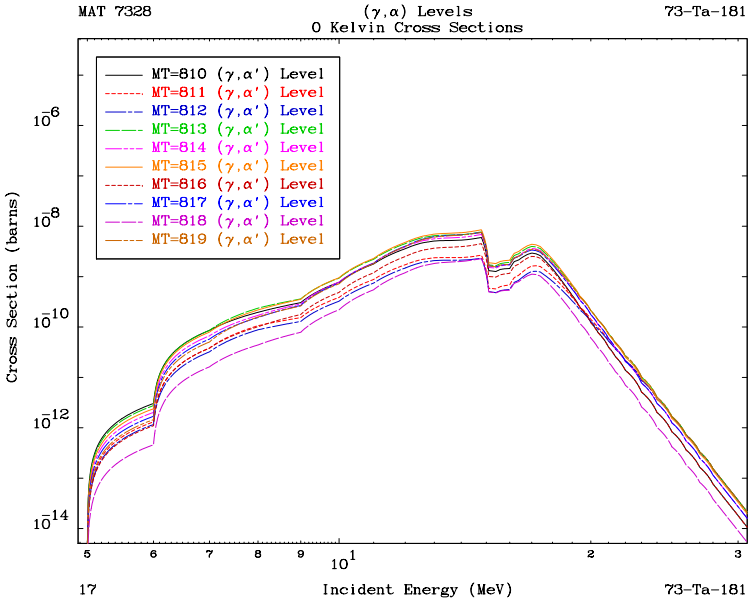
MAT 7328
(γ,α) Levels
0 Kelvin Cross Sections
73-Ta-181
MT=810 (γ,α') Level
MT=811 (γ,α') Level
MT=812 (γ,α') Level
MT=813 (γ,α') Level
MT=814 (γ,α') Level
MT=815 (γ,α') Level
MT=816 (γ,α') Level
MT=817 (γ,α') Level
MT=818 (γ,α') Level
MT=819 (γ,α') Level
Cross Section (barns)
17
Incident Energy (MeV)
73-Ta-181

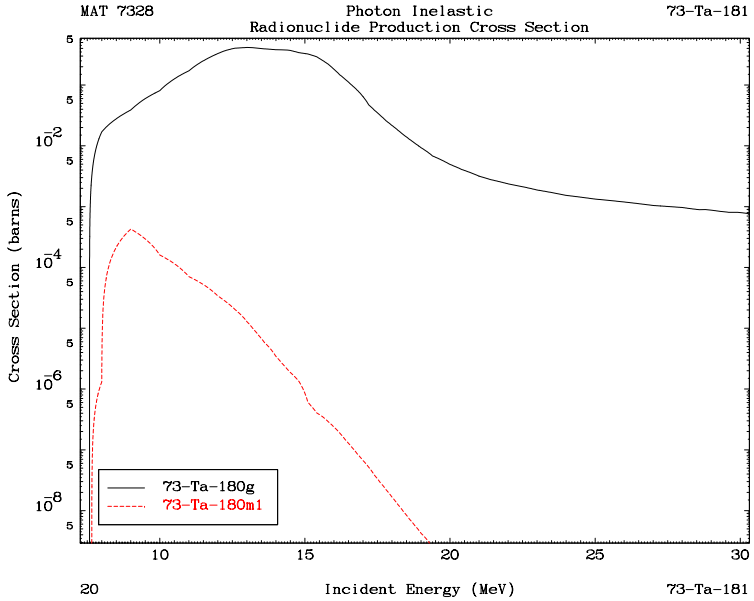
MAT 7328
Photon Inelastic
Radionuclide Production Cross Section
73-Ta-181
73-Ta-180g
73-Ta-180m1
Cross Section (barns)
20
Incident Energy (MeV)
73-Ta-181

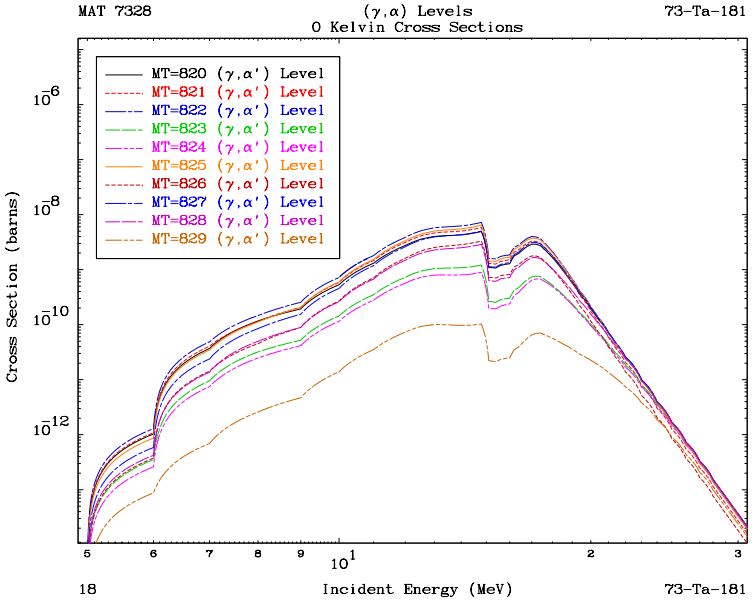
MAT 7328
(γ,α) Levels
0 Kelvin Cross Sections
73-Ta-181
MT=820 (γ,α') Level
MT=821 (γ,α') Level
MT=822 (γ,α') Level
MT=823 (γ,α') Level
MT=824 (γ,α') Level
MT=825 (γ,α') Level
MT=826 (γ,α') Level
MT=827 (γ,α') Level
MT=828 (γ,α') Level
MT=829 (γ,α') Level
Cross Section (barns)
18
Incident Energy (MeV)
73-Ta-181

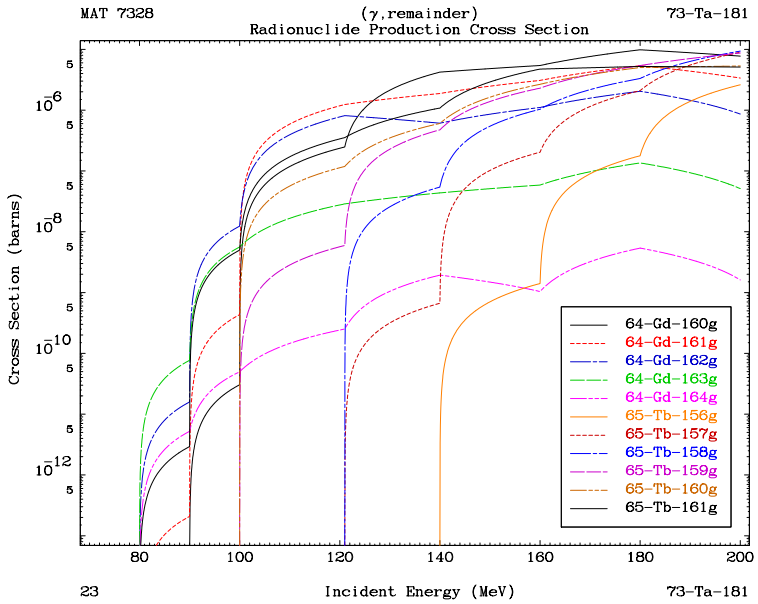
MAT 7328
(γ,remainder)
Radionuclide Production Cross Section
73-Ta-181
Cross Section (barns)
Incident Energy (MeV)
23
73-Ta-181
64-Gd-160g
64-Gd-161g
64-Gd-162g
64-Gd-163g
64-Gd-164g
65-Tb-156g
65-Tb-157g
65-Tb-158g
65-Tb-159g
65-Tb-160g
65-Tb-161g

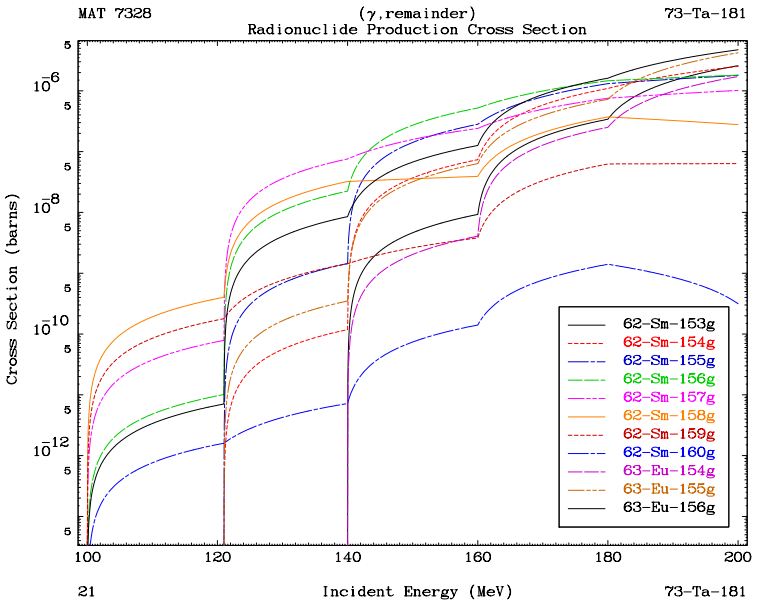
MAT 7328
(γ,remainder)
Radionuclide Production Cross Section
73-Ta-181
Cross Section (barns)
Incident Energy (MeV)
21
73-Ta-181
62-Sm-153g
62-Sm-154g
62-Sm-155g
62-Sm-156g
62-Sm-157g
62-Sm-158g
62-Sm-159g
62-Sm-160g
63-Eu-154g
63-Eu-155g
63-Eu-156g

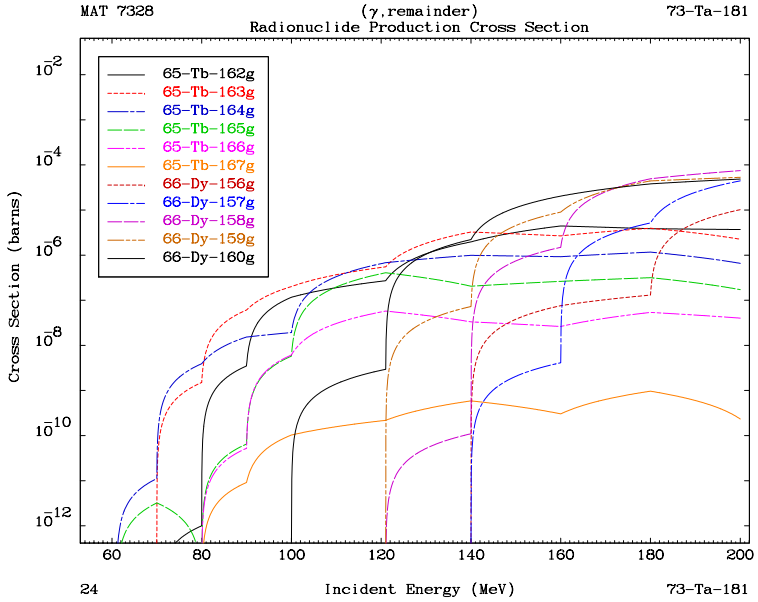
MAT 7328
(γ,remainder)
Radionuclide Production Cross Section
73-Ta-181
Cross Section (barns)
Incident Energy (MeV)
24
73-Ta-181
65-Tb-162g
65-Tb-163g
65-Tb-164g
65-Tb-165g
65-Tb-166g
65-Tb-167g
66-Dy-156g
66-Dy-157g
66-Dy-158g
66-Dy-159g
66-Dy-160g

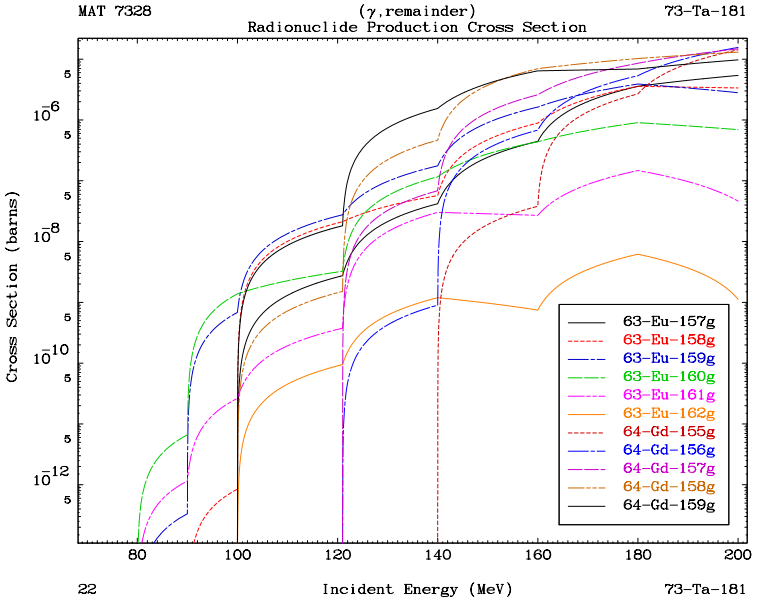
MAT 7328
(γ,remainder)
Radionuclide Production Cross Section
73-Ta-181
Cross Section (barns)
Incident Energy (MeV)
22
73-Ta-181
63-Eu-157g
63-Eu-158g
63-Eu-159g
63-Eu-160g
63-Eu-161g
63-Eu-162g
64-Gd-155g
64-Gd-156g
64-Gd-157g
64-Gd-158g
64-Gd-159g

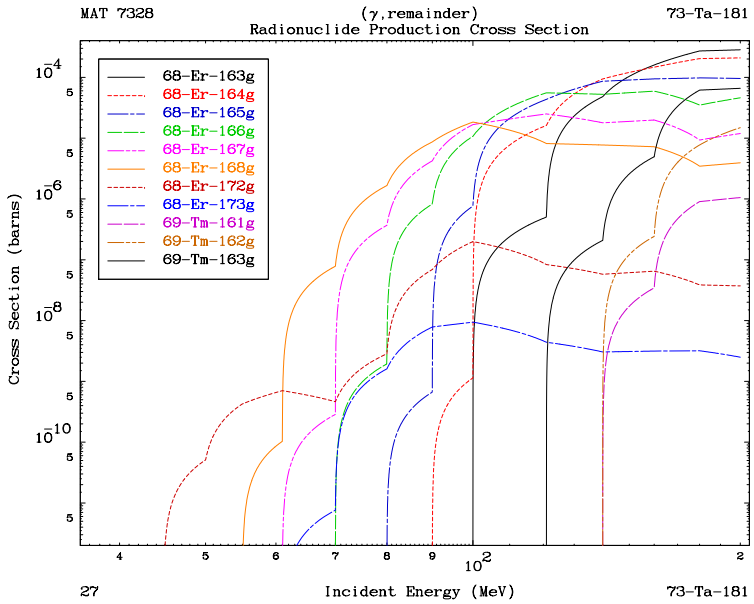
MAT 7328
(γ,remainder)
Radionuclide Production Cross Section
73-Ta-181
68-Er-163g
68-Er-164g
68-Er-165g
68-Er-166g
68-Er-167g
68-Er-168g
68-Er-172g
68-Er-173g
69-Tm-161g
69-Tm-162g
69-Tm-163g
Cross Section (barns)
Incident Energy (MeV)
27
73-Ta-181

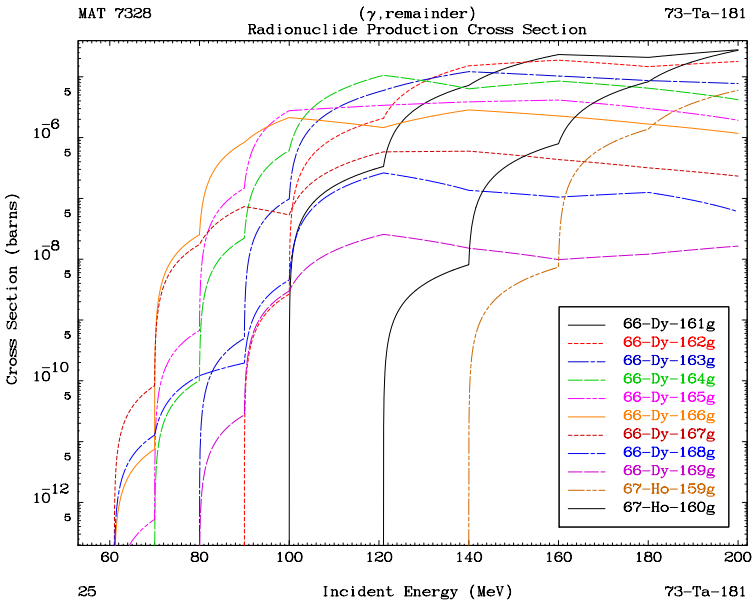
MAT 7328
(γ,remainder)
Radionuclide Production Cross Section
73-Ta-181
66-Dy-161g
66-Dy-162g
66-Dy-163g
66-Dy-164g
66-Dy-165g
66-Dy-166g
66-Dy-167g
66-Dy-168g
66-Dy-169g
67-Ho-159g
67-Ho-160g
Cross Section (barns)
Incident Energy (MeV)
25
73-Ta-181

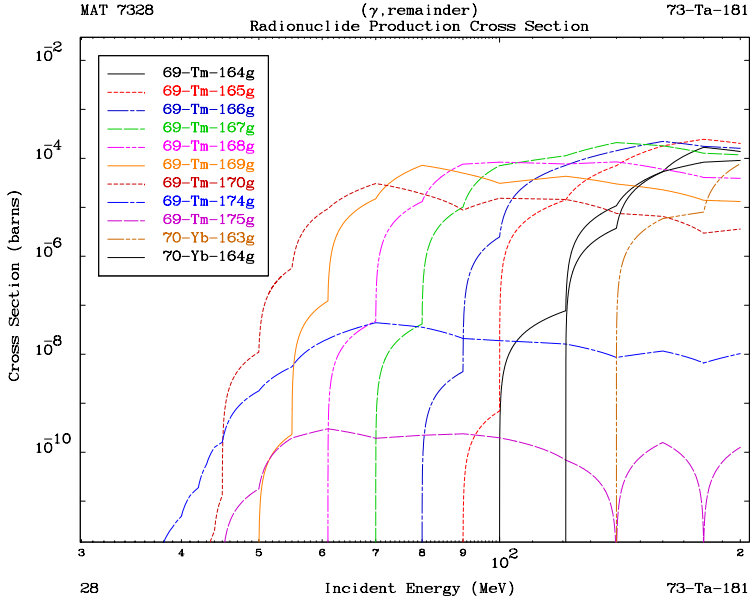
MAT 7328
(γ,remainder)
Radionuclide Production Cross Section
73-Ta-181
69-Tm-164g
69-Tm-165g
69-Tm-166g
69-Tm-167g
69-Tm-168g
69-Tm-169g
69-Tm-170g
69-Tm-174g
69-Tm-175g
70-Yb-163g
70-Yb-164g
Cross Section (barns)
Incident Energy (MeV)
28
73-Ta-181

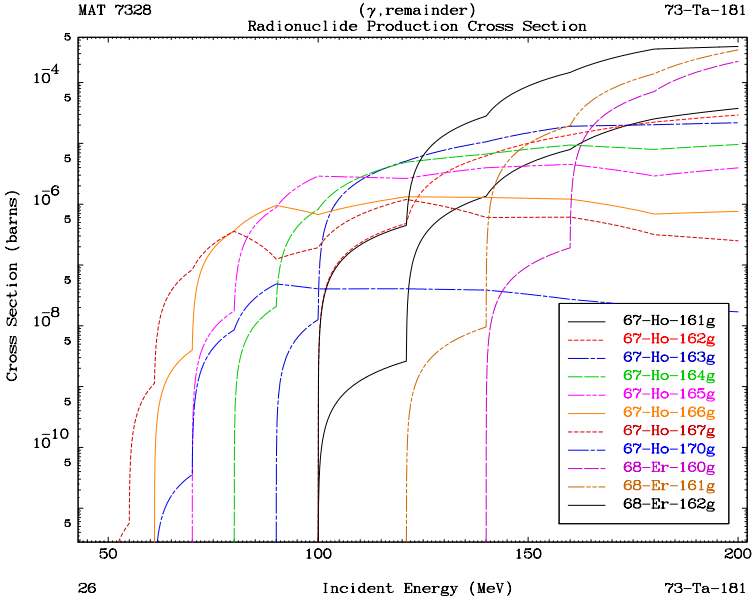
MAT 7328
(γ,remainder)
Radionuclide Production Cross Section
73-Ta-181
67-Ho-161g
67-Ho-162g
67-Ho-163g
67-Ho-164g
67-Ho-165g
67-Ho-166g
67-Ho-167g
67-Ho-170g
68-Er-160g
68-Er-161g
68-Er-162g
Cross Section (barns)
Incident Energy (MeV)
26
73-Ta-181

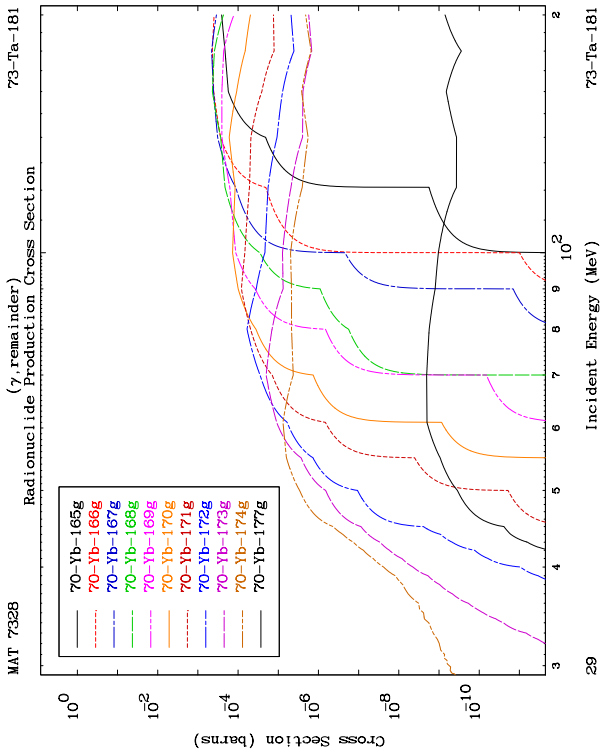
MAT 7328
73-Ta-181
(γ,remainder)
Radionuclide Production Cross Section
70-Yb-165g
70-Yb-166g
70-Yb-167g
70-Yb-168g
70-Yb-169g
70-Yb-170g
70-Yb-171g
70-Yb-172g
70-Yb-173g
70-Yb-174g
70-Yb-177g
Cross Section (barns)
Incident Energy (MeV)
29

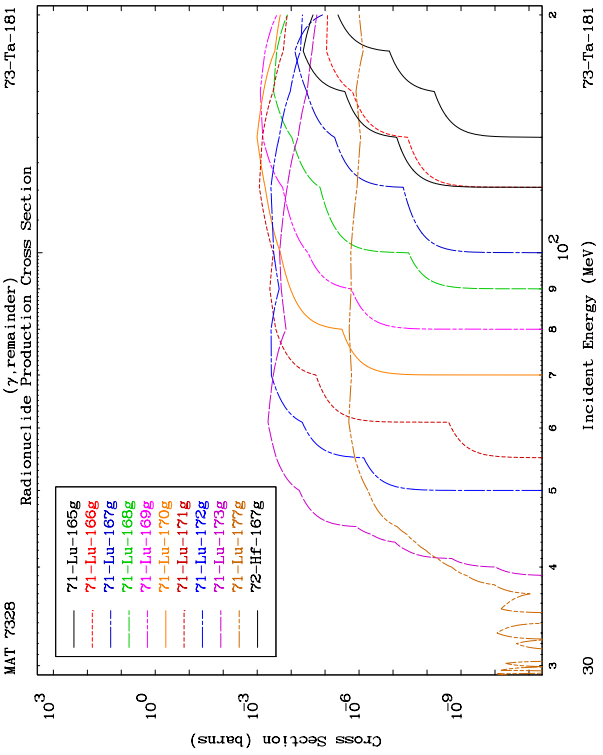
MAT 7328
73-Ta-181
(γ,remainder)
Radionuclide Production Cross Section
71-Lu-165g
71-Lu-166g
71-Lu-167g
71-Lu-168g
71-Lu-169g
71-Lu-170g
71-Lu-171g
71-Lu-172g
71-Lu-173g
71-Lu-177g
72-Hf-167g
Cross Section (barns)
Incident Energy (MeV)
30

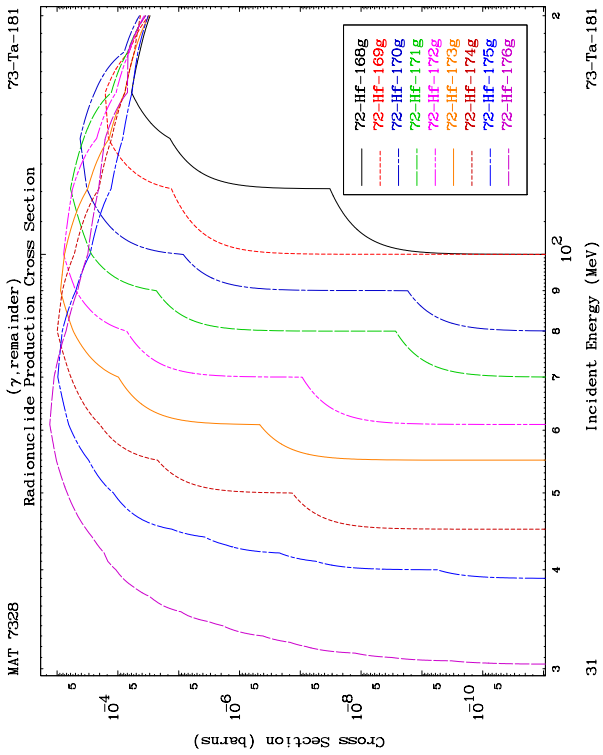
MAT 7328
73-Ta-181
(γ,remainder)
Radionuclide Production Cross Section
72-Hf-168g
72-Hf-169g
72-Hf-170g
72-Hf-171g
72-Hf-172g
72-Hf-173g
72-Hf-174g
72-Hf-175g
72-Hf-176g
Cross Section (barns)
Incident Energy (MeV)
31

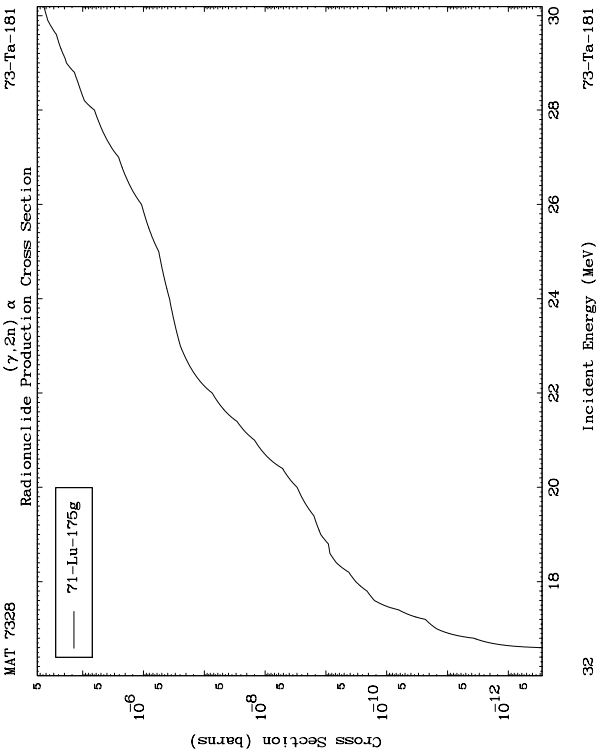
MAT 7328
73-Ta-181
(γ,2n) α
Radionuclide Production Cross Section
71-Lu-175g
Cross Section (barns)
Incident Energy (MeV)
32

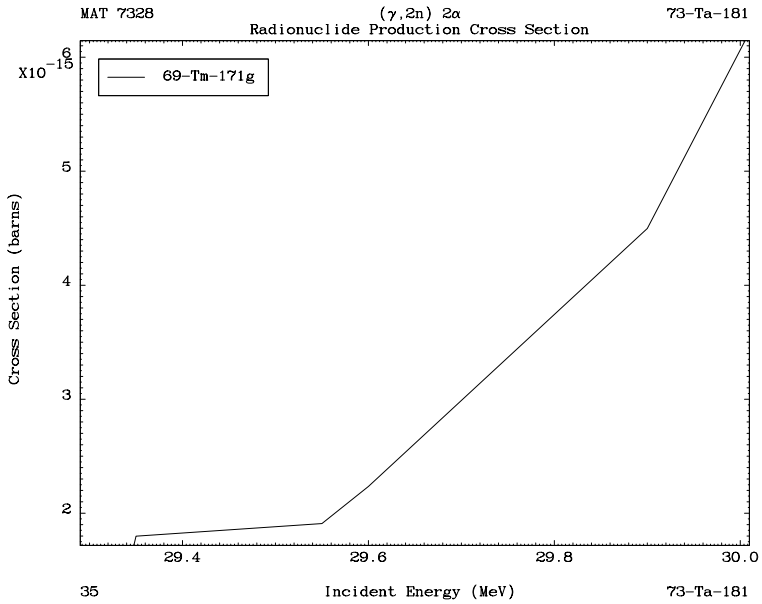
MAT 7328
(γ,2n) 2α
73-Ta-181
Radionuclide Production Cross Section
69-Tm-171g
X10^-15
Cross Section (barns)
29.4
29.6
29.8
30.0
35
Incident Energy (MeV)
73-Ta-181

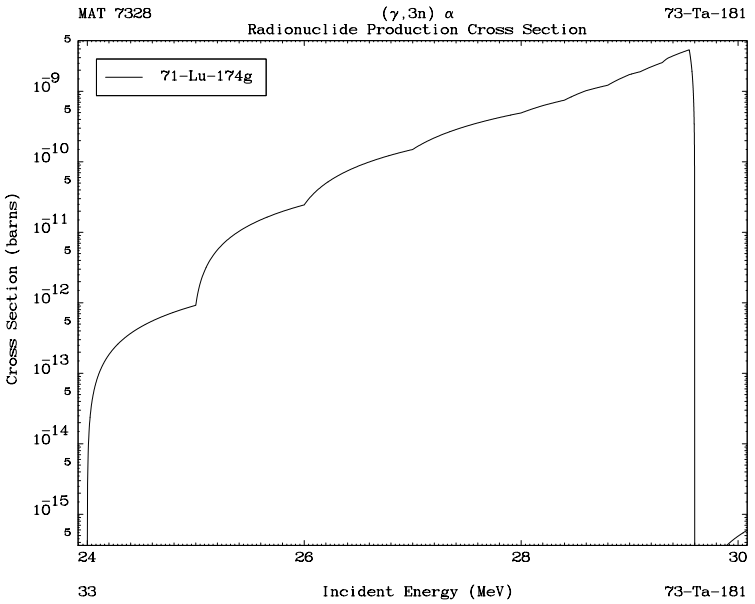
MAT 7328
(γ,3n) α
73-Ta-181
Radionuclide Production Cross Section
71-Lu-174g
Cross Section (barns)
24
26
28
30
33
Incident Energy (MeV)
73-Ta-181

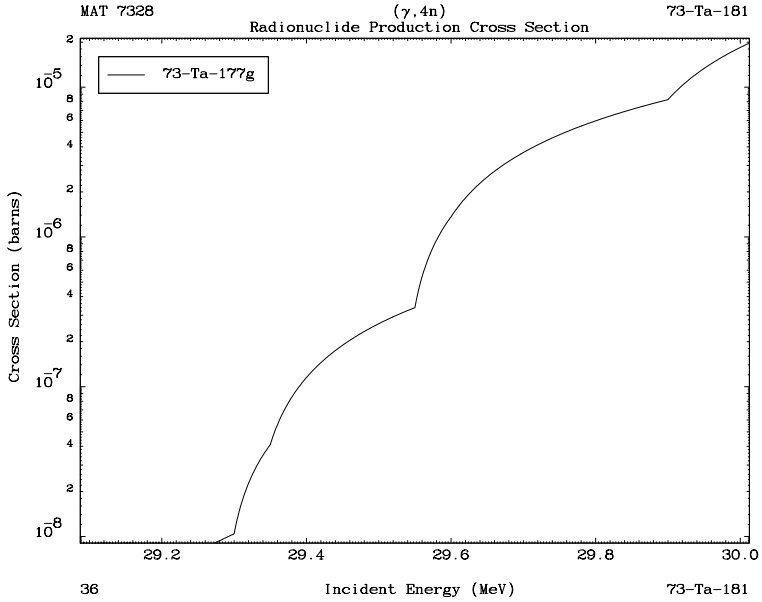
MAT 7328
(γ,4n)
73-Ta-181
Radionuclide Production Cross Section
73-Ta-177g
Cross Section (barns)
29.2
29.4
29.6
29.8
30.0
36
Incident Energy (MeV)
73-Ta-181

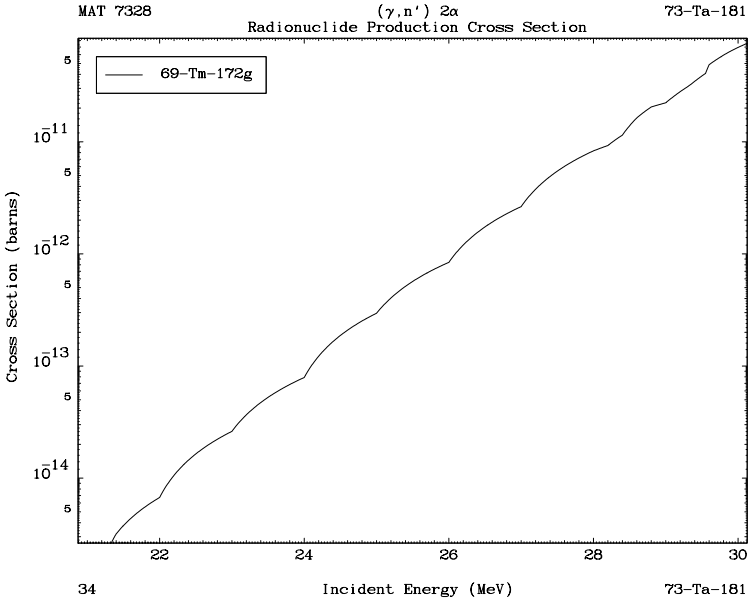
MAT 7328
(γ,n') 2α
73-Ta-181
Radionuclide Production Cross Section
69-Tm-172g
Cross Section (barns)
22
24
26
28
30
34
Incident Energy (MeV)
73-Ta-181

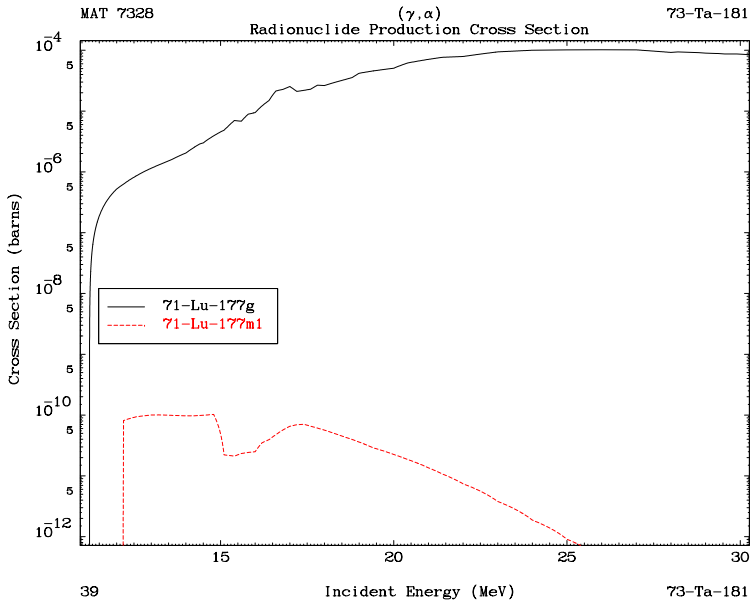
MAT 7328
(γ,α)
73-Ta-181
Radionuclide Production Cross Section
71-Lu-177g
71-Lu-177m1
Cross Section (barns)
Incident Energy (MeV)
39
73-Ta-181

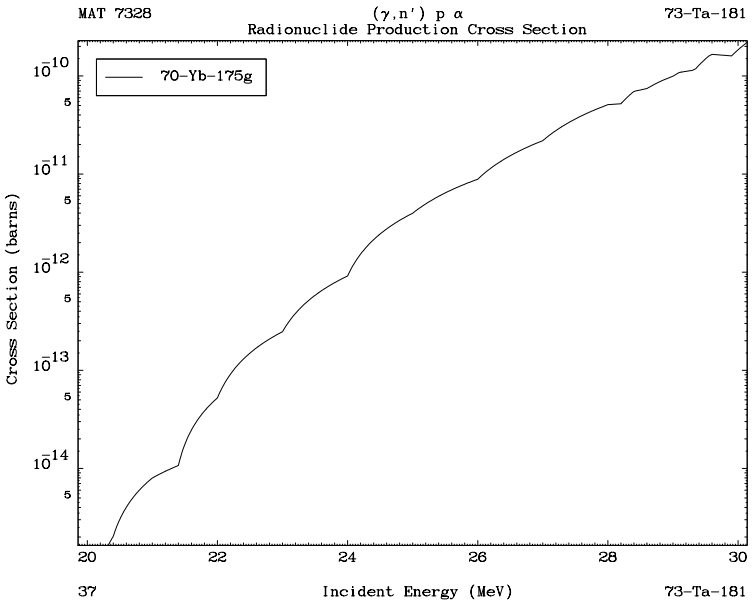
MAT 7328
(γ,n') p α
73-Ta-181
Radionuclide Production Cross Section
70-Yb-175g
Cross Section (barns)
Incident Energy (MeV)
37
73-Ta-181

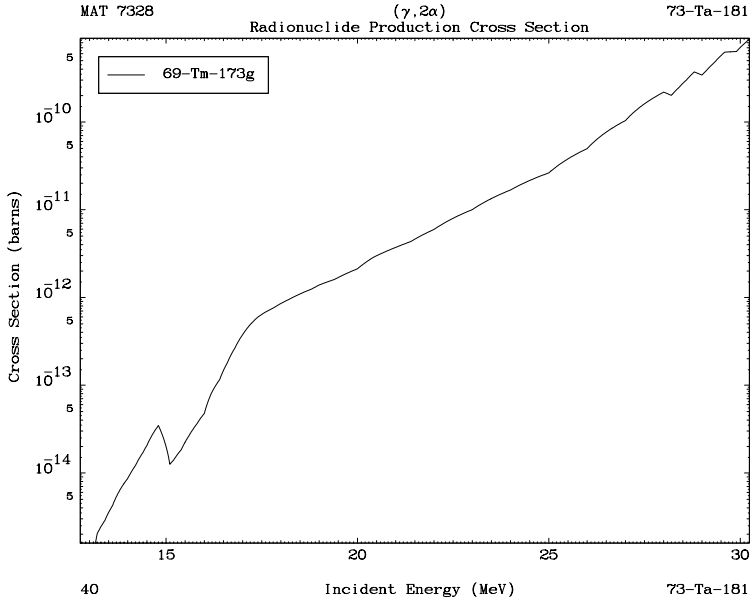
MAT 7328
(γ,2α)
73-Ta-181
Radionuclide Production Cross Section
69-Tm-173g
Cross Section (barns)
Incident Energy (MeV)
40
73-Ta-181

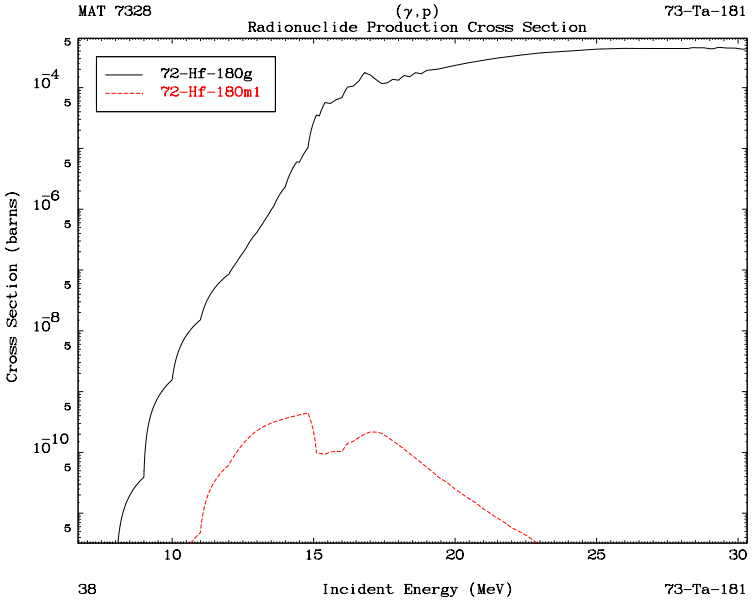
MAT 7328
(γ,p)
73-Ta-181
Radionuclide Production Cross Section
72-Hf-180g
72-Hf-180m1
Cross Section (barns)
Incident Energy (MeV)
38
73-Ta-181